FUNCTIONAL GENOMIC STUDIES OF VACCINIA VIRUS PROVIDE FUNDAMENTAL INSIGHTS INTO VIRUS-HOST INTERACTIONS

Brian Andrew Keller

A thesis submitted to the Faculty of Graduate and Postdoctoral Studies
in partial fulfillment of the requirements for the degree of

Doctorate of Philosophy in Biochemistry

Department of Biochemistry, Microbiology and Immunology
Faculty of Medicine
University of Ottawa

Abstract

The oncolytic virus field is in the midst of strong and sustained growth. The clinical utility of this class of therapeutics has been bolstered in recent years by the rise of immune checkpoint inhibition, which has the potential to work synergistically with oncolytic viruses to increase the scope of patients who respond favourably to therapy. This growth has been further driven by clear industry support with several pharmaceutical companies acquiring or developing oncolytic virus products following the 2015 FDA approval of *Talimogene laherparepvec* and the generally-accepted potential of immunotherapeutic approaches to cancer treatment. Vaccinia virus is a double-stranded DNA virus with an extensive history of vaccine use in humans and a desirable safety profile. It is a large virus with a complex lifecycle, and its history of use as a vaccine has resulted in the generation of dozens of unique strains. Although it has been studied extensively, much remains unknown about many vaccinia virus gene function(s) and the virus' interactions with cellular hosts. Vaccinia virus-based oncolytic viruses have been developed, however clinical outcomes thus far have been unsatisfactory. A more complete understanding of vaccinia virus gene functions must therefore precede the effective design of a next-generation vaccinia virus-based oncolytic candidate. With this downstream goal, we sought to (1) understand the unique oncolytic virus-relevant phenotypic properties of five clinical candidate vaccinia virus strains, and (2) generate and characterize a library of single-gene mutants of the Copenhagen strain of vaccinia virus. These studies resulted in the selection of vaccinia virus-Copenhagen as the wild-type strain of choice that will be utilized for future oncolytic virus development. Furthermore, the generation and initial characterization of an 89-member clonal library of vaccinia-Copenhagen single-gene mutants will be an important tool as we seek to generate a next-generation oncolytic virus candidate. Completed characterization studies challenge the role that viral thymidine kinase should

play in oncolytic virus design, demonstrate novel functions of the vaccinia virus gene *A47L*, and provide an understanding of the role of the vaccinia virus gene *F15L*. These studies also raise the concept of the personalized selection of oncolytic virotherapeutics. This virus library has the potential to increase the fundamental understanding of vaccinia virus biology in this field as well as in the study of vaccine development and pathogen-host interactions.

Acknowledgements

Many people have contributed to this project and to my growth over the past several years. First and foremost, I would like to thank my supervisor and mentor, Dr. John Bell, whose contributions go far beyond scientific – I have received countless wonderful opportunities, my scope has been infinitely broadened, and the lessons that I take away from my PhD will impact my career in ways that I certainly cannot yet appreciate. Thank you also to Dr. Harry Atkins, whose mentorship and scientific guidance truly helped to shape this project and who helped show me what it means to be a clinician-scientist. I would also like to express my sincere thanks to Dr. Carolina Ilkow who has impacted this work in countless ways, who has been an excellent scientific role model, and whose friendship continues to ease the challenges associated with what we do.

Thank you to the members of my thesis advisory committee – Drs. Jonathan Angel, Jennifer Beecker, and Jean-Simon Diallo, whose diverse backgrounds and areas of expertise helped to push me, but also to build the quality and scope of this project. Thank you to Dr. Guy Ungerechts, who took an interest in my progress and this project, and whose mentorship continues to be valued.

I would like to thank all the current members of the laboratory and several alumni, the majority of whom cannot be named, for their many contributions to this work. Notably, Dr. Jiahu Wang, who conceptualized transposon-mediated insertional mutagenesis of vaccinia virus and who generated the first library; and Adrian Pelin, whose bioinformatics work was critical to the ongoing success of this project and whose input into this thesis can be directly seen in many figures. Thank you to Dr. Fabrice Le Boeuf for much insight into and help with vaccinia virus-related lab techniques, as well as for editing this thesis. Likewise, thank you to Marisa Market for taking the time to carefully read and edit this thesis. Thank you to Russell Barkley, whose technical

contributions to this project are countless, and whose scientific curiosity and pursuit of a full understanding drove me to be a better teacher.

I would like to sincerely thank Catia Cemeus for her major contributions to this project and for her patience, technical support, and skill. Thank you to Julia Petryk for help with all animal experiments. I would also like to thank Drs. Jim Dimitroulakos and Carolyn Nessim, respectively, for helping with the logistical challenges associated with, and actually obtaining, surgical specimens. Thank you also to the many patients who unknowingly impacted this work for their willingness to help as we all work together to better treat cancer.

Most importantly, I would like to thank my family for their constant and continued support of all that I do; and especially Maria, who has lived and breathed all aspects of this project along with me, who unconditionally supports my interests, and who always helps me to realize where my priorities lie.

Table of Contents

List of Abbreviations

ATCC	American Type Culture Collection
CAF	Cancer-associated fibroblast
CEV	Cell-associated enveloped virion
CTL	Cytotoxic T-lymphocyte
CTLA-4	Cytotoxic T-lymphocyte-associated protein 4
DAPI	4’6’-diamidine-2’-phenylindole dihydrochloride
DNA	Deoxyribonucleic acid
ds	Double stranded
EBV	Epstein-Barr virus
EEV	Extracellular enveloped virion
EFC	Entry fusion complex
EGFR	Epidermal growth factor receptor
EV	Enveloped virion
E. coli	Escherichia coli
FFPE	Formalin-fixed, paraffin-embedded
FGF2	Fibroblast growth factor 2
GM-CSF	Granulocyte macrophage colony-stimulating factor
H3K9	Histone 3, lysine 9
HCC	Hepatocellular carcinoma
HJ	Holliday junction
HSV-1	Herpes simplex virus, type 1
Hz	Hertz
ICOS	Inducible T-cell co-stimulator
IFN	Interferon
IFNAR	IFN-α/ß receptor complex
ISG	IFN-stimulated gene
ITR	Inverted terminal repeats
IV	Immature virion
MDA5	Melanoma differentiation-associated gene 5

mM	Millimolar
MOI	Multiplicity of infection
mRNA	Messenger ribonucleic acid
MUSCLE	Multiple sequence comparison by log-expectation
MV	Mature virion
MVA	Modified Vaccinia Ankara
NCI	National Cancer Institute
NDV	Newcastle disease virus
NF- κB	Nuclear factor kappa-light-chain-enhancer of activated B cells
nr	Non-redundant database
ORF	Open reading frame
OV	Oncolytic virus
PAMP	Pathogen-associated molecular pattern
Pexa-Vec	Pexastimogene devacirepvec
PCR	Polymerase chain reaction
PD-1	Programmed cell death protein 1
PD-L1	Programmed death ligand 1
PFU	Plaque forming units
PRR	Pattern recognition receptor
RAP94	RNA polymerase-associated protein of 94 kDa
RhoA	Ras homolog gene family, member A
RIG-I	Retinoic acid induced gene I
RNA	Ribonucleic acid
RNA-seq	High-throughput deep RNA sequencing
RPMI	Roswell Park Memorial Institute
ss	Single stranded
TAA	Tumour-associated antigen
TE	Transposable element
Tp	Transposon
T-Vec	Talimogene laherparepvec

VACV	Vaccinia virus
VETF	Vaccinia early transcription factor
VGF	Vaccinia growth factor
VLTF	Vaccinia late transcription factor
VSV	Vesicular stomatitis virus
WHO	World Health Organization

List of Figures

List of Tables

1. Introduction

Preface

In recent years, oncolytic viruses (OVs) have been recognized as potential clinical agents due largely to the United States Food and Drug Administration's approval of Imlygic™. Coupled with the potential to provide synergistic anti-tumour effects with existing cancer therapeutics, the clinical interest in effective OV platforms has gained momentum. One virus platform that has been a subject of such interest is vaccinia virus (VACV). VACV is a large and genetically complex virus; as such, many unanswered questions remain about the fundamental biology of VACV. Therefore, the focus of this research project was to investigate unknown properties of VACV in the context of use as a potential OV platform. The sections that follow will describe unique biological properties of select VACV strains and investigations directed at individual gene functions of the Copenhagen strain of VACV. This research project describes the development of a novel system that can be used to study VACV biology and provides examples of how individual VACV gene products can have profound effects on viral phenotype depending on host interactions.

1.1. Human cancer

1.1.1. Epidemiology and pathophysiology

Almost half of all Canadians are expected to develop cancer at some point in their lives and approximately 25% are expected to die of their disease. Currently, cancer-related deaths represent approximately 30% of deaths in Canada, making it proportionally responsible for more fatalities than any other single cause[1]. One cancer type that has a greater focus throughout this research project is melanoma. The pathophysiology of melanoma is interesting in that it generally allows good clinical outcomes in cases of early-stage pre-metastatic disease. However metastatic melanoma is aggressive and often proves to be treatment-refractory – stage IV disease currently

carries five- and ten-year survival rates of approximately 15% and 10%, respectively[1]. Fortunately, cancer rates in general have been steadily declining over the past several years[1]. This can be attributed to therapeutic advances (most notably immune checkpoint inhibition) in several cancer types, with melanoma leading the way[2]. Advances such as these become more common as we gain insights into the pathogenesis of disease, which is occurring in the field of cancer biology at an exceptional rate.

As our understanding of cancer biology increases, so too does our appreciation for its remarkable complexity. In order to provide a framework within which to conceptualize the many forms of cancer, Drs. Hanahan and Weinberg summarized fundamental commonalities observed across most variants of the disease, which were published in a landmark paper and came to be known as the *Hallmarks of Cancer*[3]. Simply depicted, these hallmarks are: (1) the ability to infinitely replicate, (2) an insensitivity or lack of tumour suppression, (3) the ability to evade apoptosis, (4) the ability to stimulate growth through growth signal autonomy, (5) the ability to generate and sustain angiogenesis, and (6) the ability to invade distant tissues and metastasize. More recently, additions have been made to these hallmarks to reflect a contemporary view of cancer – such additions include a tumour cell's ability to evade immune detection and destruction, and a cancer cell's ability to dysregulate cellular energetics and metabolism[4]. Underlying these fundamentals, however, are two enabling characteristics – genomic instability and mutation[4].

The hypothesis that genetic mutations could be associated with cancers first came about as a result of the epidemiologic observation that common cancers increase with age[5]. In the early 20th century, Boveri hypothesized many genomic concepts that became the cornerstone of cancer research over the following decades and have contributed to what are now recognized as the hallmarks discussed above[6]. Amongst other features, Boveri predicted the presence of cell cycle

checkpoints, tumour-suppressor genes, oncogenes, the clonal origin of cancer, and the sequential changes that must occur to allow tumour progression from benign to malignant. Later researchers used similar observations to hypothesize that cancer is indeed an accumulation of multiple genetic mutations, eventually culminating in the "multi-hit hypothesis" of cancer[7], which was generated following a statistical analysis of Retinoblastoma, a disease with detectable sporadic and hereditary variants[8]. Today, many of Boveri's early hypotheses have been confirmed and it is known that inherited mutations and/or somatic alterations to relevant genes indeed contribute to oncogenesis. Overall, as the molecular observations that form our biologic understanding of cancer grow, so too does our ability to more effectively design novel anti-cancer therapeutics.

One of the inherent biological properties of most cancers is that they have adapted masterful immune evasion mechanisms through a process of immunoselection, which directly contribute to their ability to indefinitely replicate. Solid tumours are known for their ability to evade immune detection due to the downregulation or loss of HLA class I expression[9,10]. Proteins involved in the processing and presentation of antigens by HLA class I molecules have also been shown to be downregulated. Additionally, numerous inhibitory cytokines (ex. VEGF, IL-6, IL-10, TGF-β) can be produced by tumours that act to limit dendritic cell activation, which necessitate a decreased response by T cells[9,11]. Despite these measures, mechanisms are in place within the tumour microenvironment to suppress the development of even minimal anti-tumour immunity. Regulatory T cells and myeloid-derived suppressor cells are amongst a group of tumour infiltrating leukocytes that is aberrantly commonplace within many tumours, functioning to slow the immune response by secreting inhibitory cytokines, and by promoting the expression of inhibitory receptors such as cytotoxic T-lymphocyte-associated protein 4 (CTLA-4) and programmed death ligand 1 (PD-L1)[11].

1.1.2. *Therapeutic challenges*

Researchers have made tremendous progress towards the development of novel anti-cancer therapeutics, especially in recent years as our understanding of cancer biology and the potential to translate basic discoveries into clinical treatments each increase. In efforts that are often designed to address the hallmarks of cancer, novel classes of therapeutics have been created to circumvent associated therapeutic challenges.

Like with most solid cancers, traditional treatment modalities for advanced melanoma have commonly included surgery, chemotherapy, and radiation therapy. Although the quality of these treatment modalities has advanced, their lack of specificity is associated with toxicities and the majority of advanced patients do not see significant therapeutic benefit. To counter these issues, the development of biologic anti-cancer therapeutics has occurred for many indications. One example of these include the blockade of BRAF in *mtBRAF* melanoma, activating mutations of which account for approximately 50% of cases and implicate aberrant MAP kinase/ERK-signaling in disease pathogenesis[12]. Another indication for which biologic therapies have been developed is ovarian cancer. Ovarian cancers are commonly linked to aberrancies in VEGF and BRCA expression, characteristics which are shared across other indications including breast cancer, and which have been the target of efficacious biologic therapies[13-16]. These and many other biologic approaches have improved therapeutic outcomes of select patients and have importantly helped to illustrate the utility of selectively targeting activated pathways despite differences in disease site.

A more recent trend in the development of biologic therapies has been to focus on reducing immune tolerance of a tumour. Under normal physiologic conditions, immune checkpoints serve critical functions in preventing self-tolerance and protecting tissue from damage in the context of an appropriate immune response. As briefly mentioned above, however, some immune

checkpoints – such as CTLA-4 and programmed cell death protein 1 (PD-1) – can be aberrantly regulated in many cancers, which contribute to its ability to evade immune detection. Immune checkpoint inhibition, a novel class of immunotherapy that acts to "release the breaks" on the immune system, has already revolutionized the treatment of melanoma, and is being widely investigated for utility in other indications. Evidence has demonstrated that antibodies against the immune checkpoint molecules CTLA-4 and PD-L1 increase survival and durable tumour regression in previously untreated and advanced melanoma, in addition to evidence that efficacy is improved when these therapies are used concurrently[2,17]. While these findings are striking, quantitative analysis of the reported data reveals that there remains a great deal of room for improvement – the objective response rate exceeded 50% (specifically, 53%) in only one of the study cohorts[17]. Currently, the most promising strategy for improvement is to utilize a combinatorial therapeutic approach to initiate or augment a previously existing anti-tumour immunity.

1.2. Replicating oncolytic viruses

Virologists and clinicians in the early 20th century first began appreciating a link between viruses and cancer because of individual case reports of cancer regressions following natural viral infections[18]. It was not until the middle of the century, however, that directed efforts were made to use viral-based therapies to treat cancer[19-21]. In recent years, OVs have been translated into viable anti-cancer therapeutics and clinical use has been increasing. In October 2015, Amgen's *Talimogene Laherparepvec* (T-Vec), a herpes simplex virus (HSV)-1-based OV, gained provisional approval for clinical use in the United States, followed shortly thereafter by Europe.

1.2.1. Physiologic anti-viral response and inherent viral targeting of transformed cells

As the OV field matured in the final years of the 20th century and as cell biologists and clinicians began to appreciate the hallmarks of cancer, it became apparent that parallel mechanisms govern the processes of malignant transformation and viral infection. It has since been established that many aberrantly-regulated signaling pathways commonly associated with malignant transformation actually confer viral sensitivity to transformed cells and generally converge on the innate immune response, and specifically on interferon (IFN) production. Summarized in Figure 1.1, these altered pathways result in transformed cells that are able to infinitely replicate, evade apoptosis, evade immune detection, and stimulate angiogenesis[22], all properties which can leave these cells exquisitely sensitive to viral infection.

Under physiologic conditions, pattern recognition receptors (PRRs) first sense the presence of a virus when it encounters a cell. There are many types of PRRs, including the cell surface and endosomal toll-like receptor (TLR) family, various members of which can sense foreign ssRNA, dsRNA, and unmethylated DNA[23,24]. The RIG-I (retinoic acid induced gene)-like receptors melanoma differentiation-associated gene 5 (MDA5) and RIG-I have evolved to sense dsRNA and phosphorylated ssRNA, respectively, while other intracellular molecules can recognize the presence of foreign cytosolic dsDNA, including AIM2 and RNA polymerase III[23,25-27]. Interestingly, RNA polymerase III works to transcribe preferentially AT-rich DNA of invading pathogens into RNA, which can then be recognized by RIG-I[28,29]. Most relevant to this research project, pathogen-associated molecular patterns (PAMPs) from DNA viruses such as VACV are recognized by a diverse and growing array of PRRs, however most notable are TLRs[24].

Once PRRs recognize pathogenic invasion, several distinct signaling cascades can be initiated that lead to the release of inflammatory or stimulatory cytokines, the release of Type I

Figure 1.1. The oncolytic virus paradigm. When a normal cell encounters an invading pathogen such as vaccinia virus, cell-associated Pattern Recognition Receptors recognize pathogen-associated molecular patterns, initiating a complex anti-viral cascade designed to limit virus replication and spread. Central to this response is the production and release of interferon, which has both autocrine and paracrine effects, such as preventing cellular growth, inducing apoptosis, preventing angiogenesis, and the downstream activation of adaptive immunity. In a transformed cell, however, this anti-viral signaling is diminished, leaving such cells inherently sensitized to pathogenic invasion.

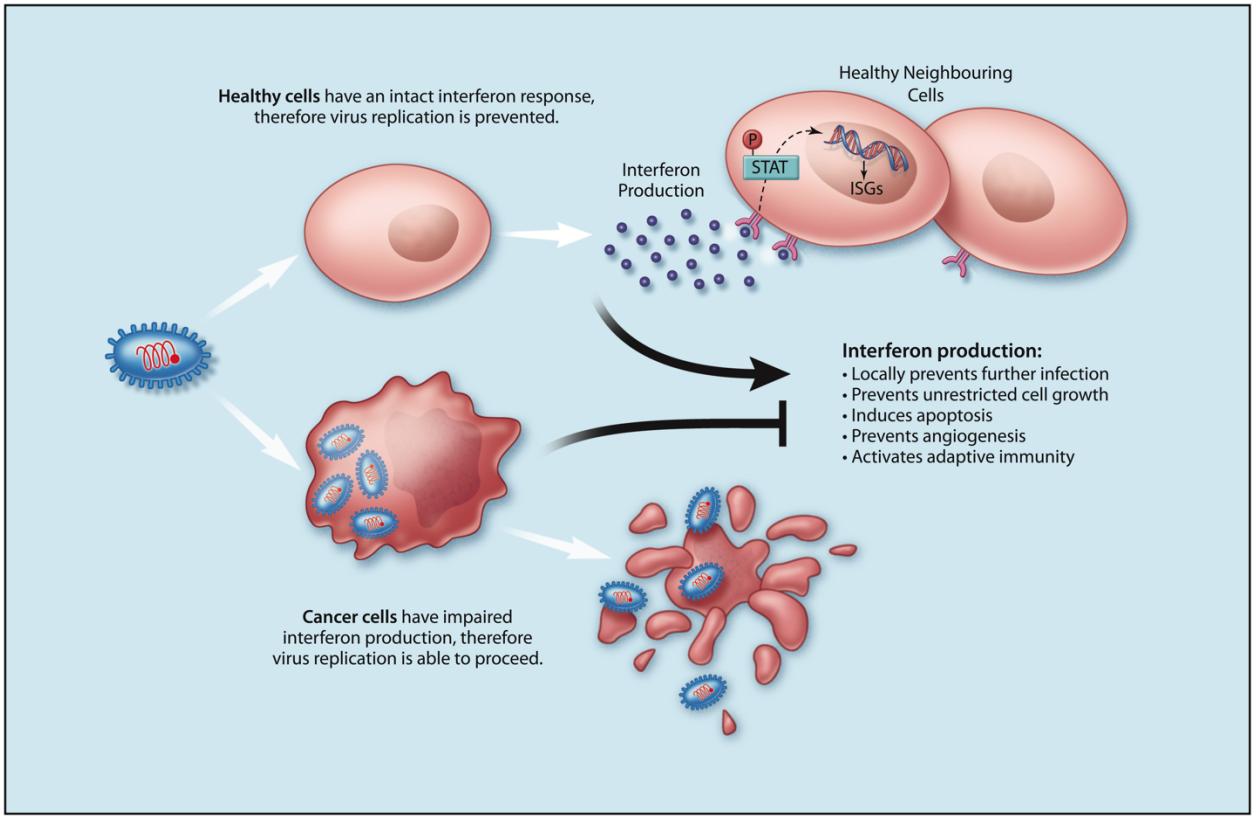

Reprinted with permission from: Keller, B. A. & Bell, J. C. *J Mol Med (Berl)* **94**, 979-991, doi:10.1007/s00109-016-1453-9 (2016).

IFN, and various forms of cellular death. The best studied of these cascades results in the cellular release of Type I IFN through a mechanism in which STING, TBK1, and IRF-3 mediate activation[24]. As summarized in Figure 1.1, the release of IFN has profound autocrine and paracrine effects on the local cellular environment that are intended to prevent the spread of infection and activate adaptive immunity. These include induction of apoptosis, the prevention of unrestricted cell growth, and the down-regulation of vascular endothelial growth factor (VEGF) – all properties which the efficient cancer cell seeks to evade[22,30]. In the physiologic milieu, the ubiquitously expressed cell surface interferon-α/ß receptor (IFNAR) complex, which is composed of two individual subunits, is typically activated in a paracrine fashion by IFN, which activates several signaling cascades and culminates in the activation of over 300 IFN-stimulated genes (ISGs)[31]. Interestingly, the majority of such ISGs do not have direct anti-viral activity, and instead encode PRRs or transcription factors, which can recognize invading virus and begin appropriate signaling to increase IFN production; this leads to significant amplification of anti-viral signaling[31]. There are, however, several protein products of ISGs with direct anti-viral activity. Such products include effectors of cytoskeletal remodeling, apoptosis, and post-transcriptional events[31].

The processes of cellular transformation and tumourigenesis are complex and they are not yet fully understood at a mechanistic level. Commonly-misregulated pathways in transformed cells, however, are involved in allowing the cancer cell to gain an evolutionary advantage, which necessitates a concession at the level of adaptive immunity, as summarized by Pikor *et al*[32]. One broad example of such misregulation is the incompatibility of physiologic anti-viral signaling with tumour development, which has been touched upon and is summarized in Figure 1.1. Specifically, IFN has been demonstrated to be protective against tumour formation and its dysfunction has been shown to increase susceptibility to cancer[33]. Key IFN signaling molecules, including various Type

I IFNs, RIG-I, STAT1, and JAK2 can be genetically or epigenetically modified in transformed cells[32,34-41]. Another commonly-misregulated pathway in many cancers, including melanoma, is the RAS-MAPK pathway. Downstream effectors have been shown to themselves be misregulated in cancers, however constitutively-upregulated wild-type or directly mutated epidermal growth factor (EGFR) have also been observed[42-45]. Consequently, the EGFR pathway has been a common therapeutic target in recent years. Misregulation of the EGFR pathway has also been directly linked to sensitivity to viral infection[46-49], which can be rationalized by its critical role in innate immunity[50-52]. Another interesting characteristic of cancer that has emerged in recent years and has profound impacts on every aspect of a cancer is the tumour microenvironment.

The tumour microenvironment is now a focus of intense study and it has emerged that many structural and molecular aspects of it impact innate immunity. Many solid tumours are known to overexpress VEGF, which has been shown to induce and sustain neovascularization – critical for tumour growth and metastasis[53-55]. Much of the previous work in the OV field has focused on this neovascularization, its relationship to efficient OV delivery, as well as the mechanisms of cell death observed in the tumour microenvironment. Interestingly, vesicular stomatitis virus (VSV) and VACV have been shown to be preferentially delivered to transformed cells upon systemic delivery, however they have also been shown to induce the recruitment of neutrophils to non-transformed cells in the tumour microenvironment[32,56-58]. It is now clear that the presence of VEGF in the tumour microenvironment sensitizes tumour endothelial cells to viral infection through a mechanism in which the transcription repressor PRD1-BF1 down-regulates the innate anti-viral response, highlighting a molecular divergence from their 'normal' counterparts[59]. Another aspect of the tumour microenvironment that has recently been shown to impact innate immunity is the presence of cancer-associated fibroblasts (CAFs). Much like how endothelial cells

created by tumour neovascularization are different from their physiologic counterparts, CAFs have diverged at the molecular level from normal fibroblasts due to a transforming growth factor-β (TGF-β)-induced reprogramming[60]. CAFs, in turn, produce increased levels of fibroblast growth factor 2 (FGF2), which reduces RIG-I expression in tumour cells, therefore antagonizing the anti-viral programming within the cell and sensitizing it to viral infection[60]. As more is discovered about the tumour microenvironment, undoubtedly more will be learned about the ability of a cancer to usurp the pathways involved in physiologic innate immunity, as these two states are incompatible. What has been established, however, are that these changes sensitize transformed and associated cells to viral infection.

1.2.2. Mechanisms of action of oncolytic virotherapy

As evidenced by the multiple cellular and structural changes that occur in the process of transformation and tumourigenesis, it is not just cancer cells themselves that are vulnerable to OV infection. Most cells in the cancer milieu likely play a role, direct or supporting, in conferring a selective growth advantage to transformed cells that results in the clinical presentation of cancer. The incompatibility of intact anti-viral signaling and tumourigenesis results in a pan-tumour vulnerability to viral infection and allows the categorization of unique mechanisms of action of OVs. At this point, the OV field recognizes three unique mechanisms of action[59-61], short summaries of which will form the basis of this section and are depicted in Figure 1.2.

1.2.2.1. Vascular collapse

A literature has been building over the past decade describing the improved efficacy of OVs in the context of concurrent therapy to block neovascularization or its associated pathways. Namely, the intratumoural administration of the oncolytic VACV JX-594 (now Pexa-Vec) into three patients with hepatitis B virus-associated hepatocellular carcinoma (HCC) resulted in the

Figure 1.2. The multiple mechanisms of action of oncolytic virotherapy. Oncolytic viruses take advantage of the unique environmental milieu associated with cancer, resulting in a multi-pronged attack with unique mechanisms of action. Namely, oncolytic viruses are able to directly infect endothelial cells associated with VEGF-induced neovascularization that occurs in many solid tumours, directly infect and lyse transformed cells, and promote the induction of anti-tumour innate and adaptive immunity. These unique mechanisms of action provide different therapeutic targets for new oncolytic viral therapeutics.

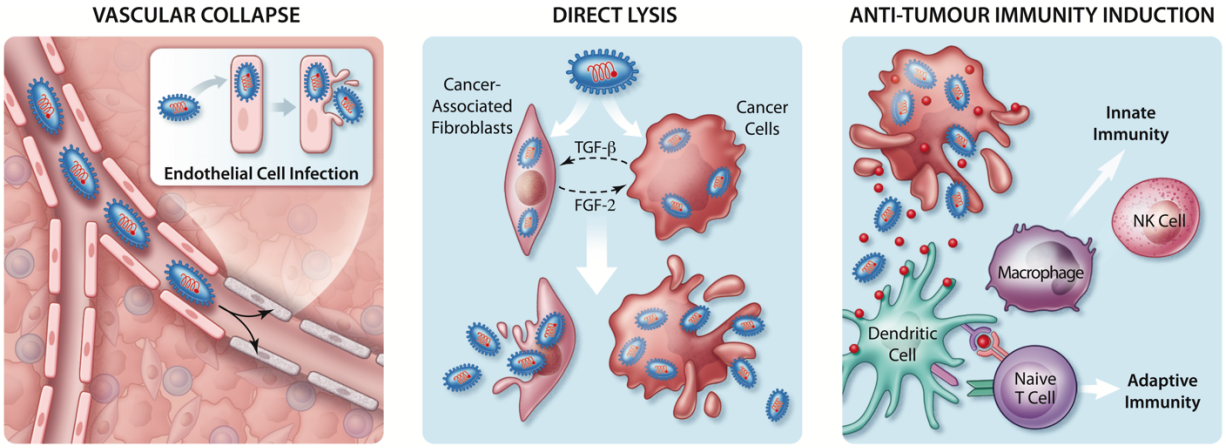

Reprinted with permission from: Keller, B. A. & Bell, J. C. *J Mol Med (Berl)* **94**, 979-991, doi:10.1007/s00109-016-1453-9 (2016).

release of cytokines with known anti-vascular activity and was associated with the shutdown of tumour vasculature[62]. Later studies made efforts to understand the mechanisms behind such therapeutic effects, which resulted in observing the sensitization of both normal respiratory epithelial cells and tumour cells to VACV internalization, replication, and cytotoxicity in an AKT-dependent fashion[63]. These authors also described an increased VACV infection of a xenograft model of human pancreatic cancer. As described above, a recent study has tied the intratumoural over-expression of VEGF to a PRD1-BF1-based mechanism in which the cellular anti-viral response is decreased[59]. Many further studies have made efforts to increase OV efficacy with concomitant anti-VEGF therapy. Unsurprisingly, several groups have therefore encoded anti-VEGF antibodies into their OV platforms of choice, most notably using VACV[64-68]. Another approach that has been used is the co-administration of OVs with the anti-VEGF antibody bevacizumab, which is clinically approved as an anti-neovascularization monotherapy and is itself used in certain cancer indications[69-71]. These experimental treatments have been used with varying successes and are at different stages of translation, however interest remains and the field will likely see this continue with future studies that can shed light into the mechanism of the apparent efficacy.

1.2.2.2. Direct cellular lysis of transformed cells

As has been established thus far, cancer cells are inherently sensitized to direct OV infection due to the anti-viral signaling compromises they make to gain an evolutionary growth advantage over their normal counterparts. Different OV platforms have viral lifecycles that are unique to them. Most central to this research project is VACV, whose viral lifecycle is such that infectious particles enter the cell, replicate exclusively in the cytoplasm and form infectious progeny, the majority of which are released upon cell lysis[72]. After undergoing multiple viral

lifecycles before causing cell death that can result in the logarithmic expansion of infectious particles, nearby transformed cells that have themselves been sensitized to viral infection are vulnerable. From the perspective of an OV, VACV has several advantages, which will be expanded on in a later section.

For over a decade at the onset of OV development, the primary focus of the field was indeed to increase replication and direct cancer cytolysis by any of several means, both biologically and chemically. As such, many studies have demonstrated the OV enhancement in many resistant cancer models. One interesting approach was the combination treatment of OVs with histone deacetylase inhibitors, which demonstrated some success in VACV, amongst other virus platforms[73]. More recently, diverse libraries of chemicals known as viral sensitizers have been screened for the ability to augment OV therapy. This is also an approach that has proven successful across diverse virus platforms and with diverse chemical libraries[74,75]. Such approaches continue to be studied as the important therapeutic utility of augmenting viral replication is clear.

1.2.2.3. Induction of anti-tumour adaptive immunity

In 2013, *Science* magazine named cancer immunotherapy the *Breakthrough of the Year*, and the clinical approach to cancer therapy has since changed dramatically[22,76]. Clinicians have added immune checkpoint inhibitors to their armamentarium, a move which has improved clinical outcomes in certain indications[2], and there is great interest in the further development of cell-based therapies. With the rise of immune checkpoint inhibition, there was a longstanding hypothesis that OVs had the potential to synergize with such therapies by breaking immune tolerance to cancer and releasing tumour-associated antigens (TAAs). Indeed, experimental evidence showing efficacy supported this, however the mechanism was not understood. Recently, Woller *et al.* demonstrated that the T cell response to several neoepitopes in an anti-PD-1-resistant CMT64 lung

adenocarcinoma model was increased following treatment with an oncolytic adenovirus, a phenomenon that was not observed with alternative inflammatory agents[77]. They also demonstrated that this increased T cell response could be cytotoxic, that the range of neoepitopes against which an increased T cell response occurred was increased with concomitant anti-PD-1 blockade in their immunocompetent model, and that this dual therapeutic approach resulted in increased efficacy compared to controls[77]. Although this was the first literature to establish a mechanism for the induction of adaptive immunity, the fact that the hypothesis existed earlier prompted several groups to begin investigating whether combined treatment of OV therapeutics with immune checkpoint inhibition would be effective. One way to do this is to encode immune checkpoint antibodies into the viral backbone itself, which was hypothesized to reduce the systemic toxicities that have been known to occur with immune checkpoint inhibitor monotherapy. This has been done using the adenovirus backbone encoding anti-CTLA-4 as well as with measles virus encoding either anti-CTLA-4 or anti-PD-L1, with varying levels of efficacy[78-80]. A more common approach, however, is to use separate therapeutic regimens to first deliver an OV of choice with the goal of breaking tumour immune tolerance[77] followed by administration of systemic immune checkpoint blockade. This approach was first utilized effectively with a Newcastle disease virus (NDV) platform in combination with systemic administration of CTLA-4 blockade in a B16 melanoma model, which allowed the authors to observe a distant therapeutic effect despite only local viral replication following intratumoural delivery[81]. Recently, this approach has been expanded upon by encoding the ligand for inducible T cell co-stimulator (ICOS) into NDV followed by the systemic administration of anti-CTLA-4, which resulted in enhanced intratumoural infiltration of activated T-cells and bilateral anti-tumour efficacy[82]. Other notable examples of combining OV therapy with systemic immune checkpoint blockade include VACV,

VSV, and Reovirus[83-87]. One exciting recent clinical development has been the publication of results from the first clinical trial of T-Vec in combination with immune checkpoint blockade. The findings were that intratumoural T-Vec administration in combination with systemic anti-CTLA-4 blockade demonstrated a tolerable safety profile and the combination therapy was more effective than either monotherapy[88]. More trials are currently in the clinic, and this continues to be an area of active investigation for which the field is sure to see the results from future studies.

1.2.3. High-throughput screening approaches

Throughout the past decade of research in the biological sciences, technological advances have allowed genome sequencing to progress to a point that overwhelming accumulation of genetic data is building without full functional validation. Similar rapid advances have occurred in the ability to manipulate genomes more rapidly and efficiently than previously possible, leading to new model systems of cancer. These insights, coupled with the biological therapeutic advances discussed above, have led to an understanding that therapeutics often have the greatest effects in similarly-activated subtypes of cancer. As such, large libraries of potentially novel therapeutics have emerged, sometimes numbering in the millions of compounds, which must be efficiently screened for function. Approaches to handling large numbers of experimental variables have therefore resulted in the development of new experimental methods, equipment, and data analysis techniques that are tailored to individual needs. The careful execution of such experiments can provide insights into complex biologic interactions.

Inherent OV shortcomings and interest in combination therapy (both expanded on below), with the added complexity of viral genetic diversity resulting in incompletely understood pathogen-host interactions, has prompted several groups to use high-throughput approaches in OV development. Two methodological reports have emerged in which transgene-expressing viruses

were able to be quantified based on their relative expression of fluorescence or bioluminescence, respectively, which makes the rapid study of viral replication possible[89,90]. High-throughput chemical library screens have been performed on various viral platforms, including HSV-1[91] and a variant of VSV[92]. These studies led to the identification of replication- or oncolysis-augmenting small molecule compounds, respectively, and a better mechanistic understanding of the two viral platforms. Taking a different approach, several more recent studies have used various RNA silencing approaches to specifically knock-down host genome targets and identify factors that were observed to impact viral parameters in VACV, HSV, and VSV[93-95]. Regardless of experimental objectives, the approach of high-throughput assays is always similar – primary screens are executed to find hits above a selected statistical threshold, secondary screens validate interesting hits, and finally independent assays are performed to ascertain biological significance; thus far in the field of OVs, such approaches have been rare[96].

1.2.4. Desirable phenotypic properties of an oncolytic virus

As the OV field has matured and as distinct mechanisms of action have been recognized, several inherent viral properties of effective OVs have been established. The above discussion makes clear that there are inherent properties that should be possessed by the optimal OV backbone. Namely, the optimal OV will replicate preferentially in cancer cells and cause subsequent oncolysis, it will be able to productively infect and lyse pathologic cells of the tumour microenvironment, and it will break immune tolerance to cancer while limiting anti-viral immunity[61,96]. Some studies suggest that viruses with increased ability to spread systemically can better evade immune destruction, especially with VACV or viruses which have been made to express certain VACV proteins[97,98]. Finally, some studies have suggested that OVs with high

intratumoural persistence will be better vectors for the delivery of therapeutic transgenes and/or pro-drugs[96].

1.3. Vaccinia virus

Vaccinia virus is a large, enveloped, dsDNA virus that replicates entirely within the cytoplasm of vertebrate and invertebrate cells[99]. It is able to form two distinct types of infectious particles: mature virions (MVs) and enveloped virions (EVs). As will be expanded upon later, MVs are the basic infectious unit of VACV, represent the majority of infectious particles, and are released upon cell lysis following cytoplasmic accumulation; EVs are essentially MVs with an additional fragile membrane wrapping, are specialized for more distant spread within the host, and have the ability to subsequently infect distant cells[99]. VACV holds important distinction as the vaccine used in the eradication of smallpox, or variola, from the human population. It is the most well-studied member of the *orthopoxvirus* genus, and is classified as a member of the family *Poxviridae*. As such, VACV has served as a prototypic model system in the broader field of virology. As the major focus of this research project is on the development and characterization of a tool utilizing previously-developed technology to manipulate the VACV genome, the current section will present a comprehensive review of the VACV literature.

1.3.1. Historical considerations

The most famous member of the Poxviridae family, variola virus, is responsible for hundreds of millions of deaths throughout human history. Early attempts at inoculating patients with material from lesions of convalescent smallpox patients had mixed results[100]. In 1798, work was published by Edward Jenner in which he described the infectious agent that was known to cause lesions on cows and their caretakers as being used to prevent smallpox; this is considered to be the first successful example of intentional vaccination. The exact origins of VACV are

unknown, however it is thought to be derived from evolution in laboratories and appears to have a shared ancestor with cowpox virus and variola virus. Throughout the duration of the smallpox eradication campaign by the World Health Organization (WHO), several vaccine strains emerged, all with unique genomic and phenotypic features[99,100]. At one time, VACV was believed to have no known natural hosts outside of humans, however several reports of bovine outbreaks in Brazil since the end of the smallpox eradication campaign have proven otherwise[101]. Reports such as these have generated questions as to the natural reservoir of VACV and raised the possibility that rodents and/or marsupials could serve as such. Interestingly, a recent report from Brazil demonstrated the serological prevalence of VACV in house cats[102]. As a consequence of the use of VACV in various aspects of public health, much has been learned about its biology.

Vaccinia virus was the first animal virus to be extensively worked with in a laboratory setting – it was the first to be purified, observed microscopically, expanded in tissue culture, to have its infectious particles accurately quantified, and to be chemically analyzed[99]. In 1961, Reich *et al.* were the first to resolve cellular RNA synthetic activity from that in purified VACV, postulating that the two processes were enzymatically or topographically distinct from one another[103]. This study led to a revision of the longstanding view that viruses were mere packets of genetic material, led to later key discoveries in RNA viruses, and to structural findings regarding viral and eukaryotic messenger RNA (mRNA)[99]. Since this time, VACV has become an important model in understanding the lifecycle of orthopoxviruses, of providing lessons in virus-host interactions as relevant replication, host-range, and immunomodulatory protein functions are uncovered, and it has been developed into a useful tool as an expression vector[99]. For many reasons, gaining a greater understanding of VACV, especially in terms of novel virus-host interactions, continues to be an area of active research.

1.3.2. Structural and genetic considerations

As will be expanded on in the following section, VACV is a large and complex virus whose ability to efficiently infect and replicate is directly tied to many aspects of its structure. Morphologically, therefore, the VACV virion is large compared to other well-studied animal viruses. Many studies utilizing scanning electron microscopy and/or cryo-electron tomography have captured images and modeled both MV and EV – a single MV particle is a barrel shape that is approximately 360 x 270 x 250 nm[99,104]. Internally, VACV consists of a dumbbell-shaped core with opposing lateral bodies between the core membrane and the dumbbell concavities[99]. The MV membrane consists of a single, continuous lipid bilayer that is tightly-associated with the developing virion as it matures[105]. As is expanded on in a later section, MVs can gain an additional wrapping from the trans-Golgi network or endosomes, which changes the morphology and size of the virion in question.

The genome of VACV virus is approximately 200kb, however the specific size can vary by strain. The genome is a linear, double-stranded DNA genome with inverted terminal repeats (ITRs) at its extremities that are joined together by hairpin loops that link the two strands together into a single uninterrupted polynucleotide chain[106]. The hairpin loops are highly conserved regions within the ITRs of the genome containing sequences of identical, but oppositely-oriented nucleotides that are critical structural components involved in the resolution of replication intermediate DNA concatemers[107]. An interesting body of work has established that highly conserved VACV genes tend to have important functions in successful viral replication, and tend to be located in the middle portion of the genome; less conserved genes, conversely, tend to be located towards the extremities of the genome and are often involved in host-range, virulence, or immunomodulation. Furthermore, VACV genes tend to be non-overlapping[99].

The convention for VACV's system of nomenclature arose before the publication of the first full genome[108,109]. When the first full genome sequence of the Copenhagen strain of VACV was published in 1990, nomenclature followed the previously-established convention[110]. This genome sequence was determined by sequencing plasmid-cloned fragments of VACV DNA that had been digested by commonly-used restriction enzymes, however naming convention was established from the results of *Hind*III digestion. In the Copenhagen genome, there are 15 *Hind*III digest sites, resulting in 16 fragments that are named according to decreasing size, with fragment A of approximately 50,000 bp down to fragment P of approximately 300 bp, which does not contain any open reading frames (ORFs). Within each fragment, ORFs were enumerated following previously-established convention, in which each ORF was numbered from left-to-right in sequence[111]. The one exception to this rule is *Hind*III fragment C, the leftmost fragment that is poorly conserved at its terminus, in which ORFs are enumerated right-to-left in an effort to establish consistency across strains within the literature. Finally, ORFs are labeled as R (for right) or L (for left) according to their direction of transcription. This naming convention is such that VACV gene *A47L* is located in the *Hind*III digest fragment A, it is the 47th ORF within fragment A, and it is transcribed in the leftward direction. This convention has persisted in the literature; however, it is interesting to note that the majority of studies establishing novel VACV gene functions have actually been done using the Western Reserve strain. Western Reserve, therefore, has its own genetic nomenclature that differs from that established for Copenhagen, however all published studies of consequence in the VACV field use the Copenhagen convention, which is also used throughout this research project.

1.3.3. Vaccinia virus lifecycle

The lifecycle of VACV is complex. Its distinct components are separated both spatially and temporally, and its output is the highly-amplified production of infectious progeny that can exist in one of three forms. As the focus of this research project is on developing a better basic understanding of VACV biology, a comprehensive overview of the lifecycle is presented in the current section. Furthermore, a schematic of the VACV lifecycle is presented in Figure 1.3.

1.3.3.1. Attachment and entry

Viral entry is defined as the moment at which the nucleoprotein core of the virion passes into the cytoplasm[112]. The understanding of properties that govern this process for VACV has been complicated by the fact that a relatively large number of proteins are involved in the processes, and also by the fact that there are two distinguishable infectious particles: MVs and EVs[99,112-114]. Electron microscopy studies have demonstrated that VACV is unique in its ability to accomplish this feat in one of two ways: either by direct fusion to the outer leaflet of a cell membrane, or by fusion to the inner leaflet of an endosomal membrane following macropinocytosis[114]. The reason for a certain strain using primarily one mechanism over another is unclear, however it appears VACV strains that have adapted for laboratory growth tend to favour direct fusion, whereas those more recently isolated from nature tend to utilize endosomal acidification, perhaps as a mechanism for penetrating the dense cellular cortex of most cells[112,115-118]. Studies using inhibitors of various cellular processes have supported a two-step entry that includes hemi-fusion and fusion/entry. Inhibitors of tyrosine protein kinases, dynamin GTPase, and actin dynamics all impair membrane fusion, while partial cholesterol depletion and inhibitors of endosomal acidification and/or membrane blebbing all impair viral core entry[119].

Figure 1.3. Vaccinia virus lifecycle. The lifecycle of vaccinia virus occurs entirely within the host cell cytoplasm and utilizes the formation of so called Virus Factories, or *virosomes*, in which the entirety of intermediate and late gene expression occurs. Prior to this, cellular attachment and entry occur, which precede the rapid expression of early genes and immune defense molecules. Mature infectious progeny is produced in one of two forms: mature virions (also known as intracellular mature virions, IMV), and extracellular virions, the formation of which is preceded by trans-Golgi processing. Following penetration of the cellular cortical actin, extracellular virions can remain attached to external cellular membrane (cell-associated virions, CEV), or can be released via an actin tail-dependent mechanism (extracellular enveloped virions, EEV). IV = immature virion, MV = mature virion, WV = wrapped virion.

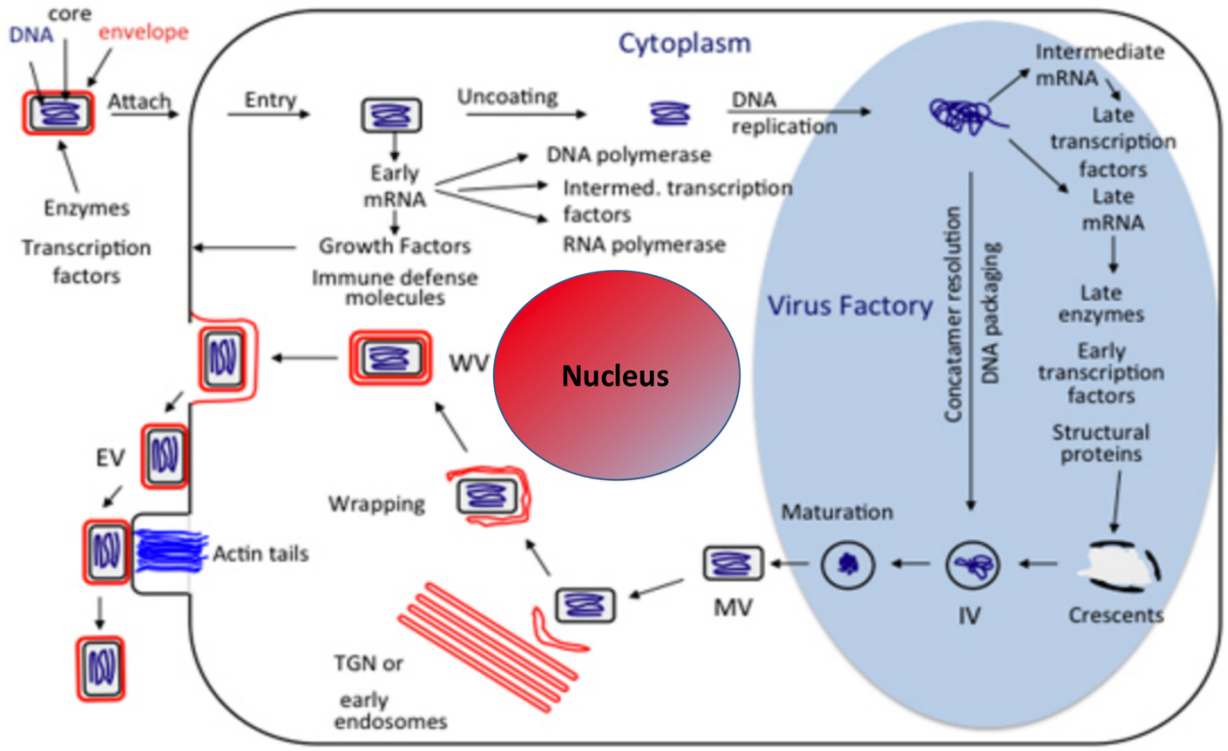

Adapted from: Moss, B. in Fields virology Vol. 2 (eds David M. Knipe & Peter M. Howley) 2129-2159 (Wolters Kluwer/Lippincott Williams & Wilkins Health, 2013).

Before beginning the entry process, in the case of EV, the outer membrane must first undergo a non-fusogenic dissolution. This process involves the EV-specific viral glycoproteins A34 and B5, and effectively reveals a MV particle upon completion[120]. It occurs via differential mechanisms depending on whether it is upon EV-cell membrane apposition, in which case the outer EV membrane is dissolved by exposure of an active region on the proximal stalk of viral B5 to cellular glycosaminoglycans[121], or via an unknown pH-dependent mechanism following endosomal internalization[114]. Once apposition occurs between the MV membrane and the cell or endosomal membrane, lipid mixing of the respective membrane leaflets leads to an intermediate state in a process that has come to be known as hemi-fusion. Attachment occurs via protein-protein interactions between four attachment proteins in the MV membrane. These four attachment proteins include D8, which can bind chondroitin sulfate[122,123], A27 and H3, which are known to bind heparan sulfate[124,125], and A26, which can bind cell membrane-associated laminin[113,126]. The entry fusion complex (EFC) is composed of at least 11 additional viral proteins, 10 of which are thought to be essential for viral replication. Although the exact protein configuration of the EFC is unknown, studies have determined various interactions between them as well as whether specific proteins compose the core or are located on the periphery of the EFC, as is the case with F9 and L1[112]. Whether following direct internalization or macropinocytosis (and non-fusogenic membrane dissolution, in the case of EV), EFC activation is triggered by the acidic environment of the late endosome. This causes dissociation of the viral fusion suppressor protein A26, which in turn triggers fusion and the release of the viral nucleoprotein core into the cytoplasm. Upon successful release of the viral core into the cell cytoplasm, early gene expression begins almost immediately[112-114].

1.3.3.2. Uncoating and message transcription

The entire VACV lifecycle has evolved for optimal efficiency in the production of progeny, a characteristic that can be appreciated almost immediately following entry. Upon entry, VACV virions are transported on microtubules to sites of transcription, and mRNA synthesis can be detected within 20 minutes of entry[99]. VACV controls the timing of the expression of individual proteins, a critical component of the complex replication cycle, at the level of transcription initiation[127]. Within the deposited core is packaged the late gene products of a virion's infectious precursor, which provides the virion with a complete early transcription system. This includes an eight-unit DNA-dependent RNA polymerase that has homology to eukaryotic and archaeal RNA polymerases, RNA polymerase-associated protein of 94 kDa (RAP94), early transcription factor, capping and methylating enzymes, poly(A) polymerase, nucleotide phosphohydrolase I, and topoisomerase[99,127-129]. Therefore, early mRNA production can begin almost immediately, and it is set up in such a way that early gene products encode enzymes and regulatory factors for intermediate gene products, which do the same for late gene products, which are components of a transcription system and will be packaged into progeny, so the cycle can begin anew[99]. In addition to enzymes and factors that influence later gene expression, early mRNAs tend to be translated into host immune defense molecules, growth factors, and DNA replication molecules. Of the approximately 200 ORFs in most VACV strains, high-throughput deep RNA sequencing (RNA-seq) studies have identified the presence of 118 ORFs before the detection of viral DNA, thus their classification as early genes[130]. Like those of eukaryotes, early VACV gene transcripts are capped to enhance their stability and to promote mRNA-ribosome interactions[131]. Early gene expression has been shown to be disrupted upon viral uncoating, which occurs following core wall breaches induced by a putative uncoating protein[99,132,133]. The presence of early steady-state mRNA then

rapidly declines due in part to the enhanced presence of early gene products and decapping enzymes D9 and D10[99].

Intermediate and late gene expression share several common characteristics that allow them to be grouped together, but remain clearly distinct from early gene expression. Most notably, a 30-50 residue long "poly(A) tail" is added to their mRNA 3' ends due to RNA polymerase slippage[134,135], their transcripts are extremely heterogenous at their 3' ends[136], and the factors that control both processes appear to be the same viruses-coded factors in each case[131]. Resolving these two sets of genes from one another was not possible until Yang *et al.* performed RNA-seq on synchronously-infected HeLa S3 cells with a virus lacking the late transcription factor G8[137]. The results of this study revealed 53 primarily intermediate genes, 38 late genes, and led to completion of the first transcriptional map of VACV[99,130,137]. Despite the similarities in the regulation of these gene sets, differences exist. Transcription of intermediate genes requires at least five known transcription factors that incorporate eight distinct early gene products, accounting for the formation of heterodimeric transcription factors[131]. Similarly, late gene transcription is initiated by a group of viral gene products that have come to be known as Vaccinia Late Transcription Factors (VLTF) and the group includes VLTF1, VLTF2, VLTF3, and VLTF4. These proteins are formed by the monomeric products of the intermediate genes *G8R*, *A1L*, *A2L*, and the early gene *H5R*, respectively[131,138]. As is evidenced by this brief overview, the viral factors regulating VACV gene expression are numerous and the list continues to grow as more are described, which should reveal further mechanistic insights into the process.

1.3.3.3. DNA replication

Poxviruses are unique in their ability to conduct DNA replication entirely in the cytoplasm of their host cell. Live cell imaging and microscopy studies have demonstrated that they do so by

setting up compartmentalized areas of replication activity termed *virosomes* or Virus Factories, which can initiate from an individual virion and eventually merge with other factories[139,140]. The mechanisms underlying VACV DNA replication are not completely understood and it remains an area of active investigation. It is only within the past decade that the field has begun to accept a relatively conventional model of RNA priming and semi-discontinuous DNA synthesis at replication forks[99]. Until important observations that VACV encodes a DNA primase[141] along with several other factors of DNA replication machinery (DNA polymerase E9, the helicase D5)[142,143], and that VACV can usurp cellular DNA ligase[144], certain structural and associated functional components of the VACV genome pointed to a self-priming model of DNA replication[99,106,145]. A recent report used directional deep sequencing of short single-stranded DNA fragments isolated from the cytoplasm of VACV-infected cells and prominent initiation points were mapped to a terminal hairpin loop as well as to the concatemeric junction of replication intermediates[146]; this work points to a DNA replication model in which leading and lagging strand synthesis is used. The current belief in the field is that the two models of DNA replication are not mutually exclusive and that it is possible these viruses use both. Regardless of the process(es) used, however, one step that is clear in VACV DNA replication is the production of DNA concatemers[145,147].

Concatemer resolution into unit-length molecules is a necessary step in the successful replication of VACV DNA[145,147]. Mature VACV genomes exists as a linear double-stranded DNA with covalently closed hairpin termini, and thus the genome is present as a continuous polynucleotide chain. As expected, therefore, replication intermediates exist as transient head-to-head or tail-to-tail concatemers, which must be appropriately resolved. It has been observed that plasmids with palindromic junction fragments that have been transfected into VACV-infected cells are resolved into linear *mini-chromosomes* with VACV DNA hairpins at either end[148]. In early

studies, it was established that the concatemeric junction can form a structure resembling a Holliday junction (HJ), which suggested the likelihood of a virally-encoded HJ resolvase[99]. Later bioinformatics studies identified *A22R* as a highly-conserved gene across poxviruses that is homologous to Escherichia coli (E. coli)'s HJ resolvase RuvC[149]. The HJ resolvase activity of A22 was established, and a subsequent study reported an A22-null mutant as lacking the ability to resolve DNA concatemers into unit-length genomes[150]. Another important component of the concatemeric resolution is the presence of a virally-encoded DNA topoisomerase, a protein which can help to relieve the supercoils that are a structural characteristic of the VACV concatemeric junction. In VACV, the *H6R* gene was shown to produce a product that could serve this role. Interestingly, an H6-null mutant produced a small plaque phenotype and demonstrated a significant decrease in the production of infectious progeny[151]. Once concatemeric resolution into unit-length genomes has occurred, subsequent packaging will allow for infectious progeny to be produced.

1.3.3.4. Virion assembly

The process of VACV virion assembly is not completely understood. The main components are clear, however, in that the immature virion (IV) is first structurally distinct as a crescent or circular particle, followed by transformation to a MV with an accompanied change in morphology to an oval or brick-shaped particle, which must occur alongside a release from the viral factory at some point in the process[99]. The limitation of the study of such particles is that the field has based their understanding almost entirely on EM images, however these have not been inconclusive. As a result, it is unclear whether crescents or IVs are single-membrane bound, double-membrane bound, or whether they associate with certain cellular organelles for their membrane. Other images that seem to show IVs open to the cytoplasm and not associated with

cellular organelles have resulted in the hypothesis that *de novo* production of IV membrane occurs, however this goes against the current belief that stable membranes must form from pre-existing membranes[99]. Whatever the exact sequence of events, several viral proteins have been implicated in virion assembly and it remains an area of active investigation[99,152,153].

The packaging of unit-length viral genomes and early transcriptional machinery are amongst the most critical components of virion assembly. Following concatemeric resolution, unit-length genomes await assembly in a state referred to as the nucleoid, which must occur in order for viral morphogenesis to continue[150]. One interesting study demonstrated that the packaging of individual nucleoids into IVs was found to occur independently of transcriptional machinery and several other enzymes in an A32-dependent manner, and that *A32L* mutants produced IVs lacking genomes and the ability to complete morphogenesis[154]. The packaging of the transcription machinery is incompletely understood, however certain components and protein-level interactions have been elucidated. One such interaction involves the previously-mentioned RAP94 – it is a critical linker between the multi-subunit RNA polymerase and vaccinia early transcription factor (VETF) – and is needed for the packaging of infectious progeny[155]. Before being released into the cytoplasm as a MV, a final IV-processing step is necessary – proteolysis. The IV still present in the virosome contains a D13 scaffold and several core precursor proteins that must be cleaved by I7 into their mature forms[153]. Once cleaved, the particle can begin its IV-MV transition, which includes the condensation of the viral core into its biconcave shape, the formation of lateral bodies, and the presence of mature proteins embedded in the MV membrane. Once the MV is released into the cytoplasm, processing can occur in one of several distinct ways, which will give the infectious particle distinct characteristics.

1.3.3.5. Wrapping and trafficking

Intracellular mature virions are the most abundant type of virus particle produced by VACV, accounting for approximately 90% of infectious progeny in a given productive cell[156]. In its core are packaged over 80 viral proteins that will be used in early stages of subsequent lifecycles. MV membrane proteins include those that are necessary for cellular entry, however others can be used to facilitate additional membrane wrapping, forming the second type of VACV infectious particle, EV. Enveloped virions are MVs that have been wrapped by additional membranes from the trans-Golgi network or endosomes[153,157,158]. In order for MVs to get to these wrapping sites, microtubule movement is exploited using an unknown mechanism. Although studies have aimed to answer this question, thus far only proteins involved in trafficking of newly-wrapped EVs to the cell periphery have been identified[159,160]. One such example is the viral protein A36, which has been shown to bind the microtubule motor protein kinesin to transport to the cell periphery, a process that may be regulated by the VACV protein A33[160]. EVs are known to incorporate at least nine VACV-derived proteins, some of which – including A27, B5, and F13 – are known to be essential to the formation of EVs. Others, including A36 and F12, are associated exclusively with the outermost membrane and are not retained by the EV but are utilized for EV trafficking[161-166]. Many of these viral proteins that are known to be closely associated with wrapping itself or the EV membrane, when mutated, are known to produce a small-plaque phenotype[99]. Many are known to interact with and modulate cytoskeletal-associated proteins at various levels, which can be explained by the EV's need to subvert the host's actin and microtubule cytoskeletal systems for efficient egress. A more detailed discussion of VACV subversion of the host's cytoskeleton will form the section that follows.

1.3.4. Vaccinia virus cytoskeletal subversion

Viruses infecting almost all organisms employ host cytoskeletal subversion as a common strategy to thrive throughout their lifecycles. Since it has been so thoroughly studied compared to many other viruses, VACV is considered to be one of the most striking examples of this. Upon VACV infection *in vitro*, simple observation of infected cells allows one to see profound changes in their morphology – they round, lose plate and cell-to-cell adhesion, and their motility is increased – all as a direct result of cytoskeletal modulation[99]. Currently, VACV's ability to interact with and modulate the host cytoskeletal framework is one of the most active areas of research in the poxvirus field, and observations that have been published over the past decade have largely formed our understanding of this[72]. This section will provide an overview discussion of what is known about virus-host interactions from the perspective of cytoskeletal modulation, and describe how VACV uses this machinery for efficient intracellular transport and egress.

1.3.4.1. Microtubule-based transport

Vaccinia virus, like most viruses, uses microtubule-based transport to move around its hosts. In the case of a large virus like VACV, the ability to hijack a cell's microtubule transport system is critical to its ability to replicate, as diffusion for a cargo of the size of a VACV virion is not possible[72,167]. Microscope-based studies examining the movement of fluorescently labeled virus particles were the first to provide clues that VACV is able to use the microtubule system of its host cell as calculations suggest that VACV MVs and EVs would have a rate of diffusion that is unable to match the observed rates of trafficking within a host cell[168]. Specifically, MV particles have been observed traveling at a rate of 3 μm/second, however based on their estimated rate of intracellular transport by diffusion, they would only be able to travel at approximately 2 μm/hour[159,168]. Therefore, microtubule-based intracellular transport of VACV MVs occurs at a rate

of approximately 5,400x what would be expected by diffusion. Conversely, several studies have directly imaged EV moving along microtubules towards the cell periphery, and it has been established that this is dependent on kinesin-1 as the microtubule-associated motor that drives this movement[72,162,169-175]. Importantly, this set of studies established the VACV-encoded proteins F12, F13, A36, and B5 as being directly implicated in intracellular EV movement, and also established microtubule-based transport as preceding actin-based transport in VACV egress.

The VACV-encoded protein A36 has been the subject of intense study because of its ability to directly interact with the light chain of kinesin-1, a protein that is part of the microtubule-associated motor complex[160,165,166,171]. As has been reviewed by Leite and Way[72], deletion of *A36R* results in a virus that is still able to produce EV[163], however these EV have diminished ability to move from the site of assembly to the cell periphery[173,175,176], and consequently have a diminished ability to successfully engage in cell-to-cell spread. Several more recent studies have established two active domains within A36 that are each responsible for direct binding to the light chain of kinesin-1. Interestingly, it has also been reported that cells infected by a Δ*A36R* VACV overexpressing the most consequential of the A36 binding motifs, WD, allowed for the viral-induced formation of actin tails, which are needed for release and efficient cell-to-cell spread[163]. Most recently, three more active motifs in the C-terminus of A36 have been described, which provide a mechanistic linkage for the induction of actin tails in EV egress, and is the first report of such a protein being able to interact with endocytic machinery[166]. In much of the literature that has expanded on the function of VACV A36, F12 has been shown to play a supporting role. Like A36, F12 is a membrane-associated protein that is only found on the outer membrane of intracellular EV, but not on extracellular EV or MV. VACV F12 is able to interact with A36, and a recombinant VACV lacking amino acids 351-458 was demonstrated to have a small plaque phenotype, a defect

in viral release, and an inability to associate with the infected cell membrane, suggesting a critical role during viral egress[161]. Subsequent imaging studies revealed that F12 functions as part of a complex with the VACV protein E2 that is involved in EV microtubule transport, but not actin nucleation, and that this complex can interact directly with kinesin-1 light chain during microtubule transport[162-164]. As mentioned, microtubule-associated transport of VACV during viral egress is one of the most active areas of the field. Although it has progressed a great deal in the past decade, the understanding of it compared to actin-based motility is lagging.

1.3.4.2. Cortical actin penetration

Once an EV reaches the cellular periphery and the cellular cortical actin, fusion with the plasma membrane and therefore a change in classification to either cell-associated EV (CEV) or extracellular EV (EEV) cannot occur until the dense cortical actin is penetrated. The cortical actin in eukaryotic cells is known to provide the cell with increased resistance to mechanical stress and also is involved in motility-related cellular processes. From the virus' perspective, however, this dense cortex represents a significant barrier to both entry and egress. To this end, VACV has adapted a mechanism that has been elegantly described. The VACV-encoded F11 protein was originally identified as a protein that is responsible for VACV-induced cell migration of infected cells[177]. Valderrama *et al.* were the first to demonstrate that F11 was involved in the migration of infected cells via Ras homolog gene family member A (RhoA) signaling, and another group later reported that F11 was essential for migration, but not contractility of infected cells[178]. More recently, F11 has been extensively studied in its context as a promoter of VACV EV release – it is able to increase the dynamics of both microtubules and also cortical actin through a mechanism involving mDia-induced actin polymerization[179,180]. The mechanism by which F11 downregulates RhoA signaling has been further established – in data that describes the inclusion of an

unprecedented (in viruses) PDZ domain within the central region of F11, it inhibits RhoA signaling by functioning as a scaffolding protein by binding Myosin-9A, a Rho GTPase-activating protein[181]. Interestingly, several of the studies reporting these findings have demonstrated a small plaque phenotype produced by the F11-null virus, which is similar to the F12-, F13-, A36-, and E2-null mutants mentioned above. Finally, F11's role in viral spread, both *in vitro* and *in vivo*, was further demonstrated when cloned into myxoma virus, a poxvirus that lacks a homologue to VACV's F11 and thus is unable to produce progeny with the ability to efficiently penetrate cortical actin[97,182].

1.3.4.3. Release of enveloped virions

The EV form of VACV can be processed in one of two ways after wrapping, transport to the cellular periphery, and penetration of the actin cortex. Upon reaching the inner cellular membrane, fusion of the EV occurs via an unknown mechanism, at which point its outer membrane is shed and it becomes part of the cell membrane. At this point, the virion is termed a CEV as it remains attached to the outer surface of the cell membrane[99]. The majority of EV remains attached to the cell surface, however the presence of CEV has also been demonstrated to induce actin polymerization and actin tail formation, a phenomenon which can propel CEV from the cell surface to become EEV[72,99,172,174,175]. Several proteins have been demonstrated to affect the release of EEV, most notably B5, A33, A34, and A36[183]. In a large body of literature, the mechanistic role of A36 in actin polymerization and EEV release has been well established – A36 is phosphorylated by Src and Abl family kinases, which induces a well-described signaling cascade involving the Rho GTPases Cdc42 and FHOD1 and culminates in the polymerization of actin, the formation of actin tails, and the release of EEV[72]. One way to easily distinguish between EEV and other forms of infectious VACV in tissue culture models is to perform satellite release assays (aka *comet*

assays) in which a known concentration of virus is used to infect cells which are covered with a liquid overlay – when infectious progeny are EEV, satellite plaques can be formed that are distant from the original plaque, forming a distinct *comet* pattern in a cell monolayer. This phenomenon was poorly understood in that it appeared the formation and position of satellite plaques occurred at rates that were incompatible with the replication kinetics of VACV until it was shown that newly-infected cells are able to repel would-be superinfecting virions. Interestingly, this is mediated by the cell surface expression of the VACV proteins A33 and A36, which mark the cells as infected[184]. Therefore, instead of internalizing superinfecting EEV, infected cells induce polymerization of actin tails and thus active repulsion across the cell surface until an uninfected neighbouring cell is located[72,184]. The ability of VACV to usurp cellular cytoskeletal machinery has been optimally-adapted for viral propagation, and as such many mechanisms that VACV uses to this end have been uncovered. Regardless, gaining a further understanding of cytoskeletal dynamics in the context of VACV infection remains an active area of investigation and future insights into novel VACV factors and established mechanisms will likely shape current opinions.

1.3.5. Oncolytic vaccinia virus

Multiple VACV platforms have been investigated for their oncolytic potential. Indeed, this field has advanced significantly as numerous clinical trials have been completed or are underway to determine the potential of VACV as an OV. The currently-active clinical studies investigating the utility of VACV-based OVs are outlined in Table 1.1. Thus far, mixed clinical benefits have been observed, however ongoing clinical trials and intense pre-clinical investigations from groups around the world will surely lead to future attempts at translation of the VACV platform into an effective OV. This section will summarize current pre-clinical and clinical knowledge from the perspective of VACV as an OV.

Table 1.1. Ongoing vaccinia virus-based oncolytic virus clinical studies. As of May 2017, there were four vaccinia virus oncolytic platforms being investigated in clinical studies worldwide. GM-CSF = granulocyte macrophage colony-stimulating factor, TK = thymidine kinase, TRIF = TIR-domain-containing adapter-inducing interferon-β, HPGD = 15-hydroxyprostaglandin dehydrogenase, **β**-gal = beta-galactosidase, **β**-gluc = beta-glucouronidase, FCU-1 = suicide gene.

Company	Trade Name	Backbone	Attenuating Mutations	Transgenes	Targeting Characteristics	Current Clinical Status
Sillajen	PexaVec (formerly JX-594)	Wyeth	TK, B18R	GM-CSF	Highly metabolic	- Three Phase I/II studies - One Phase III study
Western Oncolytics & Pfizer	WO-12	Western Reserve	Truncated TK, Deleted VGF	TRIF, HPGD	Highly metabolic	- Planning Phase I
Genelux	GL-ONC1 (GLV-1h68)	Lister	TK, F14.5, A56R	Renilla luciferase, **β**-gal, **β**-gluc	Highly metabolic	- Two Phase I studies
TransGene	TG6002	Copenhagen	TK, Ribonucleotide reductase	FCU-1	Highly metabolic	- Planning Phase I

Many groups have made efforts to design an optimal OV on the VACV backbone. Thus far, this has been attempted with several vaccine strains of VACV, however the Wyeth (Pexa-Vec) and Lister strains of VACV have progressed the furthest clinically[22]. The rationale for each of the respective groups selecting their parental strain of choice is not clear, however the overarching strategies employed by most groups have been similar and have included efforts to (1) increase the selectivity of their viruses to transformed cells, and (2) increase the potential to establish anti-tumour immunity upon infection. Cancer selectivity has primarily been accomplished by deleting the VACV-encoded thymidine kinase (TK; *J2R*), which results in a virus that is more selective to metabolically-active cells, a common characteristic of transformed cells. Deletion of *TK* was experimentally shown to produce an attenuated virus infection in mice being vaccinated with VACV vectors expressing various foreign antigens[185]. Of VACV backbones that have advanced clinically as OVs, this strategy has been utilized in the Wyeth, Lister, and Western Reserve products[186-188]. Each of these OV candidates has also utilized additional strategies to increase selectivity. Pexa-Vec additionally contains a natural *B18R* truncation, which renders the clinical candidate more susceptible to intact anti-viral effects of the healthy cell environment[22]. In addition to a *TK* deletion, the Lister-based candidate GL-ONC1 has expression cassettes inserted into the *F14.5L* and *A56R* genes, respectively[189]. Interestingly, this virus has demonstrated the ability to preferentially induce apoptosis and cytotoxicity in mutant *BRAF* melanoma, both *in vitro* and *in vivo*[190]. Similarly, the Western Reserve-based OV also harbors a deletion of Vaccinia Growth Factor (VGF, *C11R*) and has demonstrated attenuation *in vitro* and increased safety *in vivo*[191]. Each of these viruses have progressed clinically at different rates and will be discussed below. Another strategy that has been utilized in the production of clinical candidate OVs is the encoding of therapeutic transgenes into the VACV backbone. One recent study used a ΔTK-Western

Reserve strain of VACV with encoded micro RNA (miR)-34a and demonstrated increased induction of apoptosis in a model of multiple myeloma[192]. More commonly, however, the insertion of transgenes has been used in an effort to induce anti-tumour immunity after cancer-specific viral infection.

The oncolytic Wyeth platform was the first OV to encode human granulocyte macrophage colony-stimulating factor (GM-CSF) in an effort to provide the virus with the ability to break tumour immune tolerance[186]. Early *in vivo* studies in rabbits demonstrated the successful expression of virally-encoded human GM-CSF that peaked at four days following intravenous infusion or direct intratumoural delivery of the virus, which was accompanied by a significant recruitment of CD8+ and CD4+ T cells to the tumour 8-days post-infection[186]. Recently, the mechanism of action of GM-CSF-encoded OVs was clarified by Parviainen *et al.*, who utilized immunocompetent Syrian golden hamsters and the double-deleted backbone of Western Reserve encoding human GM-CSF, which is known to be active in this model. They observed the same tumour control and safety profiles previously reported, however they also observed increased proliferation and migration in splenocytes from animals treated with the GM-CSF-encoding virus[193]. Therefore, GM-CSF-encoding VACVs are able to induce the proliferation and migration of monocytes, a critical step in the induction of adaptive immunity, and presumably are involved in the subsequently-observed CTL (cytotoxic T-lymphocyte) recruitment to the tumour.

Clinically, VACV-based OVs have made impressive progress[22,61]. The leading candidate for approval at this time is Pexa-Vec, which is currently (May 2017) in the midst of recruiting for two separate studies – one Phase III study for the use of Pexa-Vec in combination with the kinase inhibitor Sorafenib in the context of HCC, and another Phase I study of Pexa-Vec in combination with the immune checkpoint inhibitor anti-CTLA-4 for advanced solid tumours

(ClinicalTrials.gov identifiers: NCT02562755 and NCT02977156, respectively). Past clinical studies with this virus have revealed several important lessons, including its tolerable safety profile[194], its ability to effectively locate to tumours following intravenous delivery[57] and disrupt tumour vasculature[56], as well as its utility across diverse indications and patient groups[195-197]. The next most advanced platform is the Lister strain VACV-based OV, GL-ONC1. Although clinical trial results appear unpublished at this time, conference presentations have demonstrated that GL-ONC1 is well-tolerated with minimal toxicity, that the delivery of transgenes to tumours occurred successfully, and that systemic administration resulted in localization of the virus to tumour sites. There are three ongoing GL-ONC1 clinical trials in different indications (NCT02759588, NCT01766739, and NCT02714374)[22]. Results have also recently been published from the first trials utilizing the above mentioned double-deleted Western Reserve-based OV. These have indicated that patients tolerated the supposed augmented virulence of the Western Reserve strain of VACV, that it was successfully delivered to tumours, and that early anti-tumour activity was observed[198,199]. Another VACV platform that has been utilized as an OV in an early study is Modified Vaccinia Ankara (MVA) encoding Epstein-Barr Virus (EBV) target antigens. In this Phase I trial, EBV-associated nasopharyngeal carcinoma was targeted as it is known to commonly express EBV-specific antigens, and antigen-expressing MVA was determined to be safe and immunogenic[200]. As evidenced by this discussion, the interest in VACV-based OV therapeutics is increasing as it provides desirable OV-relevant properties, however there are still many unknowns surrounding VACV as a pathogen that should be investigated. It is in the interest of the field to more thoroughly understand the basic biology governing the interactions between VACV and transformed cells before next-generation OV candidates will gain clinical traction; for this, improved and more comprehensive investigative tools are required.

1.4. Transposon-mediated mutagenesis

Initial observations that led to the discovery of transposable elements (TEs) were made by Barbara McClintock in maize and published as a body of work that increased the fundamental understanding of genetic diversity and for which she was awarded the 1983 Nobel Prize for Physiology or Medicine[201,202]. Shortly thereafter, investigators were able to harness the properties of TEs for use as tools in molecular biology. The earliest examples of this are described in reports of the transposition of antibiotic resistance genes between plasmids, or from TE-containing plasmid(s) into phage DNA in the context of infected cells[203-205]. Once the utility of systems such as this became apparent, they were adapted for countless purposes by groups worldwide. Most commonly, TE-mediated insertional mutagenesis has been utilized to study bacterial functional genetics, however it has also been regularly applied in an effort to discover novel oncogenes[206]. In fact, a recent body of work has led to the method known as *Tn-Seq*, in which TE-mediated insertional mutagenesis is combined with high-throughput parallel sequencing that allows the relative fitness of bacterial genes to be determined based on insertion frequencies[206,207]. TE systems have also been applied to several viral platforms, including HSV and hepatitis C virus, usually from the perspective of identifying essential viral genes[208-214]. This approach has not been applied to VACV, and the approach in various viral platforms does not appear to have been expanded to include high-throughput functional assays, which would assist in identifying downstream functions of putative ORFs or select regions within them.

Consequent to the interest in TE-mediated insertional mutagenesis for the study of gene functions, several commercially-available platforms have emerged. One such platform, now known as *PiggyBac*™, utilizes a naturally-active transposon system that was originally described by studying Baculovirus propagating in the cabbage looper moth cell line TN-368[215-217]. The

original publications identified a 2.7kb TE that was flanked by 32-bp ITRs, exhibited specificity for insertion at TTAA sites in the target genome, and could insert host genetic material into the genome of infecting Baculovirus. This naturally-occurring TE was first mobilized for experimental use in mammalian systems, including mice that were made to express a transposable red-fluorescent protein transgene and subsequently exhibited red fluorescence[218]. *PiggyBac*™'s use as a genetic tool has expanded, and hundreds of studies have since reported using it for diverse applications. Typically, the *PiggyBac*™ transposase enzyme is carried on a separate plasmid from the transposon itself, and the two are independently transfected into the host cell (supplied in *trans*). Once the transposase enzyme is expressed in mammalian cells, it works by binding to the ITR of the transposon, nicking the DNA, and freeing 3' –OH groups at each end. This results in a hydrophilic attack in which the transposon is freed from its plasmid backbone[215,219]. As explained by Woodard and Wilson, cellular genomic TTAA sequences are then subject to an additional hydrophilic attack, resulting in a staggered cut in the genomic DNA and a transient double-stranded break into which the TE can then insert[215]. There are notable advantages of using the *PiggyBac*™ system over other TE systems. Namely, insertion at TTAA sites in the target genome has been shown to lead to biased insertion towards transcription units, therefore increasing the rate of insertional mutagenesis, and although less relevant to this research project, there is less limitation in cargo size compared to similar systems[215].

1.5. Rationale, objectives, and hypothesis

As has been presented thus far, VACV is an interesting OV platform for several reasons:

- It has been utilized extensively in humans as a vaccine vector and therefore has a well-established and acceptable safety profile,

- Past clinical trials have demonstrated the cancer-selectively and efficacy of VACV-based OVs following intravenous or intratumoural delivery, and
- VACV can be engineered to express large therapeutic transgenes.

However, the study into basic VACV biology remains ongoing and the current VACV-based OV platforms were not bio-selected for potency. As a result of its large and complex genome, many of VACV's gene products remain uncharacterized. Of those that are characterized, several have functions with presumed deleterious effects from the perspective of an OV, and additional functions are likely for others. A better tool for the study of VACV is required. Therefore, this research project has been designed to address the following main objectives:

1. To understand the phenotype of five wild-type vaccine strains of VACV from the perspective of OV-relevant characteristics (replication, cytotoxicity, spread) and select a strain for the development of next-generation VACV-based OV therapeutics.
2. To construct and characterize a working library of single-gene VACV-Copenhagen mutants to allow better study of the VACV-Copenhagen genome.
3. To investigate relevant viral gene properties in the underlying context of OV development and unique pathogen-host interactions while demonstrating potential utility of this library for putative gene description and high-throughput functional genomic studies.

The remainder of this research project will present experimental evidence that relates to these objectives and supports the overall **hypothesis** that *selective interruption of VACV genes will improve the oncolytic properties of the VACV-Copenhagen backbone.* The broader research goal is to comprehensively investigate the VACV genome so that future VACV-based OV platforms can be optimally designed for therapeutic benefit.

2. Materials and Methods

Cell culture and virus. Unless further specified, all cells were purchased from the American Type Culture Collection (ATCC; Manassas, USA) and maintained according to ATCC-derived culture methods, including cell-specific growth media, as well as sub-culturing and cryopreservation techniques. The NCI-60 cell panel was obtained directly from the National Cancer Institute (Bethesda, USA) and maintained according to their guidelines. VACV strains Copenhagen, Western Reserve, Wyeth, and Lister were obtained from the ATCC. VACV-Tian Tan was a gift from Dr. David Evans (University of Alberta, Edmonton, Canada) and was previously described under the identifier *DTH-14*[220].

Virus plaque purification. Before experimentation, all wild-type VACV strains were plaque-purified for a minimum of five rounds in U-2 OS cells before expansion and purification. All clones in the working TE library were also plaque-purified in U-2 OS cells. This plaque purification was performed as many times as necessary until 100% of observed plaques in subsequent infections expressed mCherry (n = 100).

Sucrose gradient purification and virus stock generation. All viruses used in this research project were expanded in HeLa or U-2 OS cells. Following standard protocols, collected lysates were subjected to a freeze (-80ºC) and thaw cycle to lyse intact cells. Cleared lysate containing virus was then overlayed onto a 36% sucrose gradient and centrifuged at 11,500 x RPM for 90 minutes. Viral pellets were resuspended in 1mM Tris pH 9.0 and concentrations were determined via standardized plaque assay.

Creation, culture, and characterization of patient-derived cancer cell lines. Several primary cultures of patient-derived cancer cells were used in this research project. Patient-derived ovarian cancer cell lines 2028 and 2068 were gifts from Dr. Carolina Ilkow (Ottawa Hospital Research Institute, Ottawa, Canada) and were previously established from the ascites of individuals with ovarian cancer during routine paracentesis according to Ottawa Health Science Network Research Ethics Board (OHSN-REB) protocol number 20140075-01H. These cells were maintained in complete Dulbecco's Modified Eagle's medium (Corning, Manassas, USA) supplemented with 10% fetal bovine serum (Corning, Manassas, USA). Patient-derived melanoma cell lines pMel-T and pMel-X2 were gifts from Drs. Guy Ungerechts and Christine Engeland (National Center for Tumor Diseases, Heidelberg, Germany) and were generated following institutional ethics guidelines (Ethics Committee of Heidelberg University NCT MASTER, S-206/2011). These were maintained in Roswell Park Memorial Institute (RPMI)-1640 medium (Corning, Manassas, USA) supplemented with 10% fetal bovine serum, 100 µg/mL Gentamicin (Gibco – Life Technologies, Grand Island, USA), 0.1 mg/mL Normocin™ (InvivoGen, San Diego, USA), and 1 x Antibiotic-Antimycotic (Gibco – ThermoFisher Scientific, Toronto, Canada).

Melanoma Patient 12-2016 and Melanoma Patient 13-2016 primary cultures were derived from excised surgical specimens from an ulcerated chest nodular melanoma and from melanoma metastasized to the patient's left retroperitoneal pelvic lymph node, respectively. The surgeries were performed by Dr. Carolyn Nessim (Ottawa Hospital Research Institute, Ottawa, ON, Canada) and tissue was taken following the receipt of patient consent according to the Ottawa Health Science Network Research Ethics Board protocol number 20120559-01 (Appendix I). Primary cultures were established following scalpel-mediated homogenization of tumour specimens in the presence of the RPMI-based media described above, and filtering the homogenate through a 70

μm nylon mesh cell strainer (ThermoFisher Scientific, Toronto, Canada). Homogenate was maintained in culture with periodically-refreshed media until sufficient cellular proliferation occurred for experimental purposes. Both primary cultures have been cryopreserved and have proven useful as experimental models.

Basic characterization of all human-derived primary cultures was performed. Immunofluorescent staining was performed on ovarian cancer cultures using a monoclonal primary antibody against Cytokeratin 18 raised in mice (Cat. # ab55395, 1:1,000; Abcam, Toronto, Canada; Appendix II). Human-derived primary melanoma cultures were characterized at the RNA and protein levels. Reverse transcriptase PCR was performed using primers targeting the *MelanA* (TAAGGAAGGTGTCCTGTGC; AGAGACACTTTGCTGTCCCG), *Tyrosinase* (GGAAGAATGCTCCTGGCTGT; GGCTACAGACAATCTGCCAAG), and *S100A1* (TTGGCCATCTGTCCAGAACC; TGTCCACAGCATCCACATCC) genes, respectively. Immunofluorescent staining was also performed on cells in primary cultures using primary antibodies against MelanA and S100 – antibodies used were monoclonal mouse anti-human MelanA (Cat # ab140503, 1:150; Abcam, Toronto, Canada) and polyclonal rabbit anti-human S100 (Cat # ab868, 1:500; Abcam, Toronto, Canada). For primary melanoma cultures generated from patients in Ottawa, original tumour specimens were also collected, processed, and sectioned for staining purposes. Immunohistochemistry was performed using the antibodies described above, and hematoxylin and eosin staining was also performed to visualize original tumour architecture (Figures 3.3B and 3.4B).

Viral replication studies. Virus replication studies were performed using standardized protocols. When performed on cell monolayers, replication studies were multi-step (MOI 0.01). Virus

inoculation was allowed to proceed for two hours, at which point inoculum was removed, cells or patient cores were washed twice with 1 x PBS, and new culture media was applied to the system. At indicated time points, infected cells were frozen at -80ºC and viral output was determined using standardized titration methods upon thawing.

Immunohistochemistry/Immunofluorescence staining. Tumour specimens were fixed in 10% formalin for 24-48 hours and stored for longer term in 70% ethanol. Specimens were formalin-fixed and paraffin-embedded (FFPE) by the Histology Core Facility at the University of Ottawa. Likewise, tissue sectioning and hematoxylin and eosin staining was performed by the Histology Core Facility at the University of Ottawa. Immunohistochemistry was performed on FFPE tissues as previously described[221]. Immunofluorescence staining on cell cultures was performed using standardized protocols. Cells were initially grown on glass coverslips until desired density, fixed using 4% paraformaldehyde, and permeabilized using 0.1% Triton X-100. Primary antibody staining was performed for 90 minutes at room temperature. Secondary antibodies were targeted against species-specific IgG and were fluorophore-conjugated (1:500, AlexaFluor; ThermoFisher Scientific, Toronto, Canada); these were utilized for 60 minutes at room temperature. Coverslips were mounted on glass microscope slides using 4'6'-diamidine-2'-phenylindole dihydrochloride (DAPI)-containing ProLong Antifade Reagent, ThermoFisher Scientific, Toronto, Canada). After light-protected, overnight drying, cells were imaged by microscopy.

As previously mentioned, primary antibodies used to characterize primary cancer cultures include: mouse anti-human Cytokeratin 18, mouse anti-human MelanA, and rabbit anti-human S100. Rabbit anti-VACV (1:10,000; Quartett Immunodiagnostika, Berlin, Germany) was used to stain select VACV-infected tumours (Figure 3.5).

Microscopy. Imaging of live cells was performed using an EVOS FL Cell Imaging System (ThermoFisher Scientific, Toronto, Canada). Imaging of fixed cells following immunofluorescence staining was performed using a Zeiss AxioCam HRm Imager M1 (ZEISS Canada, Toronto, Canada) and an X-Cite 200DC Fluorescence Illumination System (Excelitas Technologies, Waltham, USA). Imaging of FFPE tissues following immunohistochemistry was performed using an Aperio ScanScope CS2 (Leica Biosystems, Concord, Canada).

Human biopsy core infection. Tumour specimens were obtained following the protocols established in Ottawa Health Science Network Research Ethics Board protocol number 20120559-01. Tumour specimens were taken to the Department of Pathology where a certified Pathologist Assistant would assess the tissues for diagnostic purposes. Any remaining tissue was immediately placed in RPMI-1640 medium supplemented with 10% fetal bovine serum, 100 µg/mL Gentamicin, 0.1 mg/mL Normocin™, and 1 x Antibiotic-Antimycotic, as described above. The tissue was cored with a 2-mm punch biopsy tool and the cores were allowed to incubate in media overnight at 37ºC. Tissue cores were then inoculated with 10,000 plaque forming units (PFU) of virus for two hours, at which point the inoculum was removed, the cores were washed with 1 x PBS and infected cores were allowed to incubate for 72 hours before being processed for titration.

***In vivo* melanoma virus replication studies.** Female CD1 nude mice were implanted with 1 x 10^7 M14 human melanoma cells in their bilateral sub-cutaneous flanks. Once tumours reached approximate volume of 62.5 mm^3 (5 mm x 5 mm), tumours were injected with 1 x 10^7 PFU of virus. Experimental groups included each of the wild-type VACV strains as well as ΔTK-Wyeth.

72 hours post-infection, animals were sacrificed and tumours were collected and flash frozen. Frozen tumours were homogenized at a frequency of 30 Hz for five minutes using a TissueLyser II (Qiagen, Germantown, USA). 1 x PBS was then added to homogenate and titration by standardized plaque assays was performed. Representative tissues infected with VACV were also collected and fixed in 10% formalin for 48 hours followed by 70% ethanol before being processed for immunohistochemistry.

Plaque size assays. Known concentrations of virus were used to inoculate cells of interest. Following two hours of inoculation, inoculum was removed, cells were washed with 1 x PBS and a semi-solid overlay of 3% carboxymethylcellulose, 1 x DMEM, and 10% fetal bovine serum was applied. Following a selected experimental time period, the semi-solid overlay was removed and infected monocultures were stained with 0.1% crystal violet for 30 minutes. After an overnight drying period, stained monocultures were photographed and ImageJ software (Version 1.50i; National Institutes of Health, Bethesda, USA) was used to measure plaque diameter. Measured plaques were marked to ensure no duplicate measurements.

Extracellular enveloped virus assays. Extracellular enveloped virus "comet" assays were performed following the same protocols as with plaque size assays, however a fully liquid overlay was used instead of a semi-solid overlay. Incubation periods ranged from 48 to 96 hours, during which time infected cells were placed in an incubator that remained unopened for the duration of the experiment. Following incubation in a closed incubator, infected monocultures were stained according to standardized protocols.

Quantitative extracellular enveloped virus assays were performed using a fractional titration approach that has been previously validated[222]. In short, culture supernatants, which predominantly contain released extracellular enveloped virus, were collected at selected time points post-infection and virus particles were quantified according to standardized protocols.

Vaccinia virus-Copenhagen transposable element library generation. The clonal library of VACV-Copenhagen used in this research project was derived from a previously-developed transposable element-mutagenized Copenhagen library that was optimized by Dr. Jiahu Wang (Research Associate, Dr. John Bell Laboratory). Dr. Wang cloned the sequence of *PiggyBac*™ transposase (a gift from Professor Malcolm Fraser Jr.; University of Notre Dame, Notre Dame, USA) into a pcDNA3.1 mammalian expression vector. An mCherry-expressing transposable element flanked by inverse terminal repeats was assembled by PCR and cloned into a high-copy pUC57-based vector. Following transposase vector transfection, infection, and transposable element vector transfection over a 72 hour period, transposable element-mutagenized virions were released from U-2 OS cells using a freeze (-80°C) and thaw approach.

With this library, HeLa cells were infected for 16 hours at MOIs of 0.01 and 0.1, respectively. Using a MoFlo Astrios EQ cell sorter (Beckmann Coulter Canada, Mississauga, Canada) at the University of Ottawa's Flow Cytometry and Virometry core facility, mCherry-positive cells were sorted into 96-well plates already containing U-2 OS cells in monoculture. Excess mCherry-positive cells were collected and subsequently used to infect U-2 OS cells in six-well plate format, with mCherry-positive plaques being collected 48 hours post-infection. All independent mCherry-positive cultures (see example Figure 3.8) were further expanded on HeLa cells in 12-well, and subsequently, in 10-cm plate formats. DNA was extracted from each

potentially unique virus clones (n = 228) using the QIAmp Min Elute Virus Spin Kit (Qiagen, Germantown, USA). Quality control and Next-Generation Sequencing (150 bp paired-end reads, Illumina NextSeq 500) analyses were performed by StemCore Laboratories (Ottawa Hospital Research Institute, Ottawa, Canada). Bioinformatics analysis (Adrian Pelin, Ottawa Hospital Research Institute, Ottawa, Canada) on resulting reads were inspected for the presence of inverted terminal repeat sequences flanking the TE insert. Reads which contained the inverted terminal repeat sequence were used to map back to our wild-type VACV-Copenhagen backbone reference, which allows the exact position of the insert to be determined. This analysis revealed 89 unique virus clones with unique insertion sites. Finally, unique virus clones were subjected to a minimum of five rounds of plaque purification until 100% purity was reached, as defined by the exclusive presence of mCherry-positive plaques. Unique virus stocks were then amplified and quantified according to standardized protocols.

Reverse transcription polymerase chain reaction studies. RNA was extracted from infected or uninfected cell cultures using a Trizol extraction followed by ethanol precipitation. RNA concentrations were obtained using a NanoDrop ND-1000 Spectrophotometer (ThermoFisher Scientific, Toronto, Canada). Reverse transcription was performed in a two-step reaction using a Maxima Reverse Transciptase enzyme kit (ThermoFisher Scientific, Toronto, Canada). Finally, polymerase chain reactions were performed following standardized protocols using a Mastercycler Pro PCR System (Eppendorf, Hamburg, Germany). Primers targeting melanoma diagnostic genes are presented above. Primers targeting the Tp 61 insertion clone were ATGAGGAGTATTGCGGGGCT and AGGCTTCCAAAAATTTTTCATCCGT. Primers targeting the Tp 243 insertion clone were AGACTGTCCATCTTGTCCAAGGA and

TGTTTGACTTTATGGTTAGACCCGCA. Primers targeting the Tp 250 insertion clone were AGACTGTCCATCTTGTCCAAGGA and TGTTTGACTTTATGGTTAGACCCGCA. Primers targeting the Tp 279 insertion clone were ATGGGGTTTTGCATTCCATTGAGATCAAAGATG and ACGAAAGTCCAGGTTTGATAGAGACAAACT. Primers targeting the Tp 311 insertion clone were ATGAGGAGTATTGCGGGGCT and AGGCTTCCAAAAATTTTTCATCCGT. Primers targeting the Tp 344 insertion clone were ATGGCGACTAAATTAGATTATGAGGATGC and TCGTCGGTCATCAGATCTGTAATGT. Primers targeting the VACV *C9L* gene were ACTGTAAGCATGTCCGTACCA and ATGCGT GAGTTGGATGTGTT.

Immunoblotting. Cellular or viral proteins were resolved on NuPAGE 4-12% Bis-Tris gels (Life Technologies, Carlsbad, USA) and transferred onto Immun-Blot Polyvinylidene difluoride membranes (Bio-Rad Life Sciences, Mississauga, Canada). Membranes were incubated for one hour at room temperature or overnight at 4ºC with primary antibodies or antisera. Specific products and dilutions include: 1:1,000 polyclonal goat anti-ß-Tubulin (Abcam, Toronto, Canada; ab21057), 1: 2,000 polyclonal rabbit anti-VACV F11, 1: 2,000 rabbit anti-VACV K7 antiserum, 1: 10,000 polyclonal rabbit anti-VACV A36. The antibodies against VACV proteins F11 and A36, and the antiserum against VACV K7 were generous gifts from the laboratories of Professor Michael Way (The Francis Crick Institute, London, UK) and Dr. Martina Schroeder (National University of Ireland, Maynooth, UK) and have been previously described[181,223,224]. Membranes were incubated for one hour at room temperature with horseradish peroxidase-conjugated secondary antibodies: 1: 5,000 anti-goat IgG (Jackson ImmunoResearch Laboratories, West Grove, USA; 805035180) or 1: 5,000 anti-rabbit IgG (Cell Signaling, Danvers, USA; 7074),

respectively. Proteins were detected with Supersignal West Pico chemiluminescent substrate (ThermoFisher Scientific, Toronto, Canada) followed by exposure to premium autoradiography film (Denville Scientific, Holliston, USA).

Vaccinia virus-Copenhagen B19 insertion functionality assay. The human renal cell adenocarcinoma cell line 786-O was infected for 24 hours with wild-type Copenhagen or Tp 203 (*B19R* insertion of TE) at an MOI of 0.1. After 24-hours inoculation, the supernatants from each condition were collected, passed through a 0.22 μm filter, and added to fresh monocultures of 786-O cells. VSVΔ51-GFP, a virus with neutralization sensitivity to secreted interferon, was used to inoculate each respective population at an MOI of 0.01. After 24 hours of infection, cells were imaged using an EVOS FL Cell Imaging System (ThermoFisher Scientific, Toronto, Canada).

Fluorescence-based viral replication assays. Fluorescence-based viral replication assays were performed by exploiting a previously-described direct relationship between the fluorescence intensity output of a fluorophore-expressing virus and the amount of virus in the system[90]. As schematized in Figure 2.1, a TE-mutagenized virus was used to primarily infect an experimental cell line of choice at an MOI of 0.1 or 0.01. Following initial inoculation (n = 4/virus clone), an aliquot of the input virus was left at 4°C to prevent any further freeze and thaw cycles. Inoculation was allowed to proceed for a selected period, following which the test plate was frozen at -80°C to encourage cell lysis. Meanwhile, read-out plates consisting of confluent U-2 OS cells in 96-well format were prepared, which hosted the secondary infection (n = 4/virus clone). The secondary infection was then allowed to proceed with equivalent volumes of inocula from the primary infecting virus (n = 4) as well as the output virus that had been released upon cell lysis following

Figure 2.1. Fluorescence-based high-throughput vaccinia virus replication assay. Step 1 includes the primary infection and subsequent incubation of a test cell line of choice, followed by a freeze (-80ºC) and thaw (room temperature) cycle. Step 2 includes the secondary infection with both the output of virus from the primary infection as well as the same input virus as was used for the primary infection. In Step 3, a high-throughput fluorescence readout is obtained for both samples following secondary infection, the results of which are used to calculate the relative amount of virus replication during the primary infection (Step 4).

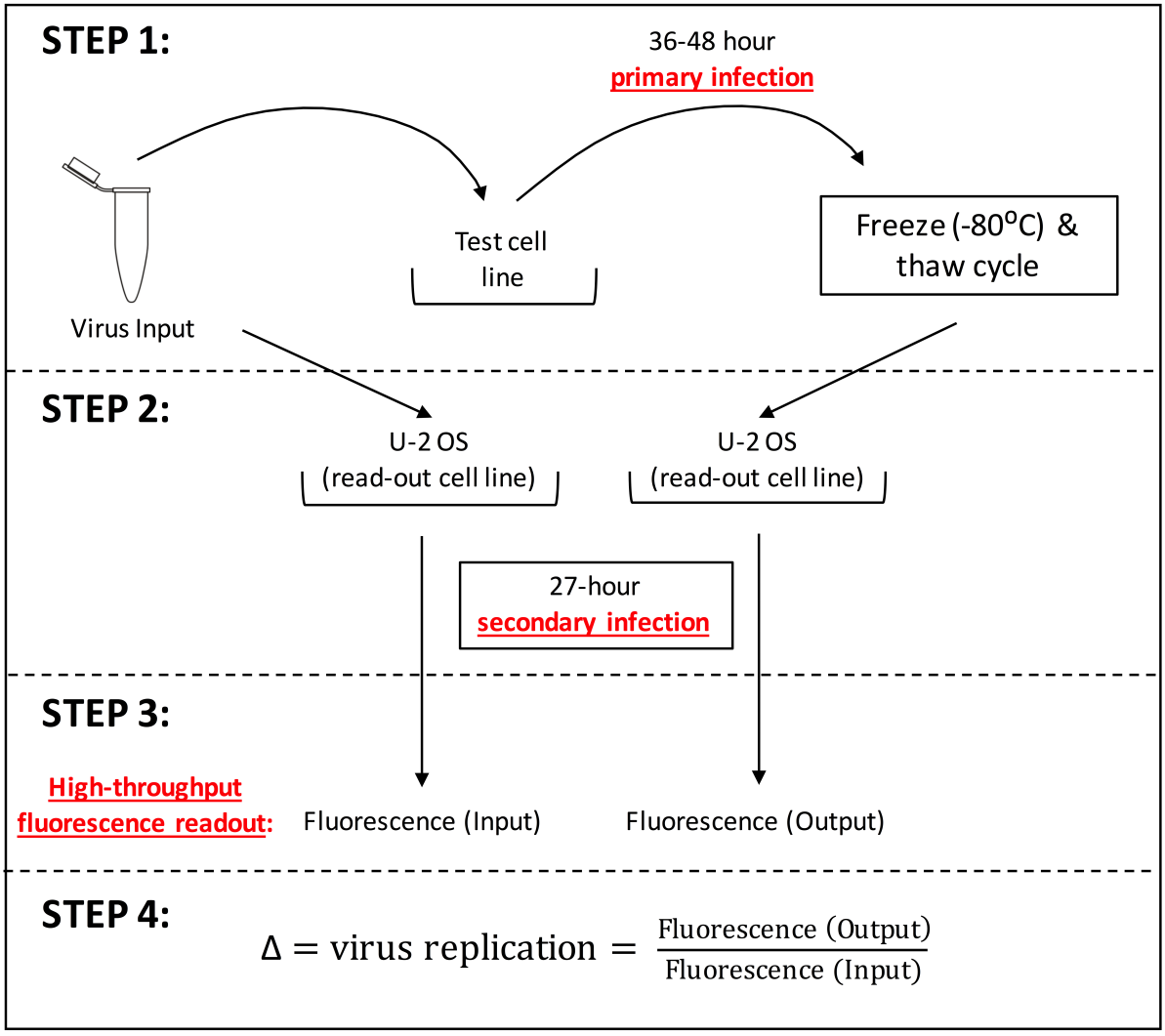
STEP 1:
36-48 hour
primary infection
Test cell line
Freeze (-80°C) & thaw cycle
Virus Input
STEP 2:
U-2 OS (read-out cell line)
U-2 OS (read-out cell line)
27-hour
secondary infection
STEP 3:
High-throughput fluorescence readout:
Fluorescence (Input)
Fluorescence (Output)
STEP 4:
Δ = virus replication = Fluorescence (Output) / Fluorescence (Input)

a thaw of the primary-infected cells (n = 4). Secondary infection was allowed to proceed for 27 hours, at which point the fluorescence output was read using a Cellomics ArrayScan VTI HCS Reader (ThermoScientific, Toronto, Canada) with the help of an Orbitor RS loading system (ThermoScientific, Toronto, Canada).

Vaccinia virus protein homology analyses. Vaccinia virus-Copenhagen proteins F15 and A47 were individually blasted against the nr database at the amino acid level. All poxvirus sequences were filtered for redundancy and duplicates and aligned together using the multiple sequence comparison by log-expectation (MUSCLE) algorithm. This alignment allowed similarity matrices to be constructed, as well as a maximum likelihood phylogeny.

In vivo **toxicity studies.** Female Balb/c mice were injected intranasally with 8 x 10^6 PFU of selected virus clones on three separate occasions (Days 1, 3, and 5). Mice were weighed at baseline (prior to first virus dose) and every day thereafter for the remainder of the experiment.

Statistics. All statistical analyses were performed using GraphPad Prism or Microsoft Excel. Where possible, statistical analyses were performed on log-transformed values. One-way ANOVAs and multiple comparisons analyses were employed for the comparison of multiple independent groups. Log-log plots were analyzed using power analyses and the slopes of their curves correspond to exponents of power-law scaling (slopes not presented). Regression values presented in these analyses were generated by solving for the power regression. P values less than 0.05 were considered significant and are annotated as follows: *$P \leq 0.05$, **$P \leq 0.01$, ***$P \leq 0.001$, ****$P \leq 0.0001$.

3. Results

3.1. Understanding unique phenotypic properties of wild-type vaccinia virus

3.1.1. In vitro replication kinetics

The underlying goal of this research project was to increase our understanding of VACV to facilitate a downstream effort aimed at bioengineering a novel VACV-based oncolytic backbone. As such, the first step was to bio-select the wild-type strain of VACV with which to conduct these studies. There are five clinical candidate strains to which we had access: Copenhagen, Western Reserve, Wyeth, Lister, and Tian Tan. The initial aim was to investigate the *in vitro* replication kinetics of each individual strain in several relevant cancer models. As a first step to gaining this understanding, a multi-step growth curve (MOI 0.01) was performed on the immortalized human cervical adenocarcinoma cell line HeLa (Figure 3.1). The mean input virus across all strains tested consisted of 2.5×10^4 PFU, with the lowest input being represented by the wild-type Copenhagen strain at 1.3×10^4 PFU. This discrepancy is attributed to the inherent inaccuracies associated with quantifying concentrations within viral preparations; despite beginning the assay with a smaller input population, the Copenhagen strain produced significantly increased progeny compared to each of the other wild-type strains of VACV as early as 24 hours post-infection. This advantage in infectious particle production was observed to be maintained at 36 and 48 hours post-infection, respectively. Similar assays were then performed in alternative immortalized human cancer models; the human melanoma cell line M14, renal cell adenocarcinoma cell line 786-O, prostate adenocarcinoma cell line PC-3, and the colorectal adenocarcinoma cell line HT-29 were all subject to *in vitro* infection by individual wild type strains of VACV. As the replication kinetics observed in HeLa cells would suggest, the Copenhagen strain was observed to produce significantly greater infectious progeny at 48 hours post-infection

Figure 3.1. Replication kinetics of distinct wild-type vaccinia virus strains. (A) A multi-step growth curve of five distinct wild-type strains of vaccinia virus in the human cervical adenocarcinoma cell line HeLa: Copenhagen, Western Reserve, Wyeth, Lister, and Tian Tan. Cells were infected at a multiplicity of infection of 0.01 and infections were allowed to proceed for the durations listed. Statistical annotations represent the analysis of variance between Copenhagen and each of the other wild-type strains. The box highlighting the 48 hour replication values has been presented in (B) so that the variability of individual means can be observed. Results shown represent three independent experiments. Statistical annotations in *A* represent the variance between wild-type Copenhagen and each of the other virus strains studied. (One-way ANOVA, *P < 0.05, **P < 0.01, ****P < 0.0001)

A

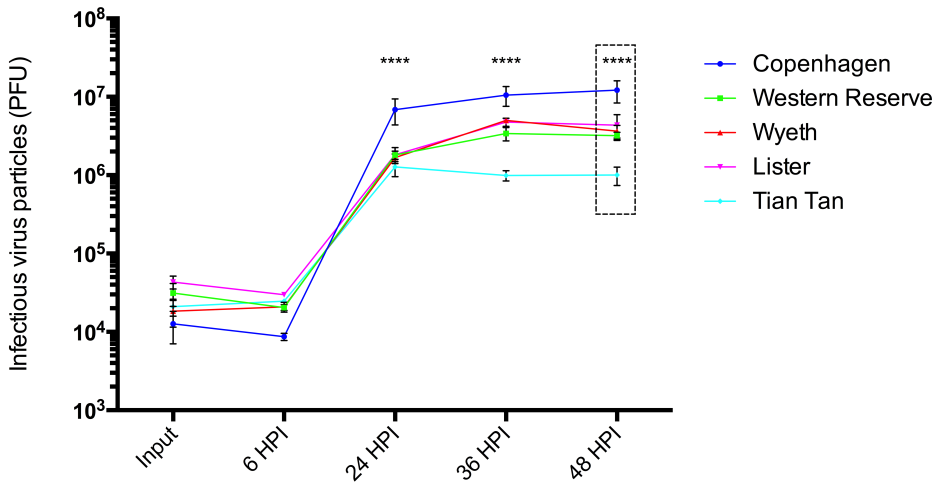
Infectious virus particles (PFU)
10^8
10^7
10^6
10^5
10^4
10^3
****
****
****
Input
6 HPI
24 HPI
36 HPI
48 HPI
Copenhagen
Western Reserve
Wyeth
Lister
Tian Tan

B

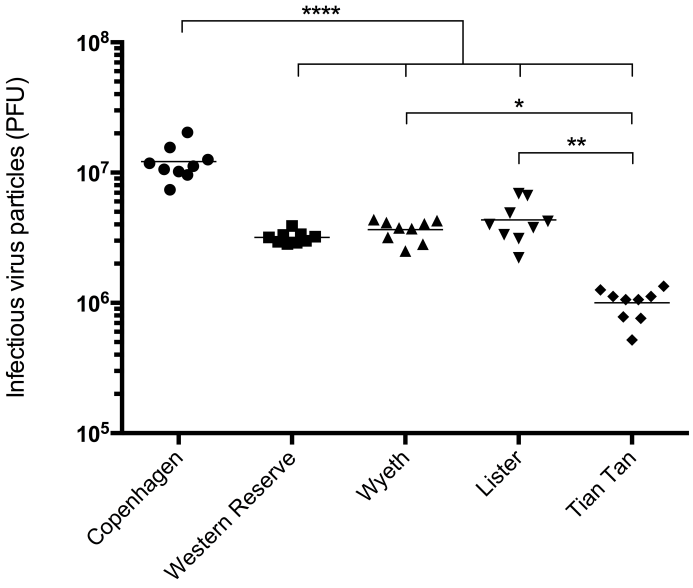
Infectious virus particles (PFU)
10^8
10^7
10^6
10^5
****
*
**
Copenhagen
Western Reserve
Wyeth
Lister
Tian Tan

compared to each of the other wild type strains (Figure 3.2). This is a finding that was observed to be consistent in more expansive cancer models and also in competition assays in which equivalent amounts of wild-type VACV were pooled and used to infect various cancer models, with NGS providing a readout of Copenhagen dominance within a diverse population (data not shown). These results suggest that the Copenhagen strain of VACV possesses an *in vitro* growth advantage compared to other wild-type strains that may have become more attenuated during their history of vaccine use.

3.1.2. Replication kinetics in patient-derived models

As a complement to these studies, an effort was made to investigate the growth properties of these five VACV strains in more clinically-relevant *in vitro* and *ex vivo* models. The data presented in Figures 3.3 and 3.4 were generated from tumour specimens taken from two individuals who presented with various degrees of advanced melanoma (Table 3.1) and underwent debulking surgery at the Ottawa Hospital (Ottawa Health Science Network Research Ethics Board protocol number 20120559-01). The gross specimen from Patient 12-2016 can be observed in Figure 3.3A and is clinically characteristic of a nodular melanoma as it was well circumscribed, ulcerated, and found on the trunk region. This diagnosis was histologically confirmed and a representative photomicrograph of Hematoxylin and eosin-stained tissue demonstrates a prevalence of epithelioid tumour cells and hyperchromatic nuclei (Figure 3.3B). Similarly, the melanoma specimen from Patient 13-2016 demonstrated similar histologic features, and the representative photomicrograph presented in Figure 3.4B also allows rudimentary nests to be observed. These features, along with the clinical presentation of numerous palpable inguinal lymph node metastases at the time of surgery (Figure 3.4B), are consistent with the more advanced disease state of this individual. In both cases, sustained *in vitro* cellular growth (Figure 3.3C, 3.4C) was

Figure 3.2. 48-hour viral replication of vaccinia virus strains in human cancer cells. The vaccinia virus strains Copenhagen, Western Reserve, Wyeth, Lister, Tian Tan, and the clinical candidate oncolytic strain ΔTK-Wyeth were used to infect various cancer cell lines at a multiplicity of infection of 0.01. Similar replication properties were observed for each of the virus strains in (A) M14 melanoma cells, (B) 786-O renal cell adenocarcinoma cells, (C) PC-3 prostate adenocarcinoma cells, and (D) HT-29 colorectal adenocarcinoma cells. Results shown represent 3 independent experiments. Statistical annotations indicate differences between Copenhagen and each of the other respective virus strains; no significant differences were observed otherwise. (One-way ANOVA, *P < 0.05, **P < 0.01, ***P < 0.001, ****P < 0.0001)

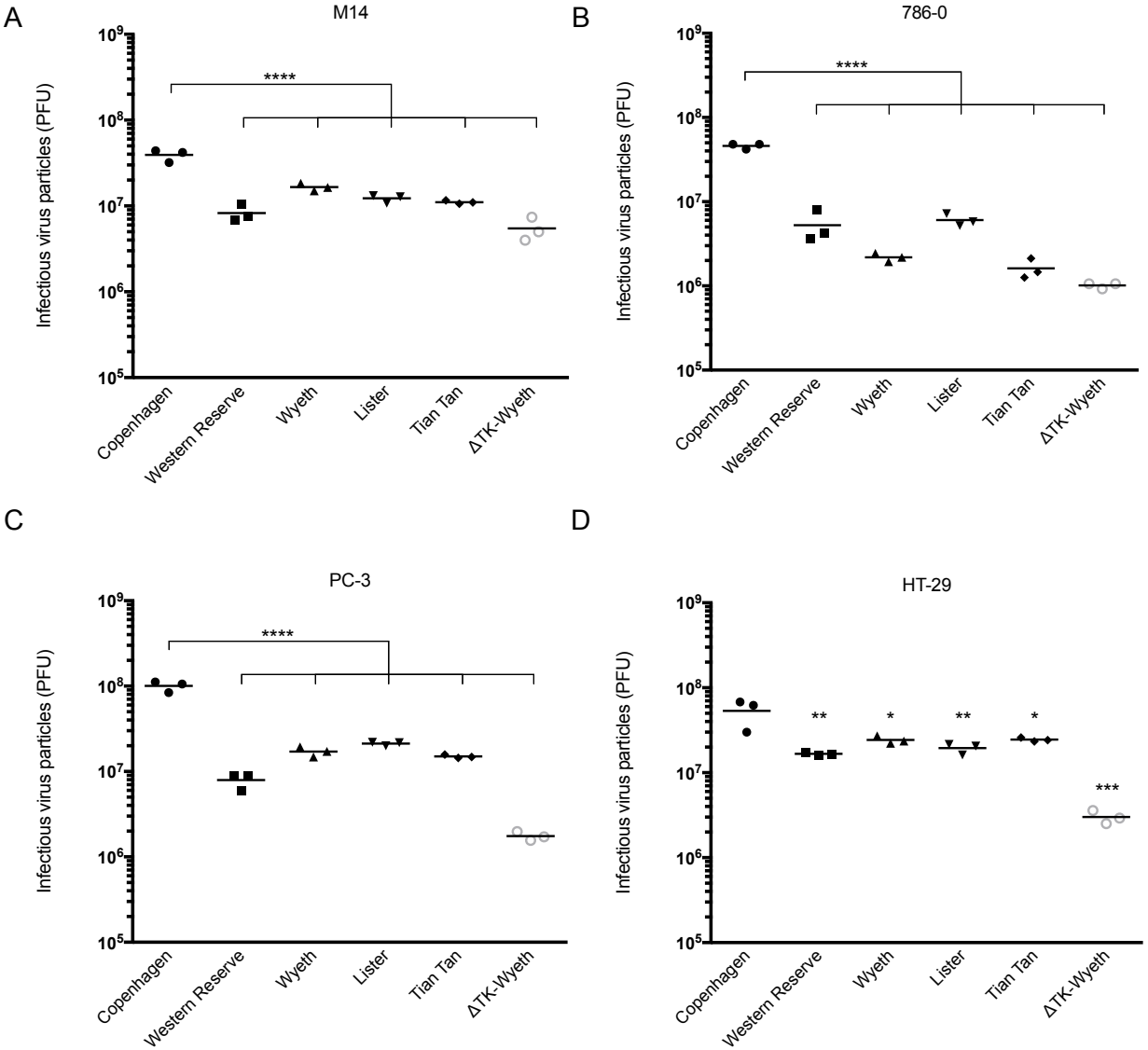
A
M14
B
786-0
C
PC-3
D
HT-29
Infectious virus particles (PFU)
10^9
10^8
10^7
10^6
10^5
****
**
*
***
Copenhagen
Western Reserve
Wyeth
Lister
Tian Tan
ΔTK-Wyeth

Table 3.1. Clinical characteristics of tumour-derived melanoma cultures. Mel-A = Melanoma antigen, AE1/3 = Cytokeratin AE1 and AE3, HMB-45 = homatropine methylbromide, Tyr = Tyrosinase.

					Pathologist Diagnosis (IHC)				RT-PCR		
Case ID	**Age**	**Sex**	**Description**	**Relevant mutations**	**Mel-A**	**S-100**	**AE1/3**	**HMB-45**	**Mel-A**	**S-100**	**Tyr**
Melanoma Pt. 12-2016	82	M	Nodular melanoma, chest; ulcerated, pedunculated; original tumour: Breslow 1.2 cm, pT4b	Unknown	+	+	-	n/a	+	+	+
Melanoma Pt. 13-2016	59	M	In-transit metastasis, left retroperitoneal pelvic lymph node; 23/28 lymph nodes positive for metastatic carcinoma	BRAF K601N	n/a	+	n/a	+	+	+	+

Figure 3.3. Vaccinia virus replication in a metastatic cutaneous melanoma model. (A) Following surgical excision, a specimen was removed from the surface of this in-transit cutaneous melanoma metastasis (Patient 12-2016), which was histologically-confirmed via hematoxylin and eosin staining (B), as well as other relevant diagnostic stains. This specimen was used to generate a primary monoculture of cells (C), which were confirmed to express the diagnostic markers MelanA, Tyrosinase, and S100 by RT-PCR (D) and at the protein level (data not shown). Wild-type strains of vaccinia virus were used to infect punch biopsy cores of the freshly-excised tumour specimen (E; input: 1×10^4 plaque forming units) as well as to probe the replication kinetics of distinct strains on the tumour-derived primary monoculture via a multi-step growth curve (F; multiplicity of infection 0.01). Error bars indicate the s.d. amongst replicates (n = 4). (One-way ANOVA, ****$P < 0.0001$; statistical annotations in *F* represent the variance between Copenhagen and the other strains studied)

A

B

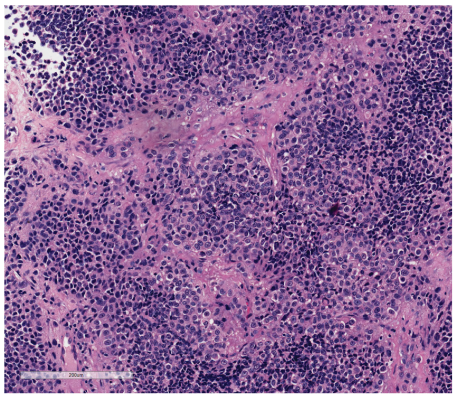

C

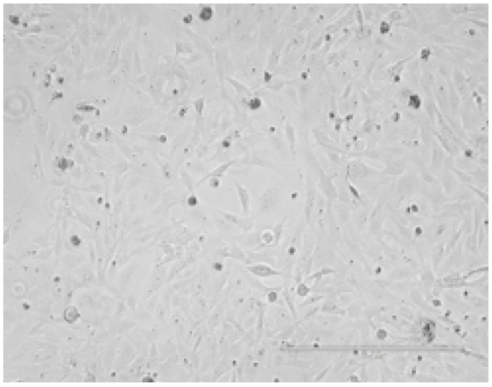

D

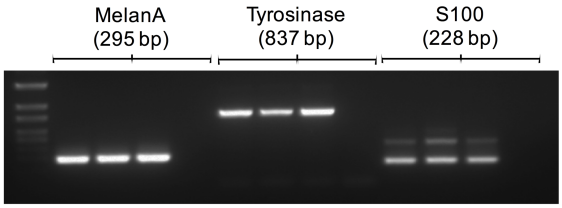

1) SK MEL 28
2) UACC 62
3) Melanoma-Pt. 12-2016
4) H_2O

E

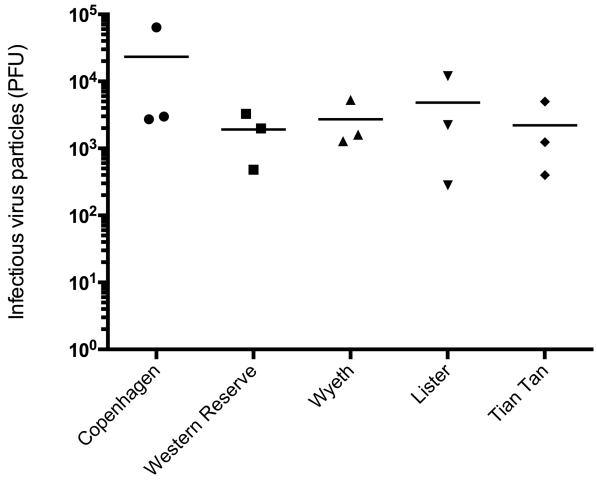

F

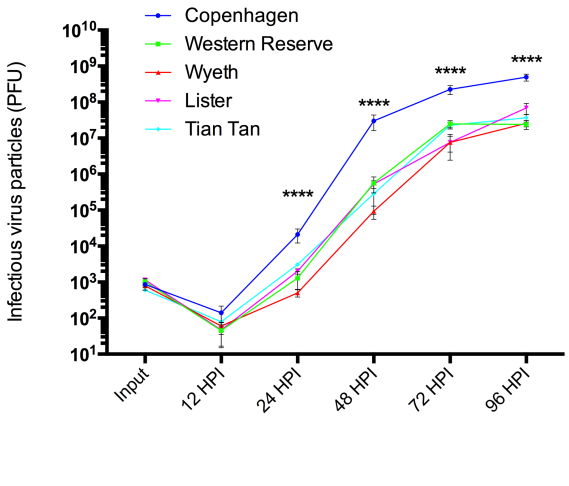

Figure 3.4. Vaccinia virus replication in inguinal lymph node metastasis melanoma model. (A) Following surgical excision, a specimen was removed from the center of this in-transit inguinal lymph node metastasis (Patient 13-2016) so as not to disturb any potential histologic margins of invasion. (B) Representative sampling allowed the tumour architecture of this specimen to be histologically-confirmed via hematoxylin and eosin staining. This specimen was used to generate a primary monoculture of cells (C), which were confirmed to express the diagnostic markers MelanA, Tyrosinase, and S100 by RT-PCR (D). Wild-type strains of vaccinia virus were used to infect punch biopsy cores of the freshly-excised tumour specimen (E; input: 1×10^4 plaque forming units) as well as to probe the replication kinetics of distinct strains on the tumour-derived primary monoculture via a multi-step growth curve (F, multiplicity of infection 0.01). Error bars indicate the s.d. amongst replicates (n = 4). (One-way ANOVA, ****$P < 0.0001$, **$P < 0.01$; statistical annotations in *F* represent the variance between Copenhagen and the other strains studied)

A

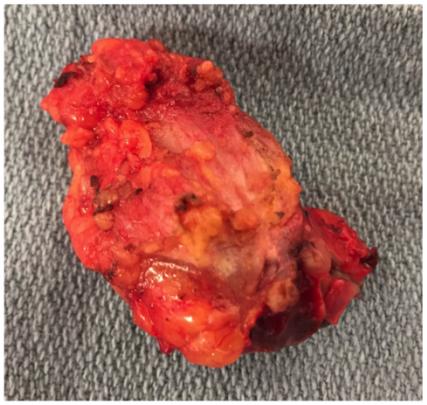

B

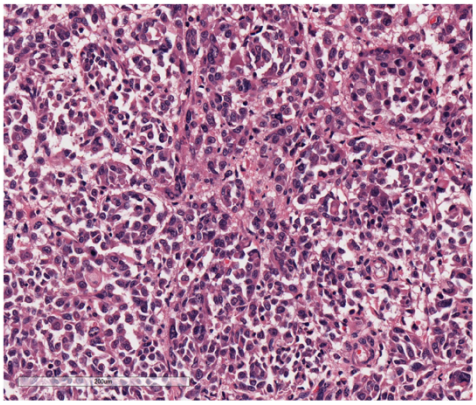

C

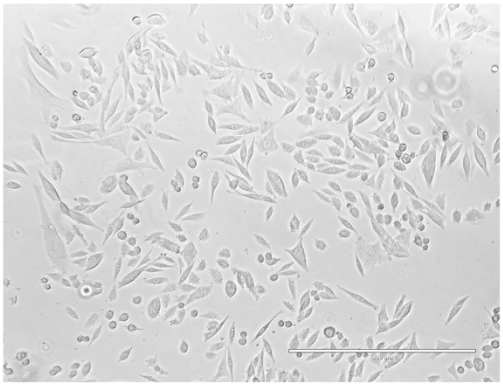

D

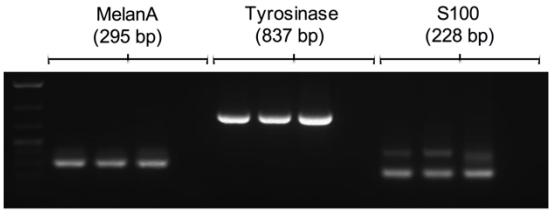

1) SK MEL 28
2) UACC 62
3) Melanoma-Pt. 13-2016
4) H_2O

E

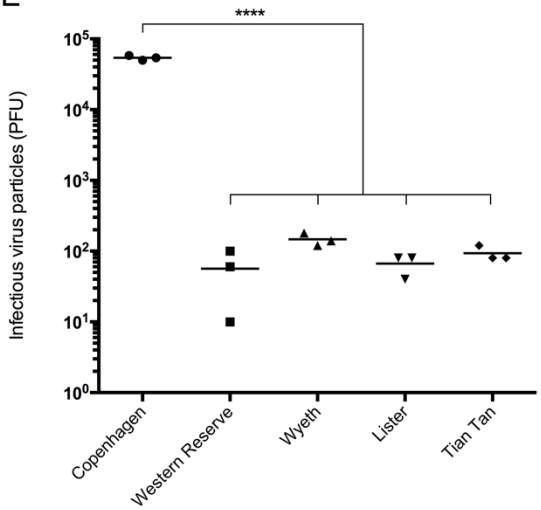

F

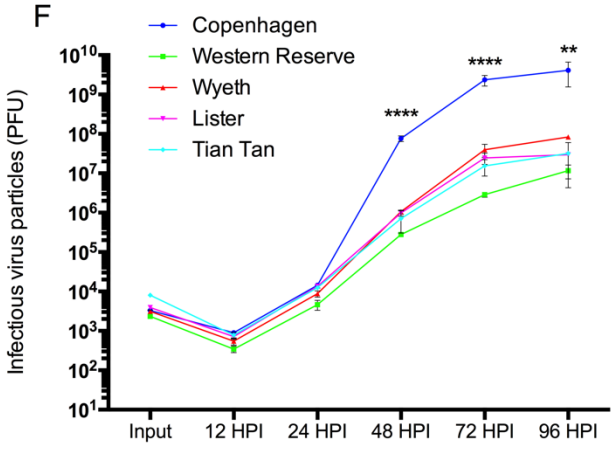

observed, and these primary cultures were found to express select melanoma diagnostic markers at the RNA level (Figures 3.3D, 3.4D). Upon obtaining each of these tissue specimens, 2-mm tumour cores were excised and each of the clinical candidate VACV strains investigated in this study were used to infect these tissues *ex vivo* (Figures 3.3E, 3.4E). Results were variable with relative equal output observed in Patient 12-2016 (Figure 3.3E) while nearly 1,000-fold higher output of Copenhagen observed in Patient 13-2016 (Figure 3.4E). Finally, multi-step growth curves were performed on the primary cultures generated from these patients – in both cases, Copenhagen is shown to have a significant growth advantage over the other wild-type strains investigated.

3.1.3. In vivo replication

With greater replication of Copenhagen when compared to the other clinical candidate strains observed *in vitro* in both immortalized and primary cancer cell lines, as well as *ex vivo* in fresh human melanoma tissues, virus replication was studied *in vivo*. The human melanoma cell line M14 was used to generate tumours in female CD1 nude mice, which were infected with individual wild-type strains of VACV as well as the current leading VACV clinical candidate ΔTK-Wyeth. The mice were sacrificed and tumours collected 72 hours post-infection, and virus output was determined by standardized plaque assay; while Copenhagen graphically appeared to replicate to a greater extent *in vivo* than each of the other strains, it reached statistical significance when compared to four of five additional strains, with the Tian Tan strain being the outlier (Figure 3.5A). By immunohistochemistry analysis, a pan-tumour spread of VACV-Copenhagen can be observed with a central region of extensive necrosis after 72 hours of virus infection (Figure 3.5B). This photomicrograph provides an interesting representation of the potential for VACV spread *in vivo*,

Figure 3.5. The replication of distinct strains of vaccinia virus in an *in vivo* melanoma model. The flanks of nude mice were implanted with bilateral sub-cutaneous M14 cells and allowed to reach approximate dimensions of 5 x 5 mm. Distinct vaccinia virus strains were then used to infect tumours via intratumoural injection of 1 x 10^7 plaque forming units of each respective virus strain. 72 hours post-infection, animals were sacrificed, tumours were collected and processed, and the recovered virus was determined by plaque assay (A). Representative photomicrographs of a Copenhagen-infected tumour (B) immunohistochemically treated with (i) a secondary control, or (ii) anti-vaccinia virus antibody demonstrates a pan-tumour infection with the Copenhagen strain of vaccinia virus. Error bars indicate the s.d. amongst at least 3 individual replicates. (One-way ANOVA, *$P < 0.05$)

A

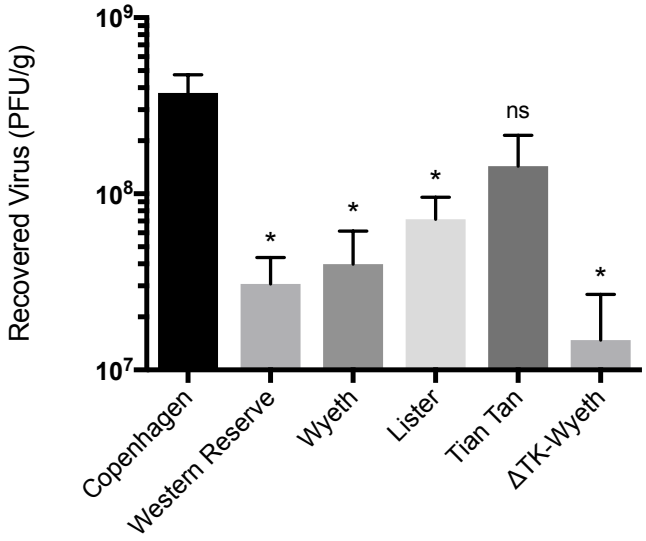
Recovered Virus (PFU/g)
10^9
10^8
10^7
ns
*
*
*
*
Copenhagen
Western Reserve
Wyeth
Lister
Tian Tan
ΔTK-Wyeth

B

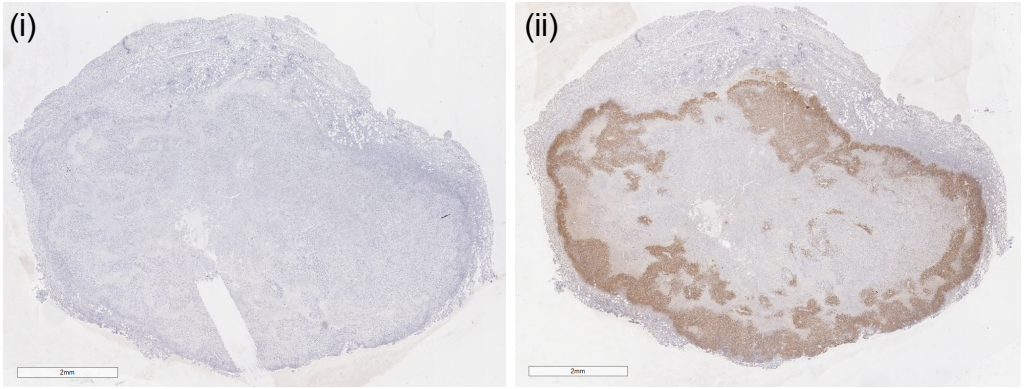
(i)
(ii)
2mm
2mm

however an immunohistochemistry-based study would have to be designed and performed systematically to make conclusions regarding cross-strain differential viral replication *in vivo*.

3.1.4. In vitro cytotoxicity and spread

To build upon the data that was generated across complementary models demonstrating the growth advantage of VACV-Copenhagen, it was decided to pursue an analysis of plaque size formation by the unique wild-type virus strains. Data from plaque size assays can provide an understanding of the cytotoxic potential of a virus strain in question over the chosen time period. A semi-solid overlay of carboxymethylcellulose was used, which minimizes any distant cell-to-cell spread that may be due to differential EEV production. Quantification of plaques produced by each strain revealed that those produced by VACV-Copenhagen are significantly larger than those produced by each of the other wild-type strains in this study plus the clinical candidate ΔTK-Wyeth (Figure 3.6). Interestingly, there was no differential plaque size phenotype produced by any of the other virus strains in this study when compared to one another.

There are two distinct forms of infectious VACV progeny that can be produced from an infected cell: IMV and EEV. Some evidence has suggested that a virus with greater propensity for EEV production may indeed be better equipped to evade host immune neutralization and therefore spread systemically to distant sites of disease[97,98]. Therefore, as an extension of the plaque size assays, an effort was made to understand the EEV-producing propensity of each of the wild-type VACV strains in this study. EEV is released from the infected cell via the polymerization of actin tails that propel its dissemination. Therefore, *in vitro*, the majority of infectious progeny in the supernatant of a monoculture is EEV that has been released, which can be quantified with a fractional titration approach using standardized plaque assays. The results from this study are presented in Figure 3.7A; by 72 hours post-infection, VACV-Copenhagen and VACV-Tian Tan

Figure 3.6. Viral-induced plaque size formation in HeLa cells. Individual strains of vaccinia virus were used to infect HeLa cells and plaque formation was allowed to proceed for 48 hours. Plaque diameters were individually measured. Results shown indicate the measurements of 20 individual plaques. (One-way ANOVA, **P < 0.01, ****P < 0.0001; statistical annotations represent the variance between Copenhagen and the other strains studied as no statistically-significant differences were otherwise observed)

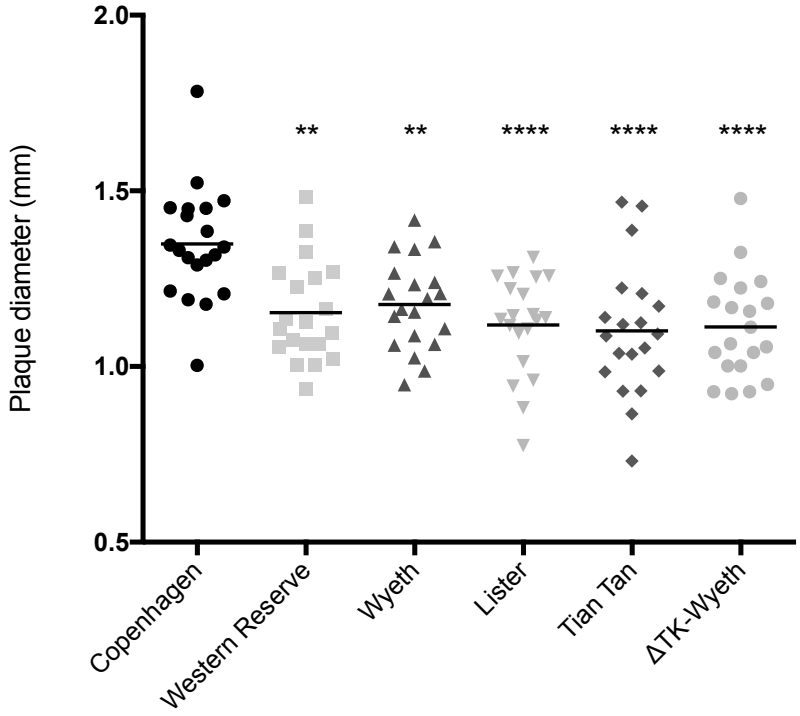
Plaque diameter (mm)
2.0
1.5
1.0
0.5
**
**
****
****
****
Copenhagen
Western Reserve
Wyeth
Lister
Tian Tan
ΔTK-Wyeth

Figure 3.7. Strain-specific extracellular enveloped virus production. Following the strain-specific infection of HeLa cells (MOI 0.01), fractional titration indicates the relative amounts of extracellular enveloped virus produced by each individual strain of vaccinia virus (A). Representative images of HeLa cells 96-hours post-infection qualitatively demonstrate the ability of individual virus strains to produce appreciable extracellular enveloped virus (B). Error bars indicate the s.d. from 3 independent experiments. Statistical annotations represent the variance between Copenhagen or Tian Tan, respectively, and each of Western Reserve, Wyeth, and Lister independently; there were no statistically-significant differences observed otherwise. (One-way ANOVA, ***$P < 0.001$, **$P < 0.01$, *$P < 0.05$)

A

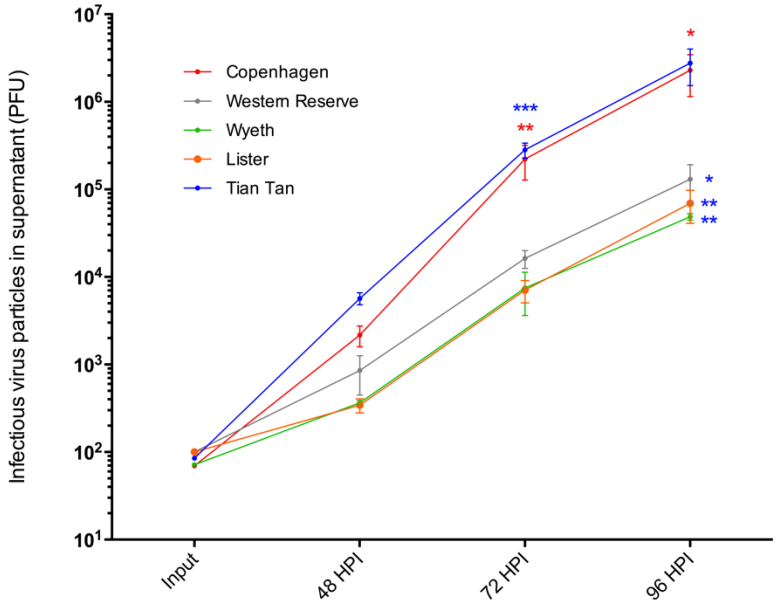
Infectious virus particles in supernatant (PFU)
10^7
10^6
10^5
10^4
10^3
10^2
10^1
Copenhagen
Western Reserve
Wyeth
Lister
Tian Tan
*
***
**
*
**
**
Input
48 HPI
72 HPI
96 HPI

B

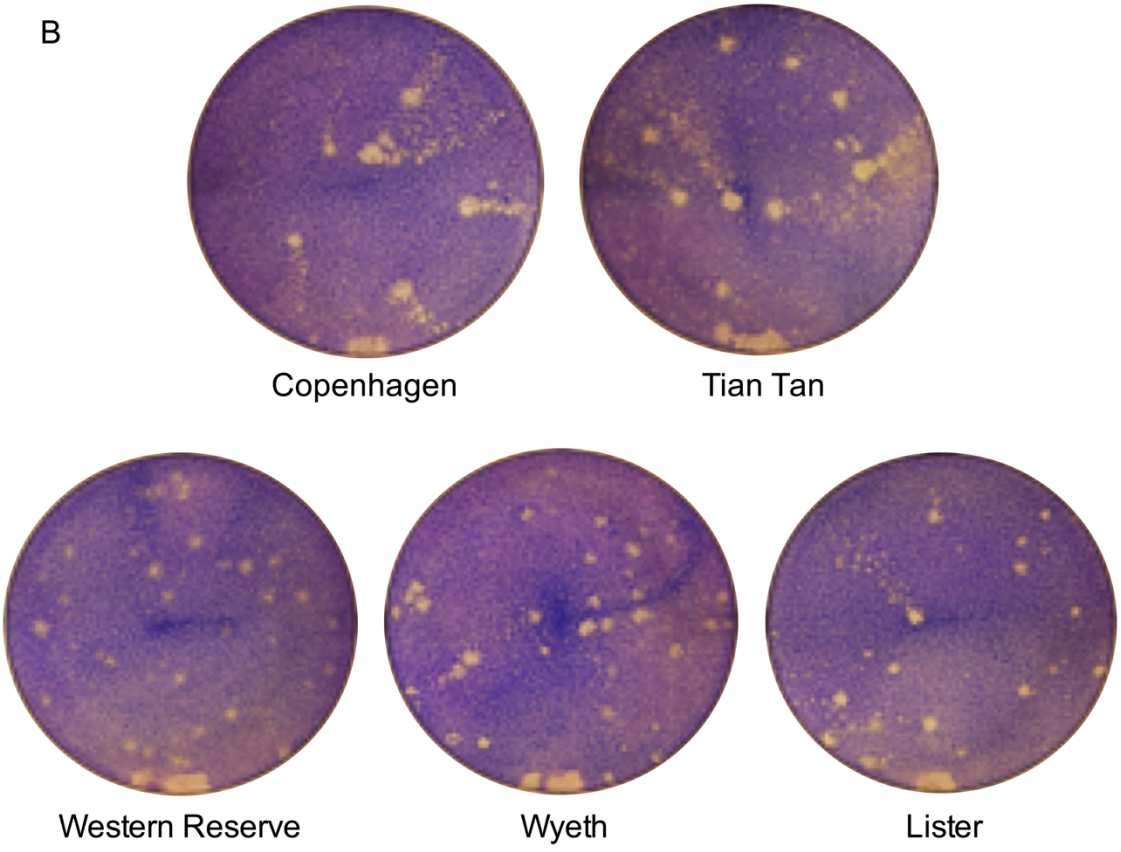
Copenhagen
Tian Tan
Western Reserve
Wyeth
Lister

produce significantly increased EEV progeny compared to each of the other wild-type strains in this study, a relationship that extends to the 96 hours post-infection time point. These results are accompanied by images of monocultures of HeLa cells that were infected with each of the listed viruses and liquid-overlayed for 96 hours (Figure 3.7B). When EEV are released from infected cells during the course of virus replication and allowed to spread via convection currents due to the use of a liquid overlay, satellite plaques can form a characteristic "comet" pattern, which can be observed in the VACV-Copenhagen and VACV-Tian Tan wells, but not to any appreciable extent in any of the other virus-infected wells.

The results presented thus far have contributed to our understanding of the phenotypic properties of VACV and how unique properties can be selected for based on the desired characteristics of a next-generation clinical candidate OV. Given the unsatisfactory clinical responses of current VACV-based candidate OVs and the poor rationale for the past selection of certain wild type backbone strains upon which to build, we thought that a systematic bioselection of available clinical candidate strains was a prudent approach. The data presented thus far demonstrates the inherent *in vitro*, *ex vivo*, and *in vivo* attenuation of the majority of clinical candidate VACV backbones. Therefore, the decision was made to focus on VACV-Copenhagen as the backbone upon which our next-generation clinical candidate OV will be built. However, the complexity of VACV contributes to the field's current incomplete understanding of its products, and a comprehensive functional genomics approach to the study of VACV has yet to be completed. A better tool is required to more completely understand OV-relevant properties of VACV on a gene-by-gene basis. The latter portion of this research project will describe studies designed to bridge this knowledge gap.

3.2. Transposon-based insertional mutagenesis of vaccinia virus-Copenhagen

3.2.1. Design of transposable element and construction of clonal library

A previously-developed TE-based mutagenesis approach to the study of VACV-Copenhagen was optimized and utilized to study individual gene components of this virus. The TE mutagenesis was completed as described above, however an NGS-based study of mutagenized virus allowed the structure of this insert to be confirmed. The results of this analysis are schematized in Figure 3.8A, which presents the important functional components that have allowed this research project to proceed. Firstly, the TE is based on the *PiggyBac*™ transposon system, which is known to target TTAA loci in the target genome for insertion, and indeed uses the sequence of *PiggyBac*™ transposase supplied *in trans* to the system on a unique vector. Any TTAA site in the VACV-Copenhagen genome is a theoretical insertion site when using this approach, and Figure 3.8A reflects this. The mobile genetic element is flanked on either side by inverted terminal repeats. Immediately downstream of the 5' ITR is a stop sequence, followed by a genetic linker sequence and a synthetic VACV early/late promoter that initiates transcription of the mCherry gene within the TE. A second stop sequence is present downstream of mCherry and before the 3' ITR.

Following the infection of HeLa cells for 16 hours, fluorescence-activated cell sorting was utilized as described above to sort individual mCherry-expressing cells into individual wells of 96-well plates already containing cells. The results of this were the expansion of potentially unique (due to insertional mutagenesis) VACV-Copenhagen-based virus clones that could be visualized due to their TE mCherry expression; a representative example of such a plate can be observed in Figure 3.8B. As described, mCherry-positive viruses were further expanded, plaque-purified, and purified through a sucrose gradient to generate a working VACV library of unique clones. NGS

Figure 3.8. Transposable element insertional mutagenesis of vaccinia virus-Copenhagen. (A) A schematic of the transposable element used in this research project is presented, which is able to insert at TTAA sites throughout the genome. (B) Flow cytometry-based sorting allowed potentially unique individual virus clones to be separated into HeLa cell-containing individual wells of 96-well plates, which then supported viral replication. Following infection, mCherry-expressing cells were harvested, expanded, and prepared for next-generation sequencing analysis.

A

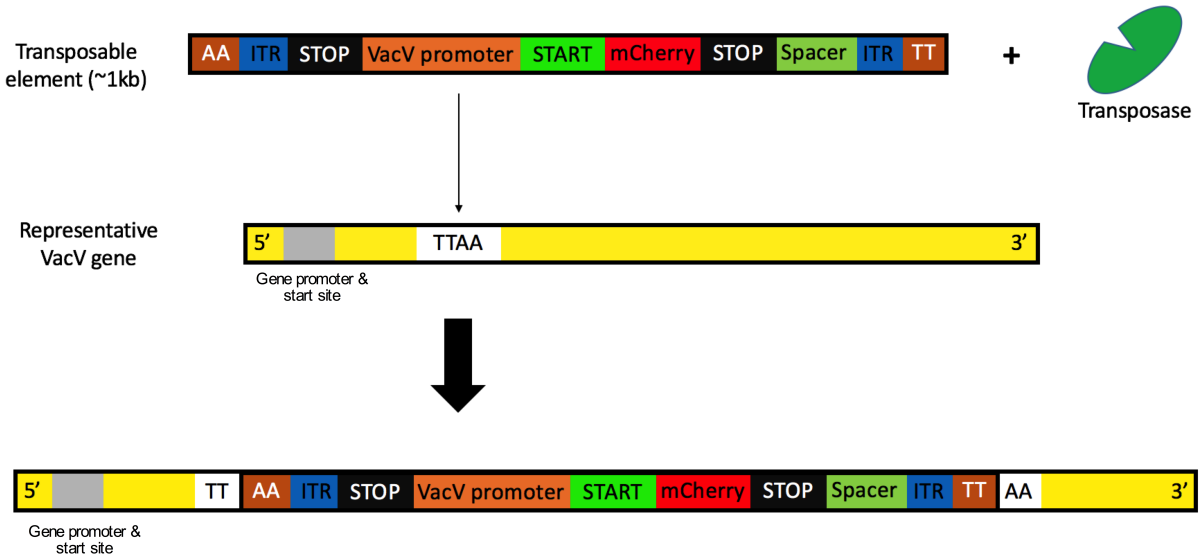
Transposable element (~1kb)
AA
ITR
STOP
VacV promoter
START
mCherry
STOP
Spacer
ITR
TT
+
Transposase
Representative VacV gene
5'
TTAA
3'
Gene promoter & start site
5'
TT
AA
ITR
STOP
VacV promoter
START
mCherry
STOP
Spacer
ITR
TT
AA
3'
Gene promoter & start site

B

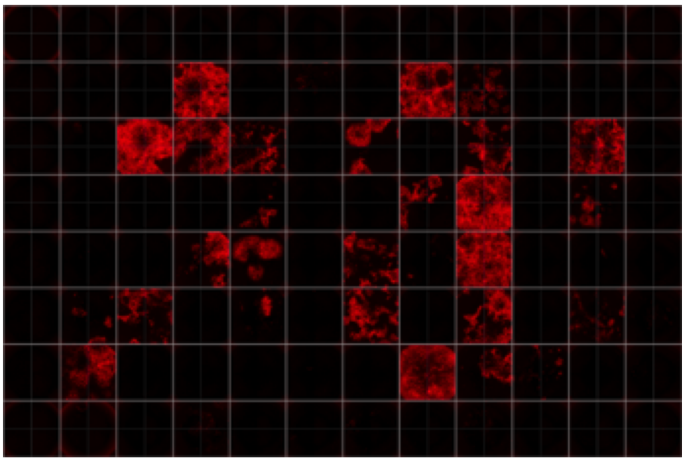

data allowed genetically redundant clones to be discarded, which resulted in a working library of 89 unique VACV-Copenhagen mutant clones. Of the 89 clones in this library, there are eight that contain intergenic insertions. Of the remaining 81 clones, there are 52 unique genes into which the TE has inserted. There are 19 genes that have been targeted by the TE in more than one place; multiple insertion mutant clones are therefore present in the working library for such genes. The overall landscape of the insertion mutants that have been used for this research project has been schematized in Figure 3.9. Of note in the distribution of insertion mutants in this working library is the propensity for insertion towards the genome extremities despite there being a relatively equal distribution of TTAA sites throughout the VACV genome. Figure 3.10 represents this, as well as the complementary paucity of observed TE insertion sites in the central region of the genome.

3.2.2. Functional effects of transposon-based insertional mutagenesis

We were able to generate VACV genomic sequencing data to verify the presence of the TE at unique sites in this library. Selection of novel clones was based on mCherry expression, so this genomic sequencing data provided specificity to what was already observed based on transgene expression. The questions of how this TE was processed both at the level of transcription and also how it affects the protein products of mutagenized genes still remain. To interrogate the effects of TE insertion on transcription, reverse transcription PCR experiments were performed in which sets of primers were designed to target regions in selected genes that surrounded the known insertion site based on NGS data. Figure 3.11 presents the results from these experiments. For each selected clone, primers targeting VACV-Copenhagen *C9L* were used as a non-mutagenized virus gene control, which can be observed in lane 2 of the control gel, as well as in each respective clone's gel in lane *iv*. For each selected gene labeled underneath that gene's clone in Figure 3.11, the primers used in lanes *i*, *ii*, and *iii* were as outlined in the schematic at the top of the figure; what

Figure 3.9. Circularized schematic of insertion loci within vaccinia-Copenhagen. Each gene within the vaccinia-Copenhagen genome is represented in this schematic by a box relative to its size. Boxes that are coloured red indicate genes that have been interrupted in at least one place by insertion of the transposable element. Boxes coloured yellow were inserted into, however to a secondary extent compared to the primary insertion sites within their respective samples. Green lines indicate intergenic sites of insertion. Non-interrupted genes are coloured blue. The unique clones highlighted in this figure compose the working library for this research project, which consists of 89 unique virus clones that span 52 unique vaccinia-Copenhagen genes and 8 mutants with integration of the transposable element in intergenic regions.

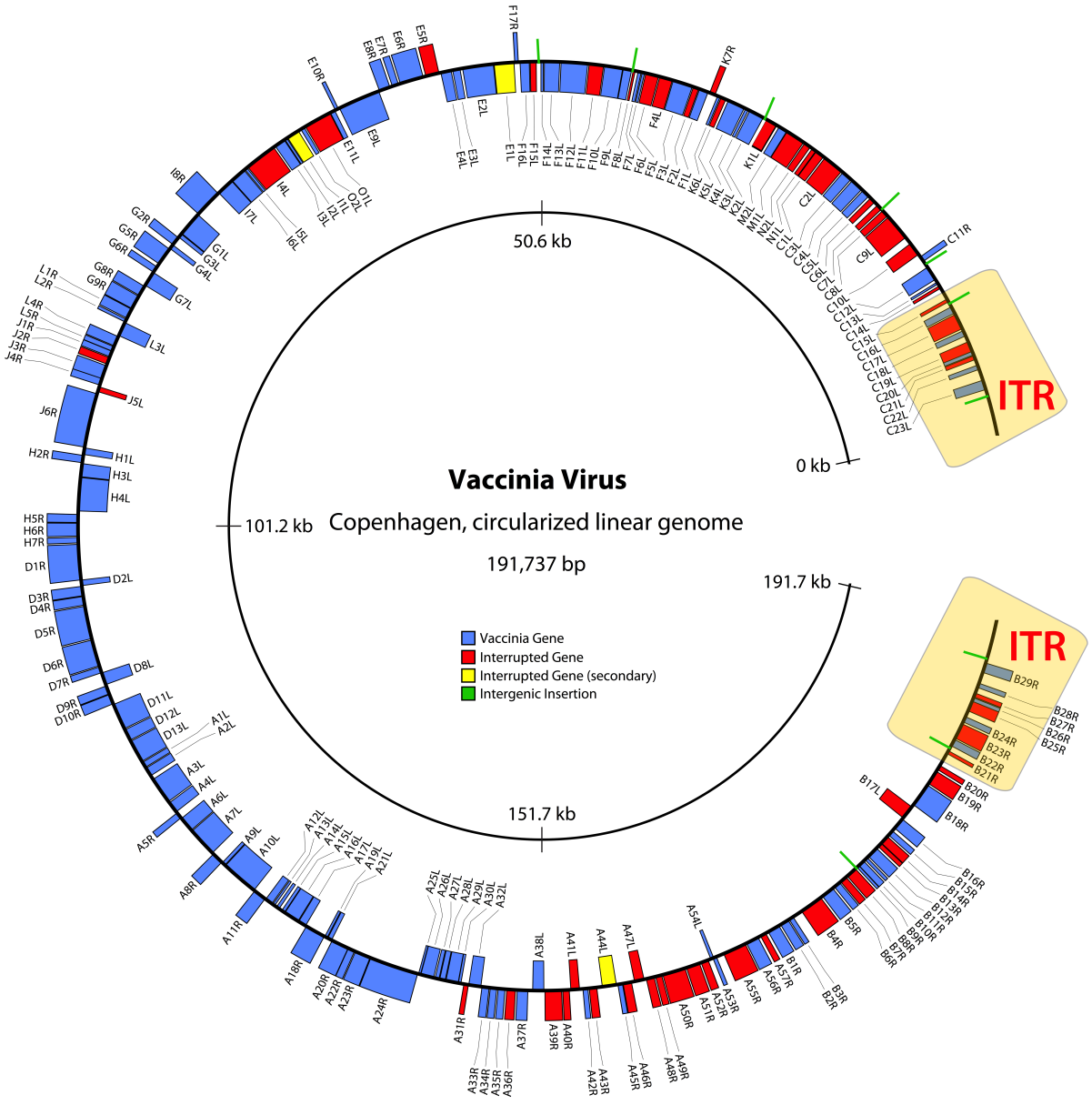
Vaccinia Virus
Copenhagen, circularized linear genome
191,737 bp
0 kb
50.6 kb
101.2 kb
151.7 kb
191.7 kb
ITR
ITR
Vaccinia Gene
Interrupted Gene
Interrupted Gene (secondary)
Intergenic Insertion

Figure 3.10. Preferential insertional mutagenesis occurs at genome extremities. (Top) A schematic indicates the frequency of TTAA sites, and thus possible transposable element integration sites, across the vaccinia virus-Copenhagen genome. Each bar represents 1kb of the genome, and the y-axis scale represents the frequency of TTAA sites within that 1kb of genome. (Bottom) A schematic outlining observed TTAA integration events within each respective 1kb of genome.

Distribution of TTAA motifs in vaccinia-Copenhagen

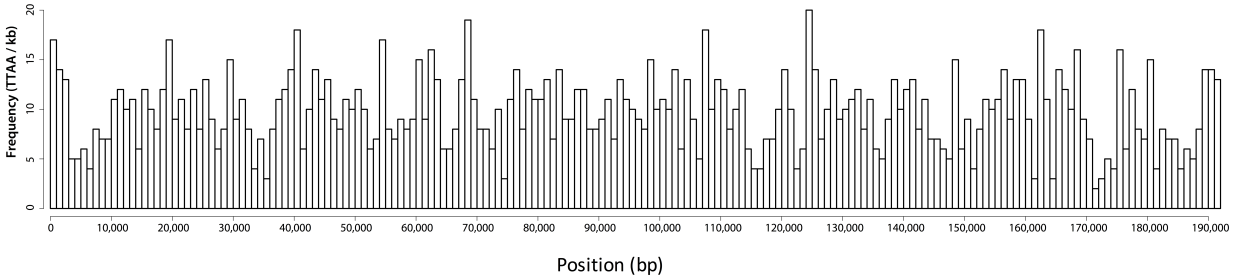

Insertion frequency of transposable element in vaccinia-Copenhagen

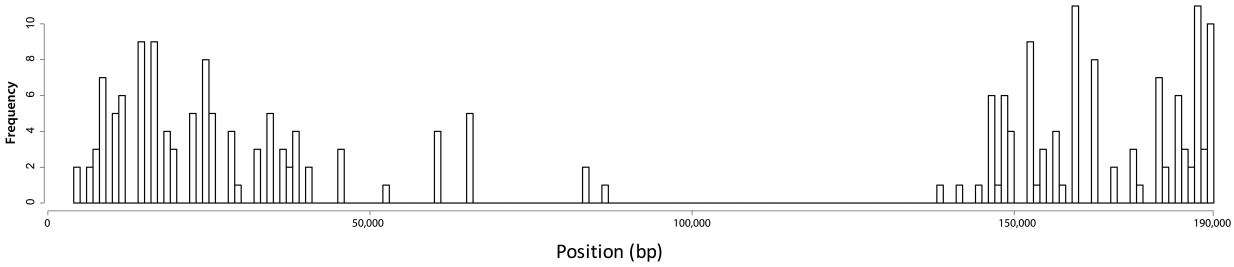

Figure 3.11. Transposable element integration at the level of messenger RNA. Reverse-transcription PCR of virus following 8-hour infection (MOI 10) of HeLa cells with the respective virus clones highlighted below each image. Primers were utilized that span the site of transposable element integration. The transposable element is approximately 1kb in size.

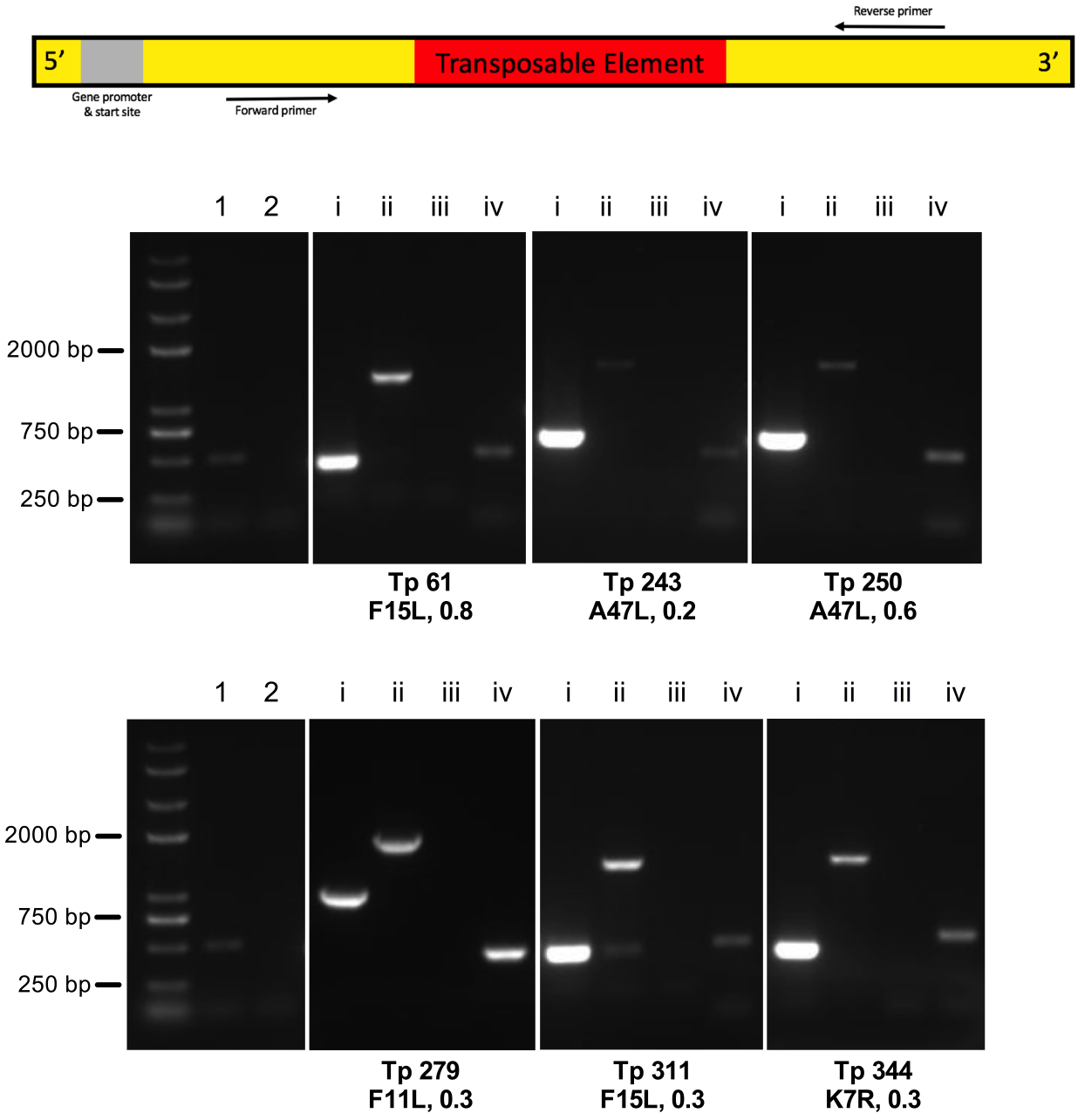

1. Wild-type Copenhagen cDNA - C9L primer pair
2. Uninfected cellular control cDNA - C9L primer pair

i. Wild-type Copehagen cDNA - gene-specific primer pair
ii. cDNA from select library clone - gene-specific primer pair
iii. Uninfected cellular control cDNA - gene specific primer pair
iv. cDNA from select library clone - C9L primer pair

differed was the treatment conditions of original cells from which the original RNA was extracted – it was from wild-type Copenhagen-infected cells, from an infection of cells with the selected clone, or from uninfected cells, respectively. As can be observed by the shift of bands in each of the lanes *i* and *ii*, the approximately 1,000 bp transposable element is present at the level of the transcript in each of the select clones.

Following confirmation of insertion at both the genomic and transcriptomic levels, the next question was how this insertion affected translation of mutagenized genes. Assays were designed to probe the presence or function of the viral proteins following insertion of the transposable element. Immunoblotting was performed against the viral proteins F11, K7, and A36; in the case of F11, an affinity-purified antibody against the residues 101-120 was used, while an unpurified anti-serum against the full-length protein was used in the case of viral K7, and a polyclonal antibody against residues 142-214 was used for A36. When cells were infected at a MOI of 10 for eight hours with the select viruses labeled in Figure 3.12A, viral protein levels could be clearly detected with the probes mentioned above. When inserting into VACV-Copenhagen *F11L* approximately 30% of the way through the gene, the antibody used in this assay detected no production of protein. Similarly, when inserting into VACV-Copenhagen *K7R* approximately 30% of the way through the gene, full-length anti-K7 anti-serum was unable to detect the presence of any viral protein. Finally, when inserting in VACV-Copenhagen *A36R* approximately 90% of the way through the gene, the antibody used in this assay detected no production of protein. In each of these cases, there was also no truncated mutant proteins produced of smaller size detected. In all cases, these Western blot results suggest that insertional mutagenesis using the transposable element in this study leads to the knockout of viral protein.

To confirm this at the functional level, a functional assay was performed that has previously been optimized in the Bell laboratory[225]. VACV-Copenhagen B19 is a functional homologue of B18 in other VACV strains, which is known to be a secreted protein able to sequester Type I and II interferons. Furthermore, VSVΔ51 is a virus with known neutralization sensitivity to Type I and II interferons and is unable to productively infect cells in their presence. Therefore, the presence of a functional protein that is able to sequester these anti-viral cytokines would create an *in vitro* microenvironment that allows replication of VSVΔ51 to proceed. In this experiment, 786-O cells were infected with either wild-type Copenhagen or Tp 203 (B19R, 0.6); supernatants from these cultures were transferred onto fresh 786-O cells following overnight culture, and VSVΔ51 was used to inoculate. Several independent replicates and conditions were utilized, and Figure 3.12B presents representative results in which VSVΔ51 is able to robustly replicate in cells whose supernatant contains a functional VACV-Copenhagen B19, while not in those whose supernatants contains a functionally knocked out B19 (Tp 203). Taken together Figure 3.12 demonstrates that the production and/or function of select affected proteins in this randomly mutagenized VACV-Copenhagen library is eliminated.

3.2.3. Understanding the effects of insertional mutagenesis on viral replication

Following the creation of this library and the verification that the VACV-Copenhagen clones that compose it are functional, the challenge was to meaningfully screen each of them to advance our understanding of VACV from an OV perspective. Because each of the insertion mutants contains an mCherry transgene, early studies with these viruses revealed a fundamental characteristic that could be exploited for experimental gain: that red fluorescence increases with increasing length and/or multiplicity of infection (Figure 3.13A). This fluorescence can be reliably quantified with the appropriate tools, and it was observed that each virus produced the same shape

Figure 3.12. Protein-level mutagenesis observed in select insertion mutants. (A) Immunoblot analysis using probes against the vaccinia virus proteins F11, K7 and A36. Anti-beta-Tubulin is used as a cellular control. (B) Supernatant transfer experiment with functional (wild-type) or dysfunctional (Tp 203; *B19R*, 0.6) vaccinia virus-Copenhagen protein B19. Vesicular Stomatitis Virus-delta 51-GFP is able to productively infect cells in the presence of functional B19 (wild-type), while unable to productively infect cells when Type I and II interferons are present.

A

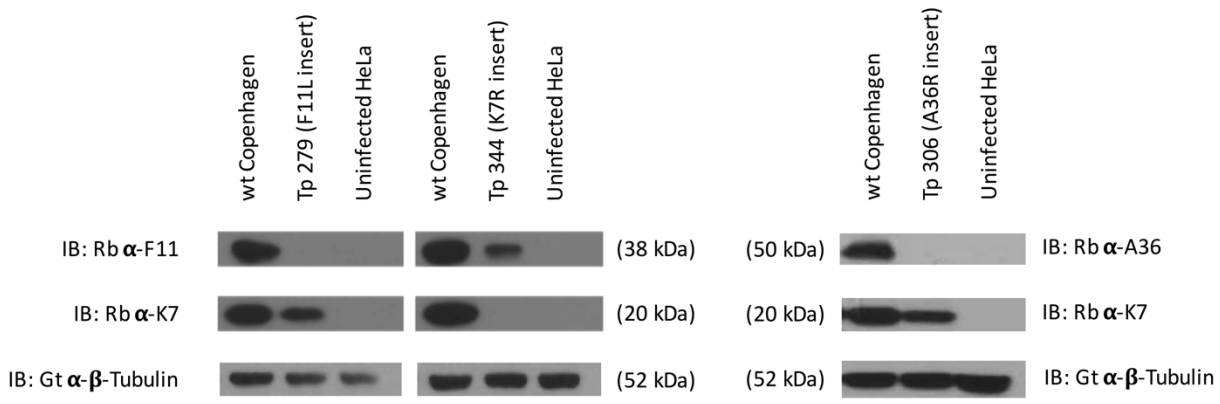
wt Copenhagen
Tp 279 (F11L insert)
Uninfected HeLa
wt Copenhagen
Tp 344 (K7R insert)
Uninfected HeLa
wt Copenhagen
Tp 306 (A36R insert)
Uninfected HeLa
IB: Rb α-F11
(38 kDa)
(50 kDa)
IB: Rb α-A36
IB: Rb α-K7
(20 kDa)
(20 kDa)
IB: Rb α-K7
IB: Gt α-β-Tubulin
(52 kDa)
(52 kDa)
IB: Gt α-β-Tubulin

B

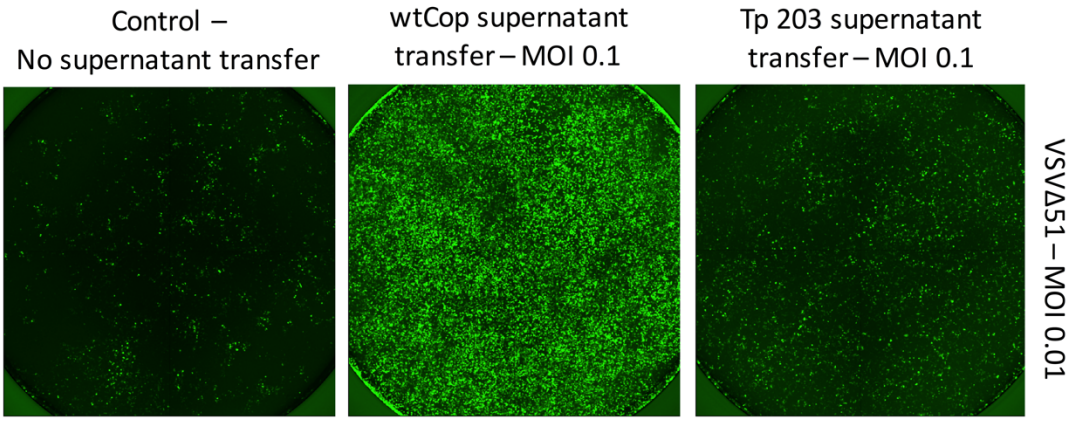
Control –
No supernatant transfer
wtCop supernatant
transfer – MOI 0.1
Tp 203 supernatant
transfer – MOI 0.1
VSVΔ51 – MOI 0.01

Figure 3.13. The direct relationship between infectious virus input and fluorescence intensity. (A) As virus infects cells of the read-out cell line, U-2 OS, fluorescence intensity increases proportionally to the concentration of virus and/or the time of infection. This intensity can be accurately quantified, plotted in a logarithmic fashion, and be observed to increase in a manner that is directly proportional to the amount of virus that is inputted to the system. (B) A virus-fluorescence intensity plot for Tp 69 (*C15L*; 0.7) and (C) A virus-fluorescence intensity plot for Tp 335 (intergenic), which are the lowest and highest fluorescence-producing viruses in this library, respectively. A non-linear power regression equation was generated by solving for the power regression.

A

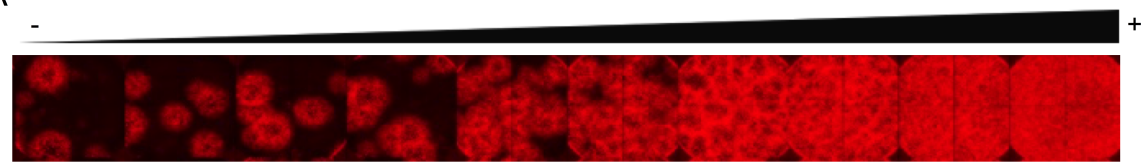
-
+

B

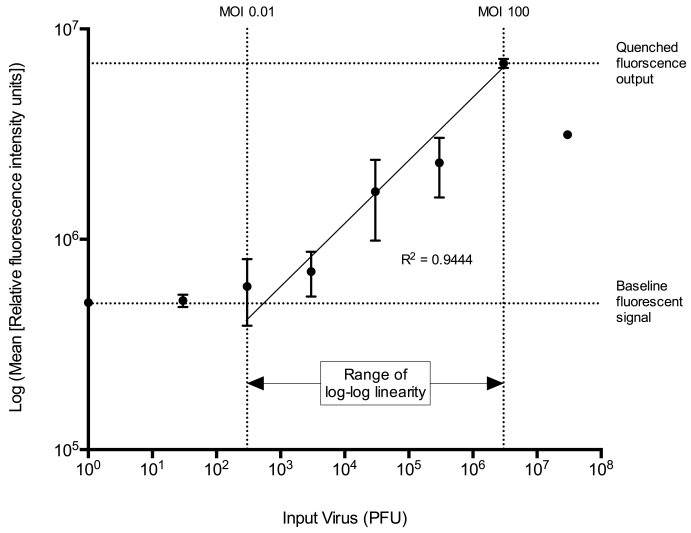
MOI 0.01
MOI 100
Quenched fluorscence output
Baseline fluorescent signal
R2 = 0.9444
Range of log-log linearity
Log (Mean [Relative fluorescence intensity units])
Input Virus (PFU)

C

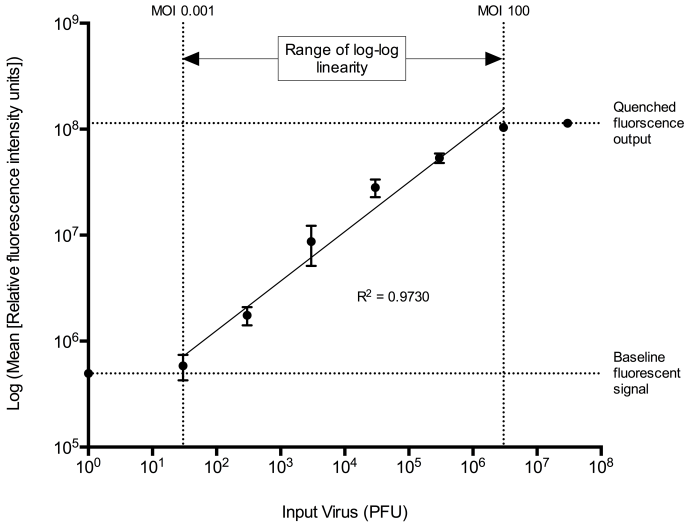
MOI 0.001
MOI 100
Range of log-log linearity
Quenched fluorscence output
Baseline fluorescent signal
R2 = 0.9730
Log (Mean [Relative fluorescence intensity units])
Input Virus (PFU)

of virus concentration vs. fluorescence intensity curve. Critically for this research project, it was observed that this is a direct relationship that begins shortly after the production of fluorescence and continues until the system (a single well in a tissue culture plate, for example) is fluorescently quenched. Interestingly, it was also observed that there is significant variability in the amount of fluorescence produced by each respective clone, and that this intensity of fluorescence is independent of the amount of virus in the system. In Figure 3.13B and C, representative virus vs. fluorescence intensity curves are presented for the viruses that were later found to reliably produce the lowest and highest values of fluorescence intensity – Tp 69 (C15L, 0.7) and Tp 335 (intergenic insertion), respectively. This shows that there is a range of fluorescent outputs that are produced by viruses in this library. What this makes clear is that direct output of fluorescent intensity by itself cannot be used as a surrogate for virus production when comparing across viruses. A method to gain meaningful replication data using this approach therefore needed to be optimized.

Typically, VACV virus concentration would be quantified on U-2 OS cells, which act as a standardized read-out cell line across experiments. As previously demonstrated in Figure 2.1, an assay was developed so that U-2 OS could be utilized as such, however the read-out itself would change from plaque assay to fluorescence output. Since comparing direct fluorescence output across virus clones is inappropriate given their unique fluorescence characteristics, and since the virus input versus fluorescence intensity curves are shaped characteristically as outlined in Figures 3.13B and C, it was determined that the fold-change from input virus to output virus could be utilized as a surrogate for virus replication. In work that optimized the utilization of such principles to screen a large panel of cells, cells from the patient-derived primary melanoma culture Patient 12-2016 were infected with each of the virus clones in the library at a MOI of 0.1 for 36 hours. Following this period of replication, U-2 OS cells were infected with both the same input virus

that originally infected the patient-derived primary cells as well as the output virus produced following 36 hours of infection. Fluorescence output was measured after 27 hours, and fold-change fluorescence was calculated from input to output; the greatest fold-change value was arbitrarily set at 1 and all other values plotted as a fraction of the greatest. These values are plotted in Figure 3.14A and range from approximately 0.16 to 1, representing a 6.33-fold change from the lowest producing virus to the highest producing virus. To confirm the validity of these results, standardized plaque assays were performed for each of the replicates used in the calculation of such values. In standard terms, these values correlated to a viral output of 4.9×10^4 PFU at the low end to a viral output of 3.1×10^5 PFU at the high end (Figure 3.14B). This represents a 6.25-fold change in virus output across the spectrum of viruses in the library. Interestingly, these optimization assays were performed on several cell lines (n = 9) using these conditions and this high degree of fold-change correlation was consistent between values of fluorescence output and PFU output in each case (data not shown).

As this data emerged, patterns of replication were observed that led to new questions about virus–host interactions and how genetically unique host cells may tolerate robust replication of some virus clones but not in others, while other cell lines may provide the optimal conditions for replication of other distinct virus strains. As such, this fluorescent-based approach to the study of viral replication was tailored for a larger panel of cell lines that represented diverse clinical indications and molecular subtypes of cancer. In addition, patient-derived cancer cell lines were studied, as were select normal cell lines. In total, 41 cell lines were screened using this approach; these cell lines include six patient-derived primary cultures of cancer, two normal (non-transformed) human cell lines, 31 members of the NCI-60 cell panel, as well as HeLa and U-2 OS

Figure 3.14. Differential replication of virus clones in a patient-derived melanoma cell line. (A) Cells derived from Patient 12-2016 were used to assess differential replication following 36-hour infection. Plotting fold-change of fluorescence demonstrates significant replication variability amongst unique viral clones. Red and green bars denote the poorest and best replicating clones, respectively. (B) By traditional titration methods, the difference in virus output following 36-hour infection is plotted for those two clones. (One-way ANOVA was performed following titration by plaque assay)

A

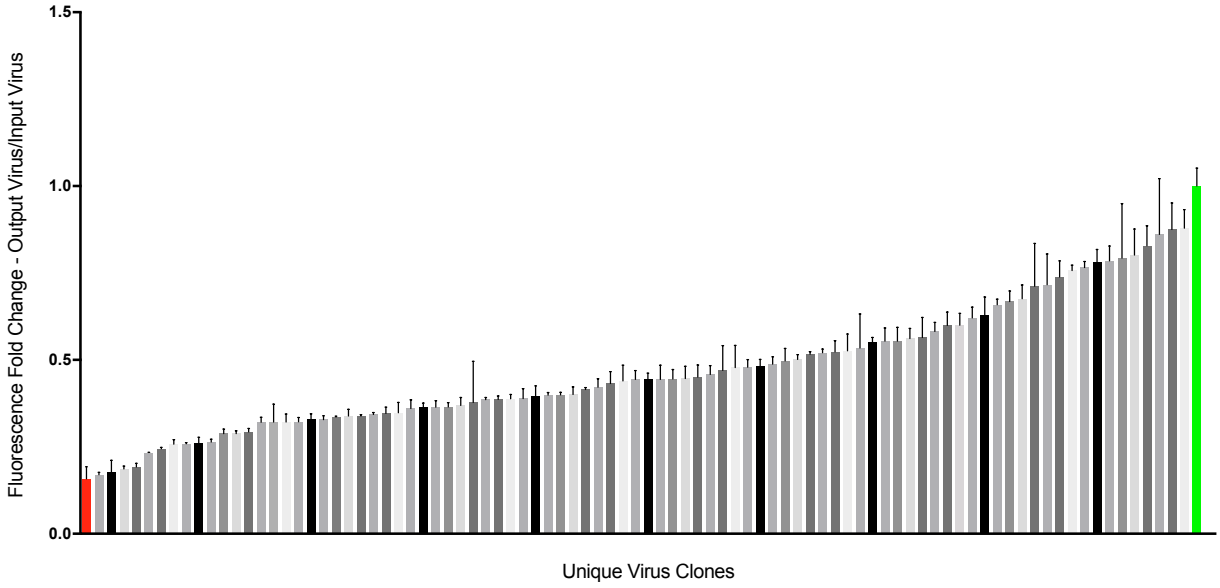
Fluorescence Fold Change - Output Virus/Input Virus
1.5
1.0
0.5
0.0
Unique Virus Clones

B

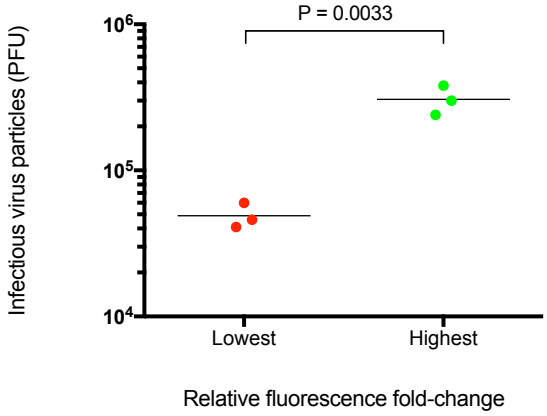
P = 0.0033
Infectious virus particles (PFU)
10^6
10^5
10^4
Lowest
Highest
Relative fluorescence fold-change

cells. The final output from the cancer cell lines in this experiment is presented in the form of a heat map in Figure 3.15 in which a green box represents a virus clone that is amongst the best replicating viruses in the library for a given cell line and a red box represents a virus clone that is amongst the poorest-replicating viruses in the library for a given cell line. The replication data has been normalized to input across the spectrum of cell lines, and as in the previous figure, the most robustly-replicating virus in each cell line was assigned a value of 1. Furthermore, in cases of multiple virus clones with insertions in the same gene, the clone that was plotted for graphical purposes is the clone with the site of insertion that is the most upstream in the gene following the viral gene start site. With the data presented in this manner, VACV-Copenhagen genes that most impact virus replication in this context can be easily identified.

3.2.4. Effects of insertional mutagenesis on cytotoxicity and viral spread

To complement this viral replication data, viral-induced cytotoxicity and cell-to-cell spread were studied by way of plaque size assays. The first attempt to understand the effects of insertional mutagenesis on plaque size were made in the human cervical carcinoma cell line HeLa. As a control in these experiments, wild-type Copenhagen was used as there was no dependence on transgene expression. The size of plaques formed by each of the virus clones were plotted and are presented in Figure 3.16A. The breadth of important data from this experiment is clear, however several specific observations have been highlighted in this figure. Interestingly, insertional mutagenesis of the VACV-Copenhagen gene *A47L* resulted in plaques that were significantly larger than any other mutants in the library. These clones have been highlighted green in Figure 3.16A and the phenotypic observations are nearly identical in each of the three mutants with *A47L* insertions (Tp 326, *A47L*, 0.1; Tp 243, *A47L*, 0.2; Tp 250, *A47L*, 0.6). On the other end of the spectrum, plaques formed by mutants with *F15L* interruptions have been highlighted in red in

Figure 3.15. Differential viral replication on a panel of 39 cancer cell lines. A schematic representation of relative replication of each clonal virus across a large panel of cancer cell lines. Each column represents an individual heat map, which allows clonal virus replication results within each cell line to be compared.

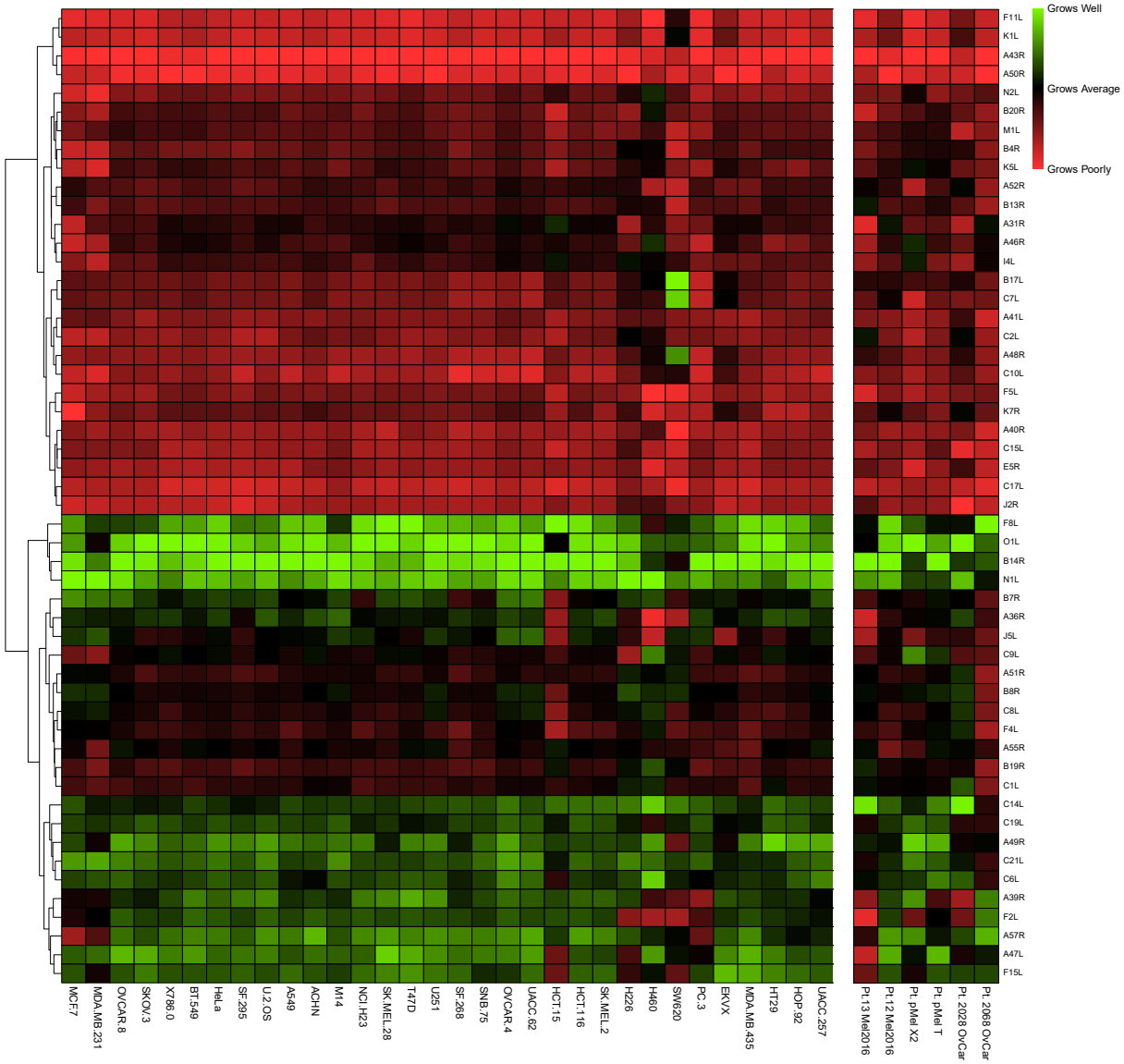
Grows Well
Grows Average
Grows Poorly
F11L
K1L
A43R
A50R
N2L
B20R
M1L
B4R
K5L
A52R
B13R
A31R
A46R
I4L
B17L
C7L
A41L
C2L
A48R
C10L
F5L
K7R
A40R
C15L
E5R
C17L
J2R
F8L
O1L
B14R
N1L
B7R
A36R
J5L
C9L
A51R
B8R
C8L
F4L
A55R
B19R
C1L
C14L
C19L
A49R
C21L
C6L
A39R
F2L
A57R
A47L
F15L
MCF7
MDA.MB.231
OVCAR.8
SKOV.3
X786.0
BT.549
HeLa
SF.295
U2.OS
A549
ACHN
M14
NCI.H23
SK.MEL.28
T47D
U251
SF.268
SNB.75
OVCAR.4
UACC.62
HCT.15
HCT.116
SK.MEL.2
H226
H460
SW620
PC.3
EKVX
MDA.MB.435
HT29
HOP.92
UACC.257
Pt.13.Mel2016
Pt.12.Mel2016
Pt. pMel X2
Pt. pMel T
Pt. 2028 OvCar
Pt. 2068 OvCar

Figure 3.16. Mean plaque size of virus clones in HeLa cells. (A) After 48 hours infection of HeLa cells, the diameter of formed plaques was measured and plotted. On the left of the figure, the red-blue-red-labeled data points correspond to the respective virus clones in (B). Similarly, the green-labeled data points on the right of *A* correspond to the *A47L* clones highlighted in green in figure (B). Results from independent plaque measurements are plotted (n = 20).

A

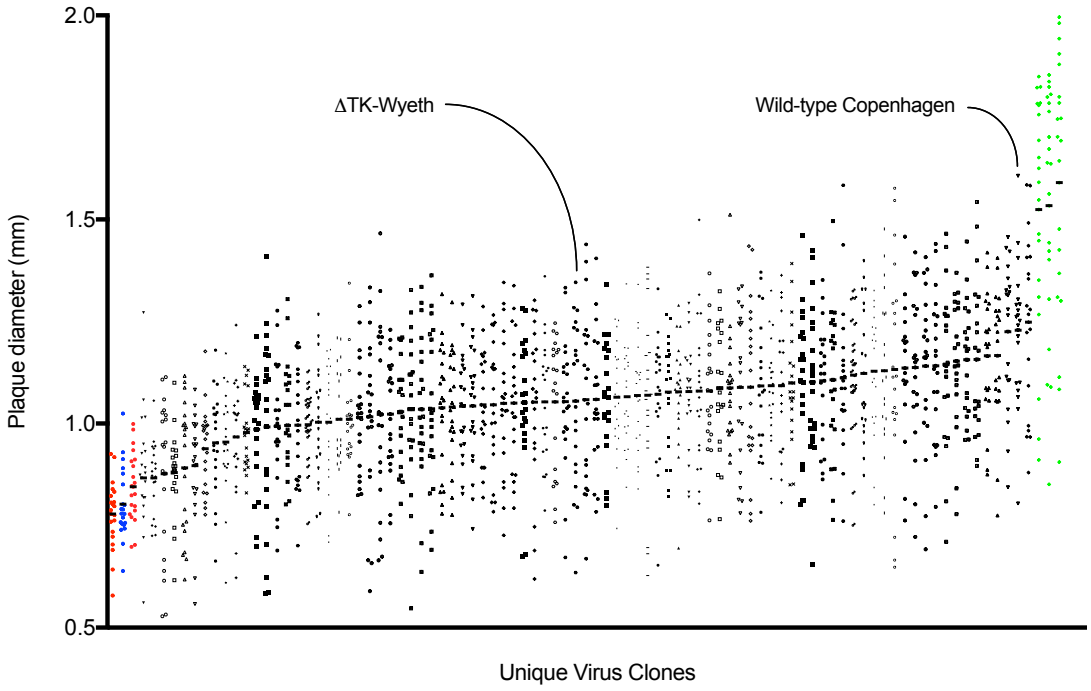
2.0
1.5
1.0
0.5
Plaque diameter (mm)
ΔTK-Wyeth
Wild-type Copenhagen
Unique Virus Clones

B

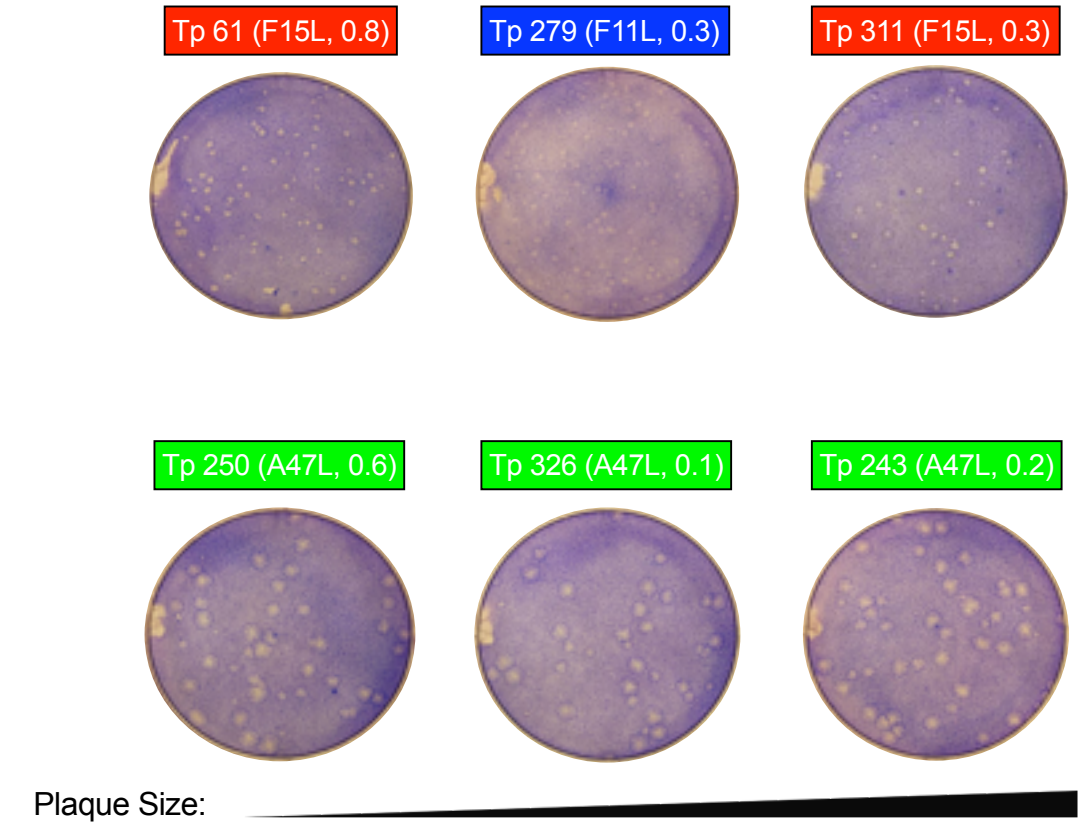
Tp 61 (F15L, 0.8)
Tp 279 (F11L, 0.3)
Tp 311 (F15L, 0.3)
Tp 250 (A47L, 0.6)
Tp 326 (A47L, 0.1)
Tp 243 (A47L, 0.2)
Plaque Size:

Figure 3.16A and are significantly smaller than wild-type Copenhagen. There are two mutants with such interruptions in this library (Tp 311, *F15L*, 0.3; Tp 61, *F15L*, 0.8), and both display the same plaque size phenotype in this experiment. Interestingly, the well-described VACV gene *F11L* is also represented in this library by insertional mutagenesis (Tp 279, *F11L*, 0.3) and the plaque phenotype observed is consistent with what would be expected of a F11 protein knockout, which is also consistent with the Western blot data presented in Figure 3.12A. Images of the plaques produced by each of the six virus clones discussed are presented in Figure 3.16B.

Given the striking results of studying plaque size in HeLa cells, similar studies were performed on additional cell lines. Figure 3.17A presents results from the same experiment on the human melanoma cell line M14. M14 cells are more sensitive to killing by VACV and cell-to-cell spread occurs more readily (as can be observed by the relatively large plaques in Figure 3.17B), however there is interestingly less infectious progeny produced from these cells when compared to HeLa cells. From these experiments, similar results were obtained as with HeLa cells – insertion mutants in VACV-Copenhagen *A47L* were observed to produce significantly larger plaques than any other clone in the library, and plaques produced by insertional mutagenesis of *F11L* and *F15L*, respectively, were small. Another interesting observation of note in this experiment was the relatively small plaques produced by the current leading VACV-based clinical candidate OV, ΔTK-Wyeth. As previously discussed, this virus is built on the VACV-Wyeth backbone, and such results are consistent with those observed with wild-type Wyeth (Figure 3.6).

3.3. Investigating the role of vaccinia virus genes *F15L* and *A47L*

3.3.1. Effects of pathogen-host interactions on viral cytotoxicity and spread

These studies were expanded on the human prostate cancer cell lines PC-3 and DU-145. Including the results discussed in Figures 3.16 and 3.17, quantitative values for plaque sizes

Figure 3.17. Mean plaque size of virus clones in a melanoma model. (A) After 48 hours infection of M14 melanoma cells, the diameter of formed plaques was measured and plotted. On the left of the figure, the red- and blue-labeled data points represent the colour-correspondent virus clones highlighted in B with insertion sites in *F11L* and at different points in *F15L*, respectively. Similarly, the green-labeled data points on the right of the figure correspond to the plaques formed by the *A47L* clones highlighted in green in figure B. Also, highlighted in A are the size of the plaques formed by ΔTK-Wyeth and wild-type Copenhagen strains. Plotted are results from independent plaque measurements (n = 20).

A

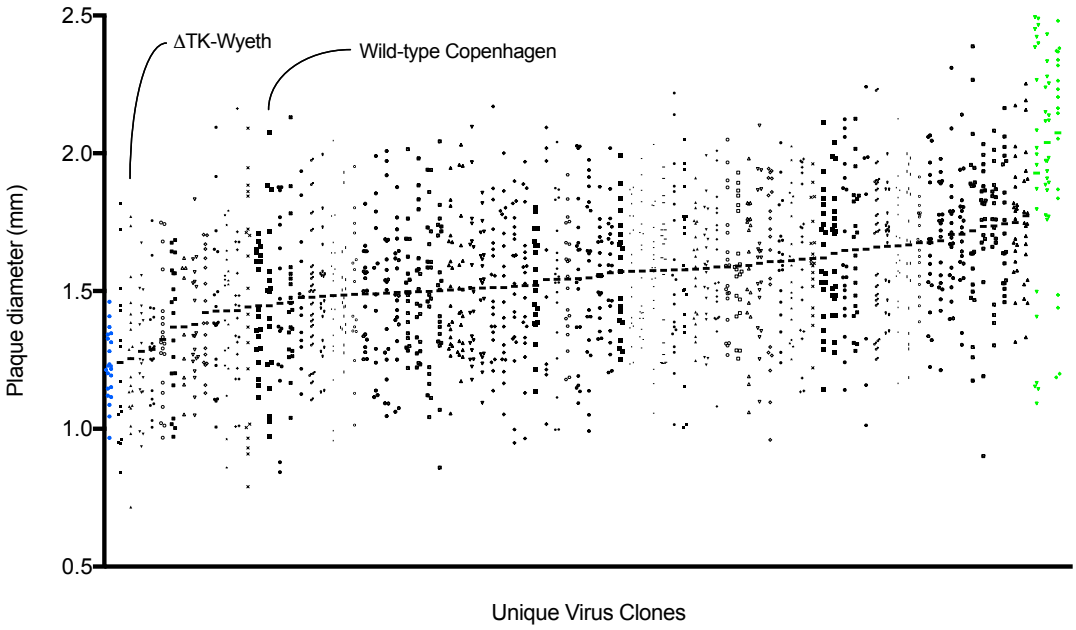
2.5
2.0
1.5
1.0
0.5
ΔTK-Wyeth
Wild-type Copenhagen
Plaque diameter (mm)
Unique Virus Clones

B

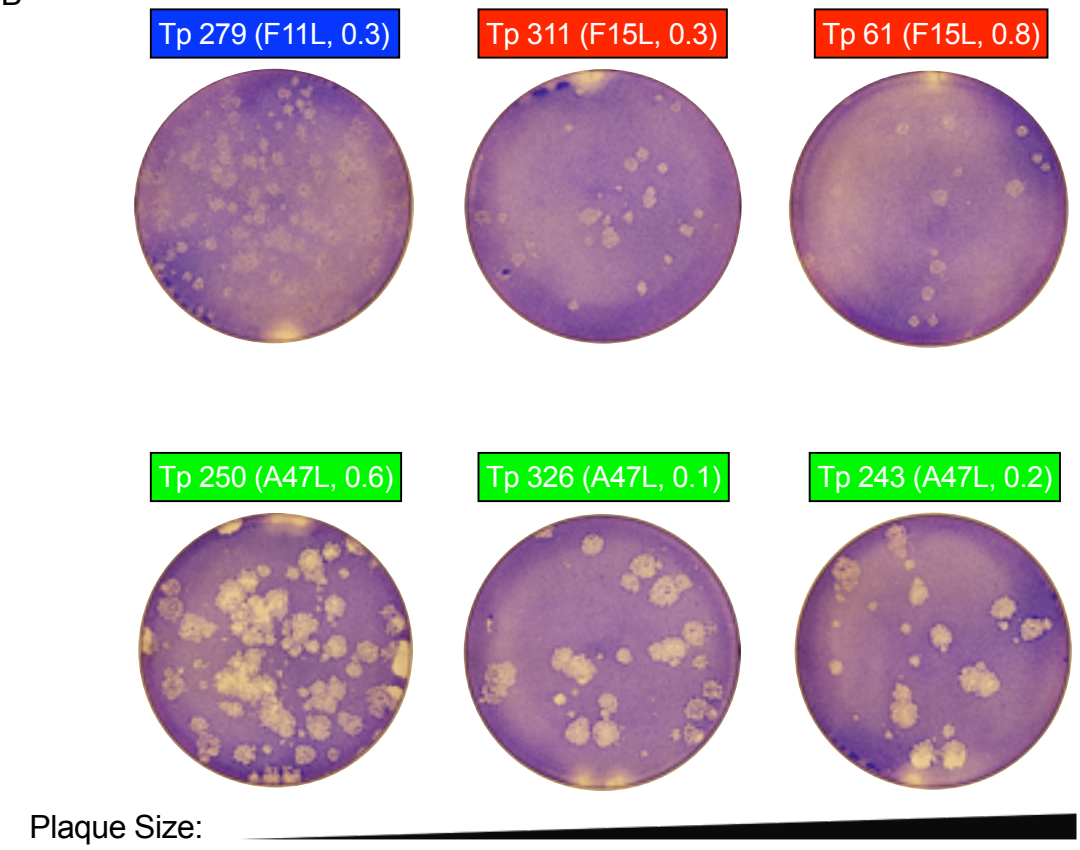
Tp 279 (F11L, 0.3)
Tp 311 (F15L, 0.3)
Tp 61 (F15L, 0.8)
Tp 250 (A47L, 0.6)
Tp 326 (A47L, 0.1)
Tp 243 (A47L, 0.2)
Plaque Size:

produced by clones Tp 311 (*F15L*, 0.3) and Tp 326 (*A47L*, 0.1) are plotted in Figure 3.18. As can be observed, the patterns discussed previously are not statistically significant in each case (note the lack of statistical significance between plaques produced by wild-type Copenhagen and Tp 311 in the human melanoma cell line M14), and the addition of further cell lines makes clear that the observed relationships in HeLa and M14 cells do not hold true in the prostate cancer cell lines in this experiment. Furthermore, plaques produced by each of the VACV-Copenhagen *A47L* mutants are not the same size as one another (data not shown), which suggests a role for this gene in cytotoxicity and/or cell-to-cell spread in some molecular sub-types of cancer (or in certain disease indications), but not in others. Taken together, these observations provide further evidence for the complexity of the pathogen–host interaction in this context.

To further expand the observations that were made in these plaque size experiments, select virus clones were used to expand the study across a larger panel of cell lines. As such, cell lines from the NCI-60 panel were chosen on which to perform these experiments and infection was allowed to proceed for 72 hours – selection criteria included cells that were known to be adherent in culture and cells whose growth characteristics resulted in a density that were appropriate for these assays. Furthermore, the experiment was supplemented with the tumour-derived primary culture Melanoma Patient 12-2016 as well as with the human osteosarcoma cell line U-2 OS. Of greatest interest to this research project, results for both Tp 311 (*F15L*, 0.3) and Tp 326 (*A47L*, 0.1) are plotted in Figures 3.19A and B, respectively, versus results obtained for wild-type Copenhagen in the same cell lines. From these studies, there are many interesting observations to be made that speak to currently-undescribed functions of both VACV-Copenhagen *F15L* and *A47L*. In 18 of the 20 cell lines studied, insertional mutagenesis of *F15L* led to the formation of smaller plaques. Of the two cell lines for which smaller plaque size was not observed, one was in

the human prostate adenocarcinoma cell line PC-3, which validates previous results at 48 hours of infection (Figure 3.18). The other was the human glioblastoma cell line SF 295. The results for insertion into VACV-Copenhagen *A47L* were less striking, however several interesting observations could also be made. Plaques were observed to be approximately the same size as those produced by wild-type Copenhagen in 11 of the 20 cell lines studied. Of the nine in which significant differences between wild-type Copenhagen and the *A47L* mutant were observed, the mean plaque size was interestingly observed to be smaller than wild-type in the human cell lines SNB 75, OVCAR.4, A549, and H460. The original finding of *A47L* mutant plaques being larger than wild-type Copenhagen at 48 hours in the human melanoma cell line M14 and the prostate adenocarcinoma cell line PC-3 were confirmed at 72 hours, and this finding was strengthened with the addition of similar results in the tumour-derived primary cells from Melanoma Patient 12-2016, the glioblastoma cell line SF 295, and the ovarian carcinoma cell line OVCAR.8. In addition to a study of the functional effects of insertional mutagenesis on VACV-Copenhagen *F15L* and *A47L*, one of the striking plaque-size phenotypes discussed earlier was that observed with the *F11L* mutant. VACV F11 is a well-described protein that is known to fundamentally modulate various aspects of the host cell cytoskeleton in the process of VACV shuttling and egress. One would expect that a deletion of this protein would lead to the production of plaques that are significantly reduced in size compared to wild-type Copenhagen. Across the 20 cell lines on which these studies were completed, this is indeed what was observed; the results are summarized in Table 3.2.

When a dynamic range of plaque size is observed across mutant VACV clones, questions can remain as to the mechanism behind this finding. For clones that are observed to induce the formation of larger plaques, it is possible that viral replication is simply more efficient and the burst size is significantly larger, or it may be that the clone in question more readily produces EEV.

Figure 3.18. 48 hour plaque size of select clones in four different cancer models. Plaque sizes formed by 3 unique virus clones are plotted – Tp 311 (*F15L*, 0.3), wild-type Copenhagen, and Tp 326 (*A47L*, 0.1). Results plotted are a result of independent plaque measurements (n = 20). (One-way ANOVA, ns = not significant, **P < 0.01, ***P < 0.001, ****P < 0.0001)

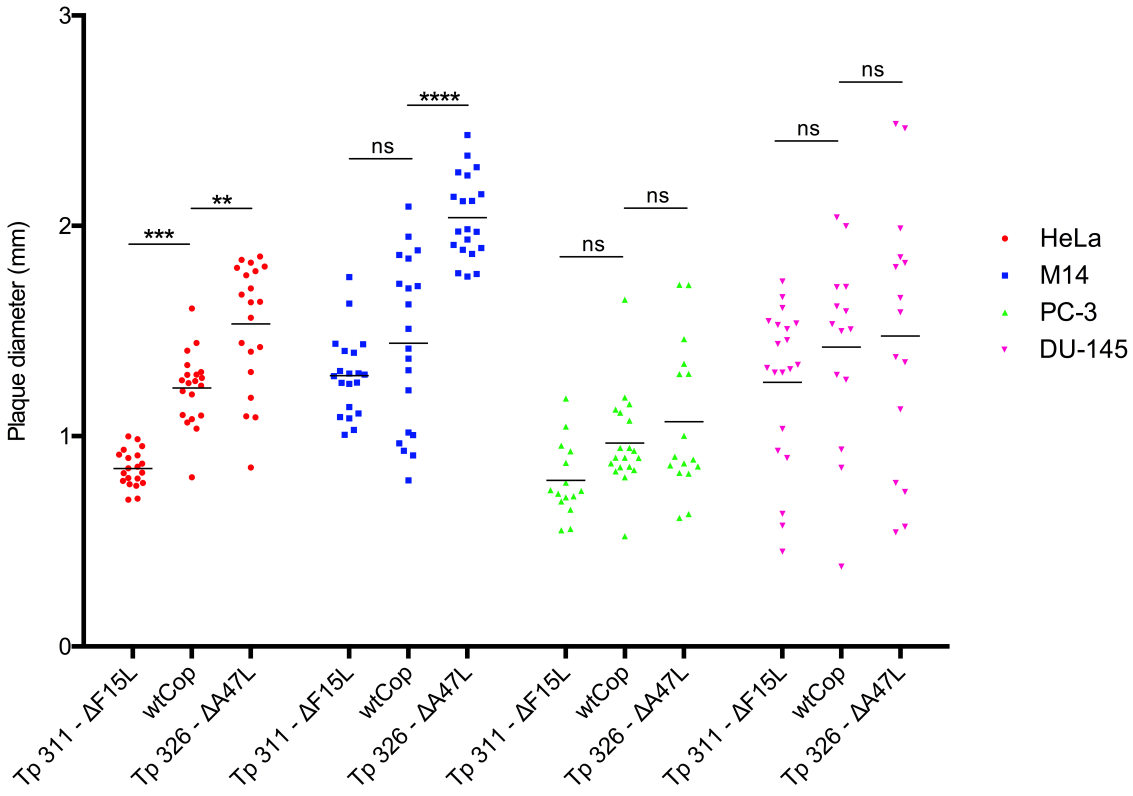
Plaque diameter (mm)
3
2
1
0
***
**
ns
****
ns
ns
ns
ns
Tp 311 - ΔF15L
wtCop
Tp 326 - ΔA47L
Tp 311 - ΔF15L
wtCop
Tp 326 - ΔA47L
Tp 311 - ΔF15L
wtCop
Tp 326 - ΔA47L
Tp 311 - ΔF15L
wtCop
Tp 326 - ΔA47L
HeLa
M14
PC-3
DU-145

Figure 3.19. Formed plaques at 72 hours post-infection in a large panel of cancer cell lines. 20 cell lines were used to study plaque size formation and determine whether cell effects could be responsible for differential plaque formation. Three unique virus clones – Tp 311 (*F15L*, 0.3), wild-type Copenhagen, Tp 326 (*A47L*, 0.1) – were utilized. (A) Results plotted for wild-type Copenhagen versus Tp 311 (*F15L*, 0.3). Each pair of unique symbols represents results from an independent cell line, denoted in the figure legend. In each pair, wild-type Copenhagen is plotted first, followed by Tp 311. (B) Results plotted for wild-type Copenhagen versus Tp 326 (*A47L*, 0.1). Each pair of unique symbols represents results from an independent cell line, denoted in the figure legend. In each pair, wild-type Copenhagen is plotted first, followed by Tp 326. Results plotted are the results of independent plaque measurements (n = 35, where possible). (One-way ANOVA between wild-type Copenhagen and Tp 311 or Tp 326, respectively; ns = not significant, *P < 0.05, **P < 0.01, ***P<0.001, ****P < 0.0001)

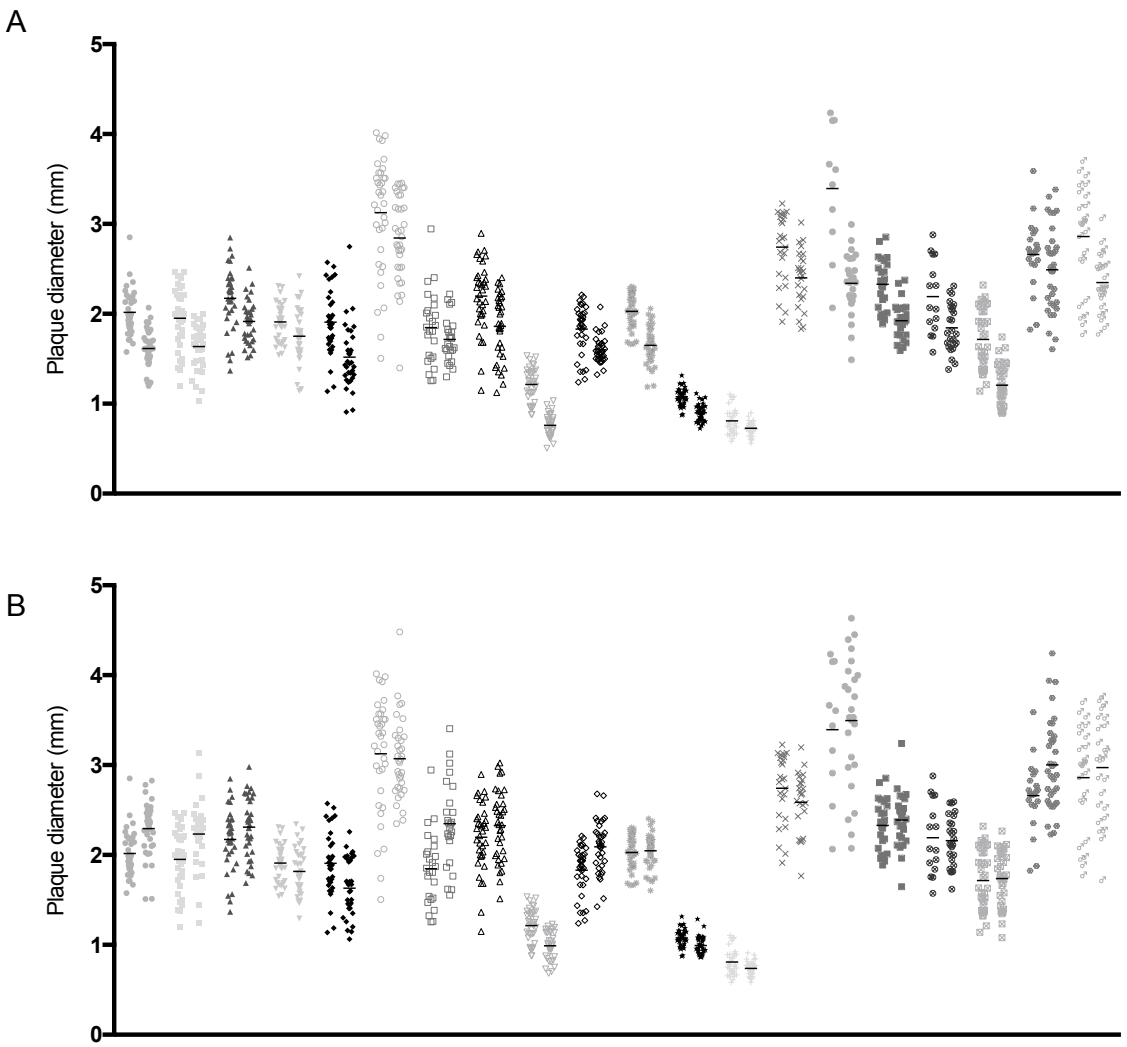

	Tp 311 *F15L*	Tp 326 *A47L*		Tp 311 *F15L*	Tp 326 *A47L*
Mel Pt. 12-2016	****	***	SK-OV-3	****	ns
M14	****	**	A549	****	***
UACC 62	***	ns	H460	**	*
SK MEL 2	*	ns	BT 549	**	ns
SNB 75	****	***	MDA-MB-231	**	ns
U251	*	ns	786-O	****	ns
SF 295	ns	***	ACHN	**	ns
SF 268	***	ns	HCT 116	****	ns
OVCAR.4	****	****	PC-3	ns	**
OVCAR.8	****	***	U-2 OS	***	ns

Table 3.2. Plaque size comparison between wild-type Copenhagen and the *F11L* mutant. Plaque size formation after 72 hours of infection. (Statistical annotations represent results from one-way ANOVA comparing results between wild-type Copenhagen and Tp 279, **P < 0.01, ***P < 0.001, ****P < 0.0001)

Disease site	Cell Line	Mean wild-type Copenhagen plaques (mm (SD) [n])	Mean Tp 279 (*F11L*, 0.3) plaques (mm (SD) [n])	P value
Melanoma	Pt. 12-2016	2.018 (0.253) [35]	1.611 (0.248) [35]	****P < 0.0001
	M14	1.951 (0.346) [35]	1.226 (0.185) [35]	****P < 0.0001
	UACC 62	2.173 (0.344) [35]	1.491 (0.164) [35]	****P < 0.0001
	SK MEL 2	1.911 (0.209) [35]	1.183 (0.140) [35]	****P < 0.0001
Central nervous system	SNB 75	1.907 (0.351) [35]	1.058 (0.131) [35]	****P < 0.0001
	U251	3.125 (0.642) [35]	2.134 (0.374) [35]	****P < 0.0001
	SF 295	1.847 (0.401) [25]	1.340 (0.220) [25]	****P < 0.0001
	SF 268	2.198 (0.391) [35]	1.584 (0.213) [35]	****P < 0.0001
Ovaries	OVCAR.4	1.214 (0.187) [35]	0.891 (0.104) [35]	****P < 0.0001
	OVCAR.8	1.829 (0.273) [35]	1.268 (0.156) [35]	****P = 0.0001
	SK-OV-3	2.027 (0.191) [35]	1.205 (1.132) [35]	****P < 0.0001
Lung	A549	1.078 (0.098) [35]	0.727 (0.055) [35]	****P < 0.0001
	H460	0.809 (0.148) [35]	0.704 (0.099) [35]	***P = 0.0009
Breast	BT 549	2.742 (0.388) [25]	1.877 (0.189) [25]	****P < 0.0001
	MDA MB 231	3.393 (0.726) [10]	1.672 (0.329) [25]	****P < 0.0001
Renal	786-O	2.330 (0.281) [25]	1.568 (0.204) [25]	****P < 0.0001
	ACHN	2.192 (0.408) [15]	1.836 (0.198) [25]	**P = 0.0054
Colorectal	HCT 116	1.715 (0.330) [35]	0.998 (0.167) [35]	****P < 0.0001
Prostate	PC-3	2.660 (0.391) [35]	2.188 (0.294) [35]	****P < 0.0001
Bone	U-2 OS	2.861 (0.583) [25]	1.757 (0.358) [13]	****P < 0.0001

To qualitatively assess the ability of select mutants to produce EEV, comet assays were performed on HeLa cells. As can be observed in Figure 3.20, there is a range of observed ability of select virus clones to produce significant satellite plaques. As previously demonstrated in Figure 3.7B, wild-type Copenhagen is able to produce satellite plaques to the point that tangible comets are observed, suggesting that more EEV are produced with this VACV strain than others; the results in this experiment confirmed those previously observed. Interestingly, insertional mutagenesis of VACV-Copenhagen *F11L*, *F15L*, and *A47L* was observed to significantly alter the degree of satellite plaque formation in HeLa cells. As expected, the *F11L* mutant was not observed to produce significant EEV or comet formation. Similarly, although the effect was less pronounced than with *F11L*, the *F15L* mutant was not observed to produce significant comet morphology in the crystal violet-stained monoculture, however rare exceptions were noted and can be observed in Figure 3.20. In contrast to virus mutants that are unable to produce appreciable EEV, the *A47L* mutants were able to produce comets with a diffuse pattern of satellite plaque dispersion compared to that observed with wild-type Copenhagen. Of additional note is the ability of the *K7R* insertion mutant to produce appreciable EEV and large comets. In contrast to the large comets observed with *A47L* mutagenesis, these were smaller, however cell cytotoxicity was more evident and demarcation of original and satellite plaques was well defined. Of interesting comparison in this assay was the inclusion of the leading VACV OV ΔTK-Wyeth, which was observed to be unable to produce appreciable satellite plaques, however well-defined plaques were evident; this finding is consistent with the inability of wild-type VACV-Wyeth to produce comets (Figure 3.6).

3.3.2. Protein-level conservation of Vaccinia virus F15 and A47

The data presented thus far is proving informative in the design of a superior next-generation VACV-based OV and there are also several observations that can add to the

Figure 3.20. Extracellular enveloped virus and comet production of select virus clones. Highlighted virus clones were allowed to infect HeLa cells for 96 hours and clones of interest are presented. Tp 279 (*F11L*, 0.3) and Tp 311 (*F15L*, 0.3) demonstrate impaired ability to produce qualitatively appreciable extracellular enveloped virions. Conversely, Tp 326 (*A47L*, 0.1) and Tp 344 (*K7R*, 0.3) demonstrate larger comet formation than wild-type Copenhagen. The clinical candidate oncolytic virus ΔTK-Wyeth was also used in this assay and results are presented here.

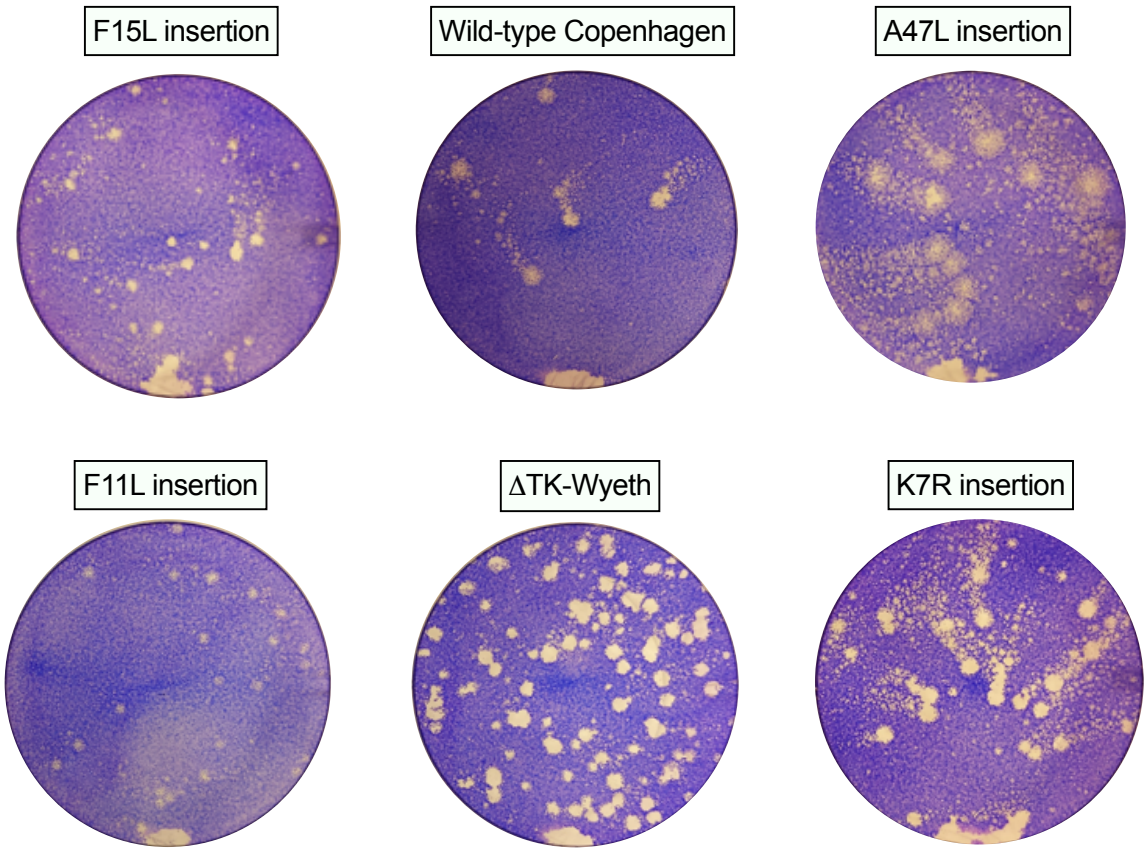
F15L insertion
Wild-type Copenhagen
A47L insertion
F11L insertion
ΔTK-Wyeth
K7R insertion

understanding of VACV functional genomics. Chief amongst these are the roles that are played by the VACV genes *F15L* and *A47L*, respectively. Currently, VACV *F15L* is an undescribed gene with unknown protein function(s); A47, conversely, has been described, however it has been described primarily for its important role in the priming of CD8 T cells, and specifically to not be involved in viral growth or plaque phenotype[226]. To gain a sense of the importance of these two proteins amongst the broader family of Poxviridae, an amino acid-level homology study was performed. The results of that for VACV-Copenhagen A47 are presented in Figure 3.21A. Homologues were identified in 12 divergent species. Nearly 100% sequence homology was identified in each of the four additional clinical candidate wild-type VACV strains presented in this study, as well as in horsepox, rabbitpox and ectromelia viruses. Also closely related, however sharing a sister group and a common ancestor to one another, are the A47 homologues in variola and camelopox viruses. More distantly related, however still at over 80% amino acid homology is a third major clade containing the A47 homologues of raccoonpox, volepox, and skunkpox. These data are also plotted in Figure 3.21B as a similarity plot, which allows for the easy comparison of amino acid sequence homology amongst all of the species discussed.

A similar analysis was performed for the amino acid sequence of VACV-Copenhagen F15. Interestingly, this as-of-yet undescribed protein was found to be highly-conserved amongst divergent Poxviridae species, which has been plotted on Figure 3.22A. It was found to have homologues in a total of 19 species with differing levels of homology. In the A47 analysis presented in Figure 3.21, there were nine species with over 90% homology to the VACV-Copenhagen variant of A47. In the case of F15, these nine species shared nearly 100% amino acid homology. There was also found to be nearly 100% sequence homology between the VACV-Copenhagen F15 and its monkeypox virus homologue, a virus which was not represented in Figure

Figure 3.21. Phylogenetic and conservation analysis of vaccinia virus-Copenhagen A47. (A) A phylogenetic tree of the Copenhagen protein A47 shows that it shares a common ancestral lineage with homologues in other vaccinia virus strains, as well as within horsepox and rabbitpox viruses, respectively. (B) Similarity analysis of Copenhagen A47 with homologues in species identified in the phylogenetic tree presented in A. The Copenhagen A47 amino acid sequence is conserved in closely-related species, denoted by orange squares.

A

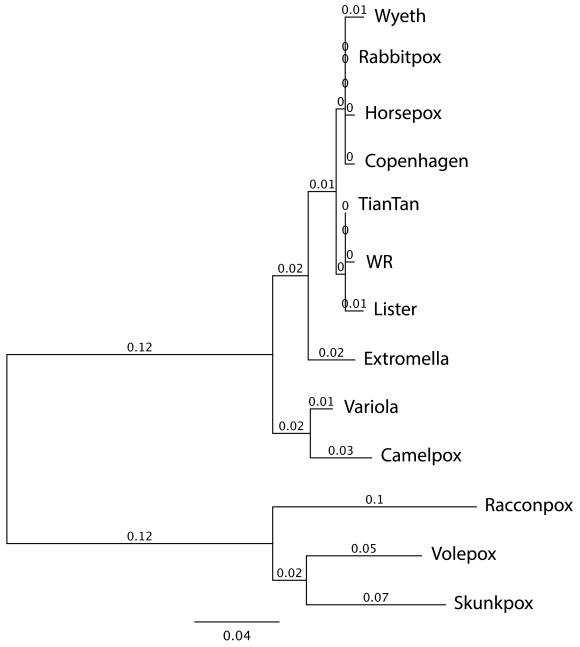
0.01
Wyeth
0
Rabbitpox
0
0
Horsepox
0
0
Copenhagen
0.01
0
TianTan
0
0
WR
0.02
0
0.01
Lister
0.12
0.02
Extromella
0.01
Variola
0.02
0.03
Camelpox
0.1
Racconpox
0.12
0.05
Volepox
0.02
0.07
Skunkpox
0.04

B

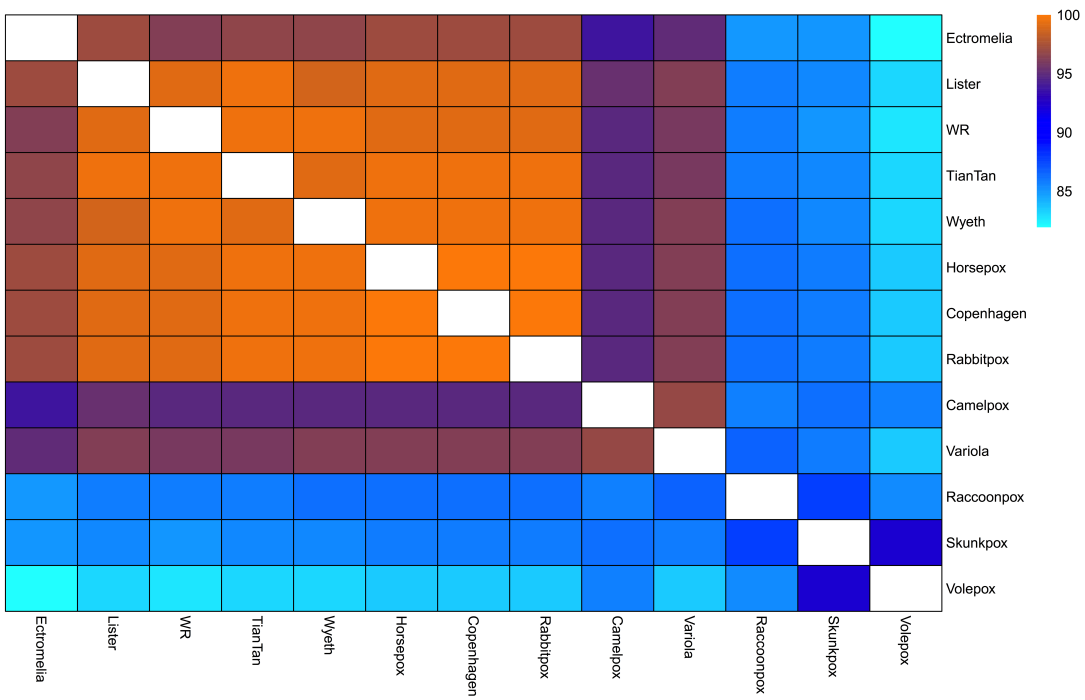
Ectromelia
Lister
WR
TianTan
Wyeth
Horsepox
Copenhagen
Rabbitpox
Camelpox
Variola
Raccoonpox
Skunkpox
Volepox
100
95
90
85

Figure 3.22. Phylogenetic and conservation analysis of vaccinia virus-Copenhagen F15. (A) The F15 protein of Copenhagen is highly conserved across all available strains of vaccinia virus as well as within other viruses within the Poxviridae family. (B) Similarity analysis of Copenhagen F15 compared with all viruses presented in the phylogeny above. Orange squares denote the intersection of viruses that share the most highly conserved amino acid sequences of F15.

A

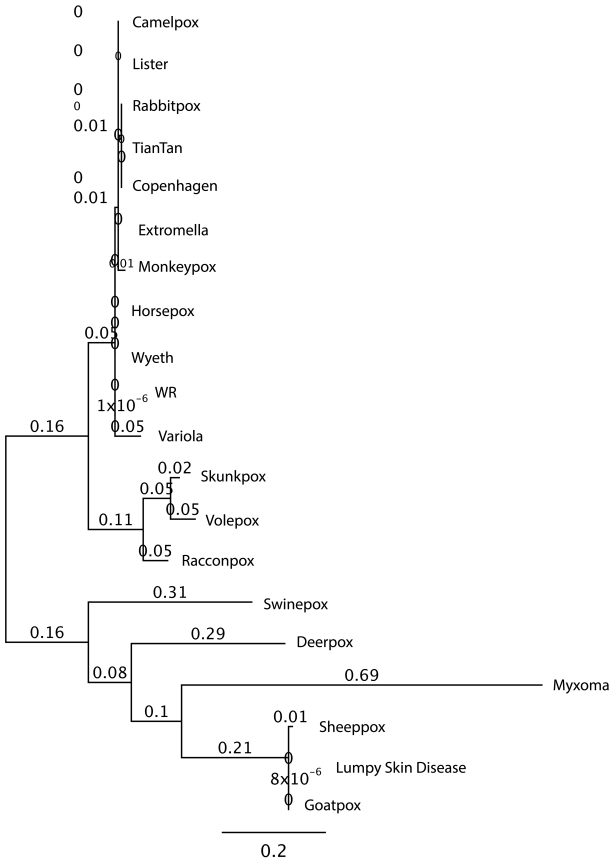
Camelpox
Lister
Rabbitpox
TianTan
Copenhagen
Extromella
Monkeypox
Horsepox
Wyeth
WR
Variola
Skunkpox
Volepox
Racconpox
Swinepox
Deerpox
Myxoma
Sheeppox
Lumpy Skin Disease
Goatpox
0.2

B

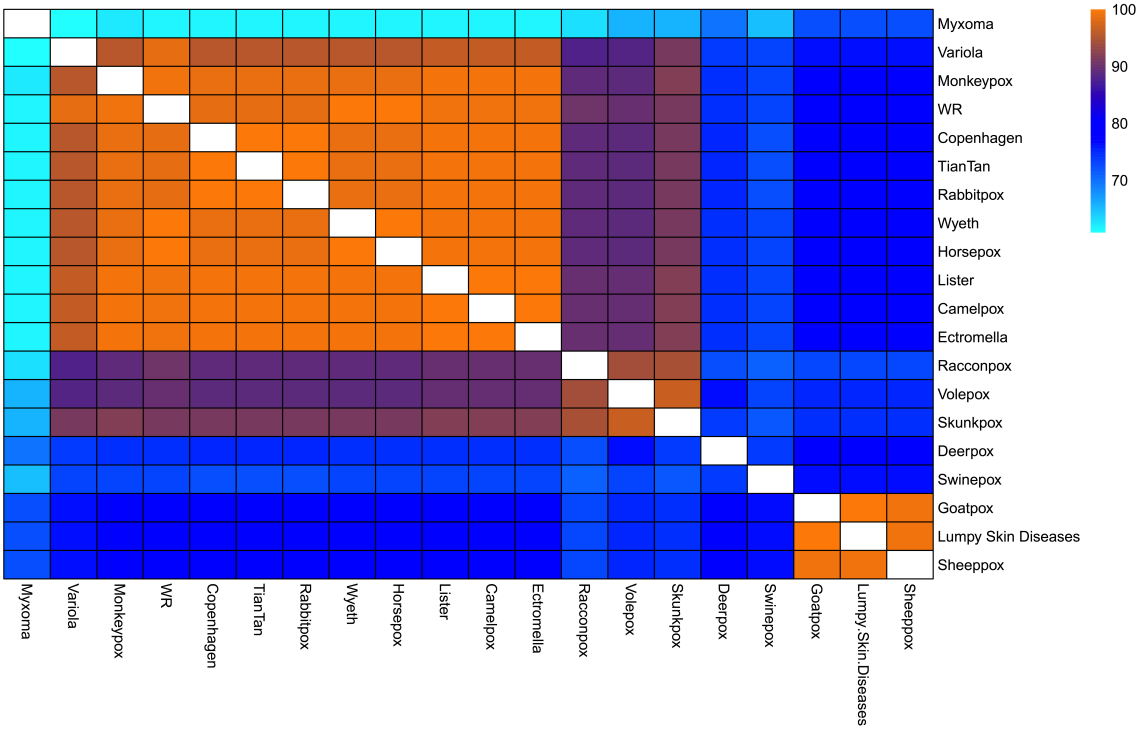
Myxoma
Variola
Monkeypox
WR
Copenhagen
TianTan
Rabbitpox
Wyeth
Horsepox
Lister
Camelpox
Ectromella
Racconpox
Volepox
Skunkpox
Deerpox
Swinepox
Goatpox
Lumpy Skin Diseases
Sheeppox
100
90
80
70

3.21. Also, notable amongst those viruses that shared high homology was each of the other wild-type VACV strains that were studied in this research project. Similar to the amino acid phylogeny presented for A47, a small sister group was formed by the F15 homologues of raccoonpox virus, volepox virus, and skunkpox virus at 80-90% homology with the VACV-Copenhagen homologue but nearly 100% homology to one another. Finally, a more divergent clade exists for homologues of this protein, however the sequence homology is lower than that described for the above-mentioned species. Swinepox virus, deerpox virus, myxoma virus, sheeppox virus, Lumpy skin disease virus, and goatpox virus were all found to have a homologue of VACV-Copenhagen F15, however amino acid sequence homology was found to be between 60-80%. All were also found to share a common F15 ancestor with one another at some point in their evolution. Interestingly, three viruses which have been said to be nearly antigenically indistinguishable from one another – goatpox virus, sheeppox virus, and Lumpy skin disease virus, were observed to have homologues of F15 which share nearly 100% amino acid sequence homology. Despite the high conservation of this protein amongst divergent species in the family, no predicted functional domains are present and the mechanism of the observed phenotype remains to be elucidated.

3.3.3. Understanding the in vivo virulence of vaccinia virus F15

To gain a further understanding on the effects of VACV-Copenhagen F15 on VACV virulence, *in vivo* toxicity assays were performed in which immunocompetent mice received three intranasal inoculations of 8×10^6 PFU of virus over a period of five days. Including the first day of virus inoculation and each day thereafter, mice were weighed and the results are plotted in Figure 3.23. The results observed support the hypothesis that the F15 mutant viruses may have a larger burst, however produced virions are not proficient at spreading to distant cells. Due to the doses selected, mice treated with wild-type Copenhagen were not observed to lose significant

Figure 3.23. Vaccinia virus F15 is a survival factor. Female Balb/c mice (n = 5 per group) were injected intranasally with 8 x 10^6 PFU of select viruses on days 1, 3, and 5. Mice injected with Tp 311 (*F15L*, 0.3) experienced a significantly increased weight loss that was observed following the second virus injection compared to those animals infected with wild-type Copenhagen. The observed weights of all treated animals did return to baseline 2 weeks following initial virus infection. (One-way ANOVA between wild-type Copenhagen and Tp 311, ***P<0.001; no statistically-significant differences were observed between animals treated with a vehicle control and wild-type Copenhagen)

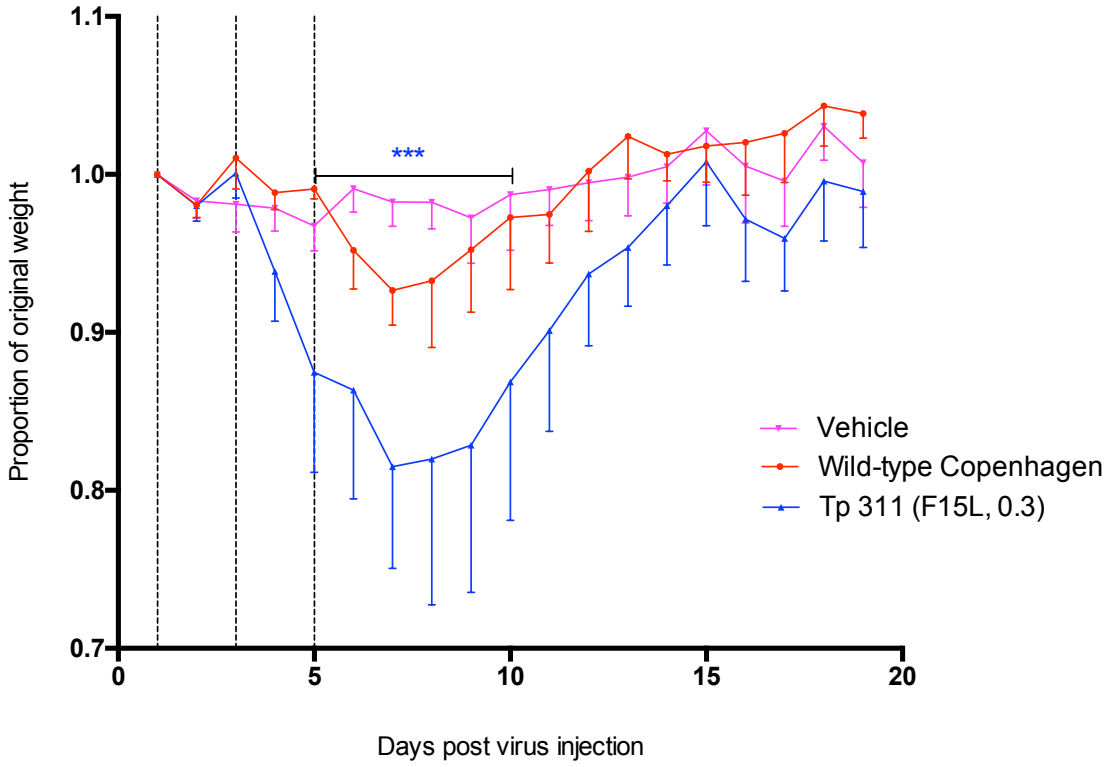
1.1
1.0
0.9
0.8
0.7
Proportion of original weight
***
0
5
10
15
20
Days post virus injection
Vehicle
Wild-type Copenhagen
Tp 311 (F15L, 0.3)

weight, while those treated with Tp 311 (F15, 0.3) were observed to lose significant weight compared to both vehicle control and, notably, mice treated with wild-type Copenhagen. These results suggest that the loss of VACV F15 may produce a more pathogenic virus strain than wild-type Copenhagen.

4. Discussion and Conclusions

4.1. Necessity for oncolytic virus backbone bioselection

For nearly two decades, the field of OV therapeutics has matured rapidly and with a clinical and translational focus. Clinical candidate OVs have been selected and tested quickly and with variable results. In the case of several candidate viruses, moderate clinical successes have been observed, which has led to the field's current situation in which dozens of clinical trials are underway and one OV that is fully approved for clinical use in the United States, Europe, and Australia[227]. This rapid pace of development is understandable and justified by the nature of the common clinical course of cancer. However, this translational appetite has also created a situation in which our understanding of the mechanisms of action of OVs is incomplete, evidenced by recent fundamental discoveries which have broadened our understanding of their utility[56,59,60]. Unfortunately, this rapid pace of clinical translation has also perhaps pressured the innovators in the field to settle on clinical products whose phenotypic characteristics are not optimal, thus providing most patients with less efficacious treatments thus far than pre-clinical data would suggest is possible. This phenomenon certainly impacts many characteristics of a virus, however even at the most basic level of strain-specific backbone selection, data has not been gathered in many cases to support the use of selected strain(s).

As described throughout this thesis, VACV is a large double-stranded DNA virus with known capacity to encode large transgenes. It also has an extensively-characterized and well-understood safety profile for use in humans due to its role in the WHO's smallpox eradication campaign[228]. Because of these and other properties, there is a high level of interest in VACV as a therapeutic platform. However, these characteristics also contribute to the biologic complexity of VACV; much remains to be elucidated despite its status as one of the most well-studied viruses.

From the perspective of a potential OV platform, a systematic study of VACV backbone candidates is yet to be completed. As such, there is a great deal of diversity of VACV backbones (wild-type strains) on which current OV candidates are built. Therefore, there is also an accompanying diversity in therapeutic benefits that have been observed with these products. Despite pre-clinical data that supports the oncolytic activity of these OVs, the one common theme that has plagued VACV OV candidates thus far is the lack of clinical efficacy. Simply, oncolytic VACV candidates have thus far proven to be too attenuated in their growth and spread for wide-ranging clinical utility. Currently, there are two VACV products in clinical trials – PexaVec and GL-ONC1, built on the Wyeth and Lister backbones, respectively. Advanced planning is also in progress for clinical trials with WO-12, an OV candidate built on the Western Reserve strain of VACV and recently acquired by Pfizer. With the goal of establishing a superior next-generation oncolytic VACV candidate, we sought to understand the phenotypic properties of each of the clinical candidate strains in an effort to select the least attenuated strain on which to build.

As demonstrated throughout Chapter 3.1 of this research project, differential replication properties exist for each of the five wild-type clinical candidate strains that were tested. As demonstrated in Figure 3.1A, although the general replication kinetics of each of the tested strains is similar in the human embryonic carcinoma cell line HeLa, wild-type Copenhagen demonstrates the production of increased progeny compared to other strains. This increased virus progeny is due to an increase in the viral burst size for Copenhagen-infected cells, leading to increased progeny as early as 12 hours post-infection (data not shown). The production of relatively greater infectious progeny peaked at 48 hours post-infection, a relationship with other wild-type strains which was observed to be relatively unchanged up to 96 hours post-infection (data not shown). This interesting observation led to the question of whether this effect was due to the fundamental

biology of VACV-Copenhagen compared to each of the other strains. Therefore, replication studies in several other *in vitro* cancer models were pursued. Interestingly, this phenomenon of the greater production of infectious progeny by VACV-Copenhagen compared to all other wild-type strains was observed to be consistent across each *in vitro* cancer model tested. Shown in Figure 3.2 are results obtained for human melanoma, renal cell carcinoma, prostate carcinoma, and colorectal adenocarcinoma. An addition to the array of viruses tested was the current leading VACV clinical candidate ΔTK-Wyeth, which consistently underperformed in terms of viral replication compared to each of the wild-type strains, including the Wyeth strain upon which it is built. The current VACV OV candidate contains attenuating mutations in the viral thymidine kinase gene *J2R* and a natural truncation of the interferon-scavenging gene *B18R* (*B19R* in Copenhagen). Interestingly, deletion of *B18R* has been shown to have a relatively neutral effect on the output of infectious progeny (Figure 3.15), however also leads to a diminished toxicity *in vivo*[229]. This relative lack of effect of *B18R* deletion on viral output coupled with the known genotype and observed replication of ΔTK-Wyeth throughout Figure 3.2 brings into question the overall attenuating effects of viral thymidine kinase deletion. To our knowledge, these simple replication studies provide the first evidence for the superior replication ability of VACV-Copenhagen in the context of head-to-head *in vitro* growth in immortalized cancer cell lines.

To position ourselves for the long-term goal of developing a superior clinical candidate oncolytic VACV, it was important to investigate whether these findings would remain consistent in more clinically-relevant specimens and non-immortalized cell cultures. To this end, surgical specimens were collected from several patients undergoing tumour debulking surgery for melanoma at the Ottawa Hospital. The original specimens obtained were histologically confirmed to be from melanoma tumours, both by hematoxylin and eosin staining, but also by a board-

certified pathologist as noted in confidential clinical records. Furthermore, the primary cultures generated were confirmed to retain expression of the melanoma markers MelanA, Tyrosinase, and S100 at the RNA level. This type of identification confirmation is critical to research such as this because of the behavior of OVs (known as the oncolytic paradigm), but also because of the logistical challenges associated with tumour specimen retrieval and primary culture generation. Possibility exists for the gross identification of cancer on tissue acquisition that is later confirmed to not be histologically-representative of such a diagnosis. Furthermore, when the successful acquisition of a cancer specimen has occurred, this specimen is undoubtedly representative of a diverse and complex tumour microenvironment that consists of more than simply transformed cancer cells. Likely, and as confirmed by the tissue sections from which photomicrographs were obtained for Figures 3.3B and 3.4B (data not shown), the specimens can consist of extensive fibrosis, fatty deposits, and vascular cells, which can all impact the growth of a culture. It is possible, for example, for fibroblast outgrowth to overtake the growth of transformed cells in tissue culture, and therefore the confirmation of expression within these primary cultures of select diagnostic markers are important to the generation and maintenance of quality *in vitro* models. Finally, with our downstream translational interests, it is important to gain an understanding of whether *in vitro* viral replication data can translate into a meaningful replication advantage when a more realistic model is utilized. Presumably, an *ex vivo* model derived from an excised human tumour specimen, which itself was infected with the viruses of interest, could appropriately represent such a model. Although it was not tested in this project, tumour-derived primary cultures are likely complex in their composition due to the complexity of their origins and their short-term existence in culture.

For this research project, data is presented for two of the specimens from which primary cell cultures were generated. *Ex vivo* infection of tumour cores from Patient 12-2016 (Figure 3.3E) revealed a mean virus output that was highest for VACV-Copenhagen, however none of the findings were statistically significant. Due to tissue limitations, these experiments were performed in triplicate and the observed mean of replication advantage for VACV-Copenhagen compared to each of the other strains did not reach a statistically significant level. This may have been remedied with increased sample size, however it is also possible that challenges associated with the tumour microenvironment preclude productive viral infection or that VACV-Copenhagen simply does not possess a replication advantage in all cases. Interestingly, cells of the primary culture derived from this patient did support productive viral replication across all strains, however the previously-observed *in vitro* growth advantage for VACV-Copenhagen was likewise observed to reach significance at 24 hours post-infection and onwards. This data supports the finding that wild-type Copenhagen causes an increased viral burst size compared to the other wild-type strains.

Alternatively, specimens from Patient 13-2016 were infected *ex vivo* and the same amount of virus was recovered from each wild-type strain except for wild-type Copenhagen, for which approximately 600-fold greater infectious virus was recovered 72 hours post-infection. Interestingly, wild-type Copenhagen is also the only virus in these two experiments (Figures 3.3E and 3.4E) for which productive viral replication can be confirmed due to the recovery of more virus than was used to inoculate the specimen at baseline. This analysis suggests that VACV-Copenhagen would indeed be the best strain upon which to consider building an oncolytic VACV due to its ability to productively infect various cancer models. Additionally, cells of the primary culture derived from this specimen were able to host productive replication in each of the wild-type strains used across these experiments. However, such as in previous studies, VACV-

Copenhagen demonstrated a growth advantage which was maintained onwards from 48 hours post-infection.

To study the ability of these virus strains to replicate *in vivo*, nude mice were allowed to grow bilateral sub-cutaneous tumours of the human melanoma cell line M14. These tumours were infected intratumourally and their ability to host productive replication was studied when they were collected and processed at 72 hours post-infection. The hypothesis of this experiment was that these tumours would recapitulate what was observed *in vitro* in M14 melanoma cells, however results from this *in vivo* model were equivocal. Greater replication and virus recovery occurred from tumours that were infected with VACV-Copenhagen compared with each of the other strains, however this did not reach a statistical level of significance when compared with VACV-Tian Tan, which is a Chinese vaccine strain that one group is currently developing as an oncolytic vector. Interestingly, infected tumours that were recovered for immunohistochemistry analysis show infection throughout the tumours (data shown for VACV-Copenhagen, Figure 3.5Bii), which does not significantly differ across virus groups, however the gross morphology of the tumour treated by VACV-Copenhagen is unique. There is a central paucity of anti-VACV staining in these tumours that is characteristic of necrosis, which is a finding that was not observed in any of the other tumours. This finding suggests that, at the time of tumour recovery and fixation, there were fewer total infected cells in the tumours that were infected with VACV-Copenhagen due to the fact that many of the infected tumour cells had already undergone necrosis. Interpreted in this way, these data lend further support to the finding that VACV-Copenhagen is a superior platform on which to build a next-generation OV, however these processes would need to be systematically studied *in vivo* to conclusively make these claims.

With the finding that the observed replication capacity of VACV-Copenhagen in several relevant cancer models is greater than in other wild-type strains, other relevant OV characteristics of cytotoxicity and cell-to-cell spread were studied. As previously discussed, there are two distinct types of infectious VACV particles that differ from one another in their ability to infect neighboring cells following an actin tail-induced propulsion, or for their propensity to remain in the cytoplasm of intact cells until lysis. It is known that each of these distinct particles can have unique impacts on the appearance of viral plaques, which can also shed light on the ability of a select strain to induce cell death. Interestingly, plaques formed by VACV-Copenhagen are significantly larger than any of the other strains studied in this research project in HeLa cells, as can be observed in Figure 3.6. This increased clearance of cells in a monolayer strongly suggests that there is greater cell death with VACV-Copenhagen than any of the other strains, and that viral replication indeed correlates to viral-induced cytotoxicity. Furthermore, the clinical candidate ΔTK-Wyeth was observed to form plaques of similar size to the other wild-type strains studied.

As there is a prevalent idea in the literature that viruses with a propensity for EEV production may be better oncolytic candidates[97,98], this property of each of the wild-type strains of virus was studied. As can be observed in Figure 3.7, HeLa cells 96 hours post-infection and under a liquid overlay show EEV release as characteristic comet formation, both when quantitative fractional titration is performed and also when qualitative analyses are performed. This finding is true of VACV-Copenhagen and VACV-Tian Tan only, however not the other three virus clones studied. The ability of these two strains to release greater EEV, and the importance of EEV release to a successful OV platform remains to be studied in depth, however these findings do speak to the unique biology of these strains compared to one another.

Taken together, these data suggest that VACV-Copenhagen has a replicative advantage over the other wild-type clinical candidate strains of VACV that were studied. This finding is consistent with other studies that date back as far as five decades, however no study to date has made an effort to characterize the oncolytic potential of unique strains of VACV in head-to-head studies and under controlled conditions, therefore resulting in its bioselection for therapeutic purposes. As discussed earlier, the clinical performance thus far for oncolytic VACV candidates has been variable – favourable treatment outcomes have only been observed in a minority of patients. To date, all patients to our knowledge that have undergone VACV cancer therapy have experienced toxicity, typically in the form of pox lesion development. It appears as though the thinking in the development of previous-generation OVs was to begin with highly-attenuated vaccine strains and modify their cancer specificity by genetic manipulation and/or their capacity to break immune tolerance with the addition of encoded cytokines. The result of these efforts are viruses that are too attenuated to induce oncolytic activity in the majority of patients, however have also been unsuccessful in eliminating virus-induced toxicities. It therefore appears clear that these viruses were developed with an incomplete understanding of their components and that this will need to be remedied in order to rationally design a superior clinical candidate OV, which was the main focus of this research project. In that sense, the compilation of data discussed thus far provides the necessary knowledge on which to build, which is the direction that was taken herein. However, in many other ways these data are hypothesis-generating and could be used as a foundation upon which to further understand the unique genetic aspects of these strains that lend to their unique phenotypes. Namely, what are the behaviors of these virus strains on normal non-transformed cells, and are they truly “oncolytic”? What are the baseline abilities of these unique virus strains to break cancer immune tolerance? What are the mechanisms that lead to a superior

burst size of VACV-Copenhagen? A more comprehensive study of these wild-type strains *in vivo* would also shed light on their suitability for use as OVs, and answering any of the mechanistic questions posed would likely shed light on fundamental cell biology. In any case, the bulk of this research project was aimed at increasing our understanding of the genetic components of VACV as they relate to OV development.

4.2. Generating a vaccinia virus-Copenhagen mutant library

Before being able to sensibly select the genetic elements of VACV-Copenhagen that may contribute to the improvement of a clinical candidate OV, it was clear that a better tool to study the virus genome needed to be developed. To date in the study of VACV, a single tool has not allowed the comprehensive study of a large portion of the VACV genome. For the most part, this lack of a comprehensive tool has led to the functional definition of VACV genes on a single gene basis, with several genes remaining undescribed. The current preferred strategy to this end uses homologous recombination; a technique for using the CRISPR-Cas9 system has recently been described, however this was shown to be labour-intensive and has not been developed for widespread use[230]. Groups that have tried to optimize an OV backbone using existing information have therefore been working with an incomplete functional picture of the viral genome. We sought to design, develop, and characterize a tool to address this shortcoming. Our selected methodology of TE insertional mutagenesis provides several advantages over traditional methods and the data presented in this research project demonstrates the ability for this tool to be utilized such that OV-relevant information can be gathered for many mutant clones at one time, which is amongst other potential uses for this tool. Not only has a VACV-focused library of guide RNAs that may be applied in a CRISPR-Cas9 approach not yet been produced, but the randomized nature of our insertional mutagenesis approach provides two clear additional benefits that can speak to the

biology of VACV. Namely, the potential for studying the active domains of select proteins into which insertion has occurred at multiple points, and secondly the potential for studying relative gene fitness using NGS-based technologies.

The design of our transposable element, as presented in Figure 3.8A, is such that successful insertion precludes the full translation of the mutagenized protein due to an amino terminus stop codon immediately downstream of the inserted TE ITR. Therefore, possibility remains for the partial production of mutagenized proteins, which may or may not affect protein function depending on the active domain of the function in question. There are many examples of this phenomenon in the literature and studying differentially-mutated proteins has indeed been a route of discovery of the active domains of VACV proteins in many cases. Furthermore, the synthetic early/late VACV promoter used in the TE likewise ensures the expression of the inserted mCherry transgene, which was also used as a selective strategy for the generation of this working library (Figure 3.8B). The fact that this selection methodology was used, importantly followed by plaque purification of mCherry-expressing virus plaques until 100% of plaques expressed this transgene, ensured the creation of a mutagenized working library composed of clonal viruses that retained the ability to produce fluorescence at each stage of their lifecycle.

As previously mentioned, one of the ways that TE mutagenesis has been recently used in the literature combines TE mutagenesis with NGS. Earlier studies used arrayed single gene mutant libraries, which exist for relatively few microorganisms, to study properties of interest namely in yeast[231,232]. It was clear that a method that would allow the high-throughput study of genes without the development of single-gene mutant libraries would be of interest for microorganisms, which led to the development of Tn-seq in 2010[233]. Thus far, this is an approach that has rarely been applied to viruses, and in fact has not been applied to VACV. Typically, bacteria have been the

focus of such studies and the seminal publication in this discipline focused on *Streptococcus pneumonia* and the ascription of fitness genes in contexts of interest. To date, Tn-seq has not been combined with the generation of a single-gene mutant library. The data presented in this research project demonstrates the ability to do so and demonstrates the ability to functionally characterize accompanying single-gene mutants in a high-throughput manner in contexts of interest. This research also hints at traditional applications of Tn-seq in the context of VACV, however the comprehensive NGS of our stored specimens will need to be completed to say this conclusively. Although data has not been presented herein that to support arguments around the relative fitness of VACV genes, the data presented does indeed hint at such arguments. Namely, presented in Figure 3.9 is a schematic of the insertion sites that are represented in the working library used throughout this research project. It is evident that the majority of insertion sites are located towards the extremities of the VACV-Copenhagen genome, which is an observation that correlates with what would be expected of a VACV mutant library that was constructed using the methodology that was used here. Based on what is known about divergent chordopoxviruses, approximately 100 genes located in the central region of the VACV genome exhibit remarkable conservation and even arrangement to other viruses; approximately half of these can also be found in entomopoxviruses. These genes are assumed or known to be involved in critical replication functions of this virus subfamily[99], and as such functional insertional mutagenesis in this gene region would be predicted to generate non-viable virus clones. There are indeed only two insertion clones in this working library that were found to be in this highly conserved region: one was found in *J2R* and the other in *J5L*. Interestingly, J2 is the VACV thymidine kinase, modification of which is common in the OV field and is commonly thought to increase cancer selectivity of OVs by directing it to highly metabolic cells while retaining virus virulence. J5, on the other hand, is known to have a more

critical role in virus replication as it partially composes the VACV EFC. It is structurally related to two other EFC proteins, A16 and G9, which suggests a common evolutionary relationship and interestingly are not represented in this working library[234]. A critical point of note regarding this *J5L* insertion mutant is that the insertion site is located at the 5' end of the gene, shortly before the gene's stop codon, therefore it is possible and perhaps probable that the protein retains full functionality.

Figure 3.10 was generated to schematize the locations of these insertion sites more clearly and to get a sense of whether TTAA frequency within the genome affects the working library that has been created. The possibilities exist that there are areas of high or low TTAA frequency in the VACV genome that inherently direct insertion frequency, or that there is a conformational disadvantage to insertion in the middle portion of the genome. As can be observed in Figure 3.10, the distribution of TTAA sites throughout the VACV-Copenhagen genome is relatively even. As expected, there are areas of higher or lower frequency, however kb-by-kb, significant variation of theoretical insertion sites across the genome does not exist. Furthermore, there is at least one TTAA site in each VACV-Copenhagen gene. When this is overlayed by the distribution of observed sites of insertional mutagenesis, the previously discussed preference for the genome extremities is evident. Although an experiment to test whether a conformational disadvantage to insertion in the middle portion of the genome was not performed, the observed insertions in *J2R* and *J5L* suggest that such a disadvantage does not exist, and perhaps more importantly, the known critical functions of the majority of these central genes would make recovery of a functional virion following insertion impossible. When these data are further overlayed with a plot demonstrating the degree of conservation amongst diverse VACV strains (data not shown), the overlap between regions of nearly 100% genomic conservation and areas of poor insertion frequency is striking.

Our observations of TE insertion favouring the extremities of the VACV genome therefore lend further support to the well-known importance of the highly-conserved central VACV genes.

4.3. Functional implications of transposable element insertion

Once the working library used in this research project was fully established, it became important to gain an understanding of the functional implications of insertion of the TE. VACV genomic sequencing data exists for each clone in this library and was used to create the Figures 3.9 and 3.10, but the next question was to understand the effects of insertion at both the level of the transcript and protein. To assess the effects at the level of the message, reverse transcription PCR was performed using cells that were infected with select clones and primer pairs that were designed to target opposing sides of the insert such that the size of the amplicon would vary by the size of the TE. These experiments were performed on selected clones that represented insertion at different positions of the VACV-Copenhagen genome and were therefore considered to be representative. Figure 3.11 presents the generated data, which suggests that, as expected, the transposable element is indeed transcribed with the virus clone.

More interesting studies were then designed to understand the effects of insertion at the level of the protein. Such studies are made challenging due to the lack of full understanding of VACV genes and proteins as well as to the lack of antibodies that are commercially available to target such proteins. In fact, all commercially available antibodies designed to recognize VACV are designed against epitopes on proteins whose function is known to be essential for virus replication. There are notable academic groups around the world who have largely shaped the study of VACV and have generated antibodies against select VACV proteins in the process, however these have all been generated for individual research purposes and are not widely available for outside use. Furthermore, many VACV genes that have been described have been

described for specific functions, however it is clear that most have additional currently undescribed phenotypic effects. Most instances of VACV protein definition have therefore occurred generally, with functional domains within proteins not being entirely understood. There are notable exceptions, one such exception being the thorough understanding that has recently accumulated for the VACV protein F11, which is known to possess a relative amino terminus functional domain with a C terminus binding site. This is an example of a protein that has been more thoroughly studied because its discovery and initial definition was transformative in virology as it was the first viral protein shown to inhibit RhoA signaling[177]. Another active area of investigation has surrounded the viral protein A36, which is known to be involved in the actin nucleation-mediated release of mature EEVs from the extracellular surface of infected cells[165]. On the immune side, there is a several-protein member class of VACV proteins that is known to inhibit the NF-κB pathway at various levels. Members of this pathway are currently an active area of focus within the VACV community as their role in modulating immune response may have implications for OVs or as vaccine candidates. One example of this protein class is the viral protein K7, which is represented in this library by Tp 344 (0.3). Finally, the soluble interferon-sequestering VACV-Copenhagen protein B19 has been defined for its ability to sequester secreted interferon, and assays have been designed to test such a phenotype. B19 is represented in this working library as Tp 203 (0.6). These four VACV-Copenhagen proteins – F11, A36, K7, B19 – were selected to further study in an effort to gain an understanding of the effects of insertional mutagenesis at the level of the protein. They were selected because their functions have been specifically defined and are known to be diverse, their deletion causes well-known phenotypes, the relative insertion sites within their respective genes are diverse (F11 – 0.3, A36 – 0.9, K7 – 0.3, B19 – 0.6), and most

importantly, reagents or functional assays exist that allow the detection of protein presence or function.

Various antibodies against the VACV proteins F11, A36, and K7 were obtained from collaborators, which enabled the immunoblotting for the presence of selected epitopes. Importantly for the present purposes, each of the antibodies used were either polyclonal, or were polyclonal antiserum as in the case of K7. As can be observed in Figure 3.12A, each of these antibodies failed to detect the presence of any protein in the mutagenized clones in question. The F11 antibody is polyclonal and the peptide used to immunize animals corresponded to residues 101-120, which has been described to include the N-terminus of the PDZ domain within VACV protein F11. This PDZ domain has been shown to be necessary to modulate the interaction between a RhoA binding domain close to the C-terminus of F11 and cellular RhoA, and the loss of this functional domain results in the inability to promote viral spread[181]. As it relates to Tp 279 (F11, 0.3), genomic insertion occurred before this region and the expected phenotype is observed. The antibody obtained against the viral protein A36 is also polyclonal and against an epitope corresponding to residues 142-214. Several NPF motifs have recently been described to be in the C-terminus of A36 and are responsible for modulating the cell-to-cell spread of VACV[166]. As for Tp 306 (A36, 0.9), TE insertion should theoretically result in the production of the first approximately 200aa of the full-length 220aa protein, therefore one would expect the presence of a diminished signal on detection with this polyclonal antibody. Interestingly, no signal is detected using this antibody, suggesting perhaps that the produced polypeptide fraction is destabilized by the loss of its C-terminus and subsequently unfit for function. Finally, the anti-VACV K7 anti-serum was raised against full-length protein and is also polyclonal, therefore one would expect a diminished binding of antibody if only partial protein production occurred. In the case of Tp 344 (K7, 0.3),

approximately 45aa of this 149aa protein would be predicted to be produced and partial binding would be expected if this was stable. Interestingly, like in the case of the previous two antibodies, the anti-K7 anti-serum failed to detect the presence of any protein. Taken together these immunoblot assays suggest that insertional mutagenesis using the transposable element in this study may actually result in functional knockout of the proteins into which insertion occurred.

Finally, the only true functional assay presented in this research project was done to validate the functional limitations of B19 following insertion into *B19R* (Tp 203, 0.6). As described above, this is an assay that has previously been described and assesses the ability of VSVΔ51 to infect or not infect in the presence or absence of Type I and II interferons. As presented in Figure 3.12B, the observed complete inability of VSVΔ51 to infect cells in the context of a supernatant transfer from cells infected with Tp 203 suggests the absence of B19 functionality. The combination of these data presented in Figure 3.12 suggests that even relative 5' genomic insertion may result in a complete functional knockout of these viral proteins; however comprehensive functional assays would need to be performed to fully assess this hypothesis.

4.4. Exploiting transgene expression for the study of virus replication

One of the advantages of the generation of a working library following TE mutagenesis with our TE specifically is that it allows the high-throughput study of VACV-Copenhagen single gene mutants by exploiting mCherry fluorescence production. As demonstrated in Figure 3.13A, the observations that led to the study of virus mutants in this way were fundamentally simplistic, which were that there is a direct relationship between the amount of infectious virus in a system versus the amount of fluorescence that is produced by that system at a given time point and across a certain range of virus concentrations (Figures 3.13A and B, respectively). Interestingly, it was quickly observed that mCherry transgene expression and therefore fluorescence intensity differs

on a clone-by-clone basis. This finding complicates the utility of fluorescence as a useful readout because there is inherent variation between baseline fluorescence, which does not correlate to the amount of virus that has been produced given a certain set of experimental conditions. To address this challenge, a two-step virus infection protocol was set up, which utilizes the same principles as standardized plaque assays to assess virus output, however it was tailored for the high-throughput quantification of this 89-virus working library across a large panel of normal and cancer cells. As described previously in Figure 2.1, this involves a primary infection using a virus clone of choice, followed by a dual secondary infection using the output of the primary infection as well as the same input that was used in the primary infection; the resulting fold-change between fluorescence output then corresponds to the amount of relative virus production, which can be compared across clones.

Differential transgene expression is a commonly-observed phenomenon in molecular biology and likely stems from our incomplete understanding of genetic regulatory elements for most species. In microorganisms and specifically in VACV, the regulation of genes is likewise incompletely understood, however the differential expression of transgenes has been observed and reported in the literature. There are several potential explanations for the differential expression of mCherry that are not necessarily tied to efficiency of virus production. The first is that at their most fundamental level, VACV genes are temporally regulated to be expressed early, intermediate, or late, and will not be expressed to high levels at other times of the viral lifecycle. Therefore, it is possible that differential transgene expression may be tied to differences in temporal gene regulation. Furthermore, gene enhancers are *cis*- or *trans*-acting regulatory elements that have been shown to act at the level of transcription to cause differential expression of certain genes. In VACV specifically, enhancer-like sequences have been characterized[235], which are generally thought to

be dependent on distance and/or orientation factors. Therefore, despite the same synthetic early/late VACV promoter regulating insert transgene expression, it is possible that secondary structures or other spatial limitations have an impact on a fluorescence intensity readout. Although the study of miRNAs in VACV has occurred, they are unlikely to be playing a role in the post-transcriptional modification of viral genes that modify transgene transcription due to the virally-encoded poly(A) polymerase, which polyadenylates viral transcripts, but also polyadenylates host miRNAs, which results in their degradation by host machinery[236]. The cause of this differential transgene expression remains unknown, however the challenge it poses to easily study virus replication was dealt with technically and therefore the principles described above have been used to study this property in a high-throughput fashion. Understanding this phenomenon is not the focus of this research project, however further study would be interesting.

4.5. High-throughput study of differential virus replication

Using the principles discussed in the previous section to study differential virus replication of the clones in this single gene mutant library is technically straightforward with accurately-quantified and arrayed virus preparations. The optimization of this technique was performed on approximately 10 cell lines following a given set of selected conditions (full data not shown), which revealed many interesting observations. Presented in Figure 3.14A are virus replication results from the patient-derived primary melanoma culture Patient 12-2016 (see also Figure 3.3). Several virus clones of choice were highlighted, which were selected to discuss interesting results. Notably, the relative replication differential that was calculated from the poorest-replicating virus (Tp 311) to the greatest-replicating virus (Tp 257) was calculated to be 6.33 and corresponds to the fold-change between these two highlighted viruses in Figure 3.14A. Interestingly, when validating traditional plaque assays were performed on the replicate infections with these virus

clones, the differential was calculated to be 6.25-times, correlating well with the results obtained by fluorescence. Such correlation was observed in each of the 10 cell lines or primary cultures studied in initial optimization experiments, providing a strong foundation upon which to build. These same principles that apply to the determination of relative virus replication using mCherry expression can also be applied using GFP expression and so a GFP-tagged version of the clinical-candidate ΔTK-Wyeth was also included in these initial replication studies. Interestingly, in the majority of cases, ΔTK-Wyeth was among the least efficiently-replicating viruses in the library tested, which correlates with the initial studies presented herein in which the wild-type clinical candidate clones were assessed. Simply, the VACV-Wyeth backbone is a more attenuated strain of virus that cannot replicate to the point of VACV-Copenhagen, even when attenuated versions of the latter are used. Finally, there are many clones in this working library that contain intergenic insertions of the TE, which presumably would have no effect on viral replication. To confirm this, viral growth curves were performed using Tp 229 and wild-type Copenhagen, and the nearly-identical growth kinetics led to the labeling of Tp 229 as "wild-type Copenhagen" for these replication studies. It was found to commonly be amongst the better-replicating virus clones for a given set of experimental conditions, however in every context there were several single gene mutants that possessed a growth advantage. To move these experiments forward, a much larger panel of cell lines for which molecular data is publicly-available were screened versus select non-transformed cell lines. These studies were designed to predict VACV mutations that might favour use as OVs, but also to understand whether it may be necessary to have tailored viral mutation landscapes in clinical candidate OVs for patients whose cancers possess a given molecular signature.

To answer these questions, a screen was performed on diverse cancer models that included a large portion of the NCI-60 cell panel supplemented with several additional cell lines of interest, including the human cervical carcinoma cell line HeLa, the human osteosarcoma cell line U-2 OS, two normal non-transformed human cell lines, and a six-member panel of patient-derived primary cultures representing both metastatic melanoma and ovarian cancer ascites. In total, relative virus replication was studied in 41 cell lines or primary cultures, including 39 different cancers, the normal human fibroblast cell line GM-38, and a primary normal human keratinocyte culture. These clustered data for cancer cell lines are summarized and presented in Figure 3.15, providing a clear example of the power of a tool such as the one developed for this research project. These data also represent head-to-head comparisons of single gene VACV mutants representing a majority of the non-essential VACV genome; to our knowledge, these results are the first of their kind and could help shape the design of next-generation OV therapeutics.

As summarized in Table 1.1, all clinical candidate VACV OV platforms to date have incorporated deletion or truncation of the VACV thymidine kinase gene *J2R*, thus providing some degree of targeting to highly metabolic cells. There are several interesting findings presented in Figure 3.15 that may be incorporated into the design of a next-generation therapeutic, however one in particular challenges the validity of this approach. Namely, Tp 255 (*J2R*, 0.8) appears to be significantly more attenuated in terms of virus replication across every cancer cell line tested. The relative attenuation of VACV following thymidine kinase deletion has been observed previously, however these observations focused on the development of effective vaccine strains, predate the development of OV platforms, and therefore this concept has not been studied in the context of transformed cells[185,237]. There exists the concept in the OV literature that cancer selectivity and targeting are increased following thymidine kinase deletion, however it has not been systematically

studied. Furthermore, the failings of previously-developed OV platforms seem to stem from virus platforms that are overly attenuated. The results presented here suggest that not only are these products developed on wild-type platforms that are more attenuated than wild-type Copenhagen at baseline, but that they were made further attenuated by design choices. Perhaps these data will help to prove the utility of VACV thymidine kinase in maintaining virulence in the context of diverse cancer models.

4.6. Effects of single gene mutations on vaccinia virus plaque size

Proficiency of viral plaque formation is a good indicator of the ability of the virus in question to efficiently cause cytolysis, and in general there are two properties that are studied in such assays. Typically, studies comment on the clarity of plaques formed given a set of experimental conditions, but also on the size of the plaques that are formed at a given time point. The killing of cells *in vitro* results in a loss of cell adherence, which can be visualized when a relevant dye such as crystal violet is used to stain remaining cell material. The complete clearance within formed virus plaques of remaining cellular material occurs with viruses that are proficient in the induction of cytolysis. Likewise, the diameter of formed plaques produced by virus at a given time point can speak to the efficiency of cell-to-cell spread, but also of killing. It stands to reason that a larger plaque occurs because of efficiently-spreading virions that can infect and carry out their lifecycle in neighboring cells, therefore resulting in a greater cell clearance. In VACV studies, plaque size is a common indicator of differential phenotype when new viral species are made and can be commonly found in the literature. As discussed previously, one of the more active areas of study in VACV occurs around VACV-induced cytoskeletal dynamics, which is thought to have fundamental implications for the efficiency of plaque formation. In the field of OV therapeutics, plaque size is often utilized as an imperfect surrogate for oncolytic effect, as many

viruses have demonstrated proficiency of plaque formation in cancer cells without causing cell death in normal cells. Furthermore, the study of viral plaque formation is another indicator of unique phenotype and can be especially useful in the study of novel phenotypes observed with mutant virus clones.

As VACV genes can have specific function(s), one of the goals of this research project was to characterize the unique biology produced by the single gene mutations that exist in this working library by studying the virus clones by more than one readout. To this end, the size of plaques produced by each of the clones in this library as well as wild-type Copenhagen and the current leading clinical VACV OV candidate was studied. The study of plaque sizes was carried out for the full library on four unique cell lines: the human cervical carcinoma cell line HeLa, the human melanoma cell line M14, and the human prostate carcinoma cell lines PC-3 and DU-145. Several notable results were observed that may impact future OV design and will provide a strong rationale for the study of virus-host interactions in the understanding of OV platforms. Plaque sizes produced by the wild-type Copenhagen virus varied in range, with it being amongst the largest observed plaques produced in HeLa, but appeared to be significantly more attenuated in M14, PC-3, and DU-145. This finding provides evidence for the importance of studying biology in diverse models because differential effects can be observed. It also brings into question the unique features of the HeLa cell line that distinguish it from others in which the full virus library was tested. Another interesting note is that the plaques produced by ΔTK-Wyeth were amongst the smallest of plaques produced in the library, even when compared to mutants with known impairment in their ability to efficiently spread, therefore producing plaques of drastically reduced size. This result provides further evidence that we may be sacrificing too much in the use of the clinical

candidate OV ΔTK-Wyeth in terms of its attenuation. Such an approach may not give a potential patient the best chance to respond favorably to treatment.

In terms of specific VACV genes whose insertional mutagenesis produced interesting results, there are several that have been highlighted in Figures 3.16 and 3.17. The first of note is with the VACV gene *F11L*, whose insertion was observed to produce a small plaque phenotype in each of the four cell lines tested. This result was predicted as the deletion of *F11L* is known to result in viruses with profound defects in cell-to-cell spread due to the absence of RhoA signaling inhibition, and indeed a small plaque phenotype has been described[181]. Furthermore, a polyclonal antibody against the PDZ domain of F11 demonstrated the complete loss of intact F11 protein in Tp 279 (*F11L*, 0.3). Another clear phenotype was observed for the clones with insertional mutagenesis of the VACV gene *A50R*. Consistently, this clone was observed to produce the single smallest or among the smallest plaque size phenotype of any clone in this library. This poor cell-to-cell spread was coupled with a poor ability to replicate (Figure 3.15) across the majority of cell lines in which these studies were performed. Mutants such as this may not be of immediate interest in the development or selection of a novel OV platform, however they may be encoded into non-VACV OV platforms to increase replication and/or virus spread and these are increasingly-relevant data that will allow us to expand our understanding of VACV biology.

Another striking phenotype that was observed was due to the insertional mutagenesis of VACV-Copenhagen *A47L*, which occurs in three independent viral clones in this library that each possess unique insertion sites. Insertional mutagenesis of this gene resulted in a plaque phenotype that was significantly larger than wild-type Copenhagen and any other virus clones in this library in Hela and M14 cells, however this phenotype was not observed in PC-3 and DU-145 cells (Figure 3.18). This result provides further evidence for the need to study such striking phenotypes across

a large panel of cell lines, and also provides evidence to further investigate differences that may exist in the molecular profile of HeLa and M14 cells versus PC-3 and DU-145 cells. Immediately obvious is that this phenotype was lost when cells derived from prostate carcinoma were studied, however it is likely that this is due to fundamental molecular differences in the host cell's ability to efficiently promote increased virus spread. Interestingly, this is a novel phenotype of VACV A47 that has not been described and whose further study may provide a mechanistic basis for understanding unique virus-host interactions.

On the other end of the phenotypic spectrum are the small plaques that were observed to be produced by virus clones with interruption of the *F15L* gene. There are two such unique clones in this library, Tp 311 (0.3) and Tp 61 (0.8), for which the same phenotype was observed in these plaque size studies. This result was first observed in HeLa cells and was interesting because of the striking phenotype that was observed, the fact that a similar phenotype was observed for both Tp 311 and Tp 61, and for the fact that VACV *F15L* remains undescribed in the literature. As presented in Figure 3.18, this observed effect was statistically significant in only one out of the four cell lines tested, however the mean plaque size was smaller than that observed for wild-type Copenhagen in each of the other three cell lines studied. Again, this provides evidence for the complexity of the biological interactions that lead to the observable plaque size phenotypes and the need to expand findings such as this to a larger panel of cells before required molecular studies can be executed.

4.7. Virus-induced cytoskeletal dynamics: implications for OV therapeutics

Virus-induced modulation of the host cell cytoskeletal system is currently one of the most active areas of investigation in the VACV field. Findings have provided many fundamental lessons in cell biology, and systematic study of the inherent complexities in VACV-host cell interactions

hold the potential to reveal novel aspects of cancer biology. As such, suitable members of the NCI-60 panel were supplemented with the human osteosarcoma cell line U-2 OS as well as the tumour-derived primary melanoma culture Patient 12-2016 to comprise a 20-member panel on which the size of plaques formed by select virus clones after 72 hours of infection was assessed. Cells were selected for these assays based on their propensity for uniform monolayer formation in culture, which is a necessary prerequisite to performing these experiments. Many interesting observations were made that (1) demonstrate the power of viral factors in modulating virus spread and cytotoxicity, and (2) suggest that viral plaque formation occurs due to a complex interplay between virus and host cell factors, which can be differentially-appreciated in unique molecular landscapes found in unique hosts.

4.7.1. Vaccinia virus F11L

To understand the power of viral factors in modulating cell-to-cell spread, the insertion mutant of F11 was studied (Tp 279, 0.3). Ubiquitously, viral plaque size was observed to be diminished compared to wild-type Copenhagen (Table 3.2), which was expected given the critical role of RhoA signaling in modulating cell-to-cell spread and given the previously-discussed properties of this clone. Studies focusing on VACV genes that have been implicated in modulating viral plaque size have overwhelmingly focused on the host cell cytoskeletal framework as a causative factor. In the case of F11, modulation is at the level of the cellular cortical actin, the nucleation of which promotes the formation of actin tails and the propulsion of EEV from the host cell surface following the completion of the viral lifecycle. At the level of microtubule transport, a similar small plaque phenotype has been observed with mutant VACV proteins A36, F12, and F13, which all directly or indirectly modulate the microtubule transport system. The modulation of other virus factors has also been shown to modify the size of observed plaques, however these

differences tend not to be as striking as those caused by the diminished ability to subvert the host cytoskeleton.

4.7.2. Vaccinia virus F15L

Similar to the results observed in these 20 cell lines for the *F11L* insertion mutant in this library are the results for the *F15L* insertion mutant Tp 311 (0.3). In 18 of the 20 cell lines studied, plaques formed by this clone were significantly smaller than those formed by wild-type Copenhagen, which suggests the profound modulation of a currently unknown host response due to a virus factor. Interestingly, these results are accompanied by the qualitative observation that this F15 mutant has a diminished ability to induce EEV formation and/or release (Figure 3.20), however it also is observed to be relatively less attenuated than other mutants in this virus library. Taken together, these results suggest that the infectious progeny are highly produced, however have a diminished ability to either (1) be wrapped with an additional membrane, (2) make it to the cell surface, or (3) be released. Furthermore, and perhaps paradoxically, Figure 3.23 suggests the possibility that VACV F15 is a survival factor as it appears to be more toxic in immunocompetent animals compared to wild-type Copenhagen. Finally, the high evolutionary conservation of F15 across divergent orthopoxviruses (Figure 3.22) suggests that it may have an important role in VACV propagation as its peptide sequence shares remarkable (near 100%) homology to species as divergent as variola virus. Although these data work to support a role for the currently undescribed VACV gene *F15L*, the mechanism(s) for these findings remains undiscovered. Interestingly, this 158-amino acid protein is not predicted to have any functional domains, so further probing studies will be necessary to gain an understanding of what this protein's role is in the lifecycle of VACV and how it accomplishes this.

Assuming that an effective OV candidate might display an *in vitro* phenotype that is the opposite of that observed with these F15 mutants, it is unlikely that incorporation of a similar mutation will result in a superior OV backbone. However, the possibility exists for encoding this VACV protein into another OV platform, such as VSV. As discussed previously, this approach has been utilized to take advantage of the phenotypic properties of VACV F11 by encoding it into a myxoma virus backbone. This resulted in an OV with increased potential to spread to distant tumour sites and displayed distant tumour control[97,182]. This increased spread phenotype was utilized in VACV to create a better OV platform[98], however these ideas have yet to be fully developed in the field. Whatever the case, the *F15L* studies presented in this research project are the first to functionally describe this unknown protein, open the door for studies to understand the mechanisms by which these phenotypes are observed, which hold the potential to increase our understanding of the complexity of virus-host interactions.

4.7.3. Vaccinia virus A47L

In many ways, the data presented describing the phenotypes that were observed given the insertional mutagenesis of VACV *A47L* is striking. The current understanding of this gene's role in the VACV lifecycle is minimal and it has been described solely as a highly-transcribed gene whose immunoprevalent protein contains many CD8+ T cell epitopes[226], therefore its deletion would be expected to result in a diminished anti-VACV CD8+ T cell response. In the data presented throughout this project, it seems to play a role in the release of EEV from infected cells as plaque assays performed under a liquid overlay demonstrate striking comets in HeLa and other cell lines (Figure 3.20). Plaque size assays performed under a semi-solid overlay strengthen these findings in cell lines for which it was observed, however this effect seems to be profoundly-regulated by host cell factors. In the 20-member cell line panel for which this was studied,

significantly-altered plaque size was observed for VACV A47 mutants in only nine of the cell lines at 72 hours post-infection. These altered plaque sizes were observed to be larger than wild-type Copenhagen in five of the nine and were surprisingly found to produce smaller plaques than wild-type Copenhagen in four of these cell lines. These data suggest that certain hosts are able to be modulated by a VACV A47 mutant in opposite ways to other hosts, and the clear comet phenotype observed in HeLa cells suggest that this altered plaque size is caused by differential EEV release. These data suggest that VACV *A47L* deletion causes differential modulation of the host cytoskeleton, however mechanisms remain currently undescribed. Furthermore, the protein-level homology of VACV A47 presented in Figure 3.21 demonstrates the presence of homologues in a smaller number of species than with F15 and the near 100% conservation in only closely-related viral species, including the other wild-type strains of VACV used in this study.

From an OV perspective, the deletion of *A47L* from a clinical candidate platform may be advantageous in select patients, however may have the opposite effect in others. Clearly, molecular mechanisms for the differential plaque sizes and EEV release would need to be understood before any conclusions could be made. However, the findings described herein raise the question of whether concepts of personalized medicine should be applied to OV therapy. Simple tumour genomic sequencing could lead to the selection of unique OV platforms if differential viral phenotypes are found to offer unique benefits in a clinical setting.

4.8. The redundancy of vaccinia virus genes complicates their functional definition

Vaccinia is a complex virus with many genes that are known to possess redundant functions to others[238]. From the perspective of viral fitness, this strategy may be beneficial when evolutionary pressures are faced. From the perspective of gaining a functional genomic understanding of the virus, this redundancy complicates matters. It is well known and has been

described in this thesis that a large central portion of the VACV genome is highly-conserved and contains genes whose functions are essential to viral replication. Many immune-modulating and host range genes, however are found in the areas represented by insertion mutants in this VACV library. There are well-known examples of redundant genes in this region that have only been defined in the context of underlying mutations of regions in which genes with redundant functions are also deleted. An excellent example of this is the VGF-encoding VACV gene *C11R*, which is a soluble factor known to bind to EGFR and promote NF-κB activation, has been described as an *in vitro* growth factor, however it behaves as an essential gene in the context of a large terminal deletion that eliminates the complicating factors of redundant genes from the genome.

A library of single gene mutants such as the one used in this research project is an incredibly useful tool for the characterization of VACV genes, however there are likely many functions masked by the presence of redundant counterparts. It is likely that subtle changes in phenotype such as increased or decreased viral replication are not easily discernible due to the nature of the assays, however experiments such as these do provide meaningful data that can be incorporated into next-generation OV backbones. Perhaps phenotypes such as the striking ones observed with F11, F15, and A47 mutants in some or all experimental contexts suggest that genes with redundant functionality do not exist in those cases. This is indeed known to be true for the unique cellular RhoA signaling regulation by VACV F11. Regardless, it is likely important to consider incorporating several gene deletions into one viral backbone in an effort to tailor an OV backbone to the phenotype of interest. Furthermore, the possibility also exists to modify a VACV backbone that already contains major gene deletions, which could independently deliver a desired OV phenotype. Overlaying such a virus with a mutant library, perhaps using the same technique

as described in this research project, could then provide even further information regarding VACV biology to unmask unappreciated genetic effects.

General Concluding Remarks

The primary objective of this work was to develop a better understanding of the genetic components of VACV, specifically for phenotypic properties that are relevant to the development of next-generation OV therapeutics. Before setting out to study the functional genomics of VACV, considerable effort was dedicated to the rational selection of the wild-type strain of the virus with properties that seemed most interesting for their oncolytic potential. This resulted in the selection of VACV-Copenhagen as the platform virus for the development of a library of single-gene mutants using a novel TE insertional mutagenesis approach. The development of the working virus library resulted in a tool that has wide-ranging utility for the study of VACV as it is composed of several dozen single gene VACV mutants. These virus mutants were described in the context of this study for their properties which are thought to impact downstream efficacy as OV therapeutics, however there are clear implications for the development of novel vaccines, furthering our understanding of VACV biology, and subsequently as a tool to better understand components of cell biology.

One of the most active areas of study in the field of VACV biology surrounds the modulation and understanding of VACV's usurping of the host cell cytoskeleton to execute its lifecycle. It is not surprising that the field has taken this turn as VACV (and most other viruses) exploits these existing intracellular transport pathways to navigate the cell as virions require unique cellular components at specific times in their lifecycle. The speed and efficiency with which VACV has evolved to replicate has made it masterful at utilizing these transport mechanisms. Some of what we understand about intracellular transport and cell motility in general has come from the basic study of VACV, however the extent of our understanding is regularly pushed. Many publications have explored the links between injury response-induced cell motility and cancer

metastasis, concepts which tie together VACV cytoskeletal dynamics and cancer progression. Some data presented in this work seems to add to the current list of VACV proteins that modulate various cytoskeletal components and the scope to which this occurs, but further mechanistic studies will need to be performed to investigate these hypotheses. In addition to the formation of this working clonal library and its initial characterization, the most interesting components to arise from this project are the VACV genes *A47L* and *F15L*. The functions of VACV A47 described in this project remain undescribed, and F15 is a functionally unknown protein. It also remains unclear how the modulation of the host cytoskeleton may impact efficacy of an OV candidate, although two separate studies have provided evidence that proficient EEV-producing virus clones stand a better chance to achieve clinical success.

From a therapeutic perspective, there are many studies that could follow those presented in this thesis in order to determine the translational possibilities of certain VACV mutations. One such finding that stands a chance of impacting the design of future OV candidates is the observation that viral thymidine kinase mutation results in a severely attenuated virus. Furthermore, the dichotomous phenotypes that were observed for VACV A47 mutant clones set the stage for the exploration of unique OVs based on a patient's molecular subtype of cancer. Greater study of the virulence and/or normal cell cytotoxicity associated with these genetic changes will be necessary.

Clarity surrounding the therapeutic potential of OVs, and interest in an effective VACV OV platform specifically, continue to grow. To date in the development of novel VACV OV therapeutics, innovations have come despite an incomplete understanding of the genetic and phenotypic landscape of the virus. It was abundantly clear at the onset of this project that a comprehensive and well-characterized tool to better understand such properties of VACV needed

to be developed and may have widespread utility. As the OV field moves towards an optimized therapeutic VACV platform and the interest in the study of basic VACV biology continues to grow, this virus library and its functional characterization could disrupt currently-held biologic beliefs and shape future OV design decisions.

References

1 Canadian Cancer Society's Advisory Committee on Cancer Statistics. Canadian Cancer Statistics 2016. (Canadian Cancer Society, Toronto, ON, 2016).

2 Postow, M. A. *et al.* Nivolumab and ipilimumab versus ipilimumab in untreated melanoma. *N Engl J Med* **372**, 2006-2017, doi:10.1056/NEJMoa1414428 (2015).

3 Hanahan, D. & Weinberg, R. A. The hallmarks of cancer. *Cell* **100**, 57-70 (2000).

4 Hanahan, D. & Weinberg, R. A. Hallmarks of cancer: the next generation. *Cell* **144**, 646-674, doi:10.1016/j.cell.2011.02.013 (2011).

5 Armitage, P. & Doll, R. The age distribution of cancer and a multi-stage theory of carcinogenesis. *Br J Cancer* **91**, 1983-1989, doi:10.1038/sj.bjc.6602297 (2004).

6 Balmain, A. Cancer genetics: from Boveri and Mendel to microarrays. *Nature reviews. Cancer* **1**, 77-82, doi:10.1038/35094086 (2001).

7 Knudson, A. G. Two genetic hits (more or less) to cancer. *Nature reviews. Cancer* **1**, 157-162, doi:10.1038/35101031 (2001).

8 Knudson, A. G., Jr. Mutation and cancer: statistical study of retinoblastoma. *Proc Natl Acad Sci U S A* **68**, 820-823 (1971).

9 Zitvogel, L., Tesniere, A. & Kroemer, G. Cancer despite immunosurveillance: immunoselection and immunosubversion. *Nat Rev Immunol* **6**, 715-727, doi:10.1038/nri1936 (2006).

10 So, T. *et al.* Haplotype loss of HLA class I antigen as an escape mechanism from immune attack in lung cancer. *Cancer Res* **65**, 5945-5952, doi:10.1158/0008-5472.CAN-04-3787 (2005).

11 Devaud, C., John, L. B., Westwood, J. A., Darcy, P. K. & Kershaw, M. H. Immune modulation of the tumor microenvironment for enhancing cancer immunotherapy. *Oncoimmunology* **2**, e25961, doi:10.4161/onci.25961 (2013).

12 Ascierto, P. A. *et al.* The role of BRAF V600 mutation in melanoma. *J Transl Med* **10**, 85, doi:10.1186/1479-5876-10-85 (2012).

13 Liu, J. F. *et al.* Combination cediranib and olaparib versus olaparib alone for women with recurrent platinum-sensitive ovarian cancer: a randomised phase 2 study. *Lancet Oncol* **15**, 1207-1214, doi:10.1016/S1470-2045(14)70391-2 (2014).

14 Jayson, G. C., Kerbel, R., Ellis, L. M. & Harris, A. L. Antiangiogenic therapy in oncology: current status and future directions. *Lancet* **388**, 518-529, doi:10.1016/S0140-6736(15)01088-0 (2016).

15 Welcsh, P. L. & King, M. C. BRCA1 and BRCA2 and the genetics of breast and ovarian cancer. *Hum Mol Genet* **10**, 705-713 (2001).

16 Arjaans, M. *et al.* VEGF pathway targeting agents, vessel normalization and tumor drug uptake: from bench to bedside. *Oncotarget* **7**, 21247-21258, doi:10.18632/oncotarget.6918 (2016).

17 Wolchok, J. D. *et al.* Nivolumab plus ipilimumab in advanced melanoma. *N Engl J Med* **369**, 122-133, doi:10.1056/NEJMoa1302369 (2013).

18 Kelly, E. & Russell, S. J. History of oncolytic viruses: genesis to genetic engineering. *Mol Ther* **15**, 651-659, doi:10.1038/sj.mt.6300108 (2007).

19 Hoster, H. A., Zanes, R. P., Jr. & Von Haam, E. Studies in Hodgkin's syndrome; the association of viral hepatitis and Hodgkin's disease; a preliminary report. *Cancer Res* **9**, 473-480 (1949).

20 Moore, A. E. The destructive effects of viruses on transplantable mouse tumors. *Acta Unio Int Contra Cancrum* **7**, 279-281 (1951).

21 Southam, C. M. & Moore, A. E. Clinical studies of viruses as antineoplastic agents with particular reference to Egypt 101 virus. *Cancer* **5**, 1025-1034 (1952).

22 Keller, B. A. & Bell, J. C. Oncolytic viruses-immunotherapeutics on the rise. *J Mol Med (Berl)* **94**, 979-991, doi:10.1007/s00109-016-1453-9 (2016).

23 Schlee, M. & Hartmann, G. The Chase for the RIG-I Ligand-Recent Advances. *Mol Ther* **18**, 1254-1262, doi:10.1038/mt.2010.90 (2010).

24 Paludan, S. R. & Bowie, A. G. Immune sensing of DNA. *Immunity* **38**, 870-880, doi:10.1016/j.immuni.2013.05.004 (2013).

25 Burckstummer, T. *et al.* An orthogonal proteomic-genomic screen identifies AIM2 as a cytoplasmic DNA sensor for the inflammasome. *Nat Immunol* **10**, 266-272, doi:10.1038/ni.1702 (2009).

26 Fernandes-Alnemri, T., Yu, J. W., Datta, P., Wu, J. & Alnemri, E. S. AIM2 activates the inflammasome and cell death in response to cytoplasmic DNA. *Nature* **458**, 509-513, doi:10.1038/nature07710 (2009).

27 Hornung, V. *et al.* AIM2 recognizes cytosolic dsDNA and forms a caspase-1-activating inflammasome with ASC. *Nature* **458**, 514-518, doi:10.1038/nature07725 (2009).

28 Chiu, Y. H., Macmillan, J. B. & Chen, Z. J. RNA polymerase III detects cytosolic DNA and induces type I interferons through the RIG-I pathway. *Cell* **138**, 576-591, doi:10.1016/j.cell.2009.06.015 (2009).

29 Ablasser, A. *et al.* RIG-I-dependent sensing of poly(dA:dT) through the induction of an RNA polymerase III-transcribed RNA intermediate. *Nat Immunol* **10**, 1065-1072, doi:10.1038/ni.1779 (2009).

30 Wu, W. Z. *et al.* Interferon alpha 2a down-regulates VEGF expression through PI3 kinase and MAP kinase signaling pathways. *J Cancer Res Clin Oncol* **131**, 169-178, doi:10.1007/s00432-004-0615-2 (2005).

31 Sadler, A. J. & Williams, B. R. Interferon-inducible antiviral effectors. *Nat Rev Immunol* **8**, 559-568, doi:10.1038/nri2314 (2008).

32 Pikor, L. A., Bell, J. C. & Diallo, J.-S. Oncolytic Viruses: Exploiting Cancer's Deal with the Devil. *Trends in Cancer* **1**, 266-277, doi:10.1016/j.trecan.2015.10.004.

33 Shankaran, V. *et al.* IFNgamma and lymphocytes prevent primary tumour development and shape tumour immunogenicity. *Nature* **410**, 1107-1111, doi:10.1038/35074122 (2001).

34 Nozawa, H. *et al.* Loss of transcription factor IRF-1 affects tumor susceptibility in mice carrying the Ha-ras transgene or nullizygosity for p53. *Genes Dev* **13**, 1240-1245 (1999).

35 Pansky, A. *et al.* Defective Jak-STAT signal transduction pathway in melanoma cells resistant to growth inhibition by interferon-alpha. *Int J Cancer* **85**, 720-725 (2000).

36 Shahid, S., Nawaz Chaudhry, M., Mahmood, N. & Sheikh, S. Mutations of the human interferon alpha-2b gene in brain tumor patients exposed to different environmental conditions. *Cancer Gene Ther* **22**, 246-261, doi:10.1038/cgt.2015.12 (2015).

37 Butcher, C. M. *et al.* Two novel JAK2 exon 12 mutations in JAK2V617F-negative polycythaemia vera patients. *Leukemia* **22**, 870-873, doi:10.1038/sj.leu.2404971 (2008).

38 Grunebach, F., Bross-Bach, U., Kanz, L. & Brossart, P. Detection of a new JAK2 D620E mutation in addition to V617F in a patient with polycythemia vera. *Leukemia* **20**, 2210-2211, doi:10.1038/sj.leu.2404419 (2006).

39 Najfeld, V., Cozza, A., Berkofsy-Fessler, W., Prchal, J. & Scalise, A. Numerical gain and structural rearrangements of JAK2, identified by FISH, characterize both JAK2617V>F-positive and -negative patients with Ph-negative MPD, myelodysplasia, and B-lymphoid neoplasms. *Exp Hematol* **35**, 1668-1676, doi:10.1016/j.exphem.2007.08.025 (2007).

40 Malinge, S. *et al.* Novel activating JAK2 mutation in a patient with Down syndrome and B-cell precursor acute lymphoblastic leukemia. *Blood* **109**, 2202-2204, doi:10.1182/blood-2006-09-045963 (2007).

41 Chiappinelli, K. B. *et al.* Inhibiting DNA Methylation Causes an Interferon Response in Cancer via dsRNA Including Endogenous Retroviruses. *Cell* **162**, 974-986, doi:10.1016/j.cell.2015.07.011 (2015).

42 Guo, G. *et al.* Ligand-Independent EGFR Signaling. *Cancer Res* **75**, 3436-3441, doi:10.1158/0008-5472.CAN-15-0989 (2015).

43 Holderfield, M., Deuker, M. M., McCormick, F. & McMahon, M. Targeting RAF kinases for cancer therapy: BRAF-mutated melanoma and beyond. *Nature reviews. Cancer* **14**, 455-467, doi:10.1038/nrc3760 (2014).

44 Nikiforov, Y. E. & Nikiforova, M. N. Molecular genetics and diagnosis of thyroid cancer. *Nat Rev Endocrinol* **7**, 569-580, doi:10.1038/nrendo.2011.142 (2011).

45 Ragab, A. *et al.* Drosophila Ras/MAPK signalling regulates innate immune responses in immune and intestinal stem cells. *EMBO J* **30**, 1123-1136, doi:10.1038/emboj.2011.4 (2011).

46 Strong, J. E., Coffey, M. C., Tang, D., Sabinin, P. & Lee, P. W. The molecular basis of viral oncolysis: usurpation of the Ras signaling pathway by reovirus. *EMBO J* **17**, 3351-3362, doi:10.1093/emboj/17.12.3351 (1998).

47 Strong, J. E. & Lee, P. W. The v-erbB oncogene confers enhanced cellular susceptibility to reovirus infection. *J Virol* **70**, 612-616 (1996).

48 Strong, J. E., Tang, D. & Lee, P. W. Evidence that the epidermal growth factor receptor on host cells confers reovirus infection efficiency. *Virology* **197**, 405-411, doi:10.1006/viro.1993.1602 (1993).

49 Parato, K. A. *et al.* The oncolytic poxvirus JX-594 selectively replicates in and destroys cancer cells driven by genetic pathways commonly activated in cancers. *Mol Ther* **20**, 749-758, doi:10.1038/mt.2011.276 (2012).

50 Oshiumi, H. *et al.* DDX60 Is Involved in RIG-I-Dependent and Independent Antiviral Responses, and Its Function Is Attenuated by Virus-Induced EGFR Activation. *Cell Rep* **11**, 1193-1207, doi:10.1016/j.celrep.2015.04.047 (2015).

51 Tummers, B. *et al.* The interferon-related developmental regulator 1 is used by human papillomavirus to suppress NFkappaB activation. *Nat Commun* **6**, 6537, doi:10.1038/ncomms7537 (2015).

52 Ueki, I. F. *et al.* Respiratory virus-induced EGFR activation suppresses IRF1-dependent interferon lambda and antiviral defense in airway epithelium. *J Exp Med* **210**, 1929-1936, doi:10.1084/jem.20121401 (2013).

53 Ferrara, N. Vascular endothelial growth factor: basic science and clinical progress. *Endocr Rev* **25**, 581-611, doi:10.1210/er.2003-0027 (2004).

54 Hicklin, D. J. & Ellis, L. M. Role of the vascular endothelial growth factor pathway in tumor growth and angiogenesis. *J Clin Oncol* **23**, 1011-1027, doi:10.1200/JCO.2005.06.081 (2005).

55 Margolin, K. Inhibition of vascular endothelial growth factor in the treatment of solid tumors. *Curr Oncol Rep* **4**, 20-28 (2002).

56 Breitbach, C. J. *et al.* Oncolytic vaccinia virus disrupts tumor-associated vasculature in humans. *Cancer Res* **73**, 1265-1275, doi:10.1158/0008-5472.CAN-12-2687 (2013).

57 Breitbach, C. J. *et al.* Intravenous delivery of a multi-mechanistic cancer-targeted oncolytic poxvirus in humans. *Nature* **477**, 99-102, doi:10.1038/nature10358 (2011).

58 Breitbach, C. J. *et al.* Targeting tumor vasculature with an oncolytic virus. *Mol Ther* **19**, 886-894, doi:10.1038/mt.2011.26 (2011).

59 Arulanandam, R. *et al.* VEGF-Mediated Induction of PRD1-BF1/Blimp1 Expression Sensitizes Tumor Vasculature to Oncolytic Virus Infection. *Cancer Cell* **28**, 210-224, doi:10.1016/j.ccell.2015.06.009 (2015).

60 Ilkow, C. S. *et al.* Reciprocal cellular cross-talk within the tumor microenvironment promotes oncolytic virus activity. *Nat Med* **21**, 530-536, doi:10.1038/nm.3848 (2015).

61 Lichty, B. D., Breitbach, C. J., Stojdl, D. F. & Bell, J. C. Going viral with cancer immunotherapy. *Nature reviews. Cancer* **14**, 559-567, doi:10.1038/nrc3770 (2014).

62 Liu, T. C., Hwang, T., Park, B. H., Bell, J. & Kirn, D. H. The targeted oncolytic poxvirus JX-594 demonstrates antitumoral, antivascular, and anti-HBV activities in patients with hepatocellular carcinoma. *Mol Ther* **16**, 1637-1642, doi:10.1038/mt.2008.143 (2008).

63 Hiley, C. T. *et al.* Vascular endothelial growth factor A promotes vaccinia virus entry into host cells via activation of the Akt pathway. *J Virol* **87**, 2781-2790, doi:10.1128/JVI.00854-12 (2013).

64 Adelfinger, M. *et al.* Preclinical Testing Oncolytic Vaccinia Virus Strain GLV-5b451 Expressing an Anti-VEGF Single-Chain Antibody for Canine Cancer Therapy. *Viruses* **7**, 4075-4092, doi:10.3390/v7072811 (2015).

65 Bazan-Peregrino, M. *et al.* Combining virotherapy and angiotherapy for the treatment of breast cancer. *Cancer Gene Ther* **20**, 461-468, doi:10.1038/cgt.2013.41 (2013).

66 Frentzen, A. *et al.* Anti-VEGF single-chain antibody GLAF-1 encoded by oncolytic vaccinia virus significantly enhances antitumor therapy. *Proc Natl Acad Sci U S A* **106**, 12915-12920, doi:10.1073/pnas.0900660106 (2009).

67 Gholami, S. *et al.* A novel vaccinia virus with dual oncolytic and anti-angiogenic therapeutic effects against triple-negative breast cancer. *Breast Cancer Res Treat* **148**, 489-499, doi:10.1007/s10549-014-3180-7 (2014).

68 Huang, T. *et al.* Expression of anti-VEGF antibody together with anti-EGFR or anti-FAP enhances tumor regression as a result of vaccinia virotherapy. *Mol Ther Oncolytics* **2**, 15003, doi:10.1038/mto.2015.3 (2015).

69 Deguchi, T. *et al.* Combination of the tumor angiogenesis inhibitor bevacizumab and intratumoral oncolytic herpes virus injections as a treatment strategy for human gastric cancers. *Hepatogastroenterology* **59**, 1844-1850, doi:10.5754/hge11566 (2012).

70 Zhang, W. *et al.* Bevacizumab with angiostatin-armed oHSV increases antiangiogenesis and decreases bevacizumab-induced invasion in U87 glioma. *Mol Ther* **20**, 37-45, doi:10.1038/mt.2011.187 (2012).

71 Tan, G. *et al.* Combination therapy of oncolytic herpes simplex virus HF10 and bevacizumab against experimental model of human breast carcinoma xenograft. *Int J Cancer* **136**, 1718-1730, doi:10.1002/ijc.29163 (2015).

72 Leite, F. & Way, M. The role of signalling and the cytoskeleton during Vaccinia Virus egress. *Virus Res* **209**, 87-99, doi:10.1016/j.virusres.2015.01.024 (2015).

73 MacTavish, H. *et al.* Enhancement of vaccinia virus based oncolysis with histone deacetylase inhibitors. *PLoS One* **5**, e14462, doi:10.1371/journal.pone.0014462 (2010).

74 McKenzie, B. A. *et al.* In vitro screen of a small molecule inhibitor drug library identifies multiple compounds that synergize with oncolytic myxoma virus against human brain tumor-initiating cells. *Neuro Oncol* **17**, 1086-1094, doi:10.1093/neuonc/nou359 (2015).

75 Diallo, J. S. *et al.* A high-throughput pharmacoviral approach identifies novel oncolytic virus sensitizers. *Mol Ther* **18**, 1123-1129, doi:10.1038/mt.2010.67 (2010).

76 Couzin-Frankel, J. Breakthrough of the year 2013. Cancer immunotherapy. *Science* **342**, 1432-1433, doi:10.1126/science.342.6165.1432 (2013).

77 Woller, N. *et al.* Viral Infection of Tumors Overcomes Resistance to PD-1-immunotherapy by Broadening Neoantigenome-directed T-cell Responses. *Mol Ther* **23**, 1630-1640, doi:10.1038/mt.2015.115 (2015).

78 Dias, J. D. *et al.* Targeted cancer immunotherapy with oncolytic adenovirus coding for a fully human monoclonal antibody specific for CTLA-4. *Gene Ther* **19**, 988-998, doi:10.1038/gt.2011.176 (2012).

79 Du, T. *et al.* Tumor-specific oncolytic adenoviruses expressing granulocyte macrophage colony-stimulating factor or anti-CTLA4 antibody for the treatment of cancers. *Cancer Gene Ther* **21**, 340-348, doi:10.1038/cgt.2014.34 (2014).

80 Engeland, C. E. *et al.* CTLA-4 and PD-L1 checkpoint blockade enhances oncolytic measles virus therapy. *Mol Ther* **22**, 1949-1959, doi:10.1038/mt.2014.160 (2014).

81 Zamarin, D. *et al.* Localized oncolytic virotherapy overcomes systemic tumor resistance to immune checkpoint blockade immunotherapy. *Sci Transl Med* **6**, 226ra232, doi:10.1126/scitranslmed.3008095 (2014).

82 Zamarin, D. *et al.* Intratumoral modulation of the inducible co-stimulator ICOS by recombinant oncolytic virus promotes systemic anti-tumour immunity. *Nat Commun* **8**, 14340, doi:10.1038/ncomms14340 (2017).

83 Ilett, E. *et al.* Prime-boost using separate oncolytic viruses in combination with checkpoint blockade improves anti-tumour therapy. *Gene Ther* **24**, 21-30, doi:10.1038/gt.2016.70 (2017).

84 Shen, W., Patnaik, M. M., Ruiz, A., Russell, S. J. & Peng, K. W. Immunovirotherapy with vesicular stomatitis virus and PD-L1 blockade enhances therapeutic outcome in murine acute myeloid leukemia. *Blood* **127**, 1449-1458, doi:10.1182/blood-2015-06-652503 (2016).

85 Rajani, K. *et al.* Combination Therapy With Reovirus and Anti-PD-1 Blockade Controls Tumor Growth Through Innate and Adaptive Immune Responses. *Mol Ther* **24**, 166-174, doi:10.1038/mt.2015.156 (2016).

86 Cockle, J. V. *et al.* Combination viroimmunotherapy with checkpoint inhibition to treat glioma, based on location-specific tumor profiling. *Neuro Oncol* **18**, 518-527, doi:10.1093/neuonc/nov173 (2016).

87 Rojas, J. J., Sampath, P., Hou, W. & Thorne, S. H. Defining Effective Combinations of Immune Checkpoint Blockade and Oncolytic Virotherapy. *Clin Cancer Res* **21**, 5543-5551, doi:10.1158/1078-0432.CCR-14-2009 (2015).

88 Puzanov, I. *et al.* Talimogene Laherparepvec in Combination With Ipilimumab in Previously Untreated, Unresectable Stage IIIB-IV Melanoma. *J Clin Oncol* **34**, 2619-2626, doi:10.1200/JCO.2016.67.1529 (2016).

89 Sen Sharma, K. *et al.* Efficient fluorescence-based imaging methods for quantitating infectivity and oncolytic efficacy of Newcastle disease virus. *J Virol Methods* **163**, 390-397, doi:10.1016/j.jviromet.2009.10.030 (2010).

90 Garcia, V. *et al.* High-throughput titration of luciferase-expressing recombinant viruses. *J Vis Exp*, 51890, doi:10.3791/51890 (2014).

91 Passer, B. J. *et al.* Identification of the ENT1 antagonists dipyridamole and dilazep as amplifiers of oncolytic herpes simplex virus-1 replication. *Cancer Res* **70**, 3890-3895, doi:10.1158/0008-5472.CAN-10-0155 (2010).

92 Diallo, J. S. *et al.* A High-throughput Pharmacoviral Approach Identifies Novel Oncolytic Virus Sensitizers. *Mol Ther* **18**, 1123-1129, doi:10.1038/mt.2010.67 (2010).

93 Workenhe, S. T., Ketela, T., Moffat, J., Cuddington, B. P. & Mossman, K. L. Genome-wide lentiviral shRNA screen identifies serine/arginine-rich splicing factor 2 as a determinant of oncolytic virus activity in breast cancer cells. *Oncogene* **35**, 2465-2474, doi:10.1038/onc.2015.303 (2016).

94 Panda, D. *et al.* RNAi screening reveals requirement for host cell secretory pathway in infection by diverse families of negative-strand RNA viruses. *Proc Natl Acad Sci U S A* **108**, 19036-19041, doi:10.1073/pnas.1113643108 (2011).

95 Sivan, G. *et al.* Human genome-wide RNAi screen reveals a role for nuclear pore proteins in poxvirus morphogenesis. *Proc Natl Acad Sci U S A* **110**, 3519-3524, doi:10.1073/pnas.1300708110 (2013).

96 Allan, K. J., Stojdl, D. F. & Swift, S. L. High-throughput screening to enhance oncolytic virus immunotherapy. *Oncolytic Virother* **5**, 15-25, doi:10.2147/OV.S66217 (2016).

97 Irwin, C. R., Favis, N. A., Agopsowicz, K. C., Hitt, M. M. & Evans, D. H. Myxoma virus oncolytic efficiency can be enhanced through chemical or genetic disruption of the actin cytoskeleton. *PLoS One* **8**, e84134, doi:10.1371/journal.pone.0084134 (2013).

98 Kirn, D. H., Wang, Y., Liang, W., Contag, C. H. & Thorne, S. H. Enhancing poxvirus oncolytic effects through increased spread and immune evasion. *Cancer Res* **68**, 2071-2075, doi:10.1158/0008-5472.CAN-07-6515 (2008).

99 Moss, B. in *Fields virology* Vol. 2 (eds David M. Knipe & Peter M. Howley) 2129-2159 (Wolters Kluwer/Lippincott Williams & Wilkins Health, 2013).

100 Damon, I. K. in *Fields virology* Vol. 2 (eds David M. Knipe & Peter M. Howley) 2160-2184 (Wolters Kluwer/Lippincott Williams & Wilkins Health, 2013).

101 Peres, M. G. *et al.* Serological study of vaccinia virus reservoirs in areas with and without official reports of outbreaks in cattle and humans in Sao Paulo, Brazil. *Arch Virol* **158**, 2433-2441, doi:10.1007/s00705-013-1740-5 (2013).

102 Costa, G. B. *et al.* Detection of Vaccinia Virus in Urban Domestic Cats, Brazil. *Emerg Infect Dis* **23**, 360-362, doi:10.3201/eid2302.161341 (2017).

103 Reich, E., Franklin, R. M., Shatkin, A. J. & Tatum, E. L. Effect of actinomycin D on cellular nucleic acid synthesis and virus production. *Science* **134**, 556-557 (1961).

104 Cyrklaff, M. *et al.* Cryo-electron tomography of vaccinia virus. *Proc Natl Acad Sci U S A* **102**, 2772-2777, doi:10.1073/pnas.0409825102 (2005).

105 Heuser, J. Deep-etch EM reveals that the early poxvirus envelope is a single membrane bilayer stabilized by a geodetic "honeycomb" surface coat. *J Cell Biol* **169**, 269-283, doi:10.1083/jcb.200412169 (2005).

106 Baroudy, B. M., Venkatesan, S. & Moss, B. Incompletely base-paired flip-flop terminal loops link the two DNA strands of the vaccinia virus genome into one uninterrupted polynucleotide chain. *Cell* **28**, 315-324 (1982).

107 Merchlinsky, M. Mutational analysis of the resolution sequence of vaccinia virus DNA: essential sequence consists of two separate AT-rich regions highly conserved among poxviruses. *J Virol* **64**, 5029-5035 (1990).

108 Mackett, M. & Archard, L. C. Conservation and variation in Orthopoxvirus genome structure. *J Gen Virol* **45**, 683-701, doi:10.1099/0022-1317-45-3-683 (1979).

109 DeFilippes, F. M. Restriction enzyme mapping of vaccinia virus DNA. *J Virol* **43**, 136-149 (1982).

110 Goebel, S. J. *et al.* The complete DNA sequence of vaccinia virus. *Virology* **179**, 247-266, 517-263 (1990).

111 Rosel, J. L., Earl, P. L., Weir, J. P. & Moss, B. Conserved TAAATG sequence at the transcriptional and translational initiation sites of vaccinia virus late genes deduced by structural and functional analysis of the HindIII H genome fragment. *J Virol* **60**, 436-449 (1986).

112 Moss, B. Membrane fusion during poxvirus entry. *Semin Cell Dev Biol* **60**, 89-96, doi:10.1016/j.semcdb.2016.07.015 (2016).

113 Moss, B. Poxvirus cell entry: how many proteins does it take? *Viruses* **4**, 688-707, doi:10.3390/v4050688 (2012).

114 Schmidt, F. I., Bleck, C. K. & Mercer, J. Poxvirus host cell entry. *Curr Opin Virol* **2**, 20-27, doi:10.1016/j.coviro.2011.11.007 (2012).

115 Carter, G. C., Law, M., Hollinshead, M. & Smith, G. L. Entry of the vaccinia virus intracellular mature virion and its interactions with glycosaminoglycans. *J Gen Virol* **86**, 1279-1290, doi:10.1099/vir.0.80831-0 (2005).

116 Townsley, A. C., Weisberg, A. S., Wagenaar, T. R. & Moss, B. Vaccinia virus entry into cells via a low-pH-dependent endosomal pathway. *J Virol* **80**, 8899-8908, doi:10.1128/JVI.01053-06 (2006).

117 Bengali, Z., Satheshkumar, P. S. & Moss, B. Orthopoxvirus species and strain differences in cell entry. *Virology* **433**, 506-512, doi:10.1016/j.virol.2012.08.044 (2012).

118 Bengali, Z. *et al.* Drosophila S2 cells are non-permissive for vaccinia virus DNA replication following entry via low pH-dependent endocytosis and early transcription. *PLoS One* **6**, e17248, doi:10.1371/journal.pone.0017248 (2011).

119 Laliberte, J. P., Weisberg, A. S. & Moss, B. The membrane fusion step of vaccinia virus entry is cooperatively mediated by multiple viral proteins and host cell components. *PLoS Pathog* **7**, e1002446, doi:10.1371/journal.ppat.1002446 (2011).

120 Law, M., Carter, G. C., Roberts, K. L., Hollinshead, M. & Smith, G. L. Ligand-induced and nonfusogenic dissolution of a viral membrane. *Proc Natl Acad Sci U S A* **103**, 5989-5994, doi:10.1073/pnas.0601025103 (2006).

121 Roberts, K. L. *et al.* Acidic residues in the membrane-proximal stalk region of vaccinia virus protein B5 are required for glycosaminoglycan-mediated disruption of the extracellular enveloped virus outer membrane. *J Gen Virol* **90**, 1582-1591, doi:10.1099/vir.0.009092-0 (2009).

122 Matho, M. H. *et al.* Murine anti-vaccinia virus D8 antibodies target different epitopes and differ in their ability to block D8 binding to CS-E. *PLoS Pathog* **10**, e1004495, doi:10.1371/journal.ppat.1004495 (2014).

123 Matho, M. H. *et al.* Structural and biochemical characterization of the vaccinia virus envelope protein D8 and its recognition by the antibody LA5. *J Virol* **86**, 8050-8058, doi:10.1128/JVI.00836-12 (2012).

124 Shih, P. C. *et al.* A turn-like structure "KKPE" segment mediates the specific binding of viral protein A27 to heparin and heparan sulfate on cell surfaces. *J Biol Chem* **284**, 36535-36546, doi:10.1074/jbc.M109.037267 (2009).

125 Lin, C. L., Chung, C. S., Heine, H. G. & Chang, W. Vaccinia virus envelope H3L protein binds to cell surface heparan sulfate and is important for intracellular mature virion morphogenesis and virus infection in vitro and in vivo. *J Virol* **74**, 3353-3365 (2000).

126 Howard, A. R., Senkevich, T. G. & Moss, B. Vaccinia virus A26 and A27 proteins form a stable complex tethered to mature virions by association with the A17 transmembrane protein. *J Virol* **82**, 12384-12391, doi:10.1128/JVI.01524-08 (2008).

127 Broyles, S. S. & Knutson, B. A. Poxvirus transcription. *Future Virology* **5**, 639-650, doi:10.2217/fvl.10.51 (2010).

128 Broyles, S. S. & Moss, B. Homology between RNA polymerases of poxviruses, prokaryotes, and eukaryotes: nucleotide sequence and transcriptional analysis of vaccinia virus genes encoding 147-kDa and 22-kDa subunits. *Proc Natl Acad Sci U S A* **83**, 3141-3145 (1986).

129 Cramer, P., Bushnell, D. A. & Kornberg, R. D. Structural basis of transcription: RNA polymerase II at 2.8 angstrom resolution. *Science* **292**, 1863-1876, doi:10.1126/science.1059493 (2001).

130 Yang, Z., Bruno, D. P., Martens, C. A., Porcella, S. F. & Moss, B. Simultaneous high-resolution analysis of vaccinia virus and host cell transcriptomes by deep RNA sequencing. *Proc Natl Acad Sci U S A* **107**, 11513-11518, doi:10.1073/pnas.1006594107 (2010).

131 Condit, R. C. & Niles, E. G. Regulation of viral transcription elongation and termination during vaccinia virus infection. *Biochim Biophys Acta* **1577**, 325-336 (2002).

132 Pedersen, K. *et al.* Characterization of vaccinia virus intracellular cores: implications for viral uncoating and core structure. *J Virol* **74**, 3525-3536 (2000).

133 Zaslavsky, V. Uncoating of vaccinia virus. *J Virol* **55**, 352-356 (1985).

134 Bertholet, C., Van Meir, E., ten Heggeler-Bordier, B. & Wittek, R. Vaccinia virus produces late mRNAs by discontinuous synthesis. *Cell* **50**, 153-162 (1987).

135 Ahn, B. Y. & Moss, B. Capped poly(A) leaders of variable lengths at the 5' ends of vaccinia virus late mRNAs. *J Virol* **63**, 226-232 (1989).

136 Mahr, A. & Roberts, B. E. Arrangement of late RNAs transcribed from a 7.1-kilobase EcoRI vaccinia virus DNA fragment. *J Virol* **49**, 510-520 (1984).

137 Yang, Z. *et al.* Expression profiling of the intermediate and late stages of poxvirus replication. *J Virol* **85**, 9899-9908, doi:10.1128/JVI.05446-11 (2011).

138 Gunasinghe, S. K., Hubbs, A. E. & Wright, C. F. A vaccinia virus late transcription factor with biochemical and molecular identity to a human cellular protein. *J Biol Chem* **273**, 27524-27530 (1998).

139 Lin, Y. C. & Evans, D. H. Vaccinia virus particles mix inefficiently, and in a way that would restrict viral recombination, in coinfected cells. *J Virol* **84**, 2432-2443, doi:10.1128/JVI.01998-09 (2010).

140 Katsafanas, G. C. & Moss, B. Colocalization of transcription and translation within cytoplasmic poxvirus factories coordinates viral expression and subjugates host functions. *Cell Host Microbe* **2**, 221-228, doi:10.1016/j.chom.2007.08.005 (2007).

141 De Silva, F. S., Lewis, W., Berglund, P., Koonin, E. V. & Moss, B. Poxvirus DNA primase. *Proc Natl Acad Sci U S A* **104**, 18724-18729, doi:10.1073/pnas.0709276104 (2007).

142 De Silva, F. S., Paran, N. & Moss, B. Products and substrate/template usage of vaccinia virus DNA primase. *Virology* **383**, 136-141, doi:10.1016/j.virol.2008.10.008 (2009).

143 Sele, C. *et al.* Low-resolution structure of vaccinia virus DNA replication machinery. *J Virol* **87**, 1679-1689, doi:10.1128/JVI.01533-12 (2013).

144 Paran, N., De Silva, F. S., Senkevich, T. G. & Moss, B. Cellular DNA ligase I is recruited to cytoplasmic vaccinia virus factories and masks the role of the vaccinia ligase in viral DNA replication. *Cell Host Microbe* **6**, 563-569, doi:10.1016/j.chom.2009.11.005 (2009).

145 Moyer, R. W. & Graves, R. L. The mechanism of cytoplasmic orthopoxvirus DNA replication. *Cell* **27**, 391-401 (1981).

146 Senkevich, T. G. *et al.* Mapping vaccinia virus DNA replication origins at nucleotide level by deep sequencing. *Proc Natl Acad Sci U S A* **112**, 10908-10913, doi:10.1073/pnas.1514809112 (2015).

147 Baroudy, B. M., Venkatesan, S. & Moss, B. Structure and replication of vaccinia virus telomeres. *Cold Spring Harb Symp Quant Biol* **47 Pt 2**, 723-729 (1983).

148 Merchlinsky, M. & Moss, B. Resolution of linear minichromosomes with hairpin ends from circular plasmids containing vaccinia virus concatemer junctions. *Cell* **45**, 879-884 (1986).

149 Garcia, A. D., Aravind, L., Koonin, E. V. & Moss, B. Bacterial-type DNA holliday junction resolvases in eukaryotic viruses. *Proc Natl Acad Sci U S A* **97**, 8926-8931, doi:10.1073/pnas.150238697 (2000).

150 Garcia, A. D. & Moss, B. Repression of vaccinia virus Holliday junction resolvase inhibits processing of viral DNA into unit-length genomes. *J Virol* **75**, 6460-6471, doi:10.1128/JVI.75.14.6460-6471.2001 (2001).

151 Da Fonseca, F. & Moss, B. Poxvirus DNA topoisomerase knockout mutant exhibits decreased infectivity associated with reduced early transcription. *Proc Natl Acad Sci U S A* **100**, 11291-11296, doi:10.1073/pnas.1534874100 (2003).

152 Condit, R. C., Moussatche, N. & Traktman, P. In a nutshell: structure and assembly of the vaccinia virion. *Adv Virus Res* **66**, 31-124, doi:10.1016/S0065-3527(06)66002-8 (2006).

153 Liu, L., Cooper, T., Howley, P. M. & Hayball, J. D. From crescent to mature virion: vaccinia virus assembly and maturation. *Viruses* **6**, 3787-3808, doi:10.3390/v6103787 (2014).

154 Cassetti, M. C., Merchlinsky, M., Wolffe, E. J., Weisberg, A. S. & Moss, B. DNA packaging mutant: repression of the vaccinia virus A32 gene results in noninfectious, DNA-deficient, spherical, enveloped particles. *J Virol* **72**, 5769-5780 (1998).

155 Yang, Z. & Moss, B. Interaction of the vaccinia virus RNA polymerase-associated 94-kilodalton protein with the early transcription factor. *J Virol* **83**, 12018-12026, doi:10.1128/JVI.01653-09 (2009).

156 Wang, D. R. *et al.* Vaccinia viral protein A27 is anchored to the viral membrane via a cooperative interaction with viral membrane protein A17. *J Biol Chem* **289**, 6639-6655, doi:10.1074/jbc.M114.547372 (2014).

157 Schmelz, M. *et al.* Assembly of vaccinia virus: the second wrapping cisterna is derived from the trans Golgi network. *J Virol* **68**, 130-147 (1994).

158 Tooze, J., Hollinshead, M., Reis, B., Radsak, K. & Kern, H. Progeny vaccinia and human cytomegalovirus particles utilize early endosomal cisternae for their envelopes. *Eur J Cell Biol* **60**, 163-178 (1993).

159 Ward, B. M. Visualization and characterization of the intracellular movement of vaccinia virus intracellular mature virions. *J Virol* **79**, 4755-4763, doi:10.1128/JVI.79.8.4755-4763.2005 (2005).

160 Ward, B. M. & Moss, B. Vaccinia virus A36R membrane protein provides a direct link between intracellular enveloped virions and the microtubule motor kinesin. *J Virol* **78**, 2486-2493 (2004).

161 Johnston, S. C. & Ward, B. M. Vaccinia virus protein F12 associates with intracellular enveloped virions through an interaction with A36. *J Virol* **83**, 1708-1717, doi:10.1128/JVI.01364-08 (2009).

162 Dodding, M. P., Newsome, T. P., Collinson, L. M., Edwards, C. & Way, M. An E2-F12 complex is required for intracellular enveloped virus morphogenesis during vaccinia infection. *Cell Microbiol* **11**, 808-824, doi:10.1111/j.1462-5822.2009.01296.x (2009).

163 Morgan, G. W. *et al.* Vaccinia protein F12 has structural similarity to kinesin light chain and contains a motor binding motif required for virion export. *PLoS Pathog* **6**, e1000785, doi:10.1371/journal.ppat.1000785 (2010).

164 Carpentier, D. C., Gao, W. N., Ewles, H., Morgan, G. W. & Smith, G. L. Vaccinia virus protein complex F12/E2 interacts with kinesin light chain isoform 2 to engage the kinesin-1 motor complex. *PLoS Pathog* **11**, e1004723, doi:10.1371/journal.ppat.1004723 (2015).

165 Horsington, J. *et al.* A36-dependent actin filament nucleation promotes release of vaccinia virus. *PLoS Pathog* **9**, e1003239, doi:10.1371/journal.ppat.1003239 (2013).

166 Snetkov, X., Weisswange, I., Pfanzelter, J., Humphries, A. C. & Way, M. NPF motifs in the vaccinia virus protein A36 recruit intersectin-1 to promote Cdc42:N-WASP-mediated viral release from infected cells. *Nat Microbiol* **1**, 16141, doi:10.1038/nmicrobiol.2016.141 (2016).

167 Greber, U. F. & Way, M. A superhighway to virus infection. *Cell* **124**, 741-754, doi:10.1016/j.cell.2006.02.018 (2006).

168 Sodeik, B. Mechanisms of viral transport in the cytoplasm. *Trends Microbiol* **8**, 465-472 (2000).

169 Dodding, M. P. & Way, M. Coupling viruses to dynein and kinesin-1. *EMBO J* **30**, 3527-3539, doi:10.1038/emboj.2011.283 (2011).

170 Geada, M. M., Galindo, I., Lorenzo, M. M., Perdiguero, B. & Blasco, R. Movements of vaccinia virus intracellular enveloped virions with GFP tagged to the F13L envelope protein. *J Gen Virol* **82**, 2747-2760, doi:10.1099/0022-1317-82-11-2747 (2001).

171 Herrero-Martinez, E., Roberts, K. L., Hollinshead, M. & Smith, G. L. Vaccinia virus intracellular enveloped virions move to the cell periphery on microtubules in the absence of the A36R protein. *J Gen Virol* **86**, 2961-2968, doi:10.1099/vir.0.81260-0 (2005).

172 Hollinshead, M. *et al.* Vaccinia virus utilizes microtubules for movement to the cell surface. *J Cell Biol* **154**, 389-402 (2001).

173 Rietdorf, J. *et al.* Kinesin-dependent movement on microtubules precedes actin-based motility of vaccinia virus. *Nat Cell Biol* **3**, 992-1000, doi:10.1038/ncb1101-992 (2001).

174 Ward, B. M. & Moss, B. Vaccinia virus intracellular movement is associated with microtubules and independent of actin tails. *J Virol* **75**, 11651-11663, doi:10.1128/JVI.75.23.11651-11663.2001 (2001).

175 Ward, B. M. & Moss, B. Visualization of intracellular movement of vaccinia virus virions containing a green fluorescent protein-B5R membrane protein chimera. *J Virol* **75**, 4802-4813, doi:10.1128/JVI.75.10.4802-4813.2001 (2001).

176 Ward, B. M., Weisberg, A. S. & Moss, B. Mapping and functional analysis of interaction sites within the cytoplasmic domains of the vaccinia virus A33R and A36R envelope proteins. *J Virol* **77**, 4113-4126 (2003).

177 Valderrama, F., Cordeiro, J. V., Schleich, S., Frischknecht, F. & Way, M. Vaccinia virus-induced cell motility requires F11L-mediated inhibition of RhoA signaling. *Science* **311**, 377-381, doi:10.1126/science.1122411 (2006).

178 Morales, I. *et al.* The vaccinia virus F11L gene product facilitates cell detachment and promotes migration. *Traffic* **9**, 1283-1298, doi:10.1111/j.1600-0854.2008.00762.x (2008).

179 Arakawa, Y., Cordeiro, J. V., Schleich, S., Newsome, T. P. & Way, M. The release of vaccinia virus from infected cells requires RhoA-mDia modulation of cortical actin. *Cell Host Microbe* **1**, 227-240, doi:10.1016/j.chom.2007.04.006 (2007).

180 Arakawa, Y., Cordeiro, J. V. & Way, M. F11L-mediated inhibition of RhoA-mDia signaling stimulates microtubule dynamics during vaccinia virus infection. *Cell Host Microbe* **1**, 213-226, doi:10.1016/j.chom.2007.04.007 (2007).

181 Handa, Y., Durkin, C. H., Dodding, M. P. & Way, M. Vaccinia virus F11 promotes viral spread by acting as a PDZ-containing scaffolding protein to bind myosin-9A and inhibit RhoA signaling. *Cell Host Microbe* **14**, 51-62, doi:10.1016/j.chom.2013.06.006 (2013).

182 Irwin, C. R. & Evans, D. H. Modulation of the myxoma virus plaque phenotype by vaccinia virus protein F11. *J Virol* **86**, 7167-7179, doi:10.1128/JVI.06936-11 (2012).

183 Breiman, A., Carpentier, D. C., Ewles, H. A. & Smith, G. L. Transport and stability of the vaccinia virus A34 protein is affected by the A33 protein. *J Gen Virol* **94**, 720-725, doi:10.1099/vir.0.049486-0 (2013).

184 Doceul, V., Hollinshead, M., van der Linden, L. & Smith, G. L. Repulsion of superinfecting virions: a mechanism for rapid virus spread. *Science* **327**, 873-876, doi:10.1126/science.1183173 (2010).

185 Buller, R. M., Smith, G. L., Cremer, K., Notkins, A. L. & Moss, B. Decreased virulence of recombinant vaccinia virus expression vectors is associated with a thymidine kinase-negative phenotype. *Nature* **317**, 813-815 (1985).

186 Kim, J. H. *et al.* Systemic armed oncolytic and immunologic therapy for cancer with JX-594, a targeted poxvirus expressing GM-CSF. *Mol Ther* **14**, 361-370, doi:10.1016/j.ymthe.2006.05.008 (2006).

187 Yang, S. *et al.* A new recombinant vaccinia with targeted deletion of three viral genes: its safety and efficacy as an oncolytic virus. *Gene Ther* **14**, 638-647, doi:10.1038/sj.gt.3302914 (2007).

188 Deng, H. *et al.* Oncolytic virotherapy for multiple myeloma using a tumour-specific double-deleted vaccinia virus. *Leukemia* **22**, 2261-2264, doi:10.1038/leu.2008.120 (2008).

189 Zhang, Q. *et al.* Eradication of solid human breast tumors in nude mice with an intravenously injected light-emitting oncolytic vaccinia virus. *Cancer Res* **67**, 10038-10046, doi:10.1158/0008-5472.CAN-07-0146 (2007).

190 Kyula, J. N. *et al.* Synergistic cytotoxicity of radiation and oncolytic Lister strain vaccinia in (V600D/E)BRAF mutant melanoma depends on JNK and TNF-alpha signaling. *Oncogene* **33**, 1700-1712, doi:10.1038/onc.2013.112 (2014).

191 McCart, J. A. *et al.* Systemic cancer therapy with a tumor-selective vaccinia virus mutant lacking thymidine kinase and vaccinia growth factor genes. *Cancer Res* **61**, 8751-8757 (2001).

192 Lei, W. *et al.* Combined expression of miR-34a and Smac mediated by oncolytic vaccinia virus synergistically promote anti-tumor effects in Multiple Myeloma. *Sci Rep* **6**, 32174, doi:10.1038/srep32174 (2016).

193 Parviainen, S. *et al.* GMCSF-armed vaccinia virus induces an antitumor immune response. *Int J Cancer* **136**, 1065-1072, doi:10.1002/ijc.29068 (2015).

194 Park, B. H. *et al.* Use of a targeted oncolytic poxvirus, JX-594, in patients with refractory primary or metastatic liver cancer: a phase I trial. *Lancet Oncol* **9**, 533-542, doi:10.1016/S1470-2045(08)70107-4 (2008).

195 Cripe, T. P. *et al.* Phase 1 study of intratumoral Pexa-Vec (JX-594), an oncolytic and immunotherapeutic vaccinia virus, in pediatric cancer patients. *Mol Ther* **23**, 602-608, doi:10.1038/mt.2014.243 (2015).

196 Breitbach, C. J., Moon, A., Burke, J., Hwang, T. H. & Kirn, D. H. A Phase 2, Open-Label, Randomized Study of Pexa-Vec (JX-594) Administered by Intratumoral Injection in Patients with Unresectable Primary Hepatocellular Carcinoma. *Methods Mol Biol* **1317**, 343-357, doi:10.1007/978-1-4939-2727-2_19 (2015).

197 Park, S. H. *et al.* Phase 1b Trial of Biweekly Intravenous Pexa-Vec (JX-594), an Oncolytic and Immunotherapeutic Vaccinia Virus in Colorectal Cancer. *Mol Ther* **23**, 1532-1540, doi:10.1038/mt.2015.109 (2015).

198 Zeh, H. J. *et al.* First-in-man study of western reserve strain oncolytic vaccinia virus: safety, systemic spread, and antitumor activity. *Mol Ther* **23**, 202-214, doi:10.1038/mt.2014.194 (2015).

199 Downs-Canner, S. *et al.* Phase 1 Study of Intravenous Oncolytic Poxvirus (vvDD) in Patients With Advanced Solid Cancers. *Mol Ther* **24**, 1492-1501, doi:10.1038/mt.2016.101 (2016).

200 Taylor, G. S. *et al.* A recombinant modified vaccinia ankara vaccine encoding Epstein-Barr Virus (EBV) target antigens: a phase I trial in UK patients with EBV-positive cancer. *Clin Cancer Res* **20**, 5009-5022, doi:10.1158/1078-0432.CCR-14-1122-T (2014).

201 McClintock, B. The significance of responses of the genome to challenge. *Science* **226**, 792-801 (1984).

202 Mc, C. B. The origin and behavior of mutable loci in maize. *Proc Natl Acad Sci U S A* **36**, 344-355 (1950).

203 Kleckner, N., Roth, J. & Botstein, D. Genetic engineering in vivo using translocatable drug-resistance elements. New methods in bacterial genetics. *J Mol Biol* **116**, 125-159 (1977).

204 Hedges, R. W. & Jacob, A. E. Transposition of ampicillin resistance from RP4 to other replicons. *Mol Gen Genet* **132**, 31-40 (1974).

205 Berg, D. E., Davies, J., Allet, B. & Rochaix, J. D. Transposition of R factor genes to bacteriophage lambda. *Proc Natl Acad Sci U S A* **72**, 3628-3632 (1975).

206 DeNicola, G. M., Karreth, F. A., Adams, D. J. & Wong, C. C. The utility of transposon mutagenesis for cancer studies in the era of genome editing. *Genome Biol* **16**, 229, doi:10.1186/s13059-015-0794-y (2015).

207 van Opijnen, T., Lazinski, D. W. & Camilli, A. Genome-Wide Fitness and Genetic Interactions Determined by Tn-seq, a High-Throughput Massively Parallel Sequencing Method for Microorganisms. *Curr Protoc Mol Biol* **106**, 7 16 11-24, doi:10.1002/0471142727.mb0716s106 (2014).

208 Thorne, L., Bailey, D. & Goodfellow, I. High-resolution functional profiling of the norovirus genome. *J Virol* **86**, 11441-11456, doi:10.1128/JVI.00439-12 (2012).

209 Brune, W. *et al.* Rapid identification of essential and nonessential herpesvirus genes by direct transposon mutagenesis. *Nat Biotechnol* **17**, 360-364, doi:10.1038/7914 (1999).

210 McMahon, C. W., Traxler, B., Grigg, M. E. & Pullen, A. M. Transposon-mediated random insertions and site-directed mutagenesis prevent the trafficking of a mouse mammary tumor virus superantigen. *Virology* **243**, 354-365, doi:10.1006/viro.1998.9071 (1998).

211 Mohl, B. S. *et al.* Random transposon-mediated mutagenesis of the essential large tegument protein pUL36 of pseudorabies virus. *J Virol* **84**, 8153-8162, doi:10.1128/JVI.00953-10 (2010).

212 Remenyi, R. *et al.* A comprehensive functional map of the hepatitis C virus genome provides a resource for probing viral proteins. *MBio* **5**, e01469-01414, doi:10.1128/mBio.01469-14 (2014).

213 Teterina, N. L. *et al.* Identification of tolerated insertion sites in poliovirus non-structural proteins. *Virology* **409**, 1-11, doi:10.1016/j.virol.2010.09.028 (2011).

214 Herod, M. R. *et al.* Employing transposon mutagenesis to investigate foot-and-mouth disease virus replication. *J Gen Virol* **96**, 3507-3518, doi:10.1099/jgv.0.000306 (2015).

215 Woodard, L. E. & Wilson, M. H. piggyBac-ing models and new therapeutic strategies. *Trends Biotechnol* **33**, 525-533, doi:10.1016/j.tibtech.2015.06.009 (2015).

216 Cary, L. C. *et al.* Transposon mutagenesis of baculoviruses: analysis of Trichoplusia ni transposon IFP2 insertions within the FP-locus of nuclear polyhedrosis viruses. *Virology* **172**, 156-169 (1989).

217 Fraser, M. J., Cary, L., Boonvisudhi, K. & Wang, H. G. Assay for movement of Lepidopteran transposon IFP2 in insect cells using a baculovirus genome as a target DNA. *Virology* **211**, 397-407, doi:10.1006/viro.1995.1422 (1995).

218 Ding, S. *et al.* Efficient transposition of the piggyBac (PB) transposon in mammalian cells and mice. *Cell* **122**, 473-483, doi:10.1016/j.cell.2005.07.013 (2005).

219 Mitra, R., Fain-Thornton, J. & Craig, N. L. piggyBac can bypass DNA synthesis during cut and paste transposition. *EMBO J* **27**, 1097-1109, doi:10.1038/emboj.2008.41 (2008).

220 Qin, L. & Evans, D. H. Genome scale patterns of recombination between coinfecting vaccinia viruses. *J Virol* **88**, 5277-5286, doi:10.1128/JVI.00022-14 (2014).

221 Keller, B. A. *et al.* Co-aggregation of RNA binding proteins in ALS spinal motor neurons: evidence of a common pathogenic mechanism. *Acta Neuropathol* **124**, 733-747, doi:10.1007/s00401-012-1035-z (2012).

222 Baker, J. L. & Ward, B. M. Development and comparison of a quantitative TaqMan-MGB real-time PCR assay to three other methods of quantifying vaccinia virions. *J Virol Methods* **196**, 126-132, doi:10.1016/j.jviromet.2013.10.026 (2014).

223 Schroder, M., Baran, M. & Bowie, A. G. Viral targeting of DEAD box protein 3 reveals its role in TBK1/IKKepsilon-mediated IRF activation. *EMBO J* **27**, 2147-2157, doi:10.1038/emboj.2008.143 (2008).

224 Rottger, S., Frischknecht, F., Reckmann, I., Smith, G. L. & Way, M. Interactions between vaccinia virus IEV membrane proteins and their roles in IEV assembly and actin tail formation. *J Virol* **73**, 2863-2875 (1999).

225 Le Boeuf, F. *et al.* Synergistic interaction between oncolytic viruses augments tumor killing. *Mol Ther* **18**, 888-895, doi:10.1038/mt.2010.44 (2010).

226 Yuen, T. J. *et al.* Analysis of A47, an immunoprevalent protein of vaccinia virus, leads to a reevaluation of the total antiviral CD8+ T cell response. *J Virol* **84**, 10220-10229, doi:10.1128/JVI.01281-10 (2010).

227 Rehman, H., Silk, A. W., Kane, M. P. & Kaufman, H. L. Into the clinic: Talimogene laherparepvec (T-VEC), a first-in-class intratumoral oncolytic viral therapy. *J Immunother Cancer* **4**, 53, doi:10.1186/s40425-016-0158-5 (2016).

228 Fenner, F. *Smallpox and its eradication*. (World Health Organization, 1988).

229 Symons, J. A., Alcami, A. & Smith, G. L. Vaccinia virus encodes a soluble type I interferon receptor of novel structure and broad species specificity. *Cell* **81**, 551-560 (1995).

230 Yuan, M. *et al.* Efficiently editing the vaccinia virus genome by using the CRISPR-Cas9 system. *J Virol* **89**, 5176-5179, doi:10.1128/JVI.00339-15 (2015).

231 Tong, A. H. *et al.* Systematic genetic analysis with ordered arrays of yeast deletion mutants. *Science* **294**, 2364-2368, doi:10.1126/science.1065810 (2001).

232 Schuldiner, M. *et al.* Exploration of the function and organization of the yeast early secretory pathway through an epistatic miniarray profile. *Cell* **123**, 507-519, doi:10.1016/j.cell.2005.08.031 (2005).

233 van Opijnen, T., Bodi, K. L. & Camilli, A. Tn-seq: high-throughput parallel sequencing for fitness and genetic interaction studies in microorganisms. *Nat Methods* **6**, 767-772, doi:10.1038/nmeth.1377 (2009).

234 Ojeda, S., Domi, A. & Moss, B. Vaccinia virus G9 protein is an essential component of the poxvirus entry-fusion complex. *J Virol* **80**, 9822-9830, doi:10.1128/JVI.00987-06 (2006).

235 Han, F., Bi, X. L., Cao, R., Wang, Y. & Wu, S. H. [Screening and application of enhancer-like sequences from vaccinia virus]. *Zhonghua Shi Yan He Lin Chuang Bing Du Xue Za Zhi* **21**, 301-303 (2007).

236 Backes, S. *et al.* Degradation of host microRNAs by poxvirus poly(A) polymerase reveals terminal RNA methylation as a protective antiviral mechanism. *Cell Host Microbe* **12**, 200-210, doi:10.1016/j.chom.2012.05.019 (2012).

237 Andrew, M. E., Coupar, B. E. & Boyle, D. B. Humoral and cell-mediated immune responses to recombinant vaccinia viruses in mice. *Immunol Cell Biol* **67 (Pt 5)**, 331-337, doi:10.1038/icb.1989.48 (1989).

238 Dobson, B. M. & Tscharke, D. C. Redundancy complicates the definition of essential genes for vaccinia virus. *J Gen Virol* **96**, 3326-3337, doi:10.1099/jgv.0.000266 (2015).

Contributions of Collaborators

Dr. Jim Dimitroulakos is the principal investigator on OHSN-REB protocol 20140075-01H that allowed for the collection, characterization, and *ex vivo* infection of human specimens. Surgical specimens were obtained from Dr. Carolyn Nessim following regulations in the above protocol. Human-derived ovarian cancer cell lines were obtained from Dr. Carolina Ilkow and were derived following paracentesis under the same OHSN-REB protocol. The human-derived melanoma cell lines pMel-T and pMel-X2 were obtained from Dr. Christine Engeland in the laboratory of Dr. Guy Ungerechts at the National Center for Tumor Diseases (Heidelberg, Germany); these were obtained following the guidelines outlined in the Ethics Committee of Heidelberg University NCT MASTER, S-206/2011. Dr. Jiahu Wang engineered the constructs and built the original VACV mutant library from which the working library used in this research project was derived. Dr. Vera Tang assisted with flow cytometry-based cell sorting (Flow Cytometry and Virometry core facility, University of Ottawa). All bioinformatics analyses (and the creation of accompanying figures) were conducted by Adrian Pelin, who also aided in the expansion of wild-type virus stocks. Anti-VACV F11 and anti-VACV A36 antibodies were obtained from Dr. Antonio Postigo in the laboratory of Professor Michael Way at the Francis Crick Institute and were previously described as outlined in Materials and Methods. Antiserum against VACV K7 was obtained from Dr. Martina Schroeder at Maynooth University and was also previously described as outlined. The VACV-Tian Tan strain was obtained from Dr. David Evans (University of Alberta, Edmonton, Canada). The experiment shown in Figure 3.12B was performed by Dr. Fabrice Le Boeuf. VACV mutant library replication studies were performed with the help of Catia Cemeus. Plaque size and EEV release assays were performed with the help of Russell Barkley. Animal studies were performed with the help of Julia Petryk.

Appendices

Appendix I: Ethics approval for attaining human tumour specimens. These are copies of the relevant portions of OHSN-REB #20120559-01H that allow human tumour specimens to be obtained for *ex vivo* research purposes, as well as the document confirming my addition to this protocol.

Ottawa Hospital
Research Institute
Institut de recherche
de l'Hôpital d'Ottawa

uOttawa

UNIVERSITY OF OTTAWA
HEART INSTITUTE
INSTITUT DE CARDIOLOGIE
DE L'UNIVERSITÉ D'OTTAWA

Ottawa Health Science Network Research Ethics Board/ Conseil d'éthique de la recherche du Réseau de science de la santé d'Ottawa
Civic Box 411 725 Parkdale Avenue, Ottawa, Ontario K1Y 4E9 613-798-5555 ext. 14902 Fax : 613-761-4311
http://www.ohri.ca/ohsn-reb

October 12, 2016

Dr. Jim Dimitroulakos
Ottawa Hospital Cancer Centre - General Campus
Department of Cancer Therapeutics
501 Smyth Road, 3rd Floor
Ottawa, ON
K1H 8L6

Dear Dr. Dimitroulakos:

RE: Protocol# - 20120559-01H **Evaluating novel therapeutic approaches in ex-vivo tumour tissue (OHSN-REB #20120559-01H)**

Renewal Expiry Date - October 26, 2017

Thank you for your e-mail dated October 4, 2016. I am pleased to inform you that your Annual Renewal Request was reviewed by the Ottawa Health Science Network Research Ethics Board (OHSN-REB) and is approved. No changes, amendments or addenda may be made in the protocol or the consent form without the OHSN-REB's review and approval.

Renewal is valid for a period of one year. Approximately one month prior to that time, a single renewal form should be sent to the REB office.

The REB no longer requires a 'valid until' date at the bottom of all approved informed consent forms. The consent forms currently approved for use by the REB are:
- English and French Patient Information and Consent Form version date May 2014.

OHSN-REB complies with the membership requirements and operates in compliance with the Tri-Council Policy Statement: Ethical Conduct for Research Involving Humans; the International Conference on Harmonization - Good Clinical Practice: Consolidated Guideline; and the provisions of the Personal Health Information Protection Act 2004.

OHSN-REB complies with the membership requirements and operates in compliance with the Tri-Council Policy Statement: Ethical Conduct for Research Involving Humans; the International Conference on Harmonization - Good Clinical Practice: Consolidated Guideline; and the provisions of the Personal Health Information Protection Act 2004.

/cb

Ottawa Hospital Research Institute
Institut de recherche de l'Hôpital d'Ottawa

uOttawa

UNIVERSITY OF OTTAWA HEART INSTITUTE
INSTITUT DE CARDIOLOGIE DE L'UNIVERSITÉ D'OTTAWA

Ottawa Health Science Network Research Ethics Board/ Conseil d'éthique de la recherche du Réseau de science de la santé d'Ottawa
Civic Box 411 725 Parkdale Avenue, Ottawa, Ontario K1Y 4E9 613-798-5555 ext. 14902 Fax : 613-761-4311
http://www.ohri.ca/ohsn-reb

Thursday, January 22, 2015

Dr. Jim Dimitroulakos
Ottawa Hospital Cancer Centre - General Campus
Department of Cancer Therapeutics
501 Smyth Road, 3rd Floor
Ottawa, ON
K1H 8L6

Dear Dr. Dimitroulakos:

Re: Protocol # 20120559-01H Evaluating novel therapeutic approaches in ex-vivo tumour tissue (OHSN-REB #20120559-01H)

Thank you for your letter dated January 9, 2015 informing us of the addition of Rebecca Auer, Brian Keller, Celia Marginean, Guillaume Martel and Avijit Chatterjee to the study as co-investigators. Our file has been updated accordingly.

OHSN-REB complies with the membership requirements and operates in compliance with the Tri-Council Policy Statement: Ethical Conduct for Research Involving Humans; the International Conference on Harmonization - Good Clinical Practice: Consolidated Guideline; and the provisions of the Personal Health Information Protection Act 2004.

Ethical approval remains in effect until October 23, 2015.

/km

Appendix II: Initial characterization of the patient-derived primary cultures that were utilized in this study whose characterization was not presented in the main text. Cultures include models derived from ovarian cancer ascites patients 2028 and 2068 that were fixed and stained with an antibody recognizing Cytokeratin-18 (A, green). Photomicrographs of the melanoma models pMel-T and pMel-X2 are shown as well as their RNA-level characterization of relevant markers of choice (B).

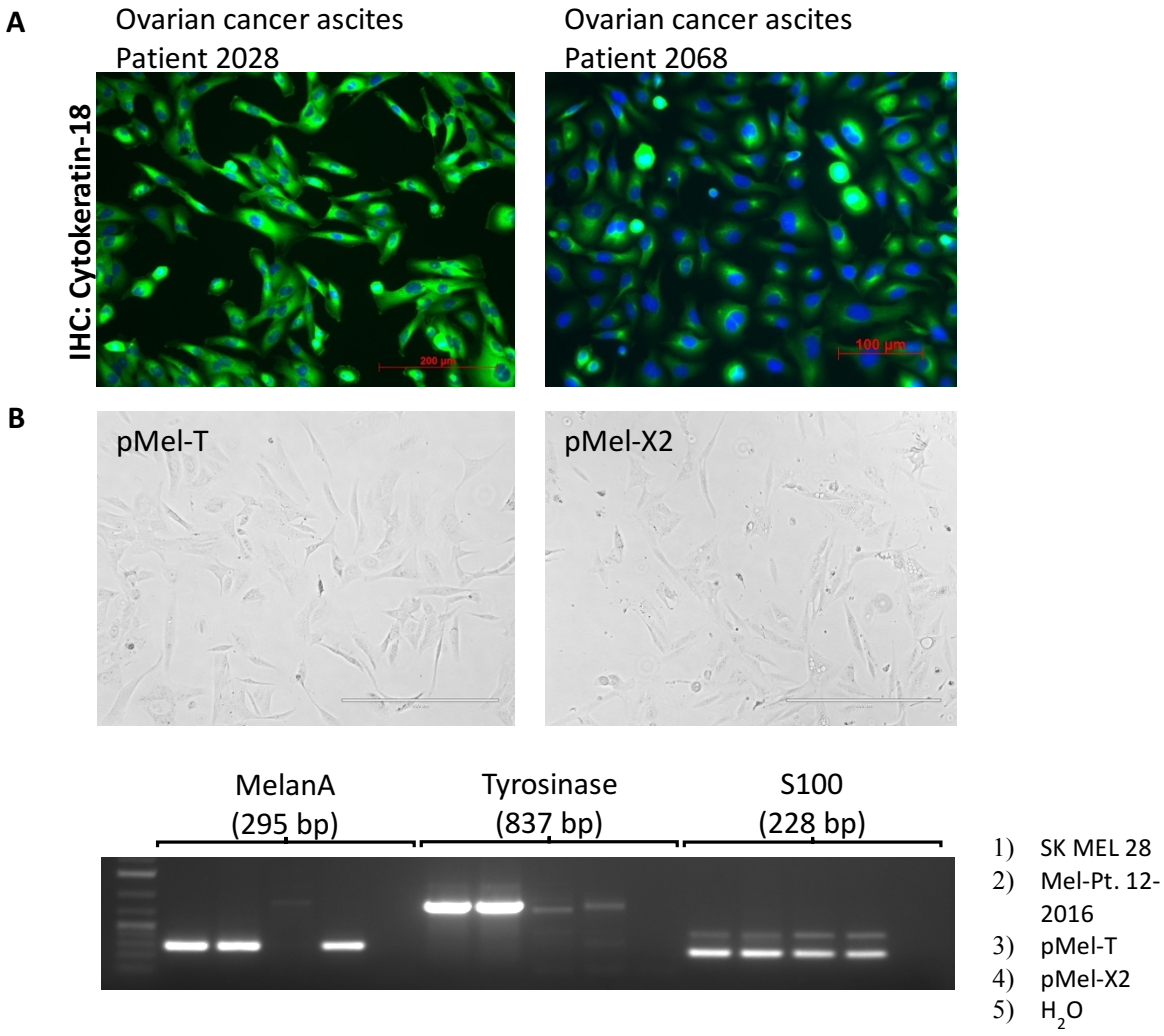
A
Ovarian cancer ascites
Patient 2028
Ovarian cancer ascites
Patient 2068
IHC: Cytokeratin-18
200 µm
100 µm
B
pMel-T
pMel-X2
MelanA
(295 bp)
Tyrosinase
(837 bp)
S100
(228 bp)
1) SK MEL 28
2) Mel-Pt. 12-2016
3) pMel-T
4) pMel-X2
5) H2O

Appendix III: Oncolytic viruses – immunotherapeutics on the rise. Reprinted with permission from the Journal of Molecular Medicine, 94 (9), 979-991. BA Keller & JC Bell (2016).

J Mol Med
DOI 10.1007/s00109-016-1453-9

REVIEW

Oncolytic viruses—immunotherapeutics on the rise

Brian A. Keller[1,2] · **John C. Bell**[1,2]

Received: 7 April 2016 / Revised: 7 July 2016 / Accepted: 27 July 2016

Abstract The oncolytic virus (OV) field has entered an exciting period in its evolution in which our basic understanding of viral biology and anti-cancer potential are being actively translated into viable therapeutic options for aggressive malignancies. OVs are naturally occurring or engineered viruses that are able to exploit cancer-specific changes in cellular signaling to specifically target cancers and their microenvironment. The direct cytolytic effect of OVs on cancer cells is known to release antigens, which can begin a cascade of events that results in the induction of anti-cancer adaptive immunity. This response is now regarded as the most critical mechanism of OV action and harnessing it can lead to the elimination of distant micrometastases as well as provide long-term anti-cancer immune surveillance. In this review, we highlight the development of the OV field, why OVs are gaining an increasingly elevated standing as members of the cancer immunotherapy armamentarium, and finally, ongoing clinical studies that are aimed at translating unique OV therapies into approved therapies for aggressive cancers.

Keywords Oncolytic viruses · Cancer · Immunotherapy · Immune checkpoint inhibitors · Combination therapy

Introduction

The fields of clinical oncology and cancer therapeutics development are in the midst of a revolution driven primarily by the successful translation of novel forms of cancer immunotherapy into clinical practice. Since *Science* magazine named Cancer Immunotherapy the Breakthrough of the Year in 2013 [1], the approach to treatment in many cancers has evolved to include immune checkpoint inhibition and cell-based immunotherapies. Beginning with the FDA approval of the cytotoxic T lymphocyte-associated antigen 4 (CTLA-4) antibody Yervoy® (developed by Bristol Myers Squibb [BMS]) in 2011, the influx of novel therapeutic agents has expanded to include those directed against programmed cell death protein 1 (PD1)—Keytruda®, developed by Merck, and another BMS product Opdivo®, both FDA approved in 2014–15 [2]. The majority of early clinical trials using these novel agents have focused on non-small cell lung cancer and melanoma, but the types of cancers being tested with monoclonal antibodies are rapidly expanding. In addition to the clinical arrival of immune checkpoint inhibitors in recent years, other players in the field of immuno-oncology are also being explored, including adoptive cell therapeutic approaches, new approaches for cytokine therapies, and more recently, inhibition of indoleamine-2,3-dioxygenase (IDO), an inhibitor of tumour immune resistance [2–4]. Despite the well-deserved excitement surrounding the field of immuno-oncology, there is still much to be learned as a minority of patients respond to these innovative therapeutics [5–7].

Oncolytic viruses (OVs) are one emerging class of therapeutic with the potential to act in synergy with novel immunotherapies to improve clinical outcomes. Oncolytic viruses are cancer-targeted viruses designed to exploit cell signaling pathways of cancer cells that are activated as they undergo malignant transformation [8]. The cellular antiviral response relies heavily on intact innate immune interferon (IFN) signaling, primarily mediated by the JAK/STAT pathway [9]. One of the well-characterized changes that occurs in the process of malignant transformation in

✉ John C. Bell
jbell@ohri.ca

[1] Centre for Innovative Cancer Therapeutics, Ottawa Hospital Research Institute, 501 Smyth Road, Ottawa, ON K1H 8L6, Canada

[2] Faculty of Medicine, University of Ottawa, Ottawa, ON, Canada

Published online: 04 August 2016

many cancers is the accumulation of mutations affecting IFN signaling [10–13]. Recently, an interesting mechanistic discovery has linked commonly-observed mutations in the tumour-suppressor gene encoding PTEN with defects in the anti-viral IFN response [14]. As summarized in Fig. 1, the results of these changes are directly implicated in oncogenesis by preventing the cell from initiating apoptosis, growth arrest, or immune stimulation [8, 15]. However, the diminished IFN response, a fundamental biological property of the malignant phenotype, also leaves the cancer cell vulnerable to OV infection [10–12]. These multiple mechanisms of action are summarized in Fig. 2 and take advantage of a number of changes in the tumour microenvironment to facilitate vascular collapse [16], cause the direct cellular lysis of both cancer cells (oncolysis) and cancer-associated fibroblasts (CAFs) [17], and perhaps most importantly, to initiate or augment existing anti-tumour immunity [8].

Clinically, OVs have moved beyond a field of investigative laboratory-based research to becoming acknowledged as validated therapeutics. This translation was significantly buoyed by the 2015 FDA approval of the herpes simplex virus 1-based Talimogene Laherparepvec (T-Vec; Imlygic™) for the treatment of advanced melanoma [18, 19]. The field is now moving towards discovering optimal viral backbones to limit toxicity and maximize anti-cancer potency, while clinical studies are being conducted to define the clinical contexts in which OVs will fit. This review summarizes our current understanding of the biology behind the utility of OVs, the most exciting viral platforms and strategies for potential clinical development, the leading branches of immuno-oncology with which OV therapeutics might synergize, and relevant clinical trials that have and will continue to define how OVs will be used.

The clinical evolution of oncolytic viruses

The concept of a clinically advantageous link between viruses and cancer treatment emerged in the early twentieth century due to observations surrounding individual case reports of cancer regressions following natural virus infection [20, 21]. At the time, viral biology was poorly understood and the ability to pursue laboratory-based studies on such agents was limited. Through the 1920s and into the 1940s, dozens of viruses were investigated for their abilities to infect and productively replicate in various cancer models [22]. The 1950s–70s saw the advancement of the field in terms of understanding appropriate models, experimenting with dozens of virus strains, and translating this knowledge into clinical experiments [21]. During this period, several meaningful clinical trials were performed [23, 24], the largest of which was a 90-patient trial investigating the use of mumps virus as an anti-cancer agent in cases of advanced non-resectable cancers [25]. The results of this and several other trials were interesting; however, many at the time dismissed the clinical utility of this novel class of anti-cancer agent due to the inherent safety risks and demonstrated lack of successful human translation. The next several decades of research into basic virology and cancer-targeted viruses yielded many fundamental insights; however, major clinical steps were delayed until the 1990s [26, 27]. An important step in the clinical advancement of OVs was the Chinese approval of the genetically modified adenovirus H101 in 2005, which was followed by a second generation of OVs that have now begun to mature in the clinic.

Imlygic™ and beyond—biological strategies for engineering superior oncolytic viruses

Amgen's Imlygic™ recently gained FDA and European approval for the treatment of advanced melanoma, with clinical trials underway to expand both the clinical indications and the strategic approach for its use. Imlygic™ (formerly OncoVEX) is built on the JS1 strain of HSV-1, which was isolated from the infected cold sore of an otherwise healthy volunteer [18]. The *ICP-34.5* gene was deleted to increase both malignant cell specificity and potency, co-incident with an *ICP-47* gene deletion to increase antigen presentation. The human cytokine granulocyte-macrophage colony-stimulating factor (GM-CSF) was added to the HSV-1 vector in an effort to enhance anti-tumour adaptive immunity and provide long-lasting anti-cancer immune surveillance [18]. This approach has proven clinically effective [28, 29], which justifies its continued investigation (Table 1). Despite the clinical activity of Imlygic™, many believe this iteration of oncolytic HSV-1 poorly capitalizes on the therapeutic potential of the OV platform and, thus, laboratory research designed to improve OV therapeutics continues.

Investigating diverse viral platforms to direct tumour selectivity

Attenuation of HSV-1 to create Imlygic™ was in part accomplished by deletion of *ICP-34.5*, a well-studied virulence gene that normally prevents infected cellular autophagy and antagonizes natural cellular interferon responses [18, 30, 31]. As an alternative strategy to create oncolytic HSV strains, groups have deleted the ribonucleotide reductase large R1 subunit gene (*UL39*) of HSV-1, creating a strain of virus that is attracted to the high metabolic physiology found in cancer cells [32–34].

Another viral backbone that has been commonly translated into human studies is adenovirus. Several different strategies

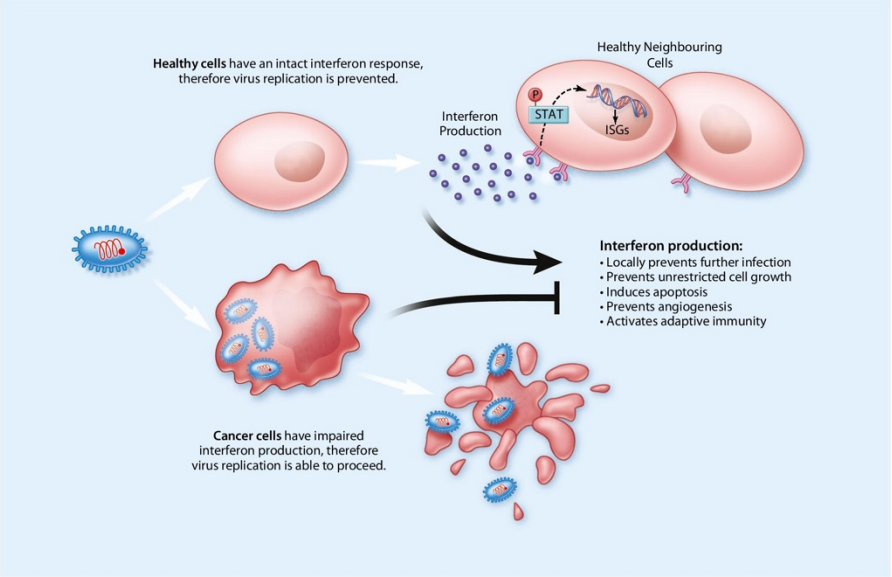

Fig. 1 Upon viral infection, the intact interferon response in healthy cells is initiated. This leads to the induction of an anti-viral state in nearby healthy cells, primarily through the JAK/STAT pathway, amongst others. This prevents the oncolytic virus infection from spreading in healthy cells, leaving normal tissues intact. In addition, an intact interferon response prevents uncensored cell growth, induces apoptosis, prevents angiogenesis, and activates an adaptive immune response—all properties that the efficient cancer cell seeks to evade. Conversely, many malignantly transformed cells have developed impairments in their cell signaling pathways necessary to initiate an interferon response, which has left them vulnerable to oncolytic virus attack. *ISG* interferon stimulated genes

have been employed to create oncolytic adenoviruses (oAds) that demonstrate selective growth in cancer cells. One strategy involves deleting the Ad *E1A* gene, which results in a virus more directed towards replication in transformed cells [35]. More recently, miRNA-controlled oAds have been developed to attenuate virulence in quiescent cells while still retaining their full lytic capacity in human-derived xenografts. This work was performed specifically by targeting the late structural protein fiber (*L5*) [36]. Finally, a popular strategy is to create transcriptionally regulated versions of oAds harboring tissue-specific promoters that can drive key virus regulatory genes [37, 38].

Similar strategies to those discussed above have been employed with Vaccinia virus (VacV) to direct virulence towards transformed cells. For instance, in the Wyeth strain of

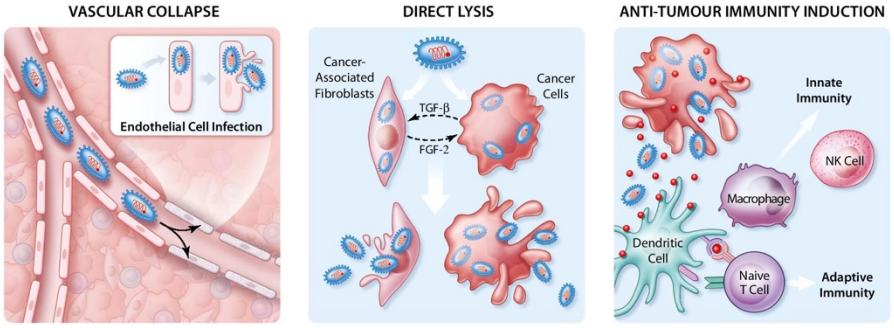

Fig. 2 Oncolytic viruses have been engineered to initiate a multi-faceted cancer attack that uses complementary mechanisms to destroy the tumour. Tumour-associated active endothelial cells are vulnerable to OV infection through a VEGF-mediated mechanism, which leads to vascular collapse and tumour starvation. The traditional mechanism of action of direct cancer cell oncolysis can now also be applied to cancer-associated fibroblasts (CAFs) as we have come to understand their vulnerability to OV attack. Finally, released tumour-specific antigens can be ingested by various antigen presenting cells, which can lead to the initiation of both innate and adaptive anti-tumour immunity

Table 1 A summary of 43 currently active oncolytic virus clinical trials (current as of April 2016)

Clinical indication	Virus platform	Primary outcome and treatment arms	Study status; trial phase	Clinicaltrials.gov. Identifier No.
Multiple cancers				
Solid tumours (locally advanced and metastatic)	Adenovirus	–Safety and recommended Phase II dose - Single-agent IV dose escalation - IV virus + Gemcitabine	Recruiting; phase I trial of VCN-01	NCT02045602
- Tumours of epithelial origin - Colorectal - Bladder	Adenovirus	- MTD and selection of reasonable administration schedule - Enadenotucirev by sub-acute fractionated IV	Recruiting; phase I/II trial of Enadenotucirev	NCT02028442
- Ovarian - Fallopian - Peritoneal	Measles virus	- Overall survival - IP infusion of MV-NIS vs. investigator's choice chemotherapy	Recruiting; phase II trial of MV-NIS	NCT02364713
Metastatic solid tumours	Adenovirus (prime) *and* MG1 (boost)	- Toxicity and objective tumour response rate - A: IV MG1MA3 virus alone - B: IM AdMA3 (vaccine prime) alone - C: AdMA3 + MG1MA3 (prime + boost)	Recruiting; phase I/II trial of MG1-MAGE-A3 ± adenovirus vaccine	NCT02285816
- Ovarian epithelial - Primary peritoneal	Measles virus	- Safety - MV-CEA and MV-NIS	Ongoing; phase I trial of MV-CEA vs. MV-NIS	NCT00408590
- Colorectal - NSCLC - Bladder - Renal cell carcinoma	Adenovirus	- Viral delivery and spread (IHC and qPCR) - IT Colo-Ad1 vs. IV Colo-Ad1	Ongoing; phase I trial of Colo-Ad1	NCT02053220
- Ovarian epithelial - Fallopian tube - Primary peritoneal	Reovirus	- Safety, progression free survival - Paclitaxel + wild-type reovirus vs. paclitaxel alone	Ongoing; phase II trial of wild-type reovirus	NCT01199263
*Metastatic or advanced epithelial tumours	Adenovirus	- MTD/MFD of IV Enadenotucirev in combination with Keytruda®	Currently recruiting; phase I trial of Enadenotucirev in combination with Keytruda®	NCT02636036
Solid organ cancers	Vaccinia	- Treatment-related adverse effects - 6 cohorts: different dosing of GL-ONC1 + eculizumab vs. GL-ONC1 alone	Not yet recruiting; Phase I trial of GL-ONC1 in combination with eculizumab	NCT02714374
Cancers of the nervous system				
Recurrent glioblastoma or gliosarcoma	Adenovirus	- Objective response (determined by MRI) - DNX-2401 ± IFN-γ	Recruiting; phase Ib trial of DNX-2401 with IFN-γ	NCT02197169
Supratentorial brain tumours	HSV-1	- Safety and tolerability - MRI-guided single dose of G207 by catheter infusion	Not yet recruiting; Phase I trial of G207	NCT02457845
Non-CNS tumours (adolescents and young adults)	HSV-1	- Safety and tolerability of IT and IV injections - IT HSV1716 (localized disease) - IV HSV1716 (metastatic disease)	Recruiting; phase I trial of HSV1716	NCT00931931
High-grade glioma (refractory or recurrent; operable)	HSV-1	- Maximum tolerated dose - IT HSV1716 + peritumoural HSV1716 post-resection; patients also receive dexamethasone	Recruiting; phase I trial of HSV1716	NCT02031965
Malignant peripheral nerve sheath tumour	Measles virus	- Best response, adverse events, maximum tolerated dose - IT injection MV-NIS; follow-up by SPECT/CT	Not yet recruiting; phase I trial of MV-NIS	NCT02700230
Recurrent glioblastoma	Adenovirus	- Adverse events - DNX2401 injection into brain parenchyma *and* temozolomide treatment	Ongoing; phase I trial of DNX2401	NCT01956734

Table 1 (continued)

Clinical indication	Virus platform	Primary outcome and treatment arms	Study status; trial phase	Clinicaltrials.gov. Identifier No.
Skin Cancer				
- Malignant melanoma - SCC	HSV-1	- Dose escalation of repeated IT virus administration - High dose vs. low dose	Recruiting; phase I trial of TBI-1401(HF10)	NCT02428036
*Unresectable melanoma (stages IIIB, IIIC, IV)	HSV-1	- Best overall response rate - IT HF10 in combination with IV Yervoy®	Recruiting; phase II trial of HF10 co-treatment with Yervoy®	NCT02272855
Recurrent cutaneous melanoma	HSV-1	- Progression-free survival - PV-10 vs. Imlygic™ vs. chemotherapy (dacarbazine or temozolomide	Recruiting; phase III trial of PV-10	NCT02288897
Melanoma (stage IIIB to IVM1c	HSV-1	- Detecting Imlygic™ DNA in blood and urine within first 3 treatment cycles - IT Imlygic™ administration	Ongoing; phase II trial of Imlygic™	NCT02014441
*Melanoma (stage IIIB to IV)	HSV-1	- Safety, tolerability, efficacy - Imlygic™ + Yervoy® vs. Yervoy® alone	Recruiting; Phase I-II trial of Imlygic™	NCT01740297
Melanoma (stage IIIB to IVM1c)	HSV-1	- Efficacy - Neoadjuvant Imlygic™ + surgery vs. surgery alone	Recruiting; phase II trial of Imlygic™	NCT02211131
*Unresected melanoma	HSV-1	- Dose limiting toxicity, progression-free survival, and overall survival - Imlygic™ + Keytruda® vs. placebo + Keytruda®	Recruiting; phase Ib/III trial of Imlygic™	NCT02263508
Melanoma (stage IIIB to IVM1c)	HSV-1	- Correlating IT CD8+ cell density to objective response rate - IT Imlygic™ administration	Recruiting; phase II trial of Imlygic™	NCT02366195
Pancreatic Cancer				
Pancreatic cancer	Adenovirus	- Maximum tolerated dose - IT LOAd703 + IV gemcitabine	Recruiting; phase I/IIa trial of LOAd703	NCT02705196
Advanced pancreatic cancer	Adenovirus	- Safety and recommended phase II dose development - IT VCN-01 + gemcitabine	Not yet recruiting; phase I trial of VCN-01	NCT02045589
*Advanced pancreatic carcinoma	Reovirus	- Safety - Reolysin® and chemotherapy + Keytruda®	Recruiting; phase Ib trial of Reolysin®	NCT02620423
Liver Cancer				
Hepatocellular carcinoma	Vaccinia	- Overall survival - Pexa-Vec + Sorafenib vs. Sorafenib alone	Recruiting; phase III trial of Pexa-Vec	NCT02562755
Hepatocellular carcinoma	HSV-1	- Dose-limiting toxicities - U/S-guided IT Imlygic™ administration	Recruiting; phase I trial of Imlygic™	NCT02509507
Colorectal Cancer				
Metastatic colorectal cancer (*mt*KRAS)	Reovirus	- Dose limiting toxicity and pharmacokinetic parameters of combination therapy - Different dose levels of Reolysin® + FOLFIRI and bevacizumab	Recruiting; phase I trial of Reolysin®	NCT01274624
Bladder Cancer				
High grade non-muscle invasive bladder cancer	Adenovirus	- Durable complete response for patients who have failed BCG therapy and refused cystectomy	Recruiting; phase III trial of CG0070	NCT02365818
Non-muscle invasive bladder cancer	Adenovirus	- Complete response - CG0070 vs. chemotherapy *or* interferon	Ongoing; phase II/III trial of CG0070	NCT01438112

Table 1 (continued)

Clinical indication	Virus platform	Primary outcome and treatment arms	Study status; trial phase	Clinicaltrials.gov. Identifier No.
Ovarian Cancer				
Ovarian cancer	Adenovirus	- Maximum tolerated dose - Experimental arm: Enadenotucirev intraperitoneal injection	Recruiting; phase I/II trial of Enadenotucirev	NCT02028117
Lung Cancer				
Malignant pleural mesothelioma	HSV-1	- Safety and efficacy - Injection of HSV1716 into tumour-bearing pleural cavity - Safety/efficacy study	Recruiting; phase I/II trial of HSV1716	NCT01721018
Mesothelioma	Vaccinia	- Determine MTD for subsequent Phase II studies - Dose escalation	Recruiting; phase I trial of GL-ONC1	NCT01766739
Multiple Myeloma				
Multiple myeloma	Measles virus	- Efficacy - UARK-21 expressing NIS + Cyclophosphamide	Recruiting; phase II trial of UARK-21	NCT02192775
Recurrent or refractory multiple myeloma	Measles virus	- Maximum tolerated dose, proportion of confirmed response - MV-NIS vs. MV-NIS + cyclophosphamide	Recruiting; phase I/II trial of MV-NIS	NCT00450814
Relapsed or refractory multiple myeloma	Reovirus	- Adverse events - Dexamethasone, bortezomib, *and* IV reovirus following treatment schedule	Recruiting; phase I trial of wild-type reovirus virus + standard of care	NCT02514382
Head and Neck Cancers				
Recurrent or metastatic SCC	Measles virus	- Maximum tolerated dose - IT injection MV-NIS	Recruiting; phase I trial of MV-NIS	NCT01846091
*Recurrent or metastatic SCC	HSV-1	- Incidence of dose limiting toxicity - Imlygic™ + Keytruda®	Not yet recruiting; Phase Ib/III trial of Imlygic™ + Keytruda®	NCT02626000
Prostate Cancer				
*Prostate Cancer	Adenovirus	- Maximum tolerated dose and dose-dependent toxicity - Intraprostatic injection of engineered virus	Recruiting; phase I trial of oncolytic adenovirus and IL-12 gene therapy	NCT02555397
*Prostate cancer	Vaccinia (prime) *and* fowlpox (boost)	- Overall survival - PROSTVAC ± GM-CSF; placebo comparitors	Ongoing but not recruiting; phase III of PROSTVAC ± GM-CSF	NCT01322490
Breast Cancer				
Breast cancer local recurrence	HSV-1	- Disease control rate - Imlygic™ initial dose IT injection + higher dose IT injections at 2 week intervals	Not yet recruiting; Phase II trial of Imlygic™	NCT02658812
Sarcoma				
Sarcoma	HSV-1	- Safety and efficacy - Imlygic™ + radiotherapy	Recruiting; phase I/II trial of Imlygic™ + radiation therapy	NCT02453191

MTD maximum tolerated dose, *IV* intravenous, *IP* intraperitoneal, *IM* intramuscular, *IT* intratumoural, *IHC* immunohistochemistry, *MV* measles virus, *HSV* herpes simplex virus, *NIS* sodium-iodide symporter, *CEA* carcinoembryonic antigen, *IFN* interferon

*Ongoing trials of OVs in combination with other immuno-oncology products

VacV, the deletion of the thymidine kinase (TK) gene has been shown to limit virus replication to highly metabolic and proliferative cancer cells. In addition, this version of Pexa-Vec has a natural *B18R* truncation, which renders the virus susceptible to intact anti-viral effects in normal cells. The TK deletion coupled with the *B18R* truncation has contributed to the clinical success of Pexa-Vec (formerly JX-594), which has entered phase III clinical trials (Table 1; ClinicalTrials.gov. identifier NCT02562755) [39–41]. Another group has explored the effects of a so-called double deleted VacV, or VVDD. This therapeutic is based on the Western Reserve (WR) strain of VacV and is attenuated by elimination of both the gene encoding Vaccinia Growth Factor (VGF) and that of thymidine kinase (TK). The wild-type version of WR is more virulent than the Wyeth strain, and the addition of these gene deletions has created a potentially more potent therapeutic. To date, VVDD has proven safe in a phase I dose-escalation trial by intratumoural injection including some hints of therapeutic benefit and is now poised for further clinical testing [42, 43]. The Lister strain of VacV has also been used in OV development, with Genelux Corporation leading the development of this approach. They have created an attenuated and cancer-targeted OV by inserting expression cassettes into the *F14.5L*, *TK*, and *A56R* genes of Lister [44], an approach that is now actively in phase I clinical trials (Table 1).

In addition to those discussed above, several other virus families have served as backbones for the development of OVs. This list includes, but is not limited to, Paramyxoviruses (Newcastle Disease virus [NDV], Measles virus [MV], Reovirus [ex. Reolysin®]) and Rhabdoviruses (Vesicular Stomatitis virus [VSV], Maraba virus). With these platforms, the strategies that have been used across the field to make effective oncolytics have remained consistent (reducing toxicity and maximizing tumour-specificity); however, opportunities exist to take advantage of the unique biology of each viral platform. For instance, MV has been engineered to allow monitoring of virus replication either by virus-directed expression of a blood marker (CEA peptide [45]) or by a cellular imaging gene like the sodium iodide symporter [46]. The naturally attenuated Reovirus strains that have made clinical strides have been demonstrated to preferentially replicate in *Ras*-activated cells, a common occurrence in many cancer types [47–49]. The Maraba virus MG1 was engineered to have two attenuating mutations creating a virus that is restricted for growth in normal cells while being hyper-virulent in cancer cells [50]. This virus has been further engineered to express a tumour antigen to boost anti-tumour immunity [51] and is therefore currently being explored for clinical use (Table 1; ClinicalTrials.gov. identifier: NCT02285816). Evidently, many bio-engineering approaches have been explored in the OV field; however, much of the work currently being done is aimed at harnessing the anti-cancer potential of the human immune system.

Strategies to maximize anti-tumour immunity

A recent focus of the OV field has been to optimize virus design or combination therapeutic strategies to improve the ability of existing platforms to induce anti-tumour immunity. One effective approach has been the inclusion of immunostimulatory transgenes and/or cytokines into candidate OVs. For instance, Imlygic™—unquestionably the most successful OV to date—encodes and expresses human GM-CSF cDNA [18, 29]. The addition of GM-CSF promotes monocyte-to-dendritic cell differentiation, thereby facilitating antigen presentation on the surface of dendritic cells following viral-induced oncolysis [8]. Another widely utilized strategy in HSV-1 is the addition of various interleukins to activate adaptive immunity through T cell activation (IL2) [52] or by doubly activating both T cells and NK cells (IL12, IL15, IL18) [53–55]. The ability to direct the co-stimulation of T cells has also been exploited in the development of HSV-1-based OVs. Specifically, B7-1 (CD80) has been cloned into the HSV backbone to help activate antigen presentation [56–58], a strategy that has also been utilized with the ligand of CD40, likely working through a PI3K-dependent mechanism [59, 60].

Similarly, approaches have been taken to create more immunostimulatory oAd and VacV OV candidates. As with Imlygic™, human GM-CSF has been encoded into both oAd and VacV candidates [41, 61, 62]. Specifically in the oncolytic VacV Pexa-Vec, ongoing phase III clinical efforts are being made following several promising phase I and II studies (Table 1; ClinicalTrials.gov. identifier NCT02562755) [41, 61]. Although there is a clear trend in the OV field of encoding human GM-CSF cDNA and/or that of other cytokines in clinical candidate strains, it is important to understand the fundamental immunology behind this strategy. The mechanisms are incompletely understood, but some evidence suggests that we can trigger the activation of immune inhibitory cells such as myeloid derived precursor cells upon cytokine-encoding viral infection [63]. More fundamental discovery must occur to understand the control of these approaches, but we believe it is important for the field to consider potential unwanted outcomes caused by stimulating undesirable immune targets.

Since the generation of oAds began prior to VacV OV development, many more strategies have been attempted in this context, especially as they relate to immune cell recruitment and activation. From the CC chemokine sub-family, two proteins have been encoded into oAds—CCL3 and RANTES (CCL5), which work to attract PMN leukocytes and T cells, respectively—positively affecting OV efficacy while recruiting immune cells to the tumour microenvironment [64, 65]. Additionally, IL4 [66] and IL12 [67, 68] have been used to elicit anti-tumour immunity; however, the toxicity risk of the latter was recently called into question in the context of oAd in a hamster pancreatic cancer model, so questions

remain [69]. Similar to the approach in HSV-1 of using B7-1 to increase T cell co-stimulation, this approach has been adapted for both VacV [70] and oAd [71] with the tumour necrosis factor receptor family member CD137 (4-1BB). Interestingly, this approach has also been adapted as a co-therapeutic approach in which the TK/VGF double-deleted strain of VacV is co-administered with a CD137 agonist, which resulted in a decreased tumour burden and increased intratumoural immune infiltrate [72].

The trend in the OV field of combining strategies to make more immunogenic clinical candidate viruses extends beyond those discussed in this review. However, this tendency reveals a fundamental truth that researchers in the OV field are accepting—current OVs are most likely to be clinically successful when they have been optimized for their ability to induce anti-tumour immunity.

Synergy between oncolytic viruses and existing immunotherapies—immune checkpoint blockade

As has been clinically well-documented, current standards of immune checkpoint inhibition (ICI) therapy, while impressive as monotherapies, are effective in only a minority of cancer patients [7, 73, 74]. This is likely because of the mechanism of action of ICIs, which by design "remove the brakes" from existing anti-tumour immune responses. Likely in many patients, pre-existing *bona fide* anti-tumour immunity is not present, and thus, there is little for an ICI therapeutic approach to augment. An objective appraisal of the OV literature will also demonstrate their limitations as monotherapies in many patients; however, it is important to understand that we are in the midst of improving early-generation products, and that by their mechanistic nature, OVs are optimally positioned to work in synergy with existing ICIs. As discussed, numerous pre-clinical and clinical (Table 1) studies are beginning to demonstrate this.

One such example occurred in a mouse tumour model with intratumoural NDV infection in combination with systemic anti-CTLA-4 administration, leading to a systemic anti-tumour effect [75]. Another example of OV synergy with ICI therapy was observed in difficult-to-treat mouse cancer models using a Semliki Forest virus platform encoding IL-12 in concert with anti-mouse-PD-1 [76]. These and other data have led to clinical studies designed to test OVs in combination with ICIs. Ongoing studies include the combination of Imlygic™ with the anti-CTLA-4 product Yervoy® (Table 1; ClinicalTrials.gov. identifier: NCT01740297) and in another study with the anti-PD1 therapy Keytruda® (Table 1; ClinicalTrials.gov. identifiers: NCT02263508 and NCT02626000). An exciting recent development in the OV field was the publication of results from the first phase Ib trial of combination Imlygic™ and Yervoy® in advanced melanoma, which demonstrated significant improvements over either monotherapy [77]. In addition, the chimeric oAd Enadenotucirev and the naturally oncolytic Reolysin® virus are being tested in combination with Keytruda® (Table 1; ClinicalTrials.gov. identifiers: NCT02636036 and NCT02620423, respectively).

While the clinical benefits of ICIs began to emerge, it became evident that systemic administration of these agents carried the potential to cause immune-related adverse events in some patients that required acute immunosuppressive therapies to manage [78, 79]. Given that OVs can often harbor and express therapeutic payloads, it was hypothesized that the intratumoural OV-induced production of an antibody against CTLA-4 could reduce toxicity while improving anti-tumour immunity. Thus, a transcriptionally targeted oAd expressing anti-CTLA-4 was generated, which demonstrated preferential tumoural replication, effective anti-CTLA-4 delivery to the tumour, and mechanistically linked T cell activation [80]. This approach of intratumoural viral-induced anti-CTLA-4 production was replicated in an oAd, which demonstrated efficacy in an immunocompetent B16 melanoma model [81]. More recently, antibodies against CTLA-4 and PD-L1 were cloned into the measles virus platform, which improved therapeutic outcomes in terms of both tumour size and overall survival. This effect was observed to be maintained when systemic administration of immune checkpoint blockade was alternatively utilized, strongly supporting the clinical rationale for co-treatment with OVs and immune checkpoint blockade [82] (Fig. 3).

Oncolytic viruses and adoptive cell therapy

Adoptive cell therapy has been developed and refined over many years to the point at which, when combined with a maximal lymphodepletion regimen, complete durable responses have been observed in a reasonable number of patients primarily suffering from melanoma [83, 84]. These positive responses are often durable, even in cases of advanced disease. Therefore, adoptive cell therapy in some form will likely play an important role in the future of anti-cancer therapy. One branch of the OV field has compiled evidence to support the combination therapy of various adoptive cell transfer approaches with OV therapeutics. In 2008, Qiao et al. studied an aggressive mouse melanoma model prone to metastases in both lymphoid and more distant organs. They infected naïve T lymphocytes with a vesicular stomatitis virus (VSV) expressing GFP and adoptively transferred them, hypothesizing that they could take advantage of the innate tumour homing ability of immune cells. They then monitored tumour growth/survival and noticed significant in vivo effects in animals treated with adoptively transferred VSV-GFP-preloaded T cells [85, 86]. This approach was similarly applied with a NDV platform in activated peripheral blood-

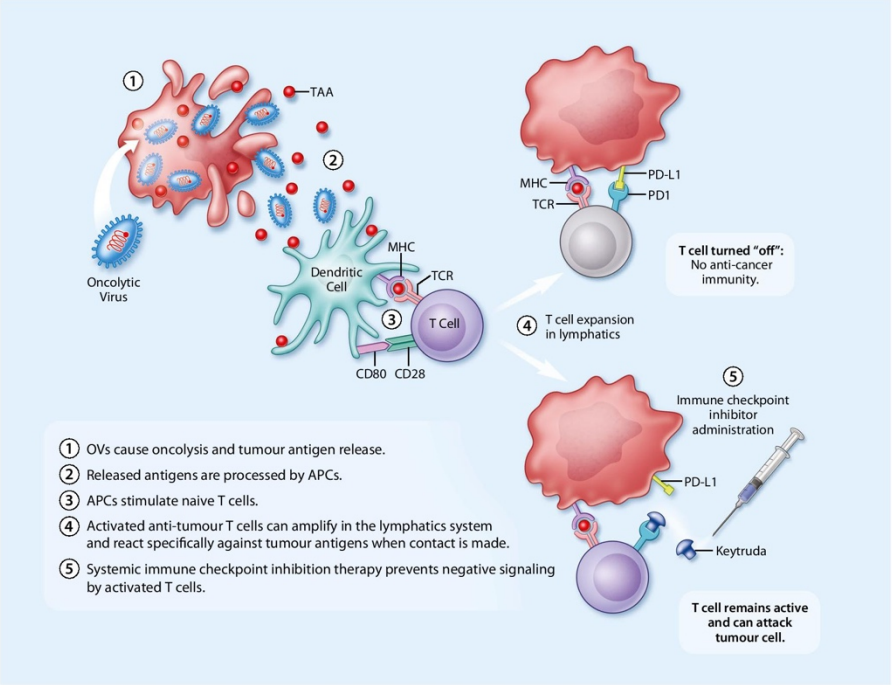

Fig. 3 Oncolytic viruses are well positioned to synergize with existing immunotherapies. Cancer cell infection and direct oncolysis leads to the release of tumour-specific antigens, which can be processed by dendritic cells for antigen presentation to naïve T cells. Now activated against the tumour antigen, these T cells can aggressively replicate within lymphoid organs before being circulated to intact tumour cells. The concomitant systemic administration of checkpoint inhibitors (ex. Keytruda®; anti-PD-1) will block the negative checkpoints on the surface of cytotoxic T cells, providing a competitive advantage for the positive regulators of T cell function to interact with the tumour cell, leading to their specific destruction. *TAA* tumour-associated antigen, *TCR* T cell receptor, *APC* antigen-presenting cell

derived T cells and tumour growth inhibition was also observed, however using a MCF-7 human breast cancer cell line [87]. In another pre-clinical model, donor splenocytes from rats harboring parvovirus-treated orthotopic PDAC tumours were adoptively transferred into naïve PDAC-bearing recipients, resulting in a significant prolonging of recipient survival [88]. In a more recent effort combining the adoptive transfer of cytotoxic T lymphocytes with OV therapy using an oAd expressing IL15, a positive therapeutic effect was observed in both human glioblastoma and gastric cancer models [89].

Cytokine-induced killer (CIK) cells have also been shown to gain an enhanced therapeutic effect when used in synergy with OV therapeutics. This has been observed using an oAd in an orthotopic rectal cancer model [90], in a patient-derived xenograft model of HCC in synergy with an HSP70-loaded oAd [91], and in an HCC model using an oAd expressing IL12 [92]. These pre-clinical studies represent attractive possibilities for future clinical translation due to the many technical benefits of working with CIK cells and their apparent efficacy benefits in early studies [93].

One of the challenges of using adoptive cell therapy is creating a situation in which the transferred cells are preferentially attracted to cancers, especially in the context of many solid tumours. Oncolytic viruses may have a mechanism by which they can help adoptively transferred cells overcome this limitation, as seen with the HSV-2-based OV that has been observed to actively pull effector T cells to the site of viral infection [94]. With the same rationale, Nishio et al. approached the less often combined CAR-T therapy with an oAd expressing IL15 as well as the RANTES chemokine. They observed that the OV therapy had a direct oncolytic effect as expected, however also worked to home the tumour antigen GD2-specific CAR-T cells to their experimental neuroblastoma model [95].

Accelerated clinical development of oncolytic viruses

As discussed, the field of OV therapeutics is in the midst of a rapid surge in clinical candidate development thanks in large

part to their synergistic potential with existing immunotherapies. It is evident that recent clinical advances in immunotherapy have changed the way oncology is practiced and changed the prognosis for many patients. Unfortunately, many patients will remain non-responders despite these advances, which is where OVs can have tremendous impacts. Dozens of clinical trials have been completed to advance the field; however, Table 1 summarizes the currently active registered clinical trials (as of April 2016; listed on ClinicalTrials.gov) involving OVs. Our group is taking a novel approach to enhancing anti-tumour immunity by encoding tumour antigens directly in an OV backbone, thus creating a true *oncolytic virus vaccine*. Heterologous "prime-boost" approaches have been in vogue in the infectious disease field for over a decade and are designed to focus the immune system on the target antigen rather than the immunizing vectors. We have adapted this strategy and are conducting a trial wherein patients receive a *priming* vaccination via intramuscular injection with a non-replicating adenovirus vector expressing a tumour antigen followed by a *boosting* vaccination with an intravenously administered rhabdovirus-based OV that encodes the same tumour antigen. In this study, we hope to combine the potent stimulation of the immune system using our novel vaccination strategy along with the benefits of OV therapy (ClinicalTrials.gov. identifier NCT02285816). Another similar approach has been employed in minimally symptomatic, chemotherapy naïve metastatic castration-resistant prostate cancer—patients have been treated with PROSTVAC immunotherapy, which uses a "prime-boost" treatment course of recombinant VacV followed by a recombinant fowl pox in an effort to generate and maintain anti-tumour immunity [96]. The field will await results of a phase III trial, which is currently underway (Table 1; ClinicalTrials.gov. identifier NCT01322490).

Future perspectives

The past decade in the OV field has been one of great progress as OVs have demonstrated themselves to be excellent potential partners to boost existing and emerging immunotherapies, and as discussed herein are poised to enhance the growing anti-cancer armament available to today's oncologist. However, there are still many unanswered questions in the OV field and there is a need to continue funding fundamental research into virus-host interactions. For instance, how can we best design vectors that overcome natural adaptive and innate anti-viral responses [97] facilitating successful systemic delivery and tumour lysis without compromising the excellent safety record OVs have enjoyed to date? These approaches have to be balanced with the need to also stimulate the immune systems of individuals with cancer to generate effective and long lasting anti-tumour immunity. Whatever the answers to these questions, it is clear the OV field has entered 'primetime', and we now seek to deliver the best possible next-generation therapeutics for our patients.

Acknowledgments BAK is supported by a Vanier Canada Graduate Scholarship. JCB is supported by the Ontario Institute of Cancer Research, the Canadian Institutes of Health Research, and the Terry Fox Foundation. We would like to acknowledge the many investigators whose basic discoveries have been translated into clinical candidate oncolytic viral therapeutics and may otherwise not be mentioned. We would like to thank Dr. C. Ilkow for the critical appraisal of this manuscript.

Compliance with ethical standards

Conflict of interest JCB is a scientific co-founder of Turnstone Biologics.

References

1. Couzin-Frankel J (2013) Breakthrough of the year 2013. Cancer immunotherapy. Science 342:1432–1433
2. Hoos A (2016) Development of immuno-oncology drugs—from CTLA4 to PD1 to the next generations. Nat Rev Drug Discov 15: 235–247
3. Sheridan C (2015) IDO inhibitors move center stage in immuno-oncology. Nat Biotechnol 33:321–322
4. Uyttenhove C, Pilotte L, Theate I, Stroobant V, Colau D, Parmentier N, Boon T, Van den Eynde BJ (2003) Evidence for a tumoral immune resistance mechanism based on tryptophan degradation by indoleamine 2,3-dioxygenase. Nat Med 9:1269–1274
5. Topalian SL, Sznol M, McDermott DF, Kluger HM, Carvajal RD, Sharfman WH, Brahmer JR, Lawrence DP, Atkins MB, Powderly JD et al (2014) Survival, durable tumor remission, and long-term safety in patients with advanced melanoma receiving nivolumab. J Clin Oncol 32:1020–1030
6. Ansell SM, Lesokhin AM, Borrello I, Halwani A, Scott EC, Gutierrez M, Schuster SJ, Millenson MM, Cattry D, Freeman GJ et al (2015) PD-1 blockade with nivolumab in relapsed or refractory Hodgkin's lymphoma. N Engl J Med 372:311–319
7. Larkin J, Chiarion-Sileni V, Gonzalez R, Grob JJ, Cowey CL, Lao CD, Schadendorf D, Dummer R, Smylie M, Rutkowski P et al (2015) Combined nivolumab and ipilimumab or monotherapy in untreated melanoma. N Engl J Med 373:23–34
8. Lichty BD, Breitbach CJ, Stojdl DF, Bell JC (2014) Going viral with cancer immunotherapy. Nat Rev Cancer 14:559–567
9. Ivashkiv LB, Donlin LT (2014) Regulation of type I interferon responses. Nat Rev Immunol 14:36–49
10. Sun WH, Pabon C, Alsayed Y, Huang PP, Jandeska S, Uddin S, Platanias LC, Rosen ST (1998) Interferon-alpha resistance in a cutaneous T-cell lymphoma cell line is associated with lack of STAT1 expression. Blood 91:570–576
11. Wong LH, Krauer KG, Hatzinisiriou I, Estcourt MJ, Hersey P, Tam ND, Edmondson S, Devenish RJ, Ralph SJ (1997) Interferon-resistant human melanoma cells are deficient in ISGF3 components, STAT1, STAT2, and p48-ISGF3gamma. J Biol Chem 272:28779–28785
12. Stojdl DF, Lichty B, Knowles S, Marius R, Atkins H, Sonenberg N, Bell JC (2000) Exploiting tumor-specific defects in the interferon pathway with a previously unknown oncolytic virus. Nat Med 6: 821–825

13. Pikor LABJC, Diallo J-S (2015) Oncolytic viruses: exploiting Cancer's deal with the devil. Trends in Cancer 1:266–277
14. Li S, Zhu M, Pan R, Fang T, Cao YY, Chen S, Zhao X, Lei CQ, Guo L, Chen Y et al (2016) The tumor suppressor PTEN has a critical role in antiviral innate immunity. Nat Immunol 17:241–249
15. Hanahan D, Weinberg RA (2011) Hallmarks of cancer: the next generation. Cell 144:646–674
16. Arulanandam R, Batenchuk C, Angarita FA, Ottolino-Perry K, Cousineau S, Mottashed A, Burgess E, Falls TJ, De Silva N, Tsang J et al (2015) VEGF-mediated induction of PRD1-BF1/Blimp1 expression sensitizes tumor vasculature to oncolytic virus infection. Cancer Cell 28:210–224
17. Ilkow CS, Marguerie M, Batenchuk C, Mayer J, Ben Neriah D, Cousineau S, Falls T, Jennings VA, Boileau M, Bellamy D et al (2015) Reciprocal cellular cross-talk within the tumor microenvironment promotes oncolytic virus activity. Nat Med 21:530–536
18. Liu BL, Robinson M, Han ZQ, Branston RH, English C, Reay P, McGrath Y, Thomas SK, Thornton M, Bullock P et al (2003) ICP34.5 deleted herpes simplex virus with enhanced oncolytic, immune stimulating, and anti-tumour properties. Gene Ther 10: 292–303
19. Kohlhapp FJ, Kaufman HL (2016) Molecular pathways: mechanism of action for Talimogene Laherparepvec, a new oncolytic virus immunotherapy. Clin Cancer Res 22:1048–1054
20. Dock G (1904) The influence of complicating diseases upon leukemia. The American Journal of Medical Sciences 127:563–592
21. Kelly E, Russell SJ (2007) History of oncolytic viruses: genesis to genetic engineering. Mol Ther 15:651–659
22. Moore AE (1951) The destructive effects of viruses on transplantable mouse tumors. Acta Unio Int Contra Cancrum 7:279–281
23. Hoster HA, Zanes RP Jr, Von Haam E (1949) Studies in Hodgkin's syndrome; the association of viral hepatitis and Hodgkin's disease; a preliminary report. Cancer Res 9:473–480
24. Southam CM, Moore AE (1952) Clinical studies of viruses as antineoplastic agents with particular reference to Egypt 101 virus. Cancer 5:1025–1034
25. Asada T (1974) Treatment of human cancer with mumps virus. Cancer 34:1907–1928
26. Liu TC, Galanis E, Kirn D (2007) Clinical trial results with oncolytic virotherapy: a century of promise, a decade of progress. Nat Clin Pract Oncol 4:101–117
27. Parato KA, Senger D, Forsyth PA, Bell JC (2005) Recent progress in the battle between oncolytic viruses and tumours. Nat Rev Cancer 5:965–976
28. Andtbacka RH, Ross M, Puzanov I, Milhem M, Collichio F, Delman KA, Amatruda T, Zager JS, Cranmer L, Hsueh E et al (2016) Patterns of clinical response with Talimogene Laherparepvec (T-VEC) in patients with melanoma treated in the OPTiM phase III clinical trial. Ann Surg Oncol. doi:10.1245/s10434-016-5286-0
29. Andtbacka RH, Kaufman HL, Collichio F, Amatruda T, Senzer N, Chesney J, Delman KA, Spitler LE, Puzanov I, Agarwala SS et al (2015) Talimogene Laherparepvec improves durable response rate in patients with advanced melanoma. J Clin Oncol 33:2780–2788
30. Orvedahl A, Alexander D, Talloczy Z, Sun Q, Wei Y, Zhang W, Burns D, Leib DA, Levine B (2007) HSV-1 ICP34.5 confers neurovirulence by targeting the Beclin 1 autophagy protein. Cell Host Microbe 1:23–35
31. Brown SM, MacLean AR, McKie EA, Harland J (1997) The herpes simplex virus virulence factor ICP34.5 and the cellular protein MyD116 complex with proliferating cell nuclear antigen through the 63-amino-acid domain conserved in ICP34.5, MyD116, and GADD34. J Virol 71:9442–9449
32. Miao L, Fraefel C, Sia KC, Newman JP, Mohamed-Bashir SA, Ng WH, Lam PY (2014) The potential application of a transcriptionally regulated oncolytic herpes simplex virus for human cancer therapy. Br J Cancer 110:94–106
33. Tyminski E, Leroy S, Terada K, Finkelstein DM, Hyatt JL, Danks MK, Potter PM, Saeki Y, Chiocca EA (2005) Brain tumor oncolysis with replication-conditional herpes simplex virus type 1 expressing the prodrug-activating genes, CYP2B1 and secreted human intestinal carboxylesterase, in combination with cyclophosphamide and irinotecan. Cancer Res 65:6850–6857
34. Kanai R, Zaupa C, Sgubin D, Antoszczyk SJ, Martuza RL, Wakimoto H, Rabkin SD (2012) Effect of gamma34.5 deletions on oncolytic herpes simplex virus activity in brain tumors. J Virol 86:4420–4431
35. Nettelbeck DM, Rivera AA, Balague C, Alemany R, Curiel DT (2002) Novel oncolytic adenoviruses targeted to melanoma: specific viral replication and cytolysis by expression of E1A mutants from the tyrosinase enhancer/promoter. Cancer Res 62:4663–4670
36. Bofill-De Ros X, Villanueva E, Fillat C (2015) Late-phase miRNA-controlled oncolytic adenovirus for selective killing of cancer cells. Oncotarget 6:6179–6190
37. Johnson TJ, Hoti N, Liu C, Chowdhury WH, Li Y, Zhang Y, Lupold SE, Deweese T, Rodriguez R (2013) Bicalutamide-activated oncolytic adenovirus for the adjuvant therapy of high-risk prostate cancer. Cancer Gene Ther 20:394–402
38. Tseng AW, Chen C, Breslin MB, Lan MS (2016) Tumor-specific promoter-driven adenoviral therapy for insulinoma. Cell Oncol (Dordr) 39:279–286
39. Kim JH, Oh JY, Park BH, Lee DE, Kim JS, Park HE, Roh MS, Je JE, Yoon JH, Thorne SH et al (2006) Systemic armed oncolytic and immunologic therapy for cancer with JX-594, a targeted poxvirus expressing GM-CSF. Mol Ther 14:361–370
40. Parato KA, Breitbach CJ, Le Boeuf F, Wang J, Storbeck C, Ilkow C, Diallo JS, Falls T, Burns J, Garcia V et al (2012) The oncolytic poxvirus JX-594 selectively replicates in and destroys cancer cells driven by genetic pathways commonly activated in cancers. Mol Ther 20:749–758
41. Breitbach CJ, Burke J, Jonker D, Stephenson J, Haas AR, Chow LQ, Nieva J, Hwang TH, Moon A, Patt R et al (2011) Intravenous delivery of a multi-mechanistic cancer-targeted oncolytic poxvirus in humans. Nature 477:99–102
42. McCart JA, Ward JM, Lee J, Hu Y, Alexander HR, Libutti SK, Moss B, Bartlett DL (2001) Systemic cancer therapy with a tumor-selective vaccinia virus mutant lacking thymidine kinase and vaccinia growth factor genes. Cancer Res 61:8751–8757
43. Zeh HJ, Downs-Canner S, McCart JA, Guo ZS, Rao UN, Ramalingam L, Thorne SH, Jones HL, Kalinski P, Wieckowski E et al (2015) First-in-man study of western reserve strain oncolytic vaccinia virus: safety, systemic spread, and antitumor activity. Mol Ther 23:202–214
44. Zhang Q, Liang C, Yu YA, Chen N, Dandekar T, Szalay AA (2009) The highly attenuated oncolytic recombinant vaccinia virus GLV-1h68: comparative genomic features and the contribution of F14.5 L inactivation. Mol Gen Genomics 282:417–435
45. Galanis E, Hartmann LC, Cliby WA, Long HJ, Peethambaram PP, Barrette BA, Kaur JS, Haluska PJ Jr, Aderca I, Zollman PJ et al (2010) Phase I trial of intraperitoneal administration of an oncolytic measles virus strain engineered to express carcinoembryonic antigen for recurrent ovarian cancer. Cancer Res 70:875–882
46. Reddi HV, Madde P, McDonough SJ, Trujillo MA, Morris JC 3rd, Myers RM, Peng KW, Russell SJ, McIver B, Eberhardt NL (2012) Preclinical efficacy of the oncolytic measles virus expressing the sodium iodide symporter in iodine non-avid anaplastic thyroid cancer: a novel therapeutic agent allowing noninvasive imaging and radioiodine therapy. Cancer Gene Ther 19:659–665
47. Coffey MC, Strong JE, Forsyth PA, Lee PW (1998) Reovirus therapy of tumors with activated Ras pathway. Science 282:1332–1334

48. Villalona-Calero MA, Lam E, Otterson GA, Zhao W, Timmons M, Subramaniam D, Hade EM, Gill GM, Coffey M, Selvaggi G et al (2016) Oncolytic reovirus in combination with chemotherapy in metastatic or recurrent non-small cell lung cancer patients with KRAS-activated tumors. Cancer 122:875–883
49. Kolb EA, Sampson V, Stabley D, Walter A, Sol-Church K, Cripe T, Hingorani P, Ahern CH, Weigel BJ, Zwiebel J et al (2015) A phase I trial and viral clearance study of reovirus (Reolysin) in children with relapsed or refractory extra-cranial solid tumors: a Children's oncology group phase I consortium report. Pediatr Blood Cancer 62:751–758
50. Brun J, McManus D, Lefebvre C, Hu K, Falls T, Atkins H, Bell JC, McCart JA, Mahoney D, Stojdl DF (2010) Identification of genetically modified Maraba virus as an oncolytic rhabdovirus. Mol Ther 18:1440–1449
51. Pol JG, Zhang L, Bridle BW, Stephenson KB, Resseguier J, Hanson S, Chen L, Kazdhan N, Bramson JL, Stojdl DF et al (2014) Maraba virus as a potent oncolytic vaccine vector. Mol Ther 22:420–429
52. Carew JF, Kooby DA, Halterman MW, Kim SH, Federoff HJ, Fong Y (2001) A novel approach to cancer therapy using an oncolytic herpes virus to package amplicons containing cytokine genes. Mol Ther 4:250–256
53. Varghese S, Rabkin SD, Liu R, Nielsen PG, Ipe T, Martuza RL (2006) Enhanced therapeutic efficacy of IL-12, but not GM-CSF, expressing oncolytic herpes simplex virus for transgenic mouse derived prostate cancers. Cancer Gene Ther 13:253–265
54. Antoszczyk S, Spyra M, Mautner VF, Kurtz A, Stemmer-Rachamimov AO, Martuza RL, Rabkin SD (2014) Treatment of orthotopic malignant peripheral nerve sheath tumors with oncolytic herpes simplex virus. Neuro-Oncology 16:1057–1066
55. Stephenson KB, Barra NG, Davies E, Ashkar AA, Lichty BD (2012) Expressing human interleukin-15 from oncolytic vesicular stomatitis virus improves survival in a murine metastatic colon adenocarcinoma model through the enhancement of anti-tumor immunity. Cancer Gene Ther 19:238–246
56. Todo T, Martuza RL, Dallman MJ, Rabkin SD (2001) In situ expression of soluble B7-1 in the context of oncolytic herpes simplex virus induces potent antitumor immunity. Cancer Res 61:153–161
57. Ino Y, Saeki Y, Fukuhara H, Todo T (2006) Triple combination of oncolytic herpes simplex virus-1 vectors armed with interleukin-12, interleukin-18, or soluble B7-1 results in enhanced antitumor efficacy. Clin Cancer Res 12:643–652
58. Fukuhara H, Ino Y, Kuroda T, Martuza RL, Todo T (2005) Triple gene-deleted oncolytic herpes simplex virus vector double-armed with interleukin 18 and soluble B7-1 constructed by bacterial artificial chromosome-mediated system. Cancer Res 65:10663–10668
59. Terada K, Wakimoto H, Tyminski E, Chiocca EA, Saeki Y (2006) Development of a rapid method to generate multiple oncolytic HSV vectors and their in vivo evaluation using syngeneic mouse tumor models. Gene Ther 13:705–714
60. Vlahava VM, Eliopoulos AG, Sourvinos G (2015) CD40 ligand exhibits a direct antiviral effect on herpes simplex virus type-1 infection via a PI3K-dependent, autophagy-independent mechanism. Cell Signal 27:1253–1263
61. Park BH, Hwang T, Liu TC, Sze DY, Kim JS, Kwon HC, Oh SY, Han SY, Yoon JH, Hong SH et al (2008) Use of a targeted oncolytic poxvirus, JX-594, in patients with refractory primary or metastatic liver cancer: a phase I trial. Lancet Oncol 9:533–542
62. Cerullo V, Pesonen S, Diaconu I, Escutenaire S, Arstila PT, Ugolini M, Nokisalmi P, Raki M, Laasonen L, Sarkioja M et al (2010) Oncolytic adenovirus coding for granulocyte macrophage colony-stimulating factor induces antitumoral immunity in cancer patients. Cancer Res 70:4297–4309
63. Fernandez A, Oliver L, Alvarez R, Fernandez LE, Lee KP, Mesa C (2014) Adjuvants and myeloid-derived suppressor cells: enemies or allies in therapeutic cancer vaccination. Hum Vaccin Immunother 10:3251–3260
64. Edukulla R, Woller N, Mundt B, Knocke S, Gurlevik E, Saborowski M, Malek N, Manns MP, Wirth T, Kuhnel F et al (2009) Antitumoral immune response by recruitment and expansion of dendritic cells in tumors infected with telomerase-dependent oncolytic viruses. Cancer Res 69:1448–1458
65. Lapteva N, Aldrich M, Weksberg D, Rollins L, Goltsova T, Chen SY, Huang XF (2009) Targeting the intratumoral dendritic cells by the oncolytic adenoviral vaccine expressing RANTES elicits potent antitumor immunity. J Immunother 32:145–156
66. Post DE, Sandberg EM, Kyle MM, Devi NS, Brat DJ, Xu Z, Tighiouart M, Van Meir EG (2007) Targeted cancer gene therapy using a hypoxia inducible factor dependent oncolytic adenovirus armed with interleukin-4. Cancer Res 67:6872–6881
67. Choi IK, Lee JS, Zhang SN, Park J, Sonn CH, Lee KM, Yun CO (2011) Oncolytic adenovirus co-expressing IL-12 and IL-18 improves tumor-specific immunity via differentiation of T cells expressing IL-12Rbeta2 or IL-18Ralpha. Gene Ther 18:898–909
68. Freytag SO, Zhang Y, Siddiqui F (2015) Preclinical toxicology of oncolytic adenovirus-mediated cytotoxic and interleukin-12 gene therapy for prostate cancer. Mol Ther Oncolytics 2
69. Poutou J, Bunuales M, Gonzalez-Aparicio M, Garcia-Aragoncillo E, Quetglas JI, Casado R, Bravo-Perez C, Alzuguren P, Hernandez-Alcoceba R (2015) Safety and antitumor effect of oncolytic and helper-dependent adenoviruses expressing interleukin-12 variants in a hamster pancreatic cancer model. Gene Ther 22:696–706
70. Kim HS, Kim-Schulze S, Kim DW, Kaufman HL (2009) Host lymphodepletion enhances the therapeutic activity of an oncolytic vaccinia virus expressing 4-1BB ligand. Cancer Res 69:8516–8525
71. Huang JH, Zhang SN, Choi KJ, Choi IK, Kim JH, Lee MG, Kim H, Yun CO (2010) Therapeutic and tumor-specific immunity induced by combination of dendritic cells and oncolytic adenovirus expressing IL-12 and 4-1BBL. Mol Ther 18:264–274
72. John LB, Howland LJ, Flynn JK, West AC, Devaud C, Duong CP, Stewart TJ, Westwood JA, Guo ZS, Bartlett DL et al (2012) Oncolytic virus and anti-4-1BB combination therapy elicits strong antitumor immunity against established cancer. Cancer Res 72:1651–1660
73. Postow MA, Chesney J, Pavlick AC, Robert C, Grossmann K, McDermott D, Linette GP, Meyer N, Giguere JK, Agarwala SS et al (2015) Nivolumab and ipilimumab versus ipilimumab in untreated melanoma. N Engl J Med 372:2006–2017
74. Robert C, Schachter J, Long GV, Arance A, Grob JJ, Mortier L, Daud A, Carlino MS, McNeil C, Lotem M et al (2015) Pembrolizumab versus ipilimumab in advanced melanoma. N Engl J Med 372:2521–2532
75. Zamarin D, Holmgaard RB, Subudhi SK, Park JS, Mansour M, Palese P, Merghoub T, Wolchok JD, Allison JP (2014) Localized oncolytic virotherapy overcomes systemic tumor resistance to immune checkpoint blockade immunotherapy. Sci Transl Med 6:226ra232
76. Quetglas JI, Labiano S, Aznar MA, Bolanos E, Azpilikueta A, Rodriguez I, Casales E, Sanchez-Paulete AR, Segura V, Smerdou C et al (2015) Virotherapy with a Semliki Forest virus-based vector encoding IL12 synergizes with PD-1/PD-L1 blockade. Cancer Immunol Res 3:449–454
77. Puzanov I, Milhem MM, Minor D, Hamid O, Li A, Chen L, Chastain M, Gorski KS, Anderson A, Chou J et al (2016) Talimogene Laherparepvec in combination with ipilimumab in previously untreated, unresectable stage IIIB-IV melanoma. J Clin Oncol 34:2619–2626
78. Chow LQ (2013) Exploring novel immune-related toxicities and endpoints with immune-checkpoint inhibitors in non-small cell lung cancer. Am Soc Clin Oncol Educ Book. doi:10.1200/EdBook_AM.2013.33.e280

79. Spain L, Diem S, Larkin J (2016) Management of toxicities of immune checkpoint inhibitors. Cancer Treat Rev 44:51–60
80. Dias JD, Hemminki O, Diaconu I, Hirvinen M, Bonetti A, Guse K, Escutenaire S, Kanerva A, Pesonen S, Loskog A et al (2012) Targeted cancer immunotherapy with oncolytic adenovirus coding for a fully human monoclonal antibody specific for CTLA-4. Gene Ther 19:988–998
81. Du T, Shi G, Li YM, Zhang JF, Tian HW, Wei YQ, Deng H, Yu DC (2014) Tumor-specific oncolytic adenoviruses expressing granulocyte macrophage colony-stimulating factor or anti-CTLA4 antibody for the treatment of cancers. Cancer Gene Ther 21:340–348
82. Engeland CE, Grossardt C, Veinalde R, Bossow S, Lutz D, Kaufmann JK, Shevchenko I, Umansky V, Nettelbeck DM, Weichert W et al (2014) CTLA-4 and PD-L1 checkpoint blockade enhances oncolytic measles virus therapy. Mol Ther 22:1949–1959
83. Rosenberg SA (2011) Cell transfer immunotherapy for metastatic solid cancer—what clinicians need to know. Nat Rev Clin Oncol 8:577–585
84. Restifo NP, Dudley ME, Rosenberg SA (2012) Adoptive immunotherapy for cancer: harnessing the T cell response. Nat Rev Immunol 12:269–281
85. Qiao J, Kottke T, Willmon C, Galivo F, Wongthida P, Diaz RM, Thompson J, Ryno P, Barber GN, Chester J et al (2008) Purging metastases in lymphoid organs using a combination of antigen-nonspecific adoptive T cell therapy, oncolytic virotherapy and immunotherapy. Nat Med 14:37–44
86. Qiao J, Wang H, Kottke T, Diaz RM, Willmon C, Hudacek A, Thompson J, Parato K, Bell J, Naik J et al (2008) Loading of oncolytic vesicular stomatitis virus onto antigen-specific T cells enhances the efficacy of adoptive T-cell therapy of tumors. Gene Ther 15:604–616
87. Pfirschke C, Schirrmacher V (2009) Cross-infection of tumor cells by contact with T lymphocytes loaded with Newcastle disease virus. Int J Oncol 34:951–962
88. Grekova S, Aprahamian M, Giese N, Schmitt S, Giese T, Falk CS, Daeffler L, Cziepluch C, Rommelaere J, Raykov Z (2010) Immune cells participate in the oncosuppressive activity of parvovirus H-1PV and are activated as a result of their abortive infection with this agent. Cancer Biol Ther 10:1280–1289
89. Yan Y, Li S, Jia T, Du X, Xu Y, Zhao Y, Li L, Liang K, Liang W, Sun H et al (2015) Combined therapy with CTL cells and oncolytic adenovirus expressing IL-15-induced enhanced antitumor activity. Tumour Biol 36:4535–4543
90. Yan Y, Xu Y, Zhao Y, Li L, Sun P, Liu H, Fan Q, Liang K, Liang W, Sun H et al (2014) Combination of E2F-1 promoter-regulated oncolytic adenovirus and cytokine-induced killer cells enhances the antitumor effects in an orthotopic rectal cancer model. Tumour Biol 35:1113–1122
91. Hu H, Qiu Y, Guo M, Huang Y, Fang L, Peng Z, Ji W, Xu Y, Shen S, Yan Y et al (2015) Targeted Hsp70 expression combined with CIK-activated immune reconstruction synergistically exerts antitumor efficacy in patient-derived hepatocellular carcinoma xenograft mouse models. Oncotarget 6:1079–1089
92. Yang Z, Zhang Q, Xu K, Shan J, Shen J, Liu L, Xu Y, Xia F, Bie P, Zhang X et al (2012) Combined therapy with cytokine-induced killer cells and oncolytic adenovirus expressing IL-12 induce enhanced antitumor activity in liver tumor model. PLoS One 7: e44802
93. Pittari G, Filippini P, Gentilcore G, Grivel JC, Rutella S (2015) Revving up natural killer cells and cytokine-induced killer cells against hematological malignancies. Front Immunol 6:230
94. Fu X, Rivera A, Tao L, Zhang X (2015) An HSV-2 based oncolytic virus can function as an attractant to guide migration of adoptively transferred T cells to tumor sites. Oncotarget 6:902–914
95. Nishio N, Diaconu I, Liu H, Cerullo V, Caruana I, Hoyos V, Bouchier-Hayes L, Savoldo B, Dotti G (2014) Armed oncolytic virus enhances immune functions of chimeric antigen receptor-modified T cells in solid tumors. Cancer Res 74:5195–5205
96. Singh P, Pal SK, Alex A, Agarwal N (2015) Development of PROSTVAC immunotherapy in prostate cancer. Future Oncol 11: 2137–2148
97. Evgin L, Acuna SA, Tanese de Souza C, Marguerie M, Lemay CG, Ilkow CS, Findlay CS, Falls T, Parato KA, Hanwell D et al (2015) Complement inhibition prevents oncolytic vaccinia virus neutralization in immune humans and cynomolgus macaques. Mol Ther 23:1066–1076

Appendix IV: A list of all clonal viruses represented in this working library and discussed throughout this thesis. Firstly, viruses are listed in numerical order. Secondly, viruses are listed in order as they are found genomically (grouped by *Hind*III digest fragments).

Clonal vaccinia virus mutant library (numerical order)

Clone ID (Tp)	Insertion
2	F4L/1.0
35	C21L/0.7
36	C6L/0.3
41	B8R/0.2
53	A51R/0.5
54	N1L/0.2
59	C8L/0.3
61	F15L/0.8
69	C15L/0.7
81	F2L/0.3
90	J5L/1.0
96	A41L/0.4
98B	B7R/0.2
106	Intergenic
112	C10L/0.4
117	A49R/0.7
130	A57R/0.5
131	A55R/0.0
133	B14R/0.1
173	C14L/0.3
177	B17L/0.8
181	Intergenic
186	Intergenic
195	Intergenic
199	B13R/0.6
201	A52R/0.9
203	B19R/0.6
205	C9L/0.6
211	Intergenic
214	A40R/0.6
219	B4R/0.6
223	F5L/0.4
225	C10L/0.8
229	Intergenic
237	A41L/0.7
243	A47L/0.2
250	A47L/0.6
254	C2L/0.3
255	J2R/0.8
257	A41L/0.9
258	A50R/0.1
261	E5R/0.0
262	C15L/0.1
263	N1L/0.4
264	C17L/0.5
268	A41L/1.0
269	A43R/0.3
270	C10L/0.1
272	B17L/0.9
275	B7R/0.1
276	B17L/0.7
279	F11L/0.3
280	K1L/0.4
285	A48R/0.9
287	C17L/1.0
288	A55R/0.3
289	C7L/1.0
292	A43R/1.0
293	C6L/0.7
297	C9L/0.9
299	B20R/0.2
304	C9L/0.1
305	K5L/0.5
306	A36R/0.9
307	C10L/0.3
311	F15L/0.3
313	C10L/1.0
314	C1L/0.7
315	A55R/0.4
316	A51R/0.9
321	C19L/0.4
323	O1L/0.2
324	M1L/0.6
325	C9L/0.8
326	A47L/0.1
327	A46R/0.6
332	I4L/0.9
333	A39R/0.1
334	N2L/0.7
335	Intergenic
336	F5L/0.2
337	I4L/0.3
339	Intergenic
344	K7R/0.3
347	A31R/0.9
348	F8L/0.8
351	O1L/0.1
353	A39R/0.7
356	F2L/0.1

Clonal vaccinia virus mutant library (genomic order)

Insertion	**Clone ID (Tp)**
Intergenic	186
C21L/0.7	35
C19L/0.4	321
C17L/0.5	264
C17L/1.0	287
Intergenic	335
C15L/0.1	262
C15L/0.7	69
C14L/0.3	173
Intergenic	211
C10L/0.1	270
C10L/0.3	307
C10L/0.4	112
C10L/0.8	225
C10L/1.0	313
C9L/0.1	304
C9L/0.6	205
C9L/0.8	325
C9L/0.9	297
C8L/0.3	59
Intergenic	195
C7L/1.0	289
C6L/0.3	36
C6L/0.7	293
C2L/0.3	254
C1L/0.7	314
N1L/0.2	54
N1L/0.4	263
N2L/0.7	334
M1L/0.6	324
K1L/0.4	280
Intergenic	229
K5L/0.5	305
K7R/0.3	344
F2L/0.1	356
F2L/0.3	81
F4L/1.0	2
F5L/0.2	336
F5L/0.4	223
F8L/0.8	348
Intergenic	106
F11L/0.3	279
Intergenic	339
F15L/0.3	311
F15L/0.8	61
E5R/0.0	261
O1L/0.1	351
O1L/0.2	323
I4L/0.3	337
I4L/0.9	332
J2R/0.8	255
J5L/1.0	90
A31R/0.9	347
A36R/0.9	306
A39R/0.1	333
A39R/0.7	353
A40R/0.6	214
A41L/0.4	96
A41L/0.7	237
A41L/0.9	257
A41L/1.0	268
A43R/0.3	269
A43R/1.0	292
A46R/0.6	327
A47L/0.1	326
A47L/0.2	243
A47L/0.6	250
A48R/0.9	285
A49R/0.7	117
A50R/0.1	258
A51R/0.5	53
A51R/0.9	316
A52R/0.9	201
A55R/0.0	131
A55R/0.3	288
A55R/0.4	315
A57R/0.5	130
B4R/0.6	219
B7R/0.1	275
B7R/0.2	98B
B8R/0.2	41
Intergenic	181
B13R/0.6	199
B14R/0.1	133
B17L/0.7	276
B17L/0.8	177
B17L/0.9	272
B19R/0.6	203
B20R/0.2	299

Curriculum Vitae

BRIAN ANDREW KELLER

EDUCATION

Doctor of Philosophy (PhD) – Biochemistry 2014 - 2017
University of Ottawa | Ottawa, Ontario
Thesis Supervisor: John C. Bell, Professor & Senior Scientist, Ottawa Hospital Research Institute

Doctor of Medicine (MD) 2012 - 2014, 2017 - 2019
University of Ottawa | Ottawa, Ontario

Master of Science (MSc) – Pathology 2010 - 2011
Western University | London, Ontario
Thesis Supervisor: Michael J. Strong, Distinguished University Professor, Western University

Bachelor of Science (BSc) – Biochemistry 2004 - 2008
Hawaii Pacific University | Honolulu, Hawaii, USA

ACADEMIC AWARDS

Research/Academic Funding (Most recent 5 years)

2016-2018	**Cancer Research Institute CLIP Grant** (Co-applicant)
2014-17	**Vanier Canada Graduate Scholarship**
2017	**Audrey J. Boyce MD/PhD Fellowship**
2017	**CIHR Michael Smith Foreign Study Supplement** (Leeds, UK)
2014-17	**University of Ottawa Excellence Scholarship**
2014-17	**CIHR CGS Doctoral Award** (Declined)
2015-16	**Judith R. Raymond Scholarship in Cancer Research**
2014-15	**Ontario Graduate Scholarship** (Declined)
2013-14	**Dr. Charles W. MacLeod MD/PhD Fellowship**
2013-14	**University of Ottawa MD/PhD Scholarship**
2013	**University of Ottawa FGPS Admission Scholarship**
2012-13	**University of Ottawa MD/PhD Scholarship**

Additional Funding/Awards

2017	**Mark Ernsting Entrepreneurship Award** (with Dr. C. Ilkow)
2016	**BioCanRx Highly Qualified Personnel travel award**
2016	**University of Ottawa BMI Department travel award**

2016 **University of Ottawa BMI Department travel award**
2016 **BioCanRx Highly Qualified Personnel travel award**
2016 **Terry Fox Research Institute travel award**
2015 **Ottawa Hospital Research Institute IMPACT Award** (with A. Pelin)
2015 **CIHR Institute Community Support travel award**

PUBLICATIONS, PRESENTATIONS, AND TEACHING

Publications

Lemay CG, **Keller BA**, Edge RE, Abei M, Bell JC, Oncolytic viruses: The best is yet to come. Curr Cancer Drug Targets. 2017 Feb 6. doi: 10.2174/1568009617666170206111609. Epub ahead of print.

Evgin L, Ilkow CS, Bourgeois-Daigneault M-C, de Souza C, Stubbert L, Huh MS, Jennings VA, Marguerie M, Acuna SA, **Keller BA**, Lefebvre C, Falls T, Le Boeuf F, Auer R, Lambris JD, McCart JA, Stojdl DF, Bell JC, Complement inhibition enables tumor delivery of LCMV glycoprotein pseudotyped viruses in the presence of anti-viral antibodies. Mol Ther Oncolytics. 2016 Nov 16;3:16027. eCollection 2016.

Keller BA & Bell JC, Oncolytic viruses – immunotherapeutics on the rise. J Mol Med (Berl). 2016 Sep;94(9):979-91. doi: 10.1007/s00109-016-1453-9. Epub 2016 Aug 4.

Monachelli G, Campos-Melo D, Droppelmann CA, **Keller BA**, De Nicola A, Deniselle M, Volkening K, Strong MJ, Expression and cellular localization of the classical progesterone receptor in healthy and amyotrophic lateral sclerosis affected spinal cord. Eur J Neurol. 2014 Feb;21(2):273-80.e11. doi: 10.1111/ene.12291. Epub 2013 Nov 7.

Droppelmann CA, Wang J, Campos-Melo D, **Keller B**, Volkening K, Hegele R, Strong MJ, Detection of a novel frameshift mutation and regions with homozygosis within ARHGEF28 gene in familial amyotrophic lateral sclerosis. Amyotroph Lateral Scler Frontotemporal Degener, 2013 Sep;14(5-6):444-51. doi: 10.3109/21678421.2012.758288. Epub 2013 Jan 4.

Keller BA, Volkening K, Droppelmann CA, Ang LC, Rademakers R, Strong MJ, Co-aggregation of RNA binding proteins in ALS motor neurons: evidence of a common pathogenic mechanism. Acta Neuropathol. 2012 Nov;124(5):733-47. doi: 10.1007/s00401-012-1035-z. Epub 2012 Sep 1.

Droppelmann CA, **Keller BA**, Campos-Melo D, Volkening K, Strong MJ, Rho guanine nucleotide exchange factor is an NFL mRNA destabilizing factor that forms cytoplasmic inclusions in amyotrophic lateral sclerosis. Neurobiol Aging. 2013 Jan;34(1): 248-62. doi: 10.1016/j.neurobiolaging.2012.06.021. Epub 2012 Jul 24.

Conference/External Seminar Oral Presentations

2017 Characterizing the phenotypic parameters of vaccinia virus using a library of single gene mutants with differential phenotypes
Institute of Cancer Research (Chelsea), Melcher & Harrington Lab Seminar
London, UK

2016 Random mutagenesis of vaccinia virus uncovers novel clinical candidate oncolytic backbones with unique phenotypes
International Conference on Replicating Oncolytic Viral Therapeutics
Vancouver, British Columbia

2016 Creating novel oncolytic vaccinia virus strains using transposon mutagenesis
German Cancer Research Center, Ungerechts Lab Seminar
Heidelberg, Germany

2016 Transposon-mediated mutagenesis for the creation of a novel oncolytic vaccinia virus
XXI International Poxvirus, Asfarvirus and Iridovirus Conference
Le Bischenberg, Strasbourg, France

2016 Augmenting the anti-tumour immunogenicity of Vaccinia virus using transposon-mediated mutagenesis
Summit for Cancer Immunotherapy
Halifax, Nova Scotia

2016 Creating and characterizing a transposon-mutagenized library of Vaccinia virus clones for the treatment of human cancer
Terry Fox Research Institute Annual Scientific Meeting
Vancouver, British Columbia

2016 Creating better oncolytic viruses for the treatment of hematologic malignancies utilizing a transposon-mutagenized library of vaccinia virus clones
Hematology Trainee Research Day – Ottawa Hospital
Ottawa, Ontario

2014 Directed evolution of vaccinia virus
Canadian Oncolytic Virus Consortium Annual Retreat
Elgin, Ontario

2012 Strengthening the argument for the role of RNA metabolism in ALS
23rd International Symposium on ALS/MND
Chicago, IL, USA

Poster Presentations (Most recent 5 years)

2016 Optimizing the vaccinia backbone for use as an oncolytic virus using insertional mutagenesis
Terry Fox Research Institute, Ontario Node Symposium
Toronto, Ontario

2016 Random mutagenesis of vaccinia virus uncovers novel clinical candidate oncolytic backbones with unique phenotypes
OHRI Research Day 2016
Ottawa, Ontario

2016 Augmenting the anti-tumour immunogenicity of vaccinia virus using transposon-mediated mutagenesis
Summit for Cancer Immunotherapy
Halifax, Nova Scotia

2016 Creating and characterizing a transposon-mutagenized library of vaccinia virus clones for the treatment of human cancer
Terry Fox Research Institute Annual Scientific Meeting
Vancouver, British Columbia

2015 Bio-engineering a vaccinia-based oncolytic virus for the treatment of cancer
OHRI IMPACT Award finalist
Ottawa, Ontario

2015 Bio-engineering a vaccinia-based oncolytic virus using transposon-mediated mutagenesis for the treatment of malignant melanoma
OHRI Research Day 2015
Ottawa, Ontario

2015 Directing recombination evolution to develop novel vaccinia virus-based therapeutics for the treatment of malignant melanoma
9th International Conference on Oncolytic Virus Therapeutics
Boston, MA, USA

2014 Directing recombination evolution to develop novel vaccinia virus-based therapeutics for the treatment of malignant melanoma
Clinical Investigator Trainee Association of Canada Annual General Meeting
Toronto, Ontario

2014 Directing recombination evolution to develop novel vaccinia virus-based therapeutics for the treatment of malignant melanoma
OHRI Research Day 2014
Ottawa, Ontario

2012 The pathogenic expression of RNA binding proteins in ALS and evidence for the histologic distinction of *mt*SOD1-ALS
London Health Research Day
London, Ontario

Teaching Experience

2017 CO-OP student supervision – Natalie Crawford (Dalhousie University)
Ottawa Hospital Research Institute, Ottawa, Ontario

2016-2017 Honours student supervision – Russell Barkley (University of Ottawa)
Ottawa Hospital Research Institute, Ottawa, Ontario

2016 Laboratory MD student supervision – Brandon Budhram (University of Ottawa)
Ottawa Hospital Research Institute, Ottawa, Ontario

2016 CO-OP student supervision – Russell Barkley (University of Ottawa)
Ottawa Hospital Research Institute, Ottawa, Ontario

2015 Summer student supervision – Nathan Fergusson (Queen's University)
Ottawa Hospital Research Institute, Ottawa, Ontario

2013 Case-Based Learning session for MD2017
University of Ottawa, Faculty of Medicine, Ottawa, Ontario

External Collaborators

- Dr. Christine Engeland (German Cancer Research Center, Heidelberg, Germany)
- Dr. Victoria Jennings (University of Leeds, Leeds, UK)
- Professor Alan Melcher (Institute of Cancer Research, London, UK)
- Dr. Antonio Postigo (Francis Crick Institute, London, UK)
- Dr. Martina Schroeder (Maynooth University, Maynooth, UK)
- Professor Michael Way (Francis Crick Institute, London, UK)